UNIL | Université de Lausanne

Unicentre
CH-1015 Lausanne
http://serval.unil.ch

Year : 2017

New Steps Towards Understanding the Hemostatic Balance and Inflammation: Dissecting the Rôle of Protein S and Gas6

Prince El adnani Raja

Prince El adnani Raja, 2017, New Steps Towards Understanding the Hemostatic Balance and Inflammation: Dissecting the Rôle of Protein S and Gas6

Originally published at : Thesis, University of Lausanne

Posted at the University of Lausanne Open Archive http://serval.unil.ch
Document URN : urn:nbn:ch:serval-BIB_04D1039545CF3

UNIL | Université de Lausanne
Faculté de biologie
et de médecine

New Steps Towards Understanding the Hemostatic Balance and Inflammation: Dissecting the Role of Protein S and Gas6

Thèse de doctorat ès sciences de la vie (PhD)

présentée à la

Faculté de biologie et de médecine
de l'Université de Lausanne

par

Raja Prince El adnani

Biologiste diplômée de l'Université Lille II, France

Jury

Prof. Président Benjamin Marsland
Prof. Tatiana Petrova, Directrice de thèse
Prof. Anne Angelillo-Scherrer, Co-directrice
Prof. Brenda R Kwak, Experte
Dr. Pascal Schneider, Expert

Lausanne 2017

New Steps Towards Understanding the Hemostatic Balance and Inflammation: Dissecting the Role of Protein S and Gas6

Raja Prince El adnani

This work was performed under the supervision of Prof. Anne Angelillo-Scherrer
at the University Clinic of Hematology and Central Hematology Laboratory
at Inselspital, Bern University Hospital, University of Bern

and

at Department of Clinical Research
University of Bern

Bern, Switzerland

Jury

Prof. President Benjamin Marsland
Prof. Tatiana Petrova, Director
Prof. Anne Angelillo-Scherrer, Co-director
Prof. Brenda R Kwak, Expert
Dr. Pascal Schneider, Expert

Lausanne 2017

Remerciements

J'ai beaucoup réfléchit avant d'écrire ces mots de remerciement…

A vrai dire, j'y pense depuis que j'ai commencé l'écriture de cette thèse.

Tout au long de la rédaction et pour chaque partie de ce travail, j'avais en tête de remercier la ou les personnes qui m'ont aidé, soutenue et rendu ma vie plus agréable en leur compagnie.

Hélas, durant ces cinq dernières années, vous étiez beaucoup à l'avoir fait…

Mes premiers mots de remerciement vont au professeur Anne Angelillo-Scherrer. Chère Anne, merci de m'avoir ouvert votre laboratoire et donné l'occasion de faire cette thèse. Oui, c'est très ordinaire comme mots de remerciement ! Mais vous Anne, vous êtes loin d'être une personne ordinaire. Donc je vous remercie plus profondément de m'avoir appris tant, d'être tout le temps disponible et encourageante quand le moral est au plus bas. Merci de m'avoir donné l'occasion de m'épanouir, d'être autonome, Merci de m'avoir fait confiance…

Je souhaite exprimer ma gratitude au Professeur Tatiana Petrova et au Professeur Brenda Kwak pour leur aide et conseils et d'avoir accepter de juger ce travail.

Mes remerciements vont aussi au Docteur Pascal Schneider pour les précieux échanges, conseils et minutieuses corrections du manuscrit.

A toi Sara, un grand merci pour ton soutien, pour les fous rires, pour les bons moments partagés, tu as un grand coeur…

A vous Claudia, Justine, Natacha, Desirée, Magdalena et tous les autres collègues à la Mu40 pour leur gentillesse et sympathie.

Ma reconnaissance va à ceux qui ont plus particulièrement assuré le soutien affectif de ce travail doctoral

Cher Papa, tu y as toujours cru (même quand je doutais fort), je te dédie cette thèse et te remercie d'être toujours là pour moi. Merci pour ton enthousiasme contagieux à l'égard de ma vie en général

A mon cher époux, Dany : merci pour ton soutien quotidien indéfectible et inconditionnel, pour ton écoute et ton amour. Cette thèse n'aurait pu être menée à bien sans ton aide. A deux, on est plus fort…

A ma fille chérie, Lyna, la douceur de ma vie.

Mes remerciements vont aussi à ma famille et mes amis qui, avec cette question récurrente, « c'est pour quand la soutenance ? », bien qu'angoissante en période fréquente de doutes, m'ont permis de ne jamais dévier de mon objectif final. Merci ma belle-mère, mes frères, ma soeur, mes beaux parents, mes beaux frères, à toi Anssar et à ta petite famille et à tous mes amis…

Table of contents

Summary

Hemostasis is the set of mechanisms that maintains blood in a fluid state under normal conditions and responds to vessel damage by the rapid formation of a clot. The equilibrium between procoagulant and anticoagulant forces is tightly balanced and the deficiency of any of the coagulation factors could leads to disequilibrium provoking bleeding or thrombosis.

Both protein S (PS) and growth arrest-specific gene 6 (Gas6) belong to the vitamin K-dependent protein family. Apart from a γ-carboxyglutamic acid-domain interaction with phospholipid membranes, PS and Gas6 also bind to the receptor tyrosine kinases Tyro3, Axl and Mer (or TAM receptors) by their carboxy-terminal globular domains. PS is an important natural anticoagulant. This is evidenced by the fact that homozygous *PROS1* deficiency promotes dramatic clinical manifestations including disseminated intravascular coagulation (DIC) and purpura fulminans (PF) that, if untreated, are incompatible with life. Heterozygous patients deficient in *PROS1* have an increased risk of thromboembolic events. Gas6 is redundant for normal homeostasis but critical for stress-responses. Therefore, inactivation of *Gas6* does not cause life-threatening developmental defects, but modulates the severity of disease related phenotypes. The pathophysiology of PF is uncertain although the imbalance between pro- and anticoagulant forces is supposed to be the etiological factor. A murine model recapitulating aspects of PS deficiencies in human is now available. The examination of PS deficiency associated PF revealed that besides extensive bleeding and thrombosis, *Pros1*$^{-/-}$ embryos displayed altered vasculature. The question was then to find out if PF could result not only from the lack of the PS anticoagulant effect, but also from the lack of PS signaling in the endothelium and its role in vascular development or both.

In order to study more in detail PF development, we used *Pros1* gene silencing by Cre inducible recombination approach in adult *Pros1*$^{lox/-}$ mice to achieve null or very low PS level. Although thrombi were found in liver, heart and lungs, *Pros1*$^{lox/-}$*Mx1Ce*$^{+}$ mice displaying low PS plasma level (16% of the level found in control mice) did not develop PF. A second strategy was to use warfarin, a vitamin K antagonist, that leads to inactive PS. Most of

Pros1+/- mice succumbed to the challenge. Among the few survivor mice, some developed PF. Histological examinations of these lesions revealed thrombosis occurring with vascular wall damage. Investigations of *Pros1*-/- embryos vasculature revealed damaged endothelium and poorly formed vessel networks further confirming that the lack of PS might disturb the vasculature development and maintenance. We also observed ongoing inflammation, altered phagocytosis and erythropoietic defects. *Gas6*-/- mice were previously described to be protected against thrombosis. To find out if PS deficiency induced PF is strictly due to the imbalance between pro- and anticoagulant factors, we hypothesize that synergic deficiency of PS and Gas6 should rebalance hemostasis in *Pros1*-/- and rescue them from PF. Surprisingly, *Pros1*-/-*Gas6*-/- embryos exhibited a more dramatic phenotype with earlier and more frequent mortality, altered vasculature, phagocytosis, inflammation and erythropoiesis indicating that PS deficiency induced PF is not only due to lack of PS anticoagulant activity but also to the lack of PS signaling involved in vasculature, phagocytosis, inflammation and erythropoiesis.

Bleeding diathesis sustained by the loss of F8 (hemophilia A :HA) or F9 (hemophilia B : HB) activity that remarkably impairs the generation of thrombin and imbalance hemostasis. Patients with severe hemophilia frequently suffer from spontaneous recurrent muscle and joint bleeding, such as hemarthrosis, which leads to severe and progressive musculoskeletal damage. The main treatment is administration of the deficient clotting factor. Complication of such therapy is the development of neutralising antibodies. The disequilibrium of the hemostatic balance caused by PS complete lack allows us hypothesize that synergic deficiency of F8/ F9 and PS might be suitable to achieve hemostasis in HA and HB and rescue *Pros1*-/- mice from PF. Attractively, *Pros1*-/-*F8*-/- and *Pros1*-/-*F9*-/- mice are viable, displayed normal hemostatic parameters and did not present PF. Fascinatingly, we observed complete prevention from acute and chronic hemarthrosis in *Pros1*-/-*F8*-/- and *Pros1*-/-*F9*-/- mice. Recombinant F8 administration in *Pros1*-/-*F8*-/- mice restored the imbalance of the coagulation and promotes DIC and thrombosis. However, no PF was observed.

Pregnancy is associated with a shift of the coagulation balance leading to a hypercoagulable state that predispose to thromboembolism. Pregnant women with partial PS inherited

deficiency have an elevated risk of late fetal loss and whether thromboprophylaxis could ameliorate pregnancy outcomes is debated. We used $Pros1^{-/-}$ mice that are fully rescued from lethality by targeting Factor VIII (FVIII) ($F8^{-/-}Pros1^{-/-}$). We did not observed pregnancy loss in $F8^{-/-}Pros1^{+/-}$ females. Differently, $F8^{-/-}Pros1^{-/-}$ females never produced a litter, demonstrating that complete lack in PS is incompatible with a positive pregnancy outcome. Examination of pregnancy in $F8^{-/-}Pros1^{-/-}$ revealed dead and macerated embryos from E11.5 onwards with no evidence of increased fibrin deposition in placentas, females liver, lung and kidney. Reduced platelet count, low fibrinogen, increased thrombin-antithrombin complexes and platelets activation in these pregnant females point to coagulation activation but no overt DIC. Treatment of $F8^{-/-}Pros1^{-/-}$ pregnant mice with enoxaparin largely prevented abortion with slightly reduced litter size. Less efficiently, aspirin also ameliorated pregnancy outcome with smaller litter as compared to enoxaparin. In summary, our findings provide evidence that the thrombotic process occurring during PS deficiency induced PF should be less central than currently admitted. PS possibly plays an additional role in vasculature development. The lack of its signaling in the endothelium might lead to vascular defects and further promotes PF. The mechanism by which PS is involved in vascular development and maintenance should be further investigated. Concomitant F8 and PS deficiency overcome $Pros1^{-/-}$ lethal phenotype, prevented hemarthrosis and perfectly restored the hemostatic balance in $F8^{-/-}Pros1^{-/-}$ mice advocating PS targeting as potential therapy for hemophilia. The absence of PF lesions in $F8^{-/-}Pros1^{-/-}$ mice after recombinant F8 injection further indicate that in PF, PS might play other role than anticoagulation. Thromboprophylaxis was very beneficial the context of very severe PS deficiency indicating that it might apply to pregnancy with inherited thrombophilias. However, litters produced under anticoagulation treatment were smaller suggesting that beyond its anticoagulation role, PS likely plays a role in uteroplacental vasculature.

Resumé

L'hémostase est l'ensemble des mécanismes maintenant le sang dans un état fluide dans des conditions normales et réagissant aux dommages vasculaires par la formation rapide d'un caillot sanguin. La balance entre forces procoagulantes et anticoagulantes est strictement équilibrée. Le déficit de l'un des facteurs de la coagulation peut provoquer un déséquilibre induisant des saignements ou des thromboses. La protéine S (PS) et le Gas6 (Growth arrest specific gene 6) appartiennent à la famille des protéines dépendantes de la vitamine K. En plus de leur interaction avec les membranes phospholipidiques grace à leur domaine riche en résidus de l'acide γ-carboxyglutamique, PS et Gas6 sont également capables de se lier aux récepteurs tyrosine kinases Tyro3, Axl et Mer (ou récepteurs TAM) grace à leur domaine carboxy-terminal globulaire. La PS est un important anticoagulant naturel. Sa déficience totale provoque une coagulation intravasculaire disséminée (CIVD) et un purpura fulminans (PF), qui sans traitement peuvent être fatals. Les patients souffrant d'une déficience en PS moins sévère présentent un risque accru d'événements thromboemboliques veineux. Gas6 est redondant pour l'homéostase normale. Cependant, il joue un rôle critique lors des réponses au stress. L'inactivation de Gas6 ne provoque pas des défauts de développement fatal mais module la sévérité des phénotypes liés aux maladies. Bien que le déséquilibre entre les forces procoagulantes et anticoagulantes est supposé être le facteur étiologique, la physiopathologie du PF est méconnue. Un modèle murin récapitulant les aspects de la déficience en PS chez l'être humain est maintenant disponible. Grâce à ce modèle murin, l'analyse du PF lié à la déficience en PS a révélé qu'en plus d'abondants saignements et de thromboses, les embryons *Pros1*$^{-/-}$ avaient des anomalies vasculaires. La question est alors de discriminer si le PF résulte non seulement de l'absence de l'effet anticoagulant de la PS, mais aussi du manque de sa signalisation dans l'endothélium et lors du développement vasculaire, ou les deux.

Afin de clarifier le mécanisme lié au développement du PF, nous avons utilisé le système de recombinaison inductible de Cre chez les souris adultes *Pros1*$^{lox/-}$ afin d'inactiver le gène *Pros1* et atteindre un taux de PS très bas voire indétectable. Bien que des thrombi aient été

observés dans leur foie, cœur et poumons, les souris $Pros1^{lox\ /-}Mx1Cre^+$ ayant un taux plasmatique de PS très faible (16% du taux constaté chez les souris témoins), n'ont pas développé de PF. Notre deuxième stratégie était d'utiliser la warfarine, un antagoniste de la vitamine K empêchant la formation de la forme active de la PS. Suite à ce traitement, seule une partie des souris $Pros1^{+/-}$ a succombé. Parmi les rares survivantes, quelques-unes ont développé un PF. Les examens histologiques de ces lésions ont révélé des thromboses et des lésions de la paroi vasculaire. L'analyse des vaisseaux des embryons $Pros1^{-/-}$ a révélé un endothélium endommagé et des réseaux vasculaires mal formés confirmant que le manque de PS pourrait perturber le développement et la maintenance du système vasculaire. Nous avons également observé des signes d'inflammation et une réduction de la phagocytose et des troubles de l'érythropoïèse. Les souris $Gas6^{-/-}$ ont été précédemment décrites comme étant protégées contre les thromboses. Pour déterminer si le PF induit par la déficience en PS est strictement dû au déséquilibre entre les facteurs procoagulants et anticoagulants, nous avons supposé que la déficience combinée en PS et en Gas6 devrait rééquilibrer l'hémostase des embryons $Pros1^{-/-}$ et les protéger contre le PF. Etonnamment, les embryons $Pros1^{-/-}Gas6^{-/-}$ ont montrés un phénotype encore plus dramatique avec une mortalité plus précoce et plus fréquente. Le réseau vasculaire, la phagocytose, l'inflammation et l'érythropoïèse étaient aussi altérés. Ceci laisse supposer que le PF induit par la déficience en PS n'est peut-être pas uniquement dû au manque de l'activité anticoagulante de la PS, mais aussi à la possible absence de la signalisation de la PS impliquée dans la vascularisation, la phagocytose, l'inflammation et l'érythropoïèse.

Dans le cadre de l'hémophilie, la perte de l'activité du facteur VIII (FVIII) (hémophilie A: HA) ou du facteur IX (FIX) (hémophilie B: HB) diminue considérablement la génération de thrombine et déséquilibre la balance hémostatique. Les patients avec une hémophilie sévère souffrent fréquemment de saignements musculaires et articulaires, comme l'hémarthrose, qui entraîne des lésions musculo-squelettiques graves et progressives. Le traitement principal étant l'administration du facteur de coagulation manquant, une thérapie qui conduit souvent au développement d'anticorps neutralisants contre les facteurs administrés. Le déséquilibre de

l'équilibre hémostatique causé par le manque complet de la PS nous a permis de supposer que le manque combiné des FVIII ou FIX et de la PS pourrait être une bonne alternative pour rééquilibrer la balance hémostatique dans le contexte de l'HA ou HB et prévenir le PF chez les souris $Pros1^{-/-}$. De manière surprenante, les souris $F8^{-/-}Pros1^{-/-}$ et $F9^{-/-}Pros1^{-/-}$ étaient viables avec des paramètres hémostatiques normaux sans aucun signe de PF. De plus, une prévention complète de l'hémarthrose aiguë a été observée chez les souris $F8^{-/-}Pros1^{-/-}$ et $F9^{-/-}Pros1^{-/-}$. Cependant, l'administration de FVIII recombinant aux souris $F8^{-/-}Pros1^{-/-}$ a ré-induit le déséquilibre de la coagulation et favorisé le développement de la CIVD et de thromboses, mais l'apparition de PF n'a toutefois pas été observée.

La grossesse est associée à un déséquilibre de la coagulation conduisant à un état hypercoagulable qui prédispose les femmes enceintes à des événements thromboemboliques. Les femmes enceintes atteintes d'une déficience héréditaire partielle en PS ont un risque accru de perte fœtale. L'effet favorable de la prophylaxie antithrombotique sur le déroulement de ces grossesses à risque est fortement débattu. Nous avons utilisé des souris $Pros1^{-/-}$ viable (grâce à leur déficience concomitante en FVIII ($F8^{-/-}Pros1^{-/-}$). Nous n'avons pas observé de perte fœtale chez les femelles $F8^{-/-}Pros1^{+/-}$. En revanche, les femelles $F8^{-/-}Pros1^{-/-}$ n'ont jamais mis bas, démontrant que la déficience complète en PS est incompatible avec une issue favorable de la grossesse. L'évaluation de la grossesse chez les femelles $F8^{-/-}Pros1^{-/-}$ a révélé des embryons morts et macérés à partir de E11.5, sans augmentation de dépôt de fibrine ni dans les organes des femelles portantes (foie, poumons et reins) ni dans les placentas de celles-ci. La diminution du nombre de plaquettes, la réduction du taux de fibrinogène et l'augmentation des complexes de thrombine-antithrombine chez ces femelles enceintes ont indiqué une activation de la coagulation, mais pas de CIVD décompensée. Le traitement des souris $F8^{-/-}Pros1^{-/-}$ portantes avec de l'énoxaparine a sensiblement diminué les pertes fœtales, les femelles ayant donné naissance à des portées légèrement réduites. L'aspirine a également amélioré le résultat de la grossesse, mais de manière moins efficace, les portées étant encore plus réduites qu'avec l'énoxaparine. En résumé, nos résultats démontrent que le processus thrombotique lors du PF (induit par la déficience complète en PS) devrait être moins central

qu'actuellement admis. En effet, la PS joue peut-être un rôle supplémentaire dans le développement vasculaire. L'absence de sa signalisation dans l'endothélium pourrait entraîner des défauts vasculaires et favoriser davantage la survenue de PF. Le mécanisme par lequel la PS est impliquée dans le développement et la maintenance vasculaire mérite d'être étudié plus à fond. La déficience concomitante en FVIII et en PS a corrigé le phénotype $Pros1^{-/-}$ létal, s'est révélée être une protection contre l'hémarthrose et a parfaitement restauré l'équilibre hémostatique chez les souris $F8^{-/-}Pros1^{-/-}$. Ces résultats spectaculaires permettent de proposer le ciblage de la PS comme traitement potentiel de l'hémophilie. L'absence de lésions de PF chez les souris $F8^{-/-}Pros1^{-/-}$ après l'injection de FVIII recombinant indique en outre que lors du PF, la PS pourrait jouer un autre rôle que l'anticoagulation. Dans la grossesse, la prophylaxie antithrombotique s'est montrée très bénéfique dans le contexte d'un déficit très sévère en PS, ce qui indique qu'elle pourrait être profitable dans le contexte de la grossesse en présence de thrombophilies héréditaires. Cependant, les portées réduites obtenues sous anticoagulation laissent suggérer qu'au-delà de son rôle d'anticoagulation, la PS joue probablement un rôle dans le système vasculaire utéro-placentaire.

List of abbreviations

ADP	adenosine diphosphate
Akt	protein kinase B
AngII	angiotensin II
APC	activated protein C
APCs	antigen presenting cells
aPL	antiphospholipid
Ark	adhesion-related kinase
BBB	blood brain barrier
BFU-Es	burst forming unit erythroid progenitors
BM	bone marrow
Brt	brain tyrosine kinase
C4BP	C4b-binding protein
Ca^{2+}	calcium
CFU-Es	colony forming unit erythroid progenitors
DCs	dendritic cells
DIC	disseminated intravascular coagulation
ds DNA	double stranded DNA
Dtk	developmental tyrosine kinase
EB	evans blue
ECs	endothelial cells
EGF	epidermal growth factor
EPCs	endothelial progenitor cells
EPO	erythropoietin
EPOR	erythropoietin receptor
ERK1/2	extracellular signal-related kinase
FV	factor V

FVII	factor VII
FVIII	factor VIII
FIX	factor IX
FX	factor X
FXI	factor XI
FFP	fresh frozen plasma
FGF	fibroblast growth factor
FNIII	fibronectin type III
FV Leiden	factor V Leiden
FVIIIa	activated FVIII
Gas6	growth arrest-specific gene 6
Gla:	gamma-carboxyglutamic acid
HELLP syndrome	hemolysis elevated liver function tests and low platelets syndrome
HRMECs	human retinal microvascular endothelial cells
IGF	insulin-like growth factor
IL-10	interleukin-10
IFN	interferon
IMT	intima media thickening
IRAK	interleukin-1 receptor associated kinase
IRAKM	interleukin-1 receptor associated kinase M
ITP	immune thrombocytopenia
K3	kunitz 3
kDa	kilodaltons
Ki	dissociation constant
LMWH	low molecular weight heparin
MHC	myosin heavy chain
MyD88s	short form of myeloid differentiation primary response gene 88
NF-κB	nuclear factor-κB

NOD2	nucleotide-binding oligomerization domain 2
PAI-1	plasminogen activator inhibitor-1
PAI-2	plasminogen activator inhibitor-2
PAR	protease activated receptors
PDGF	platelet-derived growth factor
PECAM-1	ECs adhesion protein 1
PH	phenylhydrazine
PI3K	phosphoinositide 3 kinase
PS	protein S
PT	prothrombin
PtdSer	phosphatidylserine
RBC	red blood cells
RCS	royal college of surgeons rat
rEPO	recombinant erythropoitin
rhGas6	recombinant human Gas6
ROS	reactive oxygen species
RPE	retinal pigment epithelial cells
Rse	receptor sectatoris
RTKs	receptor tyrosine kinases
S1P	sphingosine 1-phosphate receptor
SCs	sertoli cells
SHBG	steroid hormone binding globular like domain
SHBG	steroid hormone binding globular like domain
SKY	sea-related tyrosine kinase
SLE	systemic lupus erythematous
SOCS	suppressor of cytokine signalling
TAFI	thrombin activatable fibrinolytic inhibitor
TAM	Tyro3, Axl and Mer

TF	tissue factor
TIF	tyrosine kinase with immunoglobulin and fibronectin type III domains
TLRs	toll-like receptors
TOLLIP	toll interacting protein
TRAF6	tumor necrosis factor receptor associated factor 6
TReg	regulatory T cells
TTP	thrombotic thrombocytopenic purpura
TXA_2	thromboxane A_2
VE-cadherin	vascular endothelial cadherin
VEGF-A	vascular endothelial growth factor A
VEGF	vascular endothelial growth factor
VEGR-2	vascular endothelial growth factor R2
VKDP	vitamin k dependent protein
VSMC	vascular smooth cells
VTE	venous thromboembolism
WT	wild type
α-SMA	α-Smooth muscle actin

List of figures

List of tables

Chapter I. General introduction

1.1 Hemostasis and inflammation

Hemostasis is the set of mechanisms that maintains blood in a fluid state under normal conditions and responds to vessel damage by the rapid formation of a clot.

The coagulation system is characterized by the sequential, rapid and highly localized activation of a series of serine proteases, culminating in the generation of thrombin, with subsequent conversion of fibrinogen into a fibrin clot. The role of tissue factor (TF) and collagen that are localized in the subendothelial matrix is to maintain a closed circulatory system. Indeed, after vascular injury or endothelium disturbance, collagen and TF become exposed to the flowing blood allowing the formation of a clot. There, exposed collagen activates platelets that accumulate at the site of injury and TF induces thrombin generation, resulting into the conversion of fibrinogen to fibrin and platelet aggregation. Numerous positive feedback mechanisms between platelets and the coagulation system ensure the effective sealing of the vascular wound. For example, phosphatidylserine (PtdSer) exposure on the surface of activated platelets functions as the docking site for gamma-carboxyglutamic acid (GLA)-containing coagulation factors. Besides, activated platelets produce an excess of factors that promote endothelial cell survival, proliferation, and vascular repair [1].

Thrombosis related fatal and life threatening pathologies are ischemic heart disease, ischemic stroke and venous thromboembolism (VTE) comprising pulmonary embolism and deep vein thrombosis.

According to the study 'Global Burden of Diseases, Injuries and Risk Factors' initiated by the World Health Organization and the World Bank in 2010, 7 million deaths were due to ischemic heart disease and 5.9 million deaths caused by stroke. Approximately half of all stroke deaths resulted from ischemic stroke caused by thrombosis [2].

It is widely known that inflammation can activate the coagulation system and leads to consumptive coagulopathy, thrombosis and tissue damage. A link between hemostasis and

host defence was well established from early studies analysing the blood of primitive invertebrates supporting that coagulation and inflammation are finely balanced biological systems with extensive cross talks that optimize the organism response to injury and invasion by pathogens [3].

The classical example of inflammation caused coagulopathy is bacterial sepsis where acute systemic inflammatory response to infection induces endothelial injury and expression of TF. The resultant activation and consumption of coagulation factors and platelets, along with decreased fibrinolysis, disturbance of endothelial barrier function and loss of physiological antithrombotic factors create a clinical situation in which patients may be at risk for hemorrhage and arterial, venous or microvascular thrombosis. However, acute fulminant coagulopathy can also be triggered by noninfectious inflammation such as cancer, trauma, severe burns or complications of pregnancy. Besides, chronic inflammation conditions such as obesity, inflammatory bowel disease and other autoimmune disorders could also favor thrombosis [4, 5].

This work will describe the involvement and the role of two proteins in hemostasis and inflammation: Growth arrest specific gene 6 (Gas6) and protein S (PS). They are ligands for Tyro3, Axl and Mer (TAM) receptors belonging to a family of receptor tyrosine kinases (RTKs). Their downstream signalling upon Gas6/PS binding not only controls the magnitude of the immune response but is also active during inflammation resolution and recovery of tissue function via the clearance of apoptotic debris and the restoration of vascular integrity.

1.2 Identification, characterization of Gas6, protein S and TAM receptors

1.2.1 Gas6 identification

Growth arrest-specific genes or *GAS* genes expression has been studied during the different phases of the cell cycle and in different tissues. They are induced during the growth arrest phase of the cell cycle (G0), such as after serum starvation or removal of growth factors [6]. One of them is *GAS6* and encodes a vitamin K-dependent protein (VKDP) of 75 kilodaltons

(kDa) characterized by post-translational γ-carboxylation of certain glutamic acid residues by a carboxylase, using vitamin K as cofactor. In mouse, *GAS6* mRNA (2.6 kb) is expressed by serum-starved embryonic fibroblast NIH3T3 cells. Its expression decreases in the presence of fetal calf serum or under basic fibroblast growth factor stimulation. It is located on chromosome 13 at q34. Human *Gas6* cloning and sequencing revealed a high degree of homology and a similar pattern of expression in IMR90 human fibroblasts [7]. Important tissues where *Gas6* is expressed are neuronal [8], hepatic [9] and renal tissues [10]. *Gas6* is also expressed in various cell types: endothelial cells [7], vascular smooth muscle cells [11], bone marrow (BM) cells [12] and platelets [13]. Gas6 concentration in human plasma ranges from 20 to 50 μg/L [14].

1.2.2 Gas6 structure

The murine cDNA sequence of *Gas6* is 2556 nucleotides long and encodes a protein of 673 amino acid residues. With 81% identity of amino acid residues, the human *GAS6* is 2461 nucleotides long and encodes a protein of 678 amino acids. As a multidomain protein, Gas6 is composed by 4 regions: (1) region A includes the amino terminus which contains a very conserved hydrophobic stretch typically resembling a signal peptide followed by a GLA domain formed by amino acids containing GLA that confers to VKDP the ability to bind to anionic phospholipids at the cell surface (residues 1 to 87); (2) region B comprises a loop maintained by disulfide bridges called the "thrombin sensitive region" (TSR) which, in Gas6, is not sensitive to thrombin (residues 88 to 115) followed by (3) region C formed by four epidermal growth factors domains (EGF), 2 of them contain calcium-binding consensus sequences (residues 116 to 276); (4) region D, also named C terminal domain, contains the sex hormone binding globular like domain (SHBG) (residues 277 to 673) [7]; this last region has 2 subdomains with a similar structure to the globular modules of laminin G (LamG) usually found in proteins interacting with heparin [15]. (Fig 1)

Fig.1: Structure of growth arrest-specific gene 6, a multidomain vitamin K dependent protein composed by 4 regions. Region A includes the amino terminus followed by a gamma-carboxyglutamic acid domain formed by amino acids containing gamma-carboxyglutamic acid (GLA residues 1 to 87 in green). Region B comprises a loop maintained by disulfide bridges (residues 88 to 115 in blue). Region C is formed by 4 epidermal growth factors (EGF) like domains, 2 of them containing calcium-binding consensus sequences (residues 116 to 276 in light blue). Region D (C terminal) contains sex hormone binding globular (SHBG)-like domain (residues 277 to 673 in brown). This last region has 2 subdomains with a similar structure to the globular modules laminin G (LamG).

1.2.3 Protein S identification

Protein S (PS) with the S referring to Seattle, the city where this protein was purified for the first time in 1977 from human plasma as a protein with properties comparable to prothrombin (PT), factor IX (FIX) and factor X (FX) [16]. PS, a natural anticoagulant, is a VKDP of 70.69 kDa mainly synthetized by liver parenchymal cells [17], vascular endothelial cells [18], testicular Leydig cells, macrophages [19] and megakaryocytes [20]. PS circulates in human plasma at a higher concentration than Gas6 (Gas6: 20 to 50 µg/L, PS: 350 nanomolar (nM) corresponding to 25 mg/L). Sixty percent of circulating PS form a complex with C4b-binding protein (C4BP), a protein involved in the complement system. The remaining 40% circulate in free form [20, 21]. In human, two PS genes were described: *PROS1* gene, which expressed PS and *PROSP* as a pseudogene. Both are located on chromosome 3 at q11.2.

1.2.4 Protein S structure

PROS1 gene is 80 kb long and encodes a protein of 676 amino acid residues organized in a single-chain glycoprotein [20]. PS has high structural homology (~42%) with Gas6 and the modular composition is the same. However, unlike the TSR in Gas6 (disulfide bridged thumb loop), PS TSR is sensitive to cleavage action of serine proteases [7]. The multiple domains of PS are organized as following: (1) region A which contains N terminus with a 24 amino acids peptide (residues 1 to 41), followed by GLA domain required for the binding to negatively charged phospholipids (residues 42 to 86) [22]; (2) region B contains the TSR susceptible to thrombin cleavage by thrombin and activated FX (FXa); the PS anticoagulant activity is suppressed by the removal of this region [23] (residues 87 to 113); (3) in region C, four EGF-like domains in tandem are responsible for calcium binding (residues 114 to 283); (4) like in Gas6, region D or C terminus contains SHBG domain composed by two LamG known to be determinants of the PS half life and mutations [24]. Interestingly and unlike Gas6, these LamG are involved in the binding of PS to C4BP (residues 284 to 676) [21]. (Fig 2)
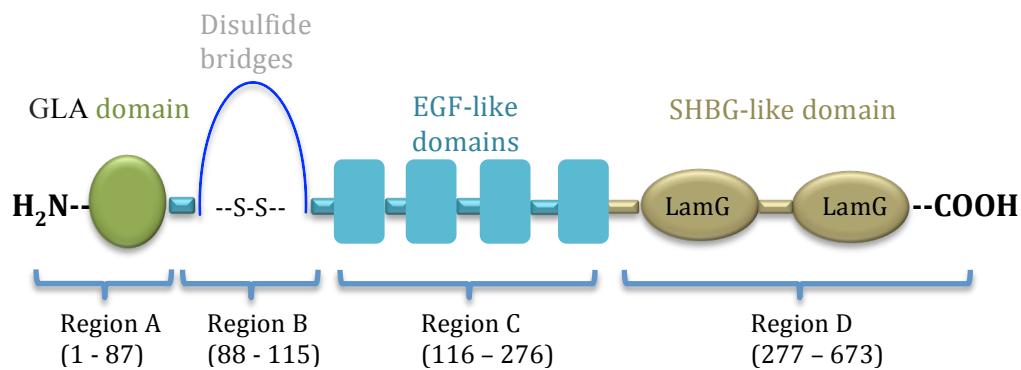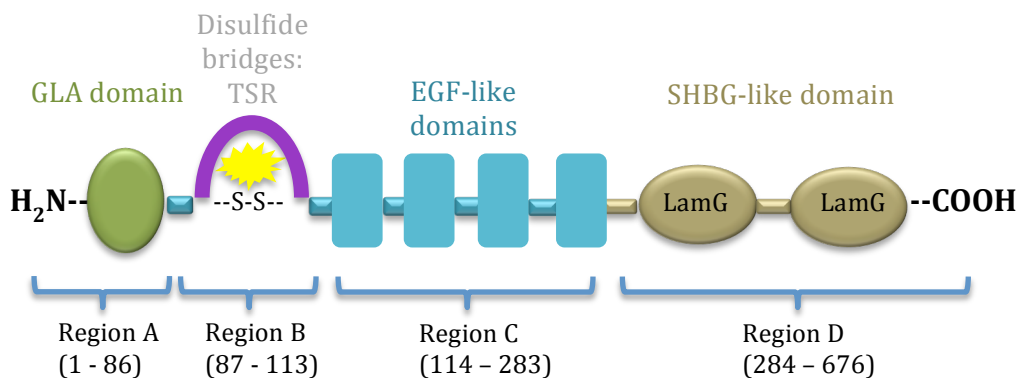

Fig.2: Structure of protein S, a multidomain vitamin K-dependent protein comprising 4 regions. Region A includes the amino terminus (N terminus) with a 24 amino acids peptide followed by a gamma-carboxyglutamic acid domain (GLA, residues 1 to 86 in green). Region B consists in a loop maintained by disulfide bridges that contains the thrombin sensitive region (TSR) susceptible to thrombin cleavage by thrombin and factor Xa (residues 87 to 113 in purple). Region C is formed by 4 epidermal growth factors (EGF)-like domains in tandem responsible for calcium binding (residues 114

to 283 in blue). The last region (C terminus) contains the sex hormone binding globular (SHBG)-like domain composed by two laminin G (LamG) involved in the binding of protein S to C4b-binding protein (residues 284 to 676 in brown).

1.2.5 TAM receptors identification

The name of the TAM receptors is derived from the first letter of its three constituents: Tyro3, Axl and Mer). They were discovered over the two last decades [25] as transmembrane RTKs and revealed incredible insights into the biology of many diseases.

The cloning of full length *Tyro3* was performed and named developmental tyrosine kinase (*Dkt*) with regard to its expression during the differentiation of murine stem cells [26]. Shortly after, 5 groups reported the cloning of *Tyro3* and referred to it as brain tyrosine kinase (*Brt*) [27], Sea related tyrosine kinase (*Sky*) [28] and receptor sectatoris (*Rse*) [29]. It was also named TIF for tyrosine kinase with immunoglobulin and fibronectin type III domains [30] for its expression in ovaries and testes, and finally Tyro3 due to its expression in mammalian central nervous system [31]. In human, it is located on chromosome 15 at q15.1. Its protein contains 890 amino acids with sizes from 100 to 140 kDa [32]. Tyro3 is most abundantly expressed in the nervous system [31] and is also found in ovary, testis, breast, lung, kidney, osteoclasts [33], retina [34], platelets [13] as well as in a number of hematopoietic cell lines including megakaryocytes, monocytes and macrophages cell lines [29].

Axl gene was named in reference to the Greek term *anexelekto* (uncontrolled) due to the abnormal cell growth in its presence. It is located on human chromosome 19 at q13.2 and encodes a protein of 894 amino acids with a molecular weight of 104 kDa. Axl expression was detected in most human cells: fibroblasts, epithelial, mesenchymal, hematopoietic cells [35] and platelets [13] suggesting an important cellular function for this receptor. It was also named *Ufo* referring to a not yet defined gene function [36] and lately named adhesion related kinase (*Ark*) based on the presence of domains of neuronal cell adhesion molecules [37].

The *Mer* gene was discovered for the first time as a viral oncogene (*v-Ryk*). Shortly after, its cellular equivalent (*c-Eyk)* was described in chicken embryonic and spleen tissue [38]. Therefore, the human *Mer* gene (*MERTK)* whose name is derived from monocytes, epithelial and reproductive tissues was cloned. *MERTK* is located on chromosome 2 at q14.1. It encodes a 999 amino acids protein with a predicted molecular weight of approximately 110 kDa, the extracellular domain of Mer possesses sites for NH2-linked glycosylation and the mature fully glycosylated form of Mer is approximately 205 [39]. It is widely expressed in tissues: testes, ovary, prostate, lung, retina and kidney. Mer is also expressed in a spectrum of cell lines of hematopoietic, epithelial and mesenchymal origin [40].

1.2.6 TAM receptors structure

In comparison to all other RTKs ectodomains where two structural modules are used repeatedly, the three TAM receptors have a different configuration of two plus two combinations. The TAM RTKs family shares structural similarities. Indeed, the amino terminal regions carry tandem immunoglobulin-related domains necessary for ligand binding. Gas6 and PS were described as the only ligands able to bind to and activate the TAM receptors [41]. This tandem is followed by tandem of fibronectin type III repeats, which are characteristic of adhesion molecules. All three TAM receptors have a single pass transmembrane domain carrying a catalytically competent protein tyrosine kinase. In many cells, the activation of this tyrosine kinase is coupled to the downstream activation of the phosphoinositide 3 kinase (PI3K)/AKT pathway [42].
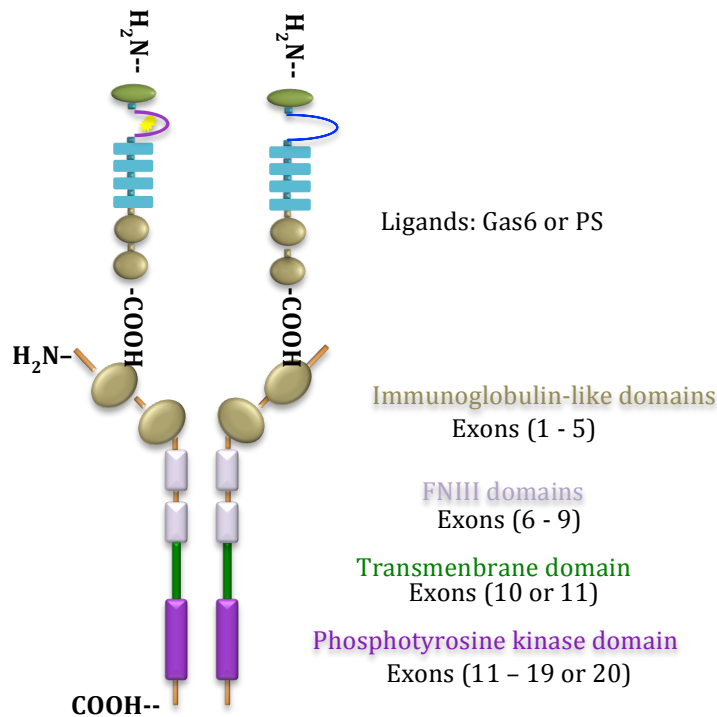
Fig.3: Structure of Tyro3, Axl and Mer receptor tyrosine kinases. The extracellular domain (N terminus) is composed by 2-immunoglobulin-like domains (residues from 1 to 5 in brown) followed by 2 fibronectin type III domains (residues from 6 to 9 in grey). The transmembrane domain is encoded by exon 10 for Tyro3 and Mer receptors and by exon 11 for Axl (in green). The cytosolic C terminus is responsible for downstream activation of Tyro3, Axl and Mer by either Gas6 or protein S (residues 11 to 19 for Tyro3 and Mer, and 12 to 20 for Axl in purple).

1.3 Gas6 and protein S roles

1.3.1 Gas6 in hemostasis

Gas6 binds to and activates the TAM RTKs with a highest affinity for Axl followed by Tyro3 and Mer [43]. This binding leads to further intracellular signaling including activation of PI3K and Akt pathways [44, 45] leading to many cellular effects.

1.3.1.1 Thrombosis and hemostasis

The generation of a murine model with complete *Gas6* deficiency (*Gas6$^{-/-}$*) provides great insights regarding the role of Gas6 in thrombosis and hemostasis. *Gas6* gene was targeted by deleting the transcription start site, the translation initiation codon, the signal peptide and the

GLA module [13]. *Gas6*^{-/-} mice are viable and fertile, and have an apparent normal phenotype. They are born at the expected Mendelian frequency. They do not exhibit thrombocytopenia or any sign of coagulopathy. *Gas6*^{-/-} mice do not suffer from spontaneous bleeding or thrombosis but interestingly, when challenged with three different thrombosis models (ligation of the abdominal vena cava, photochemical denudation of the carotid artery to induce platelet and fibrin rich thrombus and intravenous injection of collagen and epinephrine to trigger platelet dependent thromboembolism), they appeared to be protected against venous and arterial thrombosis [13]. As platelets play a key role in venous and arterial thrombosis and express Gas6 and its receptors (TAM RTKS), their functions were then investigated in *Gas6*^{-/-} mice. In contrast to *WT* (*Gas6*^{+/+}) platelets, *Gas6*^{-/-} platelets fail to form tight and irreversible plugs in response to different stimuli (adenosine diphosphate, ADP: < 10 μM, collagen: 2 μg/ml or thromboxane A$_2$, TXA$_2$, analogue U46619: 10 μM). Because ADP secretion from platelet dense granules is essential for the formation of stable aggregates, significantly impaired *Gas6*^{-/-} platelet secretion was reported after stimulation with various agonists suggesting that the protection against thrombosis could be partly due to reduced ADP release from *Gas6*^{-/-} platelets. Moreover, the altered phenotype of *Gas6*^{-/-} platelets is completely restored by treatment with recombinant Gas6. According to a study of Angelillo-Scherrer et al.[46], The loss of any one of the TAM in mice causes rebleeding in a tail clipping model and protects mice against thrombosis. Even more, two thrombosis models dependent on coagulation and platelet activation or only on platelet (ligation of the inferior vena cava and intravenous injection of tissue thromboplastin, and intrajugular injection of collagen and epinephrine, respectively) revealed the protection of *Axl*^{-/-}, *Tyro3*^{-/-} and *Mer*^{-/-} mice from thrombosis *in vivo*.

It is known that the αIIbβ3 integrin plays a critical role in platelet aggregation. In the initial phase, activation of platelets by ADP, TXA$_2$ and thrombin leads to "inside-out" signaling via αIIbβ3, which is critical for the formation of an irreversible platelet plugs [47]. Interestingly, *in vitro* data revealed that *Gas6*^{-/-}, *Axl*^{-/-}, *Tyro3*^{-/-} and *Mer*^{-/-} platelets adhere and spread out less efficiently in fibrinogen/collagen coated surfaces and disaggregate more easily suggesting a

defect in "outside-in" signaling via αIIbβ3 [46, 48]. Taking into account that Gas6 stimulates tyrosine phosphorylation of β3 integrin, it was suggested that resistance of $Axl^{-/-}$, $Tyro3^{-/-}$ and $Mer^{-/-}$ mice to thrombosis challenges could be at least in part attributed to a defect of the "outside-in" signaling of platelet via αIIbβ3 and thereby the lack of the second wave of platelet aggregation and clot retraction [46].

In human, the major source of Gas6 is plasma with a plasma concentration of 20 μg/L *versus* only a concentration 1 μg/L for platelet extracts. Plasma-derived Gas6 contributes to the stabilization of platelet aggregate formation probably by maintaining αIIbβ3 in an active state. Interestingly, platelet activation using both recombinant human Gas6 (rhGas6) and ADP revealed a synergy of Gas6 and ADP in Akt phosphorylation. Consequently, Gas6 and its receptors cooperate in the activation of PI3K pathway to achieve persistent activation of αIIbβ3 and thrombus stabilization [48].

The strong antithrombotic phenotype of $Gas6^{-/-}$ mice could be due to the platelet aggregation defect but taking into account that Gas6 is also produced by endothelium (endothelial cells, ECs and vascular smooth cells, VSMCs) [7], Tijwa et al. [49] showed that Gas6 is also acting in endothelium by promoting P-selectin, a ligand for the platelet receptor PSLG-1, to reinforce the thrombus adhesion to the vascular wall. To determine the respective contribution of nonhematopoietic (vascular cells) and hematopoietic (platelet, leucocytes) Gas6, Robins et al. [50] used a BM transplantation strategy to generate mice with selective ablation of Gas6 in the nonhematopoietic or hematopoietic compartments. Smaller thrombus size were found in mice lacking Gas6 in one of these two compartments demonstrating that Gas6 from both hematopoietic and nonhematopoietic cells have equal contribution to venous thrombus formation. Furthermore, stimulation of $Gas6^{+/+}$ ECs by thrombin revealed higher expression levels of active tissue factor (TF), a protein involved in the initiation of coagulation. Interestingly, TF expression was blunted in $Gas6^{-/-}$ ECs. Because Axl is the major Gas6 receptor expressed by ECs [49], the Gas6/Axl pathway by which Gas6 promotes TF expression in ECs was then explored. Using siRNA mediated knockdown approach, Laurence et al. [51] demonstrated that Gas6 induces Axl and c-Src localization in lipid

raft/caveolin-1–enriched microdomains that is required for Akt and ERK1/2 phosphorylation. Thus, the activation of the c-Src/Akt/ERK1/2 signaling pathway by Gas6/Axl leads to higher expression of TF in ECs.

Several studies demonstrated that platelet-derived microparticles (PMPs) are produced upon platelet activation and have a high procoagulant effect. Indeed, PMPs membranes retain all properties of the activated platelet membrane and are able to bind components of procoagulant complexes such as FVa and FVIII. In this regards, Sinauridze et al. [52] reported that the addition of PMPs to platelet free recalcified plasma accelerates initiation of thrombin generation. It was also found that the PMPs surface was approximately 50 to 100 fold more procoagulant than the surface of activated platelets.

Notwithstanding their possible harmful properties, little is still known about PMPs clearance and effects in endothelium. Recently, Happonen et al. [53] showed that PMPs are ingested in primary human ECs in a Gas6 dependent manner. Indeed, purified human platelets were stimulated with a combination of thrombin and collagen to release PMPs, which exposed PtdSer, was phagocytized by primary human ECs in a Gas6/Axl dependent manner. Moreover, erythrocyte-derived MPs were found to be ingested in the same manner (see Chapter VII: Appendices).

The characterization of *Gas6*^{-/-} mice by Angelillo-Scherrer et al. [13] pointed to the absence of spontaneous bleeding or thrombosis in these mice suggesting that Gas6 could constitute an attractive target to explore in human VTE disease. Indeed, a study of Blostein et al. [54] revealed higher Gas6 levels in a cohort of 279 patients with VTE as compare to healthy volunteers patients demonstrating an association between VTE and Gas6 levels expression and consistent with *in vivo* murine finding. In addition, analysis of single nucleotide polymorphisms (SNPs) from a cohort of 188 stroke patients indicates statistically significant differences in the *Gas6* allelic distributions as compared to 110 healthy patients [55].
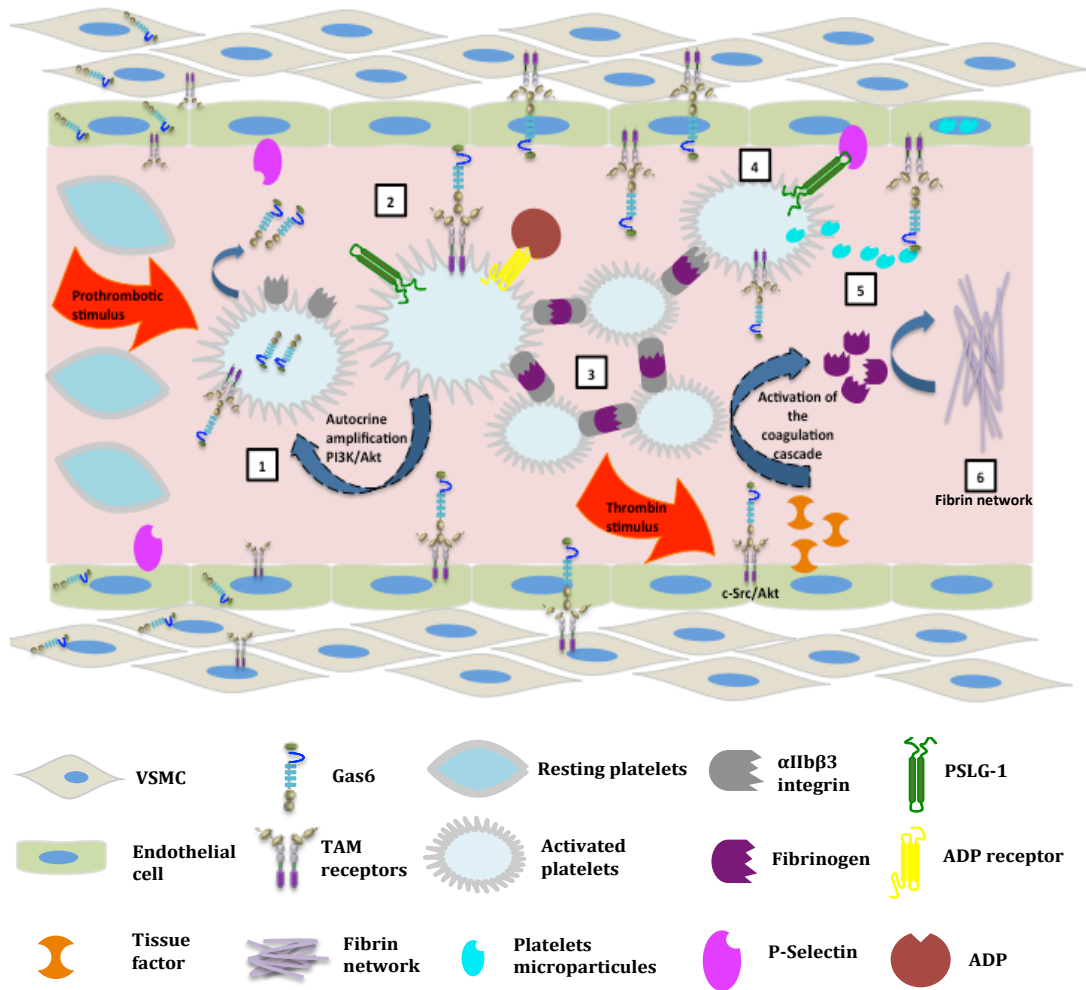
Fig.4: Six independent mechanisms of the role of Gas6 in thrombus formation and stabilization. 1. Upon a prothrombotic stimulus, activated platelet release Gas6 from their α granules. 2-3. Gas6 binding to TAM receptors perpetuates platelet aggregation and supports αIIbβ3 outside in signaling through paracrine amplification and PI3K/Akt pathway. Gas6 also exerts a synergistic effect with ADP on outside-in platelet signaling promoting further activation of αIIbβ3 that binds fibrinogen and leads to irreversible platelet aggregates. 4. Gas6 induces the expression of P-Selectin at the surface of endothelial cells and its binding to PSLG-1. 5. Activated platelet releases platelet microparticles, known to be 50 to 100 fold more procoagulant than the surface of activated platelet, that are ingested by endothelial cells in Gas6/Axl dependent manner. 6. Endothelial cells stimulation by thrombin leads to tissue factor (TF) release via Gas6/Axl/c-Src/Akt signaling and the initiation of the coagulation pathway resulting in formation of tight fibrin network.

1.3.1.2 Vasculature

The involvement of Gas6 in the vasculature was first described by Nakano et al. [11] in 1995 when they demonstrated the presence of Gas6 in rat VSMCs conditioned medium. Thus, a role for Gas6 in regulating VSMCs proliferation was addressed. Through their study, the calcium-dependent role of Gas6 suggested a potential dependent Gas6 response via its interaction with RTKs. Three years later, using a rat carotid balloon injury model, a well known model to study intracellular signal transduction through tyrosine kinase in VSMCs proliferation and migration, Melaragno et al. [56] found a time dependent Axl expression localized mainly in neointima after rat carotid injury. In addition, Gas6 was upregulated during this challenge indicating an increased activity of Gas6/Axl signaling. Furthermore, a great increase in Axl mRNA and protein levels were found in cultured VSMCs specifically treated with thrombin or angiotensin II (angII), a well characterized vasoactive agonist that binds to G protein coupled receptors. Few years later, the same group demonstrated that Axl phosphorylation upon Gas6 binding and PI3/Akt pathway activation in VSMCs leads to decreased apoptosis confirming the prominent role of Gas6/Axl signaling in vasculature maintenance [57]. Apoptosis is one of the important processes regulating VSMCs calcification but statins (lipid lowering drugs) inhibitory effect in vascular calcification is controversial. Thus clarification of the mechanism of vascular calcification via statin was awaited. Taking advantage of Gas6/Axl signaling new role in the vasculature, Son et al. [58] explored the effect of Gas6/Axl in VSMCs survival and proved that the restoration of Gas6/Axl signaling inhibits apoptosis in cultured human aortic smooth muscle cells and protected them from calcification.

Intima media thickening (IMT) is the measurement of the thickness of the two layers of the blood vessel walls: tunica intima and tunica media. It is a well-described procedure in vascular remodeling assessment after blood flow changes. ECs, VSMCs and inflammatory cells coordinate in their response during IMT. Due to its promising role in vasculature, Gas6/Axl signaling involvement in vascular remodeling initiated by flow changes was further assessed by Korshunov et al. [59]. They demonstrated that the lack of Axl leads to 30%

decrease in carotid intima, media and adventitia thickening. Moreover, in response to flow reduction, $Axl^{-/-}$ vessels display a high number of apoptotic cells as compared to $Axl^{+/+}$. The observed defects in $Axl^{-/-}$ vessels remodeling was Gas6/Axl/p-Akt dependent and further confirms the implication of Gas6/Axl pathway in vasculature.

The role of Gas6 in ECs survival and apoptosis was also studied by Healy et al. [60]. Indeed, Axl was found phosphorylated in pulmonary ECs and its phosphorylation was enhanced by the addition of exogenous Gas6. Moreover, Gas6 or Axl supplementation to growing pulmonary ECs revealed up to 54% less apoptotic cells demonstrating that Gas6/Axl signaling plays an important role in ECs survival.

Acidification (hypocarbia) condition protects ECs from apoptosis with a not well-defined mechanism. In this purpose, D'Acangelo et al. [61] evaluated survival and apoptosis of ECs in acidification setting. The study revealed that by activating Axl, Gas6 plays a key role in the acidification protective effect from apoptosis.

Endothelial progenitor cells (EPCs) play a key role in endothelium repair and vascular regeneration. Indeed, circulating EPCs accumulate at the site of tissue injury and contribute to maintain the integrity of the endothelial monolayer by replacing denuded areas of the artery [62]. In this regard, Zuo et al. [63] explored the influence of Gas6 in EPCs role in endothelium repair. They found that Gas6 treatment significantly increases EPCs proliferation and migration in a dose-dependent manner. Furthermore, the addition of a PI3K/Akt pathway inhibitor completely suppressed Gas6-related migration and proliferation effect on EPCs. Thus, Gas6 via PI3K/Akt signaling participates to EPCs vascular repair after injury.

Angiogenesis, the process of creating new blood vessels from pre-existing blood vessels, is induced by several growth factors such as vascular endothelial growth factor (VEGF), fibroblast growth factor (FGF), platelet-derived growth factor (PDGF) and insulin-like growth factor (IGF). Taking into account the relevance of the role of Gas6 in ECs proliferation and migration, Kim et al. [64] published a study where they investigated the probable implication of Gas6 neovascularization in the retina. Using human retinal microvascular endothelial cells (HRMECs), they demonstrated that Gas6 enhances

proliferation, migration and tube formation of HRMECs. Furthermore, two more angiogenesis models were assayed. In one hand, rat aortas explants sprouting vessels treated with rhGas6 were longer as compared to non-treated controls. In the other hand, neovascularization was examined in zebrafish and microinjected zebrafish embryos showed higher sub-intestinal vessels sprouting. In these three models, the extracellular signal-related kinase ERK1/2 pathway was involved highlighting a new Gas6/ERK1/2 signaling in vasculature.

The finding that ECs and VSMCs express Axl and secrete Gas6 suggests the possibility for an autocrine paracrine growth program involving both VSMCs and ECs.

Besides VSMCs and ECs, pericytes play a key role in local and systemic hemostasis and might undergo osteogenic differentiation to form mineralized nodules [65]. The mechanism that triggers this osteogenic differentiation of pericytes is not yet fully understood. To get further insights into this mechanism, Collet et al. [66] investigated the role of Axl in this process. Indeed, they demonstrated that pericytes express Gas6 and Axl and that Axl is greatly upregulated and phosphorylated along the osteogenic differentiation with the highest expression pic corresponding to cultured pericytes at confluency. Contradictory, Axl expression was highly decreased in pericytes forming mineralized nodules establishing a role of Gas6/Axl signaling in osteogenic differentiation of pericytes and vascular calcification.

It is well described that oxidative stress and reactive oxygen species (ROS) play a major role in remodeling vessels after injury. RTKs like FGF, PDGF or EGF are tyrosine phosphorylated by H_2O_2. Accordingly, Konishi et al. [67] reported that besides its activation by Gas6, Axl was also phosphorylated by H_2O_2 in VSMCs during carotid and femoral rat arteries injury. Furthermore, the addition of Axl-Fc (extracellular domain of Axl enabling neutralization of Gas6/Axl signaling) or warfarin (vitamin K antagonist that abolishes γ-carboxylation of Gas6) inhibits Axl phosphorylation demonstrating that H_2O_2 phosphorylation of Axl was Gas6-dependent. Finally, an increased Axl phosphorylation within injured arteries was found with reduced neointima formation in $Axl^{-/-}$ rat vessels after injury emphasizing the important role of Gas6/Axl in vasculature remodeling. To further clarify the mechanism by

which ROS enhance Gas6/Axl signaling in VSMCs, Cavet et al. [68] identified glutathiolated non muscle myosin heavy chain (MHC)-IIB, a well described protein in directed cells migration [69] and whose expression is upregulated in balloon injured carotid vessels [70], as a potential interacting protein which enhances Axl phosphorylation in response to Gas6 or ROS stimulation providing a direct link between Gas6/Axl signaling and cytoskeletal molecular motors, MHC-IIB.

Since VSMCs are one of the major cell types to consider when investigating aging and senescence in blood vessels and that Gas6 plays a major role in vascular remodeling, the implication of Gas6/Axl in vascular senescence process was studied by Jin et al. [71]. Using two cellular senescence models (replicative senescence by passaging VSMCs ten times or induced VSMCs senescence by treating the cells with AngII for 48h), they found that Gas6 stimulated cells exhibit a younger phenotype as compare to control cells. In addition, VSMCs treatment with either Axl specific inhibitor, FoxO3a (known as apoptosis trigger) small interfering RNA or PI3K inhibitor confirmed that Gas6 and Axl are involved in VSMCs senescence process via PI3K/Akt/FoxO signaling.

1.3.2 Gas6 in erythropoiesis

Erythropoiesis, from the Greek words 'erythro' meaning "red" and 'poiesis' meaning "to make", is the process of red blood cells (RBC) production. The constant renewal of RBC is crucial to ensure proper tissue oxygenation. Erythropoietin (EPO) was identified as a key factor in the regulation of the erythropoietic lineage [72]. Indeed, EPO binds to its receptor (EPOR) in the erythroid precursors inducing downstream signaling to promote differentiation, proliferation and anti-apoptotic processes. Across the mammalian development, the major EPO production sites shift from the liver to the kidneys along with the transition of hematopoietic tissues. In the fetal liver, hepatocytes produce EPO to support fetal liver erythropoiesis via paracrine signaling. Around birth, the erythropoiesis shift to the BM and renal EPO producing cells begin to secrete EPO [73]. Blood loss or reduced oxygen levels enhance renal and hepatic EPO secretion triggering erythropoiesis and normalizing the tissue

oxygen supply [74]. EPO also plays an important role in anemia resulting from insufficient production, excessive destruction or loss of RBC by inducing differentiation of hematopoietic stem cells to erythroblasts, which subsequently mature to RBC.

In this context, recombinant EPO (rEPO) is commonly used to treat anemia associated with several disease: myelodysplastic syndromes [75], cancer [76], chronic renal failure [77], chronic kidney diseases [78], chronic hepatitis C [79] and rheumatoid arthritis [80]. However, in many individuals, EPO treatment is not effective and patients remain hyporesponsive. The mechanism behind this refractory effect to rEPO treatment is not yet fully understood. Because Gas6 and TAM receptors are expressed in hematopoietic cells and BM stromal cells, Angelillo-Scherrer et al. [81] investigated whether Gas6 could influence erythropoiesis. Indeed by studying the liver of $Gas6^{-/-}$ embryos (the main erythropoietic site during embryogenesis), it was found that $Gas6^{-/-}$ embryo liver is reduced in size and contains less erythroblasts as compare to $Gas6^{+/+}$ embryos. Moreover, single cell suspension from E13.5 $Gas6^{-/-}$ fetal liver displays only half burst forming unit erythroid progenitors (BFU-Es) and colony forming unit erythroid progenitors (CFU-Es) as compared to $Gas6^{+/+}$. Supplementation with rGas6 restores the formation of BFU-Es and CFU-Es to the same level as in $Gas6^{+/+}$ confirming that Gas6 regulates erythroid precursors formation. The effect of the lack of Gas6 in adult mice erythropoiesis was also studied. Interestingly, $Gas6^{-/-}$ adult mice had normal hematocrit level and RBC counts without any sign of dysplasia. However, fewer reticulocytes were found in $Gas6^{-/-}$ mice essentially due to reduced erythroid progenitors reserve in BM. Further investigations of the reason behind the hematocrit levels preservation in $Gas6^{-/-}$ was elucidated by the RBC longer lifespan and impairment of their phagocytosis by macrophages. In addition, spleens from $Gas6^{-/-}$ weighed 20% less than $Gas6^{+/+}$ and spleen and BM cells flow cytometry revealed less erythroblasts as compare to $Gas6^{+/+}$.

To shed light whether the absence of Gas6 could impair response to anemia, $Gas6^{-/-}$ and $Gas6^{+/+}$ mice were challenged with two acute anemia models. In the first model, two intraperitonial injections of phenylhydrazine (PHZ) were performed to trigger rapid hemolysis. Consequently, $Gas6^{-/-}$ mice erythropoietic response and recovery from hemolytic

anemia was delayed as shown by their low level of hematocrit and RBC count. In the second model, anti mouse RBC antibody was used to induce immune hemolytic anemia. As in the first model, $Gas6^{-/-}$ mice were not able to achieve a normal hematocrit after the challenge. Even more, when treated with a more severe acute anemia challenge (three PHZ injections), most of $Gas6^{-/-}$ mice succumbed confirming a protective effect of Gas6 against life threatening acute anemia.

To examine which TAM receptor mediates Gas6 effect on erythropoiesis, erythroblasts were screened for TAM expression. Indeed, in resting condition or after EPO stimulation, erythroblasts express Axl, Tyro3 and Mer at mRNA and protein levels. Moreover, it was found that Axl mediates the major role of Gas6 in erythropoiesis as shown by the more dramatic response of $Axl^{-/-}$ to acute anemia in comparison to $Gas6^{-/-}$ mice.

Cultured $Gas6^{-/-}$ erythroblasts showed improved survival upon EPO stimulation but did not achieve $Gas6^{+/+}$ erythroblasts survival level. Interestingly, addition of rGas6 together with EPO enhances $Gas6^{-/-}$ erythroblasts survival response. Thus, alone or by synergizing with EPO, Gas6 plays an important role in erythroblasts survival.

Because erythroblasts adhesion to fibronectin is crucial for their proliferation and expansion, $Gas6^{-/-}$ erythroblasts adherence was evaluated. Remarkably, few $Gas6^{-/-}$ erythroblasts are able to correctly adhere to fibronectin and addition of rGas6 completely restores this process indicating that Gas6 is necessary for erythroblasts adherence and differentiation. To further investigate by which mechanism Gas6 acts in erythroblasts adherence and survival process, activation of PI3K/Akt and VLA4 (a fibronectin receptor) were assessed using a PI3K inhibitor and an antibody directed against anti-VLA4. Interestingly, it has been found that Gas6 enhances PI3K and VLA4 activation and that Gas6 synergizes with EPOR to activate Akt survival pathway.

Taking into account that erythroblasts maturate and differentiate within the erythroblastic islands (constituted by a central macrophage surrounded by immature erythroblasts) and that macrophages secrete erythroid inhibitory factors [82], Angelillo-Scherrer et al. investigated whether, in addition to its autocrine effect on erythroblasts, Gas6 could act in a paracrine

manner by influencing the release of the erythroid inhibitory factors from macrophages in the erythroblastic islands. Indeed, it was found that in the absence of Gas6, high levels of erythropoietic inhibitory cytokines are present indicating that Gas6 also regulates erythropoiesis via a paracrine effect.

Considering their new results regarding the autocrine and paracrine effects of Gas6 on erythropoiesis, Angelillo-Scherrer et al. [81] examined whether rGas6 treatment could be relevant in improving $Gas6^{+/+}$ mice response in acute anemia setting. Thus, in three different anemia models (PHZ induced hemolytic anemia, blood loss induced anemia and EPO resistance induced chronic anemia), the therapeutic use of rGas6, like EPO, displays a positive effect on erythropoiesis. To get further insights into the role of TAM receptors in erythropoiesis, another study from Tang et al. [83] confirmed Axl and Mer expression in all stages of developing erythroid cells: erythroid progenitors (R1), proerythroblasts (R2), basophilic erythroblasts (R3), polychromatophilic erythroblasts (R4) and orthochromatophilic erythroblasts (R5). Interestingly, $Axl^{-/-}Mer^{-/-}$ BM and spleen cells analysis by flow cytometry displayed higher R1 and reduced R3/R4 ratios as compare to WT indicating an inhibition of the erythropoietic differentiation process. Moreover, $Axl^{-/-}Mer^{-/-}$ mice are not able to correctly recover after hemolytic anemia challenge. To investigate the molecular mechanism related to the erythropoietic defect in $Axl^{-/-}Mer^{-/-}$ mice, GATA-1 (an important transcription factor in erythropoiesis) and EPOR mRNA from BM and spleen R1 progenitors were screened. Indeed, GATA-1 and EPOR transcripts are diminished in $Axl^{-/-}Mer^{-/-}$ progenitors underlining that Axl and Mer might influence erythropoiesis by regulating the expression of GATA-1 and EPOR.

EPO resistance is a risk factor for cardiovascular diseases, stroke and mortality, which are associated with treatment with high dose EPO and inability to achieve correct response to anemia. An efficient treatment for anemic patients hyporesponsive to EPO is than awaited. To mimic this clinical situation, $Gas6^{-/-}$ and Epo-TAg^{H} mice, both models with refractory response to EPO (due to EPO resistance or EPO insufficiency respectively) were co-treated with rGas6 and EPO. Strikingly, this preclinical model showed that rGas6 increased the

therapeutic activity of EPO. This last finding highlight that the use of rGas6 in association with EPO could be beneficial for patients presenting EPO resistance [81].
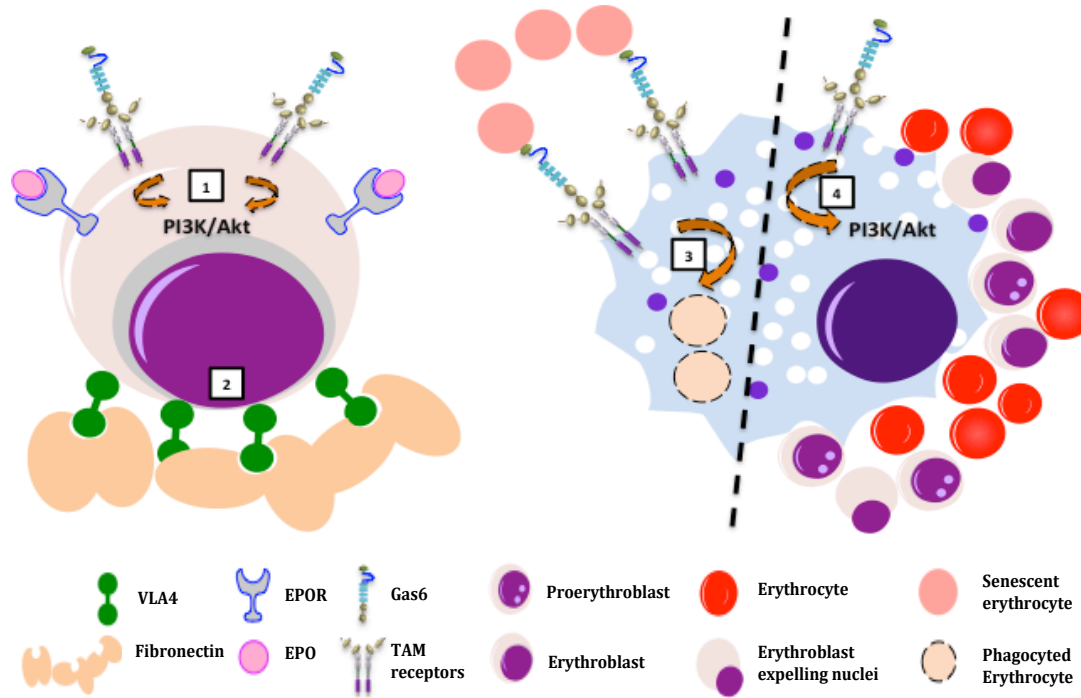
Fig.5: Representation of Gas6 mechanisms in erythropoiesis. 1. Upon EPO stimuli, erythroblasts release Gas6 that bind to its TAM receptors on the cell surface. This binding leads to activation of PI3K/Akt pathway and downstream signaling for cell proliferation and differentiation. Besides, Gas6 acts in an autocrine manner by boosting the EPOR stimulation. 2. The binding of Gas6 to TAM receptors activates the fibronectin receptor VLA4 and increases erythroblasts adhesion and differentiation. 3. Gas6 plays a key role in senescent erythrocyte phagocytosis by macrophages. It operates as a bridge between senescent erythrocyte and Gas6 receptors, thus facilitating their engulfment. 4. Erythropoietic island formed by a central macrophage surrounded by developing erythroid cells: proerythroblasts, erythroblasts, mature erythrocytes. Upon the binding of the TAM receptors to their agonist Gas6 in the macrophages surface, PI3K/Akt pathway is activated and erythroid inhibitory factors are released, thus leading to cell survival and antiapoptotic effect.

1.3.3 Protein S in hemostasis

As mentioned in paragraph 1.2.3, in human, 40% of PS circulates in a free form and the remaining 60% form a complex with C4BP. This 40% free PS, either by binding to TAM

receptors or exerting direct or indirect anticoagulant functions, have an important role in hemostasis.

1.3.3.1 Thrombosis

The first clinical observation describing severe recurrent venous thromboembolic (VTE) due to PS deficiency was made in 1984. Indeed, three family members receiving oral anticoagulant therapy and displaying normal ranges of all other proteins known to play a role in VTE diseases (protein C, antithrombin, fibrinogen and plasminogen), exhibited a half normal PS levels due to inherited *PROS1* deficiency [84]. The prevalence of PS deficiency is estimated from 0.16% to 0.21% and augments to 2% in patients with VTE [85, 86]. Interestingly, 22% of Japanese patients suffering from VTE exhibit *PROS1* mutations [87]. The $PS_{Tokushima}$ (K155E), a polymorphism of *PROS1*, exists in about 2% of the Japanese population [88]. In addition, 36% of Chinese patients with VTE have diminished PS activity levels. Factors that could influence this discrepancy are racial differences and the variance of the diagnostic tests regarding the detection of PS deficiency. Interestingly, a recent study, the multiple environmental and genetic assessment of risk factor for venous thrombosis (MEGA) highlighted that PS deficiency might be less common than previously described. In addition, it was found that PS deficiency (free PS < 53 U/dL and total PS < 68 U/dL) was not associated with VTE. Nonetheless, when lower cut-off values were applied, subjects at risk of VTE could be identified with free PS levels <33 U/dL. Paradoxically, very low levels of total PS were not associated with VTE. Furthermore, *PROS1* gene was sequenced in 48 subjects with decreased free PS levels (<46 U/dL) and copy number variations were investigated in 2718 subjects with free or total PS < 2.5th percentile. Strikingly, mutations were observed in 5 patients and 5 controls supporting the observation that inherited PS deficiency is rare in the general population. Thus, PS measurement and *PROS1* sequencing should carefully interpreted in unselected patients with VTE [89].

PS deficiency might also be acquired. Thus, Vitamin K antagonist therapy, oral

contraceptives, pregnancy, liver diseases, nephritic syndrome, disseminated intravascular coagulation (DIC) and chronic infections (like HIV) might provoke PS deficiency [90]. Acquired PS deficiency was also described as a rare complication of varicella zoster infection with development of crossreacting autoantibodies to the virus and PS [91].

In clinic, patients with hereditary PS deficiency mostly suffer from VTE. Ordinarily, the thromboembolic events could be caused by transient risk factors for VTE like surgery, trauma, immobilization, air travel, pregnancy or systemic hormonal contraception but strikingly, half of the thromboembolic events in PS deficient patients are unprovoked and these patients become symptomatic around 55 years old. Interestingly, a study from Brouwer et al. [92] revealed a nine-fold higher risk for VTE in patients with PS deficiency as compared to non-deficient patients. An additional report from Lejfering et al. [93] revealed that in thrombophilic families, free PS level could identify young subjects at risk for venous thrombosis, although the cut-off level lies far below the normal range in healthy volunteers.

Up to now, the raison behind why some PS deficient patients develop VTE while others remain unaffected is not completely explained [94]. Homozygous or compound heterozygous *PROS1* deficiencies are extremely rare with presentation soon after birth with extensive DIC and skin necrosis named purpura fulminans (PF) and death occurs within hours if untreated. (PS deficiency induced PF will be discussed in paragraph 1.3.4). Up to date, three PS deficiency types are known (Table 1).

Type of PS deficiency	Characteristics
Type I	Decreased activated protein C activity, decreased total and free PS
Type II	Decreased activated protein C activity, normal total and free PS
Type III	Decreased activated protein C activity, normal total PS and decreased free PS

Table 1: Types of protein S (PS) deficiencies.

A murine model recapitulating phenotypes of PS deficiency in human was described by Saller et al. [95]. Thus, heterozygous mice *(Pros1$^{+/-}$)* did not suffer from spontaneous thrombosis and displayed reduced PS plasma levels. They also exhibit a thrombotic phenotype *in vivo* when challenged in a TF-induced thromboembolism model. As in human, homozygous mice *(Pros1$^{-/-}$)* died *in utero* from intracranial hemorrhages and PF. One year later, another study from Burstyn et al. [96] confirmed embryonic lethality of *Pros1$^{-/-}$* mice with macroscopic blood clots and fulminant hemorrhages. In addition, plasma from *Pros1$^{+/-}$* heterozygous mice exhibited accelerated thrombin generation independent of activated protein C (APC).

1.3.3.1.1 Protein S activated protein C cofactor activity

APC plays a central role in reducing thrombin generation resulting from the sequential and rapid blood coagulation cascade steps: initiation, propagation, termination and degradation. APC has the ability to degrade the activated cofactors of the coagulation cascade: factor Va (FVa) and factor VIIIa (FVIIIa) [97] (Fig.5). The PS APC cofactor activity was described for the first time by Walker in 1980 [98]. He found that the rapidity of the inactivation of FVa by APC was increased approximately ten fold when he added plasma while an equal volume of APC-depleted plasma had no effect in FVa activity. Consequently, he assumed that in plasma, PS could be a factor that might alter the activity of APC. Few years later, Rising et al. [97] described that the presence of PS with APC accelerates twenty fold the FVa inactivation specifically by enhancing the Arg^{306} cleavage.

The ability of PS to act as APC cofactor was strictly attributed to free circulating form of PS until Maurissen et al. [99] demonstrated that PS bound to C4BP could also efficiently reduce six to eight fold FVa inactivation as compared with free PS.

The APC cofactor activity of PS was further investigated by Shen et al. [100]. Strikingly, in a purified system, they found that in the presence of both FV and PS, APC enhances the inhibition of FVIIIa activity. Moreover, APC alone or together with FV was ineffective while the combination of FV, PS and APC was more efficient in FVIIIa proteolytic inactivation.

As mentioned before, PS is a multidomain protein with GLA, TSR, EGF and LamG domain. It was demonstrated that APC interacts with PS through its EGF and GLA domains [101].
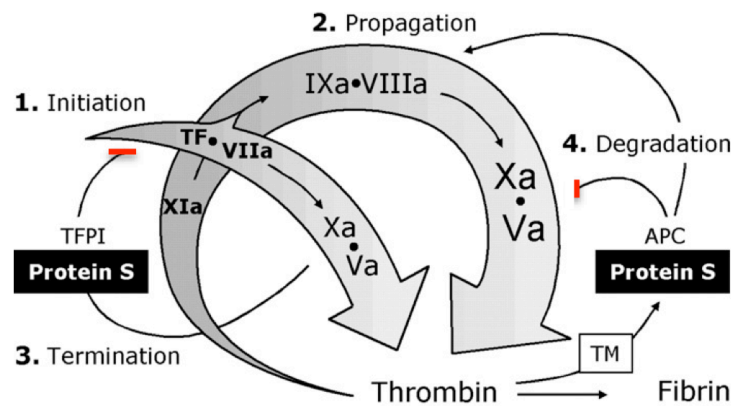

Fig.6: Scheme illustrating protein S (PS) dependent anticoagulant pathways of blood coagulation. Exposed tissue factor (TF) binds to activated factor VII (VIIa) and generate TF/VIIa transient complex known as the physiological initiator of blood coagulation (1). Subsequently, TF/VIIa activates factor X (X), and activated factor X (Xa) binds to its cofactor activated factor V (Va) on negatively charged phospholipid surfaces to generate the prothrombinase complex. Initial generated thrombin will activate cofactors V and VIII and further triggers factor XI (XI) activation from the propagation phase (2). Activated factor IX (IXa) and its cofactor activated factor VIII (VIIIa) accumulate on negatively charged phospholipids and activate additional factor X (X) to form sufficient thrombin and produce insoluble fibrin polymers. PS exerts 2 feedback mechanisms to tightly regulate thrombin generation: primarily, tissue factor pathway inhibitor (TFPI)/PS pathway inactivates FXa and subsequently shuts down TF/VIIa (3). Secondly, thrombomodulin (TM)-bound thrombin activates protein C, after which the activated protein C (APC)/PS pathway inactivates Va and VIIIa (4). Both PS dependent pathways limit thrombin generation during the initiation and propagation phases of coagulation. Adapted from Hackeng et al. [102].

1.3.3.1.2 Protein S tissue factor pathway inhibitor cofactor activity

TFPI is a Kunitz-type serine protease inhibitor, mainly synthetized by ECs, which abolish the formation of the complex TF/FVIIa through two steps feedback mechanism. The first one is the formation of FXa/TFPI complex and the second one is via the interaction of FXa/TFPI

with TF/FVIIa leading to the formation of an inactive quaternary complex and resulting in termination of TF/FVIIa catalyzed FX activation (fig6).

In 2006, an additional anticoagulant cofactor role was attributed to PS. Indeed, Hackeng et al. made two interesting observations. In one hand, PS does not inhibit thrombin generation in TFPI deficient plasma and in the other hand; the inhibitory effect of TFPI in thrombin generation was reduced in the absence of PS. They then conclude that PS might act as a cofactor of TFPI in the inhibition of TF/FVIIa catalyzed FX activation. Furthermore, it has been found that the stimulatory effect of PS on FXa inhibition by TFPI is caused by a ten fold reduction of the dissociation constant (Ki) of the FXa/TFPI complex, which diminished from 4.4 nM in the absence of PS to 0.5 nM in the presence of PS. To further investigate how PS interact with TFPI, a truncated TFPI (a form of TFPI that lacks the Kunitz-3 domain and the C terminus) was used and in this setting where PS failed to inhibit FXa. Thus, it was concluded that PS directly interacts with the kunitz 3 (K3) domain of full length TFPI [103]. Few years later, Ndonwi et al. [104] confirmed the interaction of PS specifically with K3 domain of TFPI.

The co-localization and dynamic interaction between PS and TFPI was further investigated in clinic. Thus, the effect of PS type I deficiency in TFPI plasmatic levels was evaluated by Castoldi et al. in a patient's cohort [105]. Indeed, full-length TFPI levels were lower in PS type I deficient individuals than in controls. Among these PS deficient individuals with thrombosis and under oral anticoagulant treatments, not only decreased total PS levels were found but also lower full-length TFPI levels. In addition, oral contraceptive users had reduced PS and full-length TFPI levels than non-users. Furthermore, plasma from PS deficient individuals displayed three to five folds more thrombin generation than control plasma after TF stimuli. Interestingly, the difference was only partially corrected by normalization of the PS level, full correction was only archived when TFPI levels were normalized. Additionally, it was found that free PS and full length TFPI form a complex in plasma. The conclusion of

this interesting study is that full length TFPI binds to PS in plasma and consequently is reduced in genetic and acquired PS deficiency and that probably TFPI deficiency could contributes to the hypercoagulable state associated with PS deficiency.

1.3.3.1.3 Protein S direct anticoagulant activity

The first evidence that PS could exhibit direct anticoagulant functions was established by Mitchell *et al.* in 1988 [106]. They developed a monoclonal antibody to PS and used it for PS purification. This purified PS, although identical to the conventionally purified protein as judged by SDS-PAGE, had significant anticoagulant activity in the absence of APC when measured using a FXa recalcification time method.

Another investigation from Heeb et al. [107] regarding PS direct anticoagulant action revealed that at 33 nM, PS inhibited 50% of FXa activity in an independent manner from phospholipid. This inhibitory effect was 1.6 times higher with the addition of Ca+ ions. Besides, the inhibition of prothrombinase activity by PS was 2.3 fold higher in the presence of FVa, with 50% inhibition when PS was added at 8 nM, thus demonstrating that PS, independently of APC, involves direct binding to FXa and FVa and direct inhibition of FXa. It was also reported that PS direct inhibitory effect on prothrombinase complex on endothelial and platelet surfaces could be influenced by either PS binding with C4BP or thrombin cleavage of PS [108].

The diversity of PS purification processes might have an impact on PS anticoagulant activity. In this regard, Seré et al. studied the association between the APC independent activity of PS and its phospholipid binding properties to clarify the variation in APC independent anticoagulant activity between different PS preparations. They found that 5% of total PS form multimers with hundred fold higher APC independent anticoagulant activity than the rest of PS. Furthermore, It was shown that the capacity of PS to inhibit prothrombin activation correlated with the content of multimeric PS. As this multimeric PS could not be identified in normal human plasma, it was suggested that this form of PS plays a key role in the APC

independent anticoagulant activity of PS. However, another study from Heeb et al. [109] showed that PS still has direct anticoagulant activity also in PS monomeric form. Even challenging because of their low concentration and association with the high concentration of other proteins, PS multimers were found in human plasma with comparable PS direct anticoagulant capacity.

The same group reported later that PS contains Zn^{2+} that is essential for PS direct anticoagulant activity but is lost during certain purification procedures. For example, immunoaffinity purified PS contains 1.4 ± 0.6 Zn^{2+}/mol when MonoQ purified and commercial PS contains 0.15 ± 0.15 Zn^{2+}/mol. Indeed, by isolating PS excluding ion chelators from the purification steps, they obtained Zn^{2+} containing PS that have about ten fold higher direct prothrombinase activity than the conventionally purified PS, and binds to FXa with 16 fold greater affinity. Moreover, it was revealed that the content of Zn^{2+} correlated positively with PS direct anticoagulant function in prothrombinase and clotting assays. Thus, Zn^{2+} is required for PS direct anticoagulant and this may explain the discrepancy regarding the validity of PS direct anticoagulant effect [110].

Platelets contain about 2.5% of all the PS content that is released upon platelets activation. Stavenuiter et al. [111] showed that platelets derived PS have higher direct anticoagulant effect than plasmatic PS containing Zn^{2+}, and much greater than Zn^{2+} deficient PS. Thus, platelets derived PS abolish both prothrombinase and extrinsic FXase activities. Furthermore, neutralizing antibodies against APC and TFPI have no effect on the PS direct anticoagulant effect on platelets highlighting that platelets derived PS may be essential to counterbalance procoagulant activities on platelets.

1.3.3.2 Vasculature

The first report establishing that PS have a potent mitogen effect was published by Gasic et al. in 1992 [112]. They observed that DNA synthesis was four fold higher in cultured rat

aortic SMCs treated with PS (10-50nM). This PS-related mitogenic effect was different for the free form of PS and the PS in complex with C4BP. Interestingly, PS mitogenic effect was direct without the induction of any transcription factor. Another study from Benzakour et al. [113] confirmed that PS was able to support human VSMCs growth and division. Strikingly, this investigation reported the presence of specific binding sites for PS on the surface of human VSMCs. This binding was found to be saturable and reversible.

As described before in paragraph 1.3.3.1, *Pros1*^{-/-} mice died *in utero* from DIC and PF. To investigate whether these clinical manifestations are due to the extensive thrombosis (caused by the lack of PS related anticoagulant activity) or secondary to lack of PS activity in endothelium, Burstyn et al. [96] investigated *Pros1*^{-/-} embryos at day 13.5 post coitum (E13.5) for vessels development abnormalities and functions. Indeed, immunostaining with antibody against α-smooth muscle actin (α-SMA), a VSMCs marker, revealed reduced and dispersed staining in *Pros1*^{-/-} embryos vessel walls. Co-immunostaining with an anti-vascular endothelial cadherin (VE-cadherin) antibody revealed reduced and fused expression of these markers in *Pros1*^{-/-} embryos as compared to controls. Moreover, E15.5 *Pros1*^{-/-} embryos spinal cord microvasculature staining with ECs adhesion protein 1 (PECAM-1) and fibrin, the major constituent of blood clots, indicated a considerable reduction in PECAM-1 signal in poorly formed microvessels associated with intravascular thrombosis. Defects in vessel development were also observed in *Pros1*^{-/-} embryo's yolk sacs and brain. Furthermore, the vascular networks hierarchy and morphology was 40% reduced in *Pros1*^{-/-} embryo's vasculature. Additionally, adult *Pros1*^{+/-} vessels were investigated by vascular dye extravasation. Indeed, Evans blue (EB), EB normally bound albumin and is confined to the circulation and does not leak into tissue parenchyma, was injected in *Pros1*^{+/-} tail vein. Contradictory to *WT* controls, *Pros1*^{+/-} mice displayed externally visible signs of dye extravasation into multiple organs including the gastrointestinal tract, ears, nose pad, paws, subcutaneous fascia, and brain.

Dye extravasation was measured in tissues of mouse lines with Cre driver lines designed to eliminate PS expression specifically in two different cell lineages. *Pros1*^{fl/fl}*/Tie2-Cre* mice in which PS expression is eliminated from ECs and hematopoietic lineage cells and

Pros1^{fl/fl}/Sm22-Cre mice, in which PS is eliminated from VSMCs. Interestingly, no significant difference in dye extravasation between *WT* and *Pros1^{fl/fl}/Tie2-Cre* mice. However increased EB permeation into the liver parenchyma was observed in *Pros1^{fl/fl}/Sm22*. Finally, although these results are very compelling, one question remains: is the defective vascular integrity in *Pros1^{+/−}* mice secondary to thrombosis development and perturbed blood flow during vascular development or is a direct consequence of the loss of PS dependent TAM receptor signaling or both?

A cytoprotective role was previously attributed to PS by Liu et al. [114]. Indeed, intravenous injection of 0.2 to 2 mg/kg PS to mice prior stroke challenge improved the motor neurological deficit up to 3.8 fold, reduced infarction and edema volumes up to 62%, improved post ischemic cerebral blood flow by 26% and reduced brain fibrin deposition and infiltration with neutrophils by 53%. In cultured ischemic neurons, PS displayed a protective effect from hypoxia/reoxygenation-induced apoptosis in a time and dose dependent manner. The PS cytoprotective function was further confirmed by Zhu et al. [115] using a human brain endothelial cells to study the tightness and permeability of blood brain barrier (BBB), they established that PS inhibits oxygen/glucose lack induced BBB collapse and reduced the permeability of ECs to dextran (hydrophilic polysaccharides most commonly used in vascular permeability evaluation). Interestingly, the PS related vasculoprotection effect was mediated by Tyro3. Indeed, upon PS/Tyro3 binding, sphingosine 1-phosphate receptor (S1P1) is activated inducing Rac1 (signaling GTPase involved in regulating cellular events like cells motility) dependent BBB protection. Therefore, PS was suggested as a potent therapy for hypoxic BBB damage induced neurovascular dysfunction.

Taking advantage from the reports emphasizing the new role of PS is vasculature, Fraineau et al. [116] tested whether PS could be involved in angiogenesis. Therefore, it was found that PS at 10 μg/mL suppressed the effects of proangiogenic growth factors in capillary like structures formation by ECs in Matrigel. This PS inhibitory effect was comparable with the one of the well-known angiogenesis inhibitor: endostatin. Since the vascular endothelial growth factor A (VEGF-A) is a powerful mitogen for ECs, its effect was tested in the presence of 10 μg/mL of

PS. Thus, it was demonstrated that PS significantly decreased VEGF-A induced mitogenesis but did not abolish it. The activation of the MAPK-Erk1/2 and Akt signaling is an indispensable step in mediating the mitogenic function of VEGF-A on ECs. Therefore, ECs treatment with PS before VEGF-A stimulation caused a marked decrease of VEGF-A induced Erk1/2 and Akt activation. To further examine the PS mechanistic pathway in angiogenesis, a TAM receptors gene silencing approach was used. Interestingly, it was shown that the inhibitory effect of PS on VEGF-A mitogenic function was mediated by Mer. Also, PS dephosphorylates vascular endothelial growth factor R2 (VEGR-2) on Tyr^{996}, which is sensitive to the tyrosine phosphatase SHP2. Consequently, a PS/Mer/SHP2 axis, which inhibits VEGF-A mediated VEGFR-2, MAPK Erk1/2, and Akt activation was suggested as a probable pathway of PS in vasculogenesis.

1.3.4 Protein S deficiency-induced purpura fulminans

PF is a hematological emergency characterized by skin necrosis and DIC that could rapidly progress to multi organ failure caused by thrombotic occlusion of blood vessels. PF may result from severe sepsis, an autoimmune response or benign childhood infections. It may also be a consequence of severe heritable deficiency of the natural anticoagulant protein C or PS. Early recognition and treatment of PF is essential to reduce mortality and to prevent major long-term health sequelae.

As introduced in paragraph 1.3.3.1, the complete PS deficiency is incompatible with life because of PF. Current knowledge on the molecular basis of PF is uncertain although the imbalance between pro- and anticoagulant factors is thought to be the etiological factor.

Fortunately, severe PS deficiency is a rare disease. The first case of severe *PROS1* deficiency was reported in 1990 by Mahasandana et al. [117]. A Thai girl born after preeclampsia developed 10 days after birth PF and necrotic skin lesions on the left thigh, lower abdomen and scalp. After whole blood transfusion, antibiotics and heparinisation, clinical improvement was reached. The family history was negative for thrombosis and the routine hematological examination at 3 months old revealed signs of DIC. Daily cryoprecipitate transfusion resulted

in a remarkable response with healing of necrotic skin lesions. An investigation of the etiology of these thrombotic disorders was made. Strikingly, both total and free PS were not measurable whereas protein C and antithrombin levels were within the normal range. Moreover, the analysis of the parents plasma revealed only half of the normal PS levels. The combination of oral anticoagulation therapy (warfarin) and transfusion with fresh frozen plasma (FFP) was an efficient treatment. Further examination of molecular basis behind this severe PS deficiency was performed. Indeed, the whole *PROS1* gene sequencing indicated two sequence variations: in the first allele, a frame shift leading to a TAA stop codon at position 155 and in the second allele, a nonsense mutation in exon 12 leading to a stop codon. Consequently, a compound heterozygous *PROS1* mutation was addressed [118].

One year later, another clinical report describing severe PS deficiency induced PF was published. After an uncomplicated pregnancy, a neonate developed ecchymotic areas on his scalp and lesions on both lower extremities that progressed to PF. The FFP administration every 12 hours leads to the regression of the lesions but the clinical signs of thrombosis persisted. Anticoagulant therapy was started when the patient was 5 weeks old. Despite the improvement, the intravenous administration was unsuccessful because of recurrent catheter occlusion. The intaperitoneal administration of the FFP resolved this problematic. Similarly to the first case, protein C and antithrombin levels were within the normal range and PS level was almost undetectable. Unfortunately, the molecular basis regarding this severe PS deficiency was not established because of the unavailability of the father.

The routine laboratory results in the context of PF are those of the associated DIC: prolonged plasma clotting times, thrombocytopenia, reduced plasma fibrinogen concentration, raised plasma fibrin degradation products and sometimes, microangiopathic hemolysis. Unfortunately, these abnormalities are not specific to PF and could arise in DIC of any cause. Additionally, protein C and PS quantification is mandatory since PF is usually associated with reduced protein C or PS levels (<5%). However, it is important to take into account that healthy neonates show low and highly variable physiological level of PC and PS (15–55 IU/dl) as compared to older children and adults, which progressively augments during the

first six months of life. Unlike testing in adults, the interpretation of PS levels in neonates is not complicated since C4BP is present at very low levels at birth. Crucially, PC and PS level should be carefully interpreted since the FFP infusion contains exogenous PC and PS.

The manifestation of DIC is usually associated with significantly diminished plasmatic PC and PS because of consumption of these natural anticoagulants. Thus, the demonstration of DIC and decreased PC and PS level is not enough to address the underlying cause of PF. The evaluation of PC and PS level in the parents of a neonate with PF could be informative since the demonstration of a partial reduction in PC or PS in both parents is favorably indicative of severe heritable PC or PS deficiency in the affected neonate. Finally, it should be noticed that in healthy women postpartum, PS level is physiologically reduced and is not necessarily a strict indication of partial heritable PS deficiency [119].

1.3.5 Protein S in pregnancy

1.3.5.1 Hemostasis in pregnancy

Pregnancy is associated with various physiological changes, which may affect most of the body system. Some of these changes start immediately after conception and continue through delivery to the postpartum period in order to accommodate both the maternal and fetal needs. The hematologic system adapts by different mechanisms such as an increased use of cofactors necessary for fetal hematopoiesis like iron-sulfur, vitamin B12 and folic acid, and preparation for bleeding at delivery necessitating enhanced hemostatic function. These changes simplify healthy pregnancy but besides, they could increase the risks of developing thrombotic events like VTE.

One of the major hematologic changes during pregnancy is the augmentation of blood and plasma volume. Indeed, it increases by 10% to 15% at 6 to 12 weeks of gestation, and expands rapidly until 30 to 34 weeks. The total gain is 30% to 50% above that found in nonpregnant women. Plasma volume reduces immediately after delivery. At three weeks postpartum, it remains elevated by 10% to 15% as compared to nonpregnant women, but it generally reaches normal nonpregnant levels at six weeks postpartum [120, 121].

RBC mass augments by 20% to 30% at 8 to 10 weeks of pregnancy and gradually increases above nonpregnant levels by the end of pregnancy in women taking iron supplements. Moreover, RBC life span is slightly decreased during normal pregnancy [122]. The main moderator of the RBC augmentation mass is the upregulation of EPO levels, which stimulates RBC production. Indeed, a study from Milman et al. revealed that EPO levels increase by 50% in normal pregnancies. Interestingly, the resulting increased RBC mass partially supports the higher metabolic requirement for oxygen during pregnancy [123] (Table 2).

Usually, pregnancy is associated with a modest decrease in hemoglobin levels named physiological or dilutional anemia of pregnancy. This decrease is due to the high plasma volume expansion and low RBC mass increase. The disproportion between the rates at which plasma and RBCs are added to the maternal circulation occurs typically at 28 to 36 weeks of pregnancy. By the end of the pregnancy, hemoglobin concentration increases due to cessation of plasma expansion and continuing increase in hemoglobin mass [124]. Nonetheless, a report from Stephansson et al. indicated that the absence of physiologic anemia could be a risk factor for stillbirth [125]. In general, physiologic anemia of pregnancy should resolve by six weeks postpartum since plasma volume has returned to normal by that time (Table 2).

Regularly, leukocytosis is observed during pregnancy and is mainly due to increased circulating neutrophils. The neutrophil count starts increasing in the second month of pregnancy to reach its maximal level in the second or third trimester [126]. The white blood cell count decreases to normal range by the sixth day postpartum. In addition, lymphocyte and monocyte counts remain generally unchanged in healthy women with normal pregnancies. However, the basophil count could decrease and the eosinophil count could slightly increase [127] (Table 2).

In pregnancy, the balance between hemostatic and fibrinolytic systems is disturbed in order to prevent excessive hemorrhage during placental separation. Pregnant women displayed a relative hypercoagulable state marked by higher levels of coagulation factors, decreased fibrinolysis, and amplified platelet activity. In addition, factors like nitric oxide, endothelin, estrogen, progesterone and prostacyclin play a prominent role in the vascular bed to ensure

the vascular tone modification in order to boost uteroplacental blood flow.

During uncomplicated pregnancy, platelet counts are usually within the normal range or slightly lower as compared to nonpregnant women [128]. Differently, pregnancies with gestational thrombocytopenia are characterized by a slight diminution in platelet count occurring in the third trimester. It is not associated with maternal, fetal, or neonatal sequelae and spontaneously resolves during postpartum [129]. Three to four weeks after delivery, the platelet counts is enhanced before returning to baseline [130] (Table 2).

It should be taking into account that gestational thrombocytopenia is distinct from other various thrombocytopenia's causes. Indeed, severe preeclampsia, hemolysis elevated liver function tests and low platelets (HELLP) syndrome, thrombotic thrombocytopenic purpura (TTP), immune thrombocytopenia (ITP), antiphospholipid syndrome, and drug-induced thrombocytopenia are characterized by more severe thrombocytopenia and/or other hematologic disorders.

Pregnancy is also associated with a shift of the coagulation balance. Indeed, increased concentration of clotting factors, decreased concentration of some of the natural anticoagulants and diminished fibrinolytic activity occur in order to maintain placental function during pregnancy and meet the delivery's hemostatic challenge. Consequently, these changes in blood coagulation and fibrinolysis, principally around term and the immediate postpartum period, create a state of hypercoagulability protecting pregnant women from fatal hemorrhage during delivery but predisposing them to thromboembolism [131] (Table 2).

Hematology	Nonpregnant adult	First trimester	Second trimester	Third trimester
Erythropoietin (units/L)	4-27	12-25	8-67	14-222
Ferritin (ng/mL)	10-150	6-130	2-230	0-116
Folate, red blood cell (ng/mL)	150-450	137-589	94-828	109-663
Folate, serum (ng/mL)	5.4-18.0	2.6-15.0	0.8-24.0	1.4-20.7
Haptoglobin (mg/mL)	25-250	130 +/- 43	115 +/- 50	135 +/- 65
Hemoglobin (g/dL)	12-15.8	11.6-13.9	9.7-14.8	9.5-15.0
Hematocrit (%)	35.4-44.4	31.0-41.0	30.0-39.0	28.0-40.0
Iron, total binding capacity (mcg/dL)	251-406	278-403	Not reported	359-609
Iron, serum (mcg/dL)	41-141	72-143	44-178	30-193
Mean corpuscular hemoglobin (pg/cell)	27-32	30-32	30-33	29-32
Mean corpuscular volume (xm3)	79-93	81-96	82-97	81-99
Platelet (x109/L)	165-415	174-391	155-409	146-429
Mean platelet volume (mcm3)	6.4-11.0	7.7-10.3	7.8-10.2	8.2-10.4
Red blood cell count (x106/mm3)	4.00-5.20	3.42-4.55	2.81-4.49	2.71-4.43
Red cell distribution width (%)	<14.5	12.5-14.1	13.4-13.6	12.7-15.3
White blood cell count (x103/mm3)	3.5-9.1	5.7-13.6	5.6-14.8	5.9-16.9
Neutrophils (x103/mm3)	1.4-4.6	3.6-10.1	3.8-12.3	3.9-13.1
Lymphocytes (x103/mm3)	0.7-4.6	1.1-3.6	0.9-3.9	1.0-3.6
Monocytes (x103/mm3)	0.1-0.7	0.1-1.1	0.1-1.1	0.1-1.4
Eosinophils (x103/mm3)	0-0.6	0-0.6	0-0.6	0-0.6
Basophils (x103/mm3)	0-0.2	0-0.1	0-0.1	0-0.1

Coagulation	Nonpregnant adult	First trimester	Second trimester	Third trimester
Antithrombin, functional (%)	70-130	89-114	78-126	82-116
D-dimer (mcg/mL)	0.22-0.74	0.05-0.95	0.32-1.29	0.13-1.7
Factor V (%)	50-150	75-95	72-96	60-88
Factor VII (%)	50-150	100-146	95-153	149-211
Factor VIII (%)	50-150	90-210	97-312	143-353
Factor IX (%)	50-150	103-172	154-217	164-235
Factor XI (%)	50-150	80-127	82-144	65-123
Factor XII (%)	50-150	78-124	90-151	129-194
Fibrinogen (mg/dL)	211-496	244-510	291-538	301-696
Homocysteine (mmol/L)	4.4-10.8	3.34-11	2.0-26.9	3.2-21.4
International Normalized Ratio	0.9-1.04◊	0.86-1.08	0.83-1.02	0.80-1.09
Partial thromboplastin time, activated (second)	26.3-39.4	23.0-38.9	22.9-38.1	22.6-35.0
Plasminogen activator inhibitor-1 (PAI-1) antigen (pg/mL)	17.3 +/− 5.7	17.7 +/− 1.9	Not reported	66.4 +/− 4.9
Plasminogen activator inhibitor-1 (PAI-1) activity (arbitrary units)	9.3 +/− 1.9	9.0 +/− 0.8	Not reported	31.4 +/− 3.0
Prothrombin time (second)	12.7-15.4	9.7-13.5	9.5-13.4	9.6-12.9
Protein C, functional (%)	70-130	78-121	83-133	67-135
Protein S, total (%)	70-140	39-105	27-101	33-101
Protein S, free (%)	70-140	34-133	19-113	20-65
Protein S, functional activity (%)	65-140	57-95	42-68	16-42
Tissue plasminogen activator (ng/mL)	1.6-13	1.8-6.0	2.36-6.6	3.34-9.20
Tissue plasminogen activator inhibitor-1 (ng/mL)	4-43	16-33	36-55	67-92
von Willebrand factor antigen (%)	75-125	62-318	90-247	84-422
ADAMTS-13, von Willebrand cleaving protease	40-170	40-160	22-135	38-105

Table 2: Hematological and coagulation parameters range in pregnant and nonpregnant women across the 3 trimesters. Adapted from UpToDate® 2016 (www.uptodate.com). The following coagulation factors are upregulated by ≈ 2 fold: factor VII, VIII, XII and von Willebrand factor. In addition, thrombin activatable fibrinolytic inhibitor (TAFI), plasminogen activator inhibitor-1 (PAI-1), tissue plasminogen activator (TPA) and products of fibrinolysis are also increased. Protein C, factor V and factor IX are unchanged or marginally increased. Protein S and antithrombin are 20% lower during

pregnancy as compared to baseline levels.

During pregnancy, thrombin cleavage products are enhanced. Indeed, an investigation from Francalanci et al. [132] revealed a progressive upregulation of plasmatic concentration of fibrin degradation products during normal pregnancy.

During the postpartum period, the hematological and coagulation parameters return to the normal range. The normalization might vary depending on the factor, but all return to the baseline level by 6 to 8 weeks after delivery [130].

1.3.5.2 Thrombophilia and pregnancy

Thrombophilia is a disorder that predisposes to develop venous thrombosis and increases the risk for VTE. Two distinct categories are known: acquired thrombophilia and inherited thrombophilia.

Antiphospholipid antibody syndrome is the most common cause of acquired thrombophilia provoking VTE in pregnancy. Moreover, recurrent fetal loss is one of the clinical criteria included in the definition of the antiphospholipid (aPL) syndrome [133]. aPL antibodies are a group of autoantibodies that display a wide range of target specificities and affinities, all recognizing various combinations of phospholipids, phospholipid-binding proteins, or both. The term aPL syndrome was first used to describe the clinical association between aPL antibodies and a syndrome of hypercoagulability. The commonly known aPL are lupus anticoagulants, anticardiolipin antibodies and anti-ß2-glycoprotein 1 antibodies [134]. A metaanalysis from Opatrny et al. [135] concluded a strong association between aPL and recurrent pregnancy loss.

Deficiencies or mutations of anticoagulant proteins are the main cause of inherited thrombophilia. The most frequent abnormalities are factor V Leiden (FV Leiden) mutation and the prothrombin gene mutation. In this regard, an analysis from Gerhardt et al. [136] indicates that the relative risk of pregnancy associated VTE was as high as 43.7% due to FV

Leiden mutation. Besides, G20210A prothrombin gene mutation was associated to 16.9% of VTE during pregnancy. Furthermore, Benedetto et al. [137] reported in their review that in pregnancy, predictive rates of VTE in women with inherited thrombophilias were: 1:500 for patients carrying heterozygous mutation for FV Leiden, 1:200 for those with heterozygous mutation for prothrombin G20210A. The accumulation of more than a single mutation seems to increase the VTE incidence. Therefore, predictive rates of VTE in women with double heterozygocity were 4.6:100 (Table 2).

As explained in paragraph 1.3.6.1, the coagulation balance is shifted to a hypercoagulable state as a physiological symptom of pregnancy and PS, protein C and antithrombin levels reduction are all concomitant with thrombophilia during pregnancy. According to Benedetto et al. [137], a pregnant woman carrying protein C deficiency displays a VTE risk of 1:113, 1:42 when antithrombin deficiency type 2, and 1:3 for antithrombin deficiency type 1 (Table 2).

Thrombophilia	Odds ratio general population	Annual incidence of first VTE (%)	Odds ratio in pregnancy (95% onfidence interval)
Antithrombin deficiency	28.2	1.77	4.69 (1.30–16.96)
Protein C deficiency	24.1	1.52	4.76 (2.15–10.57)
Protein S deficiency	30.6	1.9	3.19 (1.48–6.86)
Factor V Leiden	7.5	0.49	Homozygous 34.4 (9.86–120.0) Heterozygous 8.32 (5.44–12.70)
Prothrombin gene mutation	5.2	0.34	Homozygous 26.36 (1.24–559.2) Heterozygous 6.80 (2.46–19.77)

Table 3: Venous thromboembolism (VTE) risk during pregnancy with inherited thrombophilia. Adapted from Battinelli et al. [138].

1.3.5.3 Inherited thrombophilia: protein S deficiency

As mentioned in the previous paragraph, PS deficiency is an inherited thrombophilia factor leading to VTE during pregnancy. A report from Seligsohn et al. [86] revealed that pregnant women with PS inherited deficiency have also an elevated risk of late fetal loss. The efficacy of anticoagulation therapy in improving pregnancy's outcome in women with inherited PS was investigated by Brenner et al. [139]. They found that 75% of pregnant patients with different inherited thrombophilias including inherited PS treated by low molecular weight heparin (LMWH) enoxaparin gave birth as compared to only 20% of the untreated

pregnancies. Another study from Kupferminc et al. [140] investigated the beneficial effect of enoxaparin and low aspirin dose prophylaxis in 33 women with either fetal loss, pre-eclampsia, abruption placentae or intrauterine growth retardation, and a thrombophilic defect including PS deficiency. They found that with this prophylaxis, only 9% of the pregnancies exhibit thrombotic events. Three years later, a report from Gris et al. [141] indicated a more beneficial effect using enoxaparin from the 8th week (77% live births) than using a low dose aspirin treatment (14% live births). Folkeringa et al. also showed in a prospective study that anticoagulant treatment during pregnancy lowers the high fetal loss rate in women with hereditary deficiency of PS [142]. Indeed, fetal loss rates were 0% in deficient women with thromboprophylaxis versus 45% in deficient women without, further pointing to a very beneficial role of thromboprophylaxis to improve pregnancy outcome in women with inherited thrombophilia including PS deficiency. Differently, a randomized clinical trial performed by Kaandrop et al. [143] using three treatments: aspirin and heparin, aspirin alone or placebo revealed that among 299 pregnant women with a history of previous unexplained miscarriage, the live-birth rates were 69.1% in aspirin and heparin treated group, 61.6% in the aspirin treated group and 67.0% in the placebo group. These results pointed that neither aspirin combined with heparin nor aspirin alone improved pregnancies outcome. An answer to the question whether the use or heparin alone or combined with aspirin could be beneficial is still awaited.

In this regards, Rodger et al. [144] published recently a protocol for a systematic review and individual patient data meta-analysis in order to investigate the risk/benefit ratio of LMWH in preventing placenta-mediated pregnancy complications. This ambitious study named AFFIRM (an individual patient data meta-analysis of LMWH for prevention of placenta-mediated pregnancy complications) will integrate individual patient data from recent randomized controlled trials of LMWH for the prevention of recurrent placenta-mediated pregnancy complications. The overall objective of this meta-analysis will be to inform clinical practice and develop clinical practice guidelines.

A very recent review from Professor Middeldrop during the annual meeting of the American society of hematology in 2016 summarized the recent finding in the field of pregnancy and inherited thrombophilia [145]. Indeed, It was highlighted that numerous studies have investigated the association between inherited thrombophilia and various pregnancy complications, ranging from a single miscarriage to intrauterine fetal death, preeclampsia, HELLP (hemolysis, elevated liver enzymes, and low platelets), and placental abruption. However, no evidence-based solution on subsequent therapeutic consequences was established. Interestingly, a multicenter, investigator initiated randomized clinical trial, named anticoagulants for living fetus (ALIFE) assembling about 15 years of various clinical trials piloted around the world, revealed that LMWH does not increase the chance of live birth in women with unexplained recurrent miscarriage. However, it is still unclear whether this is also the case for women with inherited thrombophilia. Remarkably in this study, the subgroup of women with inherited thrombophilia (n=547) showed a trend toward a benefit of LMWH and aspirin (relative risk for live birth, 1.31 [95% CI, 0.74- 2.33] for the LMWH and aspirin vs placebo; relative risk for live birth, 1.22 [95% CI, 0.69-2.16] for aspirin, with corresponding absolute difference in live birth rates of 16.3% [95% CI, 218.2% to 50.8%] and 11.8% [95% CI, 221.1% to 44.6%], respectively). According to these encouraging results, the ALIFE2 trial was initiated, and is recruiting patients since 2013 in the Netherlands, United Kingdom, and Belgium, and hopefully soon in the United States and Slovenia.

1.3.6 Role of Gas6 and Protein S in phagocytosis and inflammation

1.3.6.1 Phagocytosis

Phagocytosis was described for the first time by Metchnikoff in 1908 as an important immune defence mechanism by which specialized cells engulf and kill pathogens. Analogously, efferocytosis is the clearance of unwanted cells comprising excess cells generated during development, transformed or malignant cells capable of tumorigenesis, apoptotic cells, cell debris and cells irreparably damaged by cytotoxic agents. Both phagocytosis and

efferocytosis are necessary for maintenance of overall health and homeostasis, and prevention of autoimmunity, pathogen burden or cancer.

Following an inflammatory stimulus, neutrophils are the first cells to enter to the injured site, where they can ingest microbial invaders and cellular debris. Hallmarks of inflammation eradication and tissue repair include the inhibition of the neutrophils influx and clearance of apoptotic neutrophils [146]. In this context, Bosurgi et al. investigated the role of Axl and Mer in the efferocytosis of apoptotic neutrophils generated consequently to azoxymethane and dextran sulfate sodium induced inflammation in mice colon cancer. Interestingly, they found that the percentages of $Ly6G^+$ neutrophils and $F4/80^+$ $CD11b^+$ macrophages were not altered in *WT* and $Axl^{-/-}Mer^{-/-}$ mice in resting condition. Differently, immunohistochemical and FACS analyses showed a higher number of $TUNEL^+/Ly6G^+$ apoptotic neutrophils in the lamina propria of $Axl^{-/-}Mer^{-/-}$ mice as compared to *WT* mice. Moreover, apoptotic neutrophils labelled with CellTracker dye and cocultured with $Axl^{-/-}Mer^{-/-}$ BM derived macrophages demonstrated a significant reduction in phagocytic activity of apoptotic neutrophils as compared to *WT* macrophages. Thus, Axl and Mer modulate inflammation in the intestinal lamina propria by phagocyting apoptotic neutrophils. Since macrophages express the TAM agonists PS and Gas6, TAM might signal in an autocrine manner in macrophages [147]. The role of Mer in clearance of apoptotic cells was also investigated by Scott et al. [148] by treating adult mice with dexamethasone to induce apoptosis of cortical thymocytes. Indeed, they observed that the thymi of $Mer^{-/-}$ mice exhibit seven fold more remnant apoptotic thymocytes as compared to *WT* mice thymi. The authors further examined the role of macrophages in the clearance of apoptotic cells. Irradiated $Mer^{-/-}$ mice reconstituted with *WT* BM showed clearance of dexamethasone induced apoptotic thymocytes almost at normal levels. Intriguingly, the converse experiment in which $Mer^{-/-}$ BM was transferred into irradiated *WT* mice showed normal removal of apoptotic cells. It was suggested that this compensation was due to radioresistant *WT* macrophages. However, *in vitro* setting confirmed that both $Mer^{-/-}$ and *WT* macrophages bound equally to apoptotic

thymocytes but $Mer^{-/-}$ macrophages had a dramatic deficit in phagocytosis of apoptotic thymocytes but not of Listeria, latex beads, or opsonized particles. Another report from Cohen et al. [149] further confirmed the role of Mer in phagocytosis. Since autoimmune diseases, for example, systemic lupus erythematous (SLE), are associated with diminished phagocytosis of apoptotic cells and debris, and consistent with a role for Mer in the clearance of apoptotic cells, Cohen et al. demonstrated that mice lacking the intracellular kinase domain of Mer had delayed clearance of exogenously administered apoptotic cells and spontaneous progress of additional serological manifestations of SLE.

The downstream signaling upon Mer phosphorylation is involved in distinct cellular activities. Indeed, Tibrewal et al. [150] identified a *MERTK* mutation, Y867F, in which Mer failed to stimulate actin cytoskeleton reorganization and lost its phagocytic activity.

In addition to Mer, Axl and Tyro3 have phagocytic activity. Seitz et al. [151] proved that $Axl^{-/-}$, $Tyro3^{-/-}$, and $Axl^{-/-}Mer^{-/-}$ macrophages phagocyted 40 to 50% less apoptotic thymocytes as compared to *WT*. It was also highlighted in this report that depending on the phagocyte type, involvement of the Tyro3, Axl and Mer in the removal of apoptotic cells may be different. Therefore, $Mer^{-/-}$ BM derived dendritic cells (DCs) phagocyted normal level of apoptotic thymocytes whereas $Axl^{-/-}$, $Tyro3^{-/-}$, and $Axl^{-/-}Mer^{-/-}$ mice all had severe deficits in this process.

During apoptosis, PtdSer is exposed on the outer leaflet of the plasma membrane. As described in paragraph 1.2.2, Gas6 binds to its receptors via the C-terminal globular domain. It was reported by Nakano et al. [152] that Gas6 binds to PtdSer via the N-terminal GLA domain and that Axl presence facilitated this interaction by decreasing the K_d value by approximately 30%. Furthermore, a study from Anderson et al. [153] evaluating the role of PS in phagocytosis revealed that PS binds PtdSer expressed on the apoptotic cell surface in a Ca^{2+}-dependent manner. Indeed, it was demonstrated that either serum or purified PS addition to cultured macrophage enhances phagocytosis of apoptotic cells and that serum immunodepletion of PS inhibited this prophagocytic activity.

Inherited blindness is classically studied with the royal college of surgeons rat (RCS) model in which retinal pigment epithelial (RPE) cells fail to phagocytose shed outer segments resulting in photoreceptor cells death and retinal dystrophy. Interestingly, D'Cruz et al. [154] mapped the locus responsible for inherited retinal dystrophy in these rats to *Mertk* by positional cloning approach. It was found that RCS displayed a small DNA deletion in the *Mertk* gene. Consequently, Mertk was described as a probable responsible of RPE phagocytosis defect causing retinal dystrophy. Shortly after and in line with these results, Gal et al. [155] screened the human orthologue, *MERTK,* in 328 DNA samples from individuals with various retinal dystrophies. Remarkably, three *MERTK* mutations in three individuals with retinitis pigmentosa were described further confirming the role of Mertk in RPE phagocytosis and retinal degeneration.

Although *in vitro* experiments have implicated Gas6 as the critical TAM ligand for this process, Prasad et al. [34] demonstrated that *Gas6$^{-/-}$* mice have a histologically intact retina with no photoreceptor degeneration. It has been shown that in addition to Mertk, RPE cells express Tyro3 and that PS, also expressed by RPE cells, activates both of these receptors suggesting that their biologically appropriate ligand in these cells is PS.

Spermatogenesis is the development of the sperm cells within the male reproductive organs, the testes. During this process, the apoptotic spermatogenic cells and residual bodies are phagocytosed and degraded by Sertoli cells (SCs) via a not well know mechanism. A report from Xiong et al. [156] revealed that Gas6 addition to cultured SCs rises five fold their phagocytic activity. Furthermore, SCs lacking the TAM receptors exhibited 7.6 fold less phagocytic activity as compared to *WT*. Besides, *Mertk$^{-/-}$* SCs had 35% reduction in phagocytosis of apoptotic spermatogenic cells as compared to *WT* cells. This phagocytic defect was attributed to a compromised binding of the SCs to apoptotic germ cells.

Mammalian nervous system undergoes extensive activity in order to accomplish its precise neural connectivity. Although microglial cells are responsible for a portion of synapses

uptake, the remaining phagocytic mechanisms are still poorly understood. In this regards, Chung et al. [157] reported a novel role for astrocytes in engulfing central nervous system synapses. Interestingly, in an *in vitro* engulfment assay, astrocytes cultured in the presence of synaptosomes and 5% serum or PS significantly augmented the amount of synaptosomes engulfed by astrocytes. It was demonstrated that this process involves the MERTK phagocytic pathway. Importantly, *Mertk*$^{-/-}$ astrocytes phagocyted 58% less synaptosomes. The same results were demonstrated *in vivo* where mice deficient in Mertk pathway fail to improve their retinogeniculate networks and had excess excitatory and inhibitory functional synapses known to be responsible of several neurological diseases.

As evoked in paragraph 1.3.1.1, the mechanism regarding the clearance of PMPs is not completely understood. The work of Happonen et al. [158] fairly demonstrated that vascular Gas6 and Axl mediated the uptake of PMPs by ECs. Since circulating PMPs were not elevated in *Gas6*$^{-/-}$ as compare to *WT* mice, it was suggested that this endothelium specific phagocytic activity could serve to eliminate PMPs generated at injured site (see Chapter VII: Appendices).

1.3.6.2 Inflammation

Inflammation was described at the basis of a significant number of diseases. Since many years, researchers are hardly investigating the effects of inflammation on health and possible preventive medical applications. In a recent review of Nature journal [159], Professor Buckley declared that acute inflammation is an unstable state that either resolves or become chronic. Traditional models of inflammation suggest that inflammation resolves after the elimination of the pro-inflammatory mediators that first originated the response. However, several anti-inflammatory agents have now been discovered, including steroids, nitric oxide, adenosine and interleukin-10 (IL-10), as well as regulatory T (TReg) cells. These mediators restrain inflammation. Another step forward was the molecular characterization of numerous distinct biochemical pathways that are actively turned on during inflammation, and lead to the

production of mediators responsible of reparatory functions. Experiments implicating genetic deletion models or pharmacological synthesis compounds provided new insights into understanding the inflammatory process.

Activation of DCs, known as the professional antigen presenting cells (APCs), initiate T cell activation. However, the magnitude of DCs activation must be strictly controlled because if unrestrained, DCs responses can lead to pathological conditions with overactive immune responses, such as allergy, autoimmunity and chronic inflammatory diseases [160, 161].

Toll-like receptors (TLRs) are known as a set of mediators that activate host defences responsible for local inflammation, the recruitment of effector cells, and the secretion of cytokines that modulate both the innate and adaptive immune responses [162]. Interestingly, TLRs are highly expressed in DCs and macrophages, which drive the innate immune response. Subsequently, TLRs activation in DCs provokes secretion of cytokines and costimulatory molecules that afterward, coordinate the adaptive immune response [163].

It was extensively studied that unrestrained DCs activation, sustained by elevated levels of type I IFNs, could lead to autoimmune diseases like SLE, Sjögren's syndrome and psoriasis [164]. As illustrated in Fig.7, TLRs activation in DCs is modulated by negative regulators responsible of the inhibition of this activation [165]. Indeed, TRIAD3A (a ring finger protein that binds to the cytoplasmic tail of several TLRs) promotes degradation of certain TLRs. The short form of myeloid differentiation primary response gene 88 (MyD88s) antagonizes MyD88 functions. Inhibitory proteins such as suppressor of cytokine signaling 1 (SOCS1), interleukin-1 receptor associated kinase M (IRAKM), Toll interacting protein (TOLLIP), IRAK2c and IRAK2d suppress IRAK function and targets various stages of the TLRs signaling pathways. PI3K negatively regulates some TLRs responses through an unknown mechanism. A20 deubiquitylates tumor necrosis factor receptor associated factor 6 (TRAF6) and affects both MyD88-dependent and MyD88-independent pathways. Nucleotide-binding oligomerization domain 2 (NOD2) might inhibit TLR2 signaling by suppressing nuclear factor-κB (NF-κB) activity [165] Fig.7.
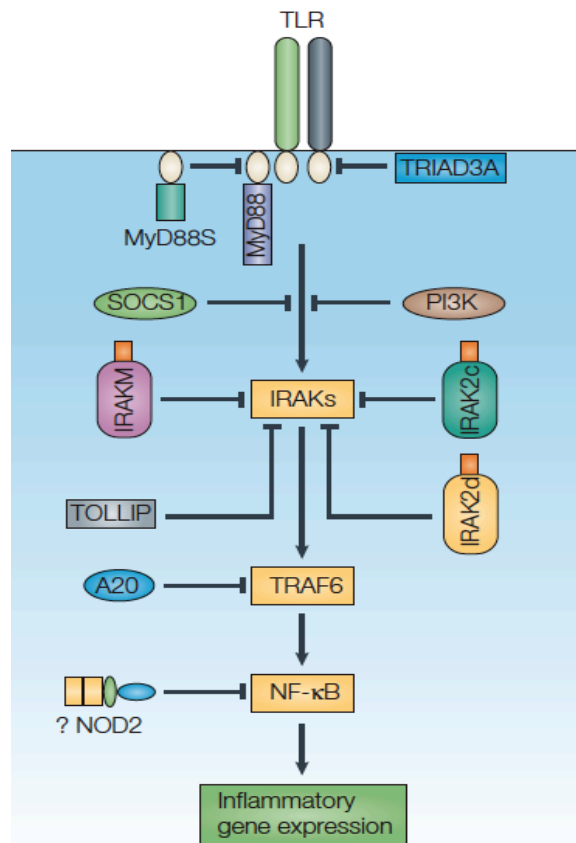
Fig.7: Overview of intracellular toll-like receptor (TLRs) regulators. TLRs signaling pathways are tightly regulated by endogenous regulators at multiple levels. TRIAD3A (a ring finger protein that binds to the cytoplasmic tail of several TLRs) promotes ubiquitylation and degradation of certain TLRs. The short form of myeloid differentiation primary response gene 88 (MyD88s) antagonizes MyD88 functions. Inhibitory proteins such as SOCS1 (suppressor of cytokine signaling 1), IRAKM (interleukin 1 receptor associated kinase M), TOLLIP (Toll-interacting protein), IRAK2c and IRAK2d suppress IRAK function by targeting various stages of the TLRs signaling pathways. Phosphatidylinositol 3-kinase (PI3K) negatively regulates some TLRs responses through an unknown mechanism. A20 deubiquitylates TRAF6 (tumor necrosis factor receptor associated factor 6) and affects both MyD88-dependent and MyD88-independent pathways. Nucleotide-binding oligomerization domain 2 might (NOD2) inhibit TLR2 signaling by suppressing nuclear factor-κB (NF-κB) activity. Adapted from Liew et al. [165].

Although the cited mechanisms above demonstrate news insights into TLRs inhibition, the pathway regarding their negative regulation remains still unclear.

TAM RTKs involvement in inflammation was first described by Lu et al. [33]. It was shown that Tyro3, Axl and Mertk play a crucial immunoregulatory role. Indeed, mice lacking these three receptors displayed a severe lymphoproliferative disorders illustrated by the aberrant growth of peripheral lymphoid organs due to the hyperproliferation of B and T lymphocytes and systemic autoimmune diseases characterized by high blood titters of antibodies directed against normal cellular antigens, like nucleoproteins and double stranded DNA (ds DNA).

Since TAM receptors are not expressed by lymphocytes, the immune defects observed in the TAM knockout mice were suggested to be cells nonautonomous. Consequently, it was proposed that Tyro 3, Axl and Mertk are responsible of downregulating the immune response via DCs and macrophages and thereby play a prominent role in returning the immune system to baseline after pathogen or toxin clearance.

Results of previous studies performed by Camenisch et al. [166] were consistent with the regulation of this APCs functions by TAM receptors. Indeed, $Mertk^{-/-}$ mice were hypersensitive to lipopolysaccharide (LPS) induced endotoxemia with $Mertk^{-/-}$ macrophages expressing high levels of NF-κB. It was also found that the excessive release of TNF-alpha caused tissue damage and mice death. Remarkably, these phenotypes were significantly more pronounced in the TAM triple knockout mice [33]. Few years later, the same authors further investigated how TAM receptors function in the DCs subset of APCs. Interestingly, they described a new pathway of TAM in mediating negative regulation of both TLRs activation and cytokine production in APCs and suggested that this pathway regulates APCs activation. Indeed, upon TLRs activation, an initial burst of cytokines is released which is further amplified by a feed-forward loop through cytokine receptors. In meanwhile, cytokine activation of the type I interferon receptor (IFNAR) and signal transducer and activator of transcription 1 (STAT1) triggers Axl activation. Activated TAM subsequently induce the transcription of SOCS genes and the pleiotropic inhibition of both cytokine receptors and TLRs signaling pathways (red pathways). This final TAM driven inhibitory phase is also dependent on the IFNAR/STAT1 signaling cassette, which is physically associated with TAM receptors [167] Fig.8.
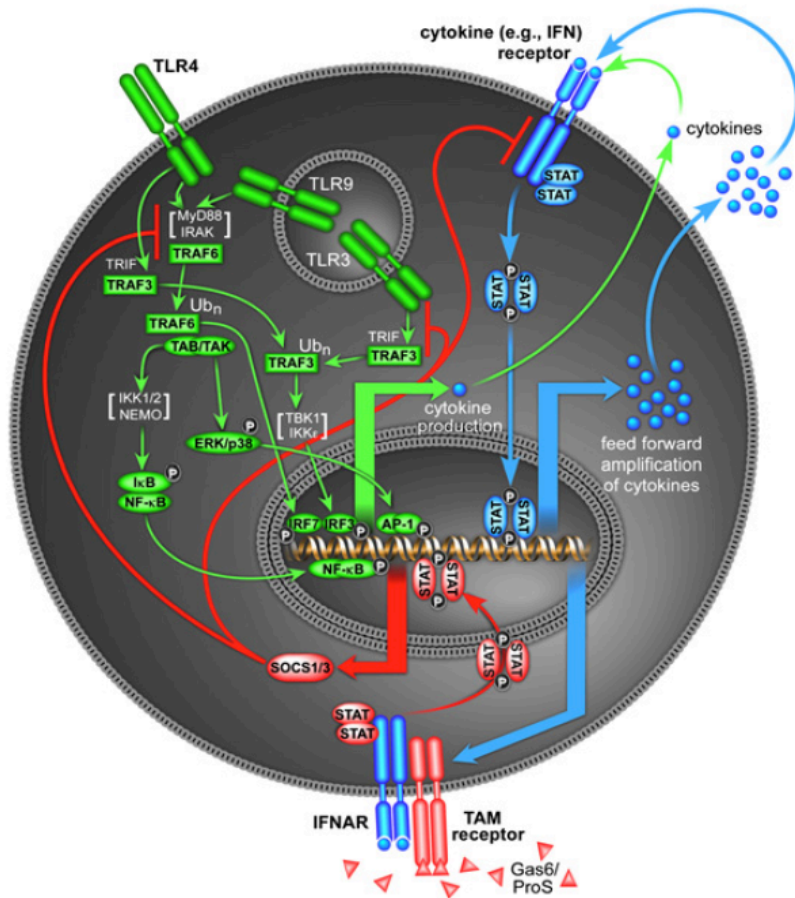
Fig.8: Scheme illustrating the activation of Toll-like receptors (TLRs) and downstream signaling. Upon TLRs activation, an initial burst of cytokines is released that is secondly amplified by a feed-forward loop through cytokine receptors (blue pathways). In meanwhile, cytokine activation of the type I interferon receptor / signal transducer and activator of transcription 1 (IFNAR/STAT1) triggers Axl activation. Subsequently, TAM signaling is upregulated and further induces the transcription of suppressor of cytokine signaling (SOCS) genes and the pleiotropic inhibition of both cytokine receptors and TLRs signaling pathways (red pathways). This final TAM driven inhibitory phase is also dependent on the IFNAR/STAT1 signaling cassette, which is physically associated with TAM receptors. Adapted from [167].

IFN-alpha plays an important role in the generation of DCs with high antigen presenting competences from peripheral blood monocytes [168]. Besides, it was revealed that Axl expression is regulated by IFN-alpha [169]. Rising evidence that DCs differentiate from

monocytes in SLE, where high levels of IFN-alpha circulates, and in line with immunotherapeutic studies highlighting IFN and DCs as promising targets, Scutera et al. [170] reported that during their IFN-alpha driven differentiation, human DCs exposed cell surface Axl. Additionally, it was shown that Gas6 protects these cells from serum deprivation induced apoptosis and stimulates their chemotaxis in an Axl dependent manner. Thus, it was proposed that IFN-alpha controls DCs survival and migration via a Gas6/Axl signaling.

A recent study from Carrera et al. [171] further shed light on the negative feedback mechanism by which activated T cells control DCs activation and adjust the extent of the immune response. For the first time, it was demonstrated that both human and mice activated DCs activate T cells that release PS. Therefore, secreted PS initiates the anti-inflammatory TAM signaling pathway in DCs. Thus, by releasing PS, activated T cells regulate DCs activity and avoid exacerbated inflammation.

T cells do not contribute to the physiological plasmatic amounts of PS since mice lacking PS in T cells *(Pros1$^{flox/flox}$ Cd4-Cre$^+$* mice)* exhibited comparable PS levels as compared to *WT* controls. Intriguingly, this study revealed that blood-circulating PS did not balance the lack of PS expression by activated T cells needed to control DCs activity. It was then proposed that PS acts locally as an immunomodulatory protein at the physical T cell- DCs interface. Thus, synchronized PS secretion and the exposure of PtdSer on activated T cells should allow the localization and the bioactivity of PS at the T cell membrane surface, engaging TAM signaling in DCs following T cell priming in lymphoid organs.

Sepsis is characterized by an overwhelming systemic inflammation caused by an infection and is a leading cause of death in the intensive care unit. There have been no proven pharmacological therapies for sepsis

Based on the reports highlighting the role of TAM receptors and Gas6 in inflammation, Burnier al. (manuscript in revision, chapter VII, Appendices) hypothesized that Gas6 and its receptors might be involved in protection against systemic inflammatory response to infection and/or in the development of immune dysfunction observed in severe sepsis. In order to test this hypothesis, they performed experimental studies using *Gas6$^{+/+}$* and *Gas6$^{-/-}$* mice. First, it

67

was observed that *Gas6*^{-/-} mice displayed the same vulnerability to endotoxin challenge as described in *Mertk*^{-/-} mice [166], characterized by a reduced survival associated with an overproduction of TNF-α. Survival curves after endotoxin challenge in *Axl*^{-/-} and *Tyro3*^{-/-} were comparable to those of *Mertk*^{-/-} and *Gas6*^{-/-} mice. Second, *Gas6*^{-/-} mice were also more susceptible to death in the CLP model. Gas6 plasma concentrations were enhanced in models of endotoxemia and microbial peritonitis (inoculation of *E. coli* in the peritoneum and cecal ligation puncture). Therefore, it was suggested that endogenous Gas6 plays a key role in the regulation of the death/over-inflammatory process, which acts through Gas6 receptors as a negative feedback. Besides, it had been shown that TLR4 stimulation by endotoxin activated monocytic cells, which secrete TNF-α and other cytokines. Gas6 then binds to its cognate receptors and thereby prevents an over-stimulation of monocytic cells as it was postulated previously. Consequently, in severe sepsis, a protective role was attributed to Gas6 for its effect in dampening the inflammation state of macrophages.

Data in mice are corroborated by observations in humans. Indeed, it was found that in healthy volunteers, Gas6 levels raised in plasma in response to endotoxin, reaching its maximal concentration at 90 min and sustained for the next 4.5 h.

A study of Gibot et al [172] confirmed the correlation between Gas6 levels and septic related mortality. Patients requiring renal support exhibited higher Gas6 concentration than those without need for hemofiltration (76.5 versus 10.5pg/ml respectively). Although there was a progressive decline in Gas6 concentration in survivors, nonsurvivors had persistently elevated Gas6 levels. It was concluded that plasmatic Gas6 levels correlate with disease severity, particularly with renal and hepatic dysfunction in septic shock.

Another report from Ekman et al. [173] revealed that patients with severe sepsis, sepsis, infection or SIRS displayed double Gas6 levels as compared to the controls. sAxl was also upregulated in the patient groups compared to the controls. Additionally, Gas6 and sAxl correlated with some other inflammatory markers implying a role in systemic inflammation.

A recent report of Stalder et al. [174] studied a cohort of 129 septic patients. Gas6 level was 238% in non-survivors versus 167% in survivors. Furthermore, sAxl was found increased in non-survivors. It was concluded that Gas6 plasma level might predict mortality of septic patients.

1.4 Aims of the thesis

Hemostasis is guaranteed by the equilibrium between procoagulant and anticoagulant forces which are tightly balanced. Deficiency of any of the coagulation factors could lead to disequilibrium provoking bleeding or thrombosis. Protein S (PS) is a natural anticoagulant regulating thrombin generation. It acts as a cofactor for activated protein C (APC) and tissue factor pathway inhibitor (TFPI), and also has a direct anticoagulant activity. Besides its role as an anticoagulant, the downstream signaling of PS binding to the TAM receptors exerts multiple cellular effects like phagocytosis, inflammation and angiogenesis. Purpura fulminans (PF) is characterized by disseminated intravascular coagulation and hemorrhagic **infarction** of the skin that could rapidly progress to multi organ failure and death. PF may result from severe sepsis, an autoimmune response or benign childhood infections. PS complete deficiency also causes PF and DIC and leads to death if untreated. Early recognition and treatment of PF is essential to reduce mortality and to prevent major long-term health sequelae. Current knowledge on the molecular basis of PF is uncertain although the imbalance between pro- and anticoagulant factors is thought to be the etiological factor. This thesis will be divided in three part:

1. New insights into purpura fulminans induced by protein S deficiency

PS deficiency induced PF will be investigated using several strategies. The first strategy will be to mimic severe acquired PS deficiency using *Pros1* gene silencing by poly I: C-inducible *Mx1-Cre^{+}* in mice. The resulted null or low level of PS in *Pros1$^{lox/-}$Mx1Cre^{+}* adult mice will probably trigger PF and allow the monitoring of PF lesions development. The second strategy will be to treat *Pros1$^{+/-}$* mice with warfarin, a vitamin K antagonist, to further drop plasmatic PS and reproduce PF. The monitoring and investigations of developed PF lesions will provide more insights into the molecular basis of PF.

Gas6, a protein sharing 44% similarity with PS is however described to display prothrombotic effects by its function in thrombus stabilization and as TF activity inducer. Like PS, Gas6 is also a ligand for TAM receptors and exerts various cellular

effects like phagocytosis, inflammation and angiogenesis. Since PF etiology is supposed to result from imbalance between pro- and anticoagulant factors, our third strategy will be to combine Gas6 and PS deficiencies to investigate if the *Gas6*[^-/-] antithrombotic phenotype could rebalance hemostasis in *Pros1*[^-/-] mice and rescue them from fatal PF. We hypothesize that the results obtained using these three strategies will bring new insights into PF development mechanisms.

2. Targeting anticoagulant protein S to achieve hemostasis in hemophilia

Bleeding diathesis caused by the loss of *F8* (hemophilia A :HA) or *F9* (hemophilia B : HB) activity results from impaired thrombin generation and imbalanced hemostasis. Patients with severe hemophilia frequently suffer from spontaneous recurrent muscle and joint bleeding, such as hemarthrosis, which leads to severe and progressive musculoskeletal damage. The main treatment is the administration of the deficient coagulation factor. Complication of such therapy is the development of neutralising antibodies. The disequilibrium of the hemostatic balance caused by PS complete lack allows us to hypothesize that the combined deficiency in F8/ F9 and PS might be suitable to achieve hemostasis in HA and HB and rescue *Pros1*[^-/-] mice from PF. If *Pros1*[^-/-] mice are rescued, *F8*[^-/-]*Pros1*[^-/-] and *F9*[^-/-]*Pros1*[^-/-] mice will be investigated to evaluate hemostasis in complete PS deficiency.

3. Pregnancy and protein S deficiency

Pregnancy is associated with a shift of the coagulation balance with increased concentration of coagulation factors, decreased concentration of some of the natural anticoagulants and diminished fibrinolytic activity leading to a hypercoagulable state that protects pregnant women from fatal hemorrhage during delivery but predispose them to thromboembolism. Pregnant women with partial PS inherited thrombophilia have an elevated risk of late fetal loss and whether thromboprophylaxis could ameliorate pregnancy outcomes is intensely debated. We will investigate pregnancy in *Pros1*[^+/-] mice

71

by blood cell count, coagulation tests and histology of pregnant mice and embryos. Heparin or aspirin alone or a combination of both will be used for thromboprophylaxis. If viable $F8^{-/-}Pros1^{-/-}$ and $F9^{-/-}Pros1^{-/-}$ mice are obtained, the effect of PS complete deficiency will be investigated.

Chapter II. New insights into purpura fulminans induced by protein S deficiency

(Manuscript in final preparation)

Chapter II. New insights into purpura fulminans induced by protein S deficiency

Raja Prince[1,2], Sara Calzavarini[1,2], Desiré Reina Caro[1,2], Claudia Quarroz[1,2], José A. Fernández[3], Yasuhiro Matsumura[4], François Saller[5], John H. Griffin[3], Anne Angelillo-Scherrer[1,2]

1) Department of Hematology and Central Hematology Laboratory, Inselspital, Bern University Hospital, University of Bern, CH-3010 Bern, Switzerland

2) Department of Clinical Research, University of Bern, Murtenstrasse 31, CH-3010 Bern, Switzerland

3) Department of Molecular and Experimental Medicine, The Scripps Research Institute, La Jolla, California 92037, USA

4) Division of Developmental Therapeutics, Research Centre for Innovative Oncology, National Cancer Centre Hospital East, Chiba, Japan

5) INSERM & UMR-S 1176, Université Paris-Sud, Université Paris-Saclay, 94270 Le Kremlin-Bicêtre, France

Correspondence to: Prof. Anne Angelillo-Scherrer
                     Department of Hematology and Central Hematology Laboratory
                     Inselspital
                     Bern University Hospital
                     University of Bern
                     CH-3010 Bern
                     Switzerland
                     Phone: +41 31 632 33 02
                     e-mail: anne.angelillo-scherrer@insel.ch

Abstract

Purpura fulminans (PF) is characterized by disseminated intravascular coagulation and hemorrhagic infarction of the skin that could rapidly progress to multi organ failure and death. Early recognition and treatment of PF is essential to reduce mortality and to prevent major long-term health sequelae. Current knowledge on the molecular basis of PF is uncertain although the imbalance between pro- and anticoagulant factors is thought to be the etiological factor. PS complete deficiency causes PF. We found that in mice, very low circulating PS level (16% of the level found in control mice) is sufficient to protect against PF. Warfarin treatment induced PF only in a few $Pros1^{+/-}$ mice. The evaluation of the formed skin lesions over time revealed thrombi occurring with vascular wall damage. $Pros1^{-/-}$ embryonic vasculature examination displayed dorsal disturbed vasculature with reduced vascular volume and less vessels branching. Furthermore, $Pros1^{-/-}$ embryos vasculature was altered before PF starts. Inadequate phagocytosis and erythropoiesis, and more inflammation were observed during PF. Gas6 is a procoagulant factor. However, combined deficiency in Gas6 and PS did not rescue $Pros1^{-/-}$ from fatal PF, the $Pros1^{-/-}Gas6^{-/-}$ phenotype appearing more dramatic with earlier and more frequent embryonic death from PF. Our findings provide evidence that the thrombotic process occurring during PS deficiency induced PF should be less central than currently admitted. The lack of PS signaling in the endothelium might lead to vascular defects that further promote PF.

2.1 Introduction

Protein S (PS) is a vitamin K-dependent protein (VKDP) functioning as natural anticoagulant in the blood. It acts as a cofactor of activated protein C (APC) and tissue factor pathway inhibitor (TFPI), and also displays a direct anticoagulant activity. It is a protein of 70.69 kDa and is characterized by post-translational γ-carboxylation of certain glutamic acid residues by a carboxylase, using vitamin K as cofactor. PS is mainly synthetized by liver parenchymal cells [17], vascular endothelial cells [18], testicular Leydig cells, macrophages [19] and megakaryocytes [20]. It circulates in human plasma at a concentration of 350 nanomolar (nM) corresponding to 25 μg/mL of which 60% forms a complex with C4b-binding protein (C4BP), a protein involved in the complement system. The remaining 40% circulates in a free form [20, 21]. In human, two PS genes were described: *PROS1* gene, which expressed PS and *PROSP* as a pseudogene.

In clinic, patients with hereditary parcial PS deficiency mostly suffer from venous thromboembolism (VTE). The thromboembolic events could be caused by transient risk factors for VTE. However, half of the thromboembolic events in PS deficient patients are unprovoked and these patients become symptomatic around 55 years old. Brouwer et al. [92] found a 9-fold higher risk for VTE in patients with PS deficiency as compared to non deficient patients. In thrombophilic families, Lejfering et al. [93] indicated that free PS levels could identify young subjects at risk for venous thrombosis, although the cut-off level lies far below the normal range in healthy volunteers. Up to now, the raison behind why some PS deficient patients develop VTE while others remain unaffected is not completely explained [94]. The prevalence is estimated from 0.16% to 0.21% and augments to 2% in patients with VTE [85, 86]. The multiple environmental and genetic assessment of risk factor for venous thrombosis (MEGA) study highlighted that PS deficiency might be less common than previously described. It was found that PS deficiency was not associated with VTE. Nonetheless, when lower cut-off values were applied, subjects at risk of VTE could be identified with low free PS levels. Paradoxically, very low levels of total PS were not

associated with VTE [89].

Homozygous or compound heterozygous *PROS1* deficiencies are extremely rare with presentation soon after birth with a combination of extensive disseminated intravascular coagulation (DIC) and skin necrosis named purpura fulminans (PF). Death occurs within hours if untreated. A murine model recapitulating phenotypes of PS deficiency in human was described by Saller et al. [95]. Thus, heterozygous mice *(Pros1$^{+/-}$)* did not suffer from spontaneous thrombosis and displayed reduced PS plasma levels. They also exhibit a thrombotic phenotype *in vivo* when challenged in a tissue factor (TF) induced thromboembolism model. As in human, homozygous mice *(Pros1$^{-/-}$)* died *in utero* from intracranial hemorrhages and PF. Burstyn et al. [96] confirmed embryonic lethality of *Pros1$^{-/-}$* mice with macroscopic blood clots and fulminant hemorrhages. Plasma from *Pros1$^{+/-}$* heterozygous mice exhibited accelerated thrombin generation independent of activated protein C (APC). The vascular networks hierarchy and morphology was 40% reduced with poorly formed microvessels in *Pros1$^{-/-}$* embryos as compared to *WT*. Since the role of PS in vasculature was previously addressed in several studies [112] [113] [114] [116], one question remains: is the defective vascular integrity in *Pros1$^{-/-}$* embryos secondary to increased thrombosis and perturbed blood flow during vascular development or is a direct consequence of the loss of PS signaling in the vasculature or both?

Growth arrest specific gene 6 (Gas6) is a VKDP of 75 kilodaltons (kDa). Gas6 mRNA was found expressed by serum-starved embryonic mouse fibroblast NIH3T3 cells. *Gas6* clonage and sequencing revealed a high degree of homology and a similar pattern of expression in IMR90 human fibroblasts [7]. Important tissues where *Gas6* is expressed are neuronal [8], hepatic [9] and renal tissue [10]. *Gas6* is also expressed in various cell types: endothelial cells (ECs) [7], vascular smooth muscle cells [11], bone marrow (BM) [12] and platelet [13]. Gas6 concentration in human plasma range from 20 to 50 μg/L [14].

Gas6 binds to and activates the Tyro3, Axl and Mer (TAM) receptor tyrosine kinases (RTKs) with a highest affinity for Axl followed by Tyro3 and Mertk [43]. This binding leads to

further intracellular signaling including activation of PI3K and Akt pathways [44, 45] resulting in many cellular effects.

PS has high structural homology (~42%) with Gas6 and the modular composition is the same. However, unlike the thrombin sensitive region (TSR) in Gas6, PS TSR is sensitive to the cleavage action of serine proteases [7]. PS also binds to and activates the TAM receptors. The downstream signaling is involved in phagocytosis, angiogenesis and immunity.

The generation of a murine model with complete $Gas6$ deficiency ($Gas6^{-/-}$) provides great insights regarding the role of Gas6 in thrombosis. $Gas6^{-/-}$ mice were viable, fertile, had an apparent normal phenotype. $Gas6^{-/-}$ mice did not suffer from spontaneous bleeding or thrombosis but interestingly, when challenged with different thrombosis models, they were protected against venous and arterial thrombosis [13]. Gas6 also acts in endothelium by promoting P-selectin, a ligand for the platelet receptor PSLG-1, to reinforce the thrombus adhesion to the vascular wall [49]. Furthermore, it was found that ECs stimulation by thrombin leads to tissue factor release via Gas6/Axl/c-Src/Akt signaling and the initiation of the coagulation pathway resulting in formation of tight fibrin networks [51]. Platelet-derived microparticles (PMPs) are produced upon platelet activation and have a high procoagulant effect [52]. Recently, Happonen et al. showed that PMPs are ingested in primary human ECs in a Gas6/Axl dependent manner [53]. In human, higher Gas6 levels were found in a cohort of patients with VTE as compared to healthy volunteers patients demonstrating an association between VTE and Gas6 levels expression and consistent with in $vivo$ murine findings [54]. In addition, analysis of single nucleotide polymorphisms (SNPs) from a cohort of stroke patients indicates statistically significant differences in the $Gas6$ allelic distributions as compared to healthy patients [55].

Gas6 plays a prominent role in erythropoiesis. Upon erythropoietin (EPO) stimuli, erythroblasts release Gas6 that bind to its TAM receptors on the cell surface. This binding leads to the activation of PI3K/Akt pathway and downstream signaling for cells proliferation and differentiation. Besides, Gas6 acts in an autocrine manner by boosting the erythropoietin receptor (EPOR) stimulation. The binding of Gas6 to TAM receptors activate the fibronectin

receptor VLA4 and increases erythroblasts adhesion and differentiation. Gas6 plays an important role in senescent RBC phagocytosis by macrophages [81].

PS complete deficiency induced PF is a quite enigmatic pathology. Its development mechanism is poorly understood although the imbalance between anticoagulant and procoagulant factors is thought to be the etiological factor. Recent findings suggested that PF could result not only from the lack of the PS anticoagulant effect, but may also be due to the lack of PS in the endothelium and its role in vascular development [96].

In the present report, we used three approaches to investigate the development of PF. Firstly, we mimicked severe PS deficiency using *Pros1* gene silencing by poly I: C-inducible *Mx1-Cre$^+$* in adult *Pros1$^{lox/-}$* mice. Secondly, we treated adult *Pros1$^{lox/-}$* mice with warfarin, a vitamin K antagonist, to further drop plasmatic PS and reproduce PF. Since *Gas6$^{-/-}$* mice are protected against thrombosis, our third strategy was to combine PS and Gas6 deficiency to assess if the hemostatic balance could be achieved and *Pros1$^{-/-}$* embryos rescued from fatal PF. The monitoring and investigations of developed PF lesions provided new insights into the PF development mechanism.

2.2 Material and methods

Generation of conditional floxed and knockout mice

Pros1$^{+/-}$, Gas6$^{-/-}$, Pros1$^{lox/lox}$ and *Pros1$^{lox/l-}$* mice were progeny of the original colonies, with a genetic background of 50% 129/Sv x 50% C57BL/6J, as described previously [81, 95]. *Mx1-Cre* mice with C57BL/6J background were obtained from The Jackson Laboratory. The Swiss Federal Veterinary Office approved the experiments. *Pros1$^{+/-}$* mice were genotyped by a multiplex PCR that amplifies the WT (+), lox and the null (-) alleles of *Pros1* gene at the same time, using primers previously described [95].

Pros1$^{lox/lox}$ and *Pros1$^{lox/l-}$* mice were mated with the *Mx1-Cre* mice to obtain *Pros1$^{lox/lox}$Mx1-Cre$^+$* and *Pros1$^{lox/l-}$Mx1-Cre$^+$* mice. Excision of genomic *Pros1* sequences was determined by PCR using the following primers P1: 5'-CGCGTCTGGCAGTAAAA-3' and P2: 5'-

CTAGGCCACAGAATTGAAAGATCT-3' yielding a 100-bp control band and 324-bp mutant band.

Pros1 gene silencing using Mx1- Cre system

8-10 weeks old _Pros1$^{lox/lox}$Mx1-Cre$^+$_ and _Pros1$^{lox/l-}$Mx1-Cre$^+$_ mice received an intraperiteal (i.p) injection of 250 μg of poly I: C (10μg/g) every other day for a total of three doses to eliminate _Pros1_ gene mainly in the liver and hematopoietic cells. Mice were monitored for 2 months.

Preparation of murine plasma and measurement of PS antigen by ELISA

Mice were anesthetized with pentobarbital (40 mg/kg) and whole blood was drawn from the inferior vena cava into 3.13% citrate (1 vol anticoagulant/9 vol blood). Blood was centrifuged at 2400 g for 10 min at room temperature (RT), to obtain platelet-poor plasma (PPP).

Wells from 96-well plates (Maxisorb, Thermo) were coated with 50 μL per well of 10 μg/mL of rabbit polyclonal anti-human PS (DAKO Cytomation) and incubated overnight at 4°C. After 3 washes with TBS buffer (0.05 M tris (hydroxymethyl)aminomethane, 0.15 M NaCl, pH 7.5, 0.05% Tween 20), the plate was blocked with TBS-BSA 2%. Diluted plasma samples (dilution range: 1:300-1:600) were added to the wells and incubated at RT for 2 h. After 3 washings, 50 μL of 1μg/mL biotinylated chicken polyclonal anti-murine protein S were added and incubated for 2 h at RT. Signal was amplified by streptavidin-HRP conjugated 19 horseradish peroxidase (Thermo) was added and plates incubated for 1 h. The plates were washed 3 times and 100 μL TMB substrate (KPL) was added. Reactions were stopped by adding 100 μL HCl (1M). Absorbance was measure at 450 nm. Standard curves were set up by using serial dilution of pooled normal plasma obtained from 14 healthy mice (8 males and 6 females, 7–12 weeks old). Results were expressed in percentage relative to the pooled normal plasma.

Tissue processing and sectioning, immunohistochemistry and microscopy

Liver, heart, lung, ear sections (4 μm) and sagittal embryos sections (5 μm) were performed

from paraffin embedded tissues. No pre-treatment was applied. Tissues were stained with hematoxylin/eosin, Masson Trichrome or Prussian blue. Whole slides were scanned using 3D HISTECH Panoramic 250 Flash II, with 20x (NA 0.8), 40x (NA 0.95) air objectives. Images processing was done using Panoramic Viewer software.

Warfarin per os treatment

8 to 10 weeks old mice received daily 0.8 mg warfarin for a total of 5 doses. Warfarin was freshly prepared before administration by dissolving 5 mg of warfarin (L1G59, Bristol-Myers Squibb) in 15 ml H_2O. A stainless steel feeding needle (FTSS-20S-38, Instech) was used. Mice were monitored during 12 days.

Timed matings and embryos harvesting

Pros1$^{+/-}$ timed matings were set to generate E14, E16 and E17.5 embryos. Mating was confirmed by detection of a vaginal plug and defined as day 0.5 pc. Embryos were harvested by dissecting the female uterus. Viability was assessed under a stereomicroscope (M80, Leica) coupled to a camera (MC170 HD, Leica) and photographed. DNA was extracted from the tails for genotyping. Embryos were then fixed in 4% paraformaldehyde (PFA) and embedded in paraffin.

Whole embryo or embryonic dorsal skin whole mount and immunofluorescence

Collected E11 embryos or embryonic dorsal skin (E16) were rinsed several times with ice-cold PBS and fixed in PFA 4% overnight. After 3 washings with ice-cold PBS (15 min each), they were incubated overnight in blocking buffer containing 0.5% BSA, 5% donkey serum (AbD Serotec), 0.3% Triton X-100, 0.1% Sodium Azide and PBS. The following antibodies (Abs) were used: PE conjugated anti-mouse PECAM1 (561073, BD Biosciences) 1:400 dilution; PE conjugated anti-mouse Ter119 (12-5921, Ebiosciences) 1:400 dilution; anti-mouse Lyve1 (MAB2125, R&D Systems) and anti-mouse VE Cadherin (ab33168, Abcam), both Abs were diluted 1:200 and Alexa Fluor 488 conjugated goat anti-rabbit (ab150077,

Abcam) used as secondary Ab at 1:500 dilution; anti-human fibrin (mAb clone 102-10) [175] at a final concentration of 15.6 μg/mL and secondary Ab Alexa Fluor 488 conjugated goat anti-human, (A-11013, ThermoFisher) 1:500 dilution; anti-mouse F4/80 (ab6640, Abcam) 1:100 dilution and secondary Ab Alexa Fluor 568 conjugated goat anti-rat (ab175476, Abcam) 1:500 dilution. Tissues were incubated in primary Abs overnight then extensively washed with washing buffer (0.3% Triton X-100 in PBS) before overnight incubation with secondary Abs. Next, stained tissues were washed 10 times (30 minutes each) and fixed in PFA 4%, mounted with ProLong Gold Antifade Mountant (P36930, ThermoFisher), dried overnight before microscopic observation. Tissues collection, incubation and washing steps were performed at 4°C. Staining was examined using the Zeiss LSM710 Laser scanning microscope for Z stacks (whole tissue thickness was identified by the top and bottom limits of fluorescence signal detection). EC Plan-Neofluar 40x/1.30 Oil DIC M27 /a=0.21mm was used as objective.

Images were acquired and optimized with ZEN system software. Imaris software (Bitplane AG, Switzerland) was used for visualisation of 3D confocal data, volume and surface rendering. Blood vascular networks, volume and branching, lymphatic vasculature volume were quantitatively estimated by unbiased stereological method [176]. Surface-related distribution was assessed by STEPanizer software [177].

Colony forming assay from embryonic liver

Single-cell suspensions from E14 fetal livers were prepared from finely minced livers using scissors. Next, cell aggregates were disrupted by passage through a 26-gauge needle. After a washing step with Iscove's MEM (31980048, Lifetechnologies) supplemented with 2% FBS (10082147, Lifetechnologies), 2.10^5 cell were plated with MethoCult™ medium (GF M3434, StemCell technologies) in Pre-tested 35 mm culture dishes (#27100, StemCell technologies). BFU-E were counted at day 7 and CFU-E at 12 days.

Flow cytometry on embryonic liver single-cell suspensions

Single-cell suspensions from E14 fetal livers were prepared as described above. Cells were then washed twice in FACS buffer (PBS with 2% FBS). After a centrifugation step, the remaining cell pellet was resuspended and incubated for 5 min at 4 °C in FACS buffer containing 1% FC block (anti-CD16/CD32, eBioscience). After an additional centrifugation, 2.10^5 cells were incubated for 30 min on ice with FITC conjugated anti-mouse CD71 (553266, BD Biosciences) diluted 1:200 and anti-mouse Ter119-PE (553673, BD Biosciences) diluted 1:200. Cells were then washed in FACS buffer, centrifuged at 1500 g for 5 min at 4°C and fixed in 2% PFA. Cells were analysed using an LSR II flow cytometer (BD Biosciences) and FACS Diva 7.0 software (BD Biosciences). Gating strategy was defined according to literature [178]. Cell-surface markers CD71, Ter119 and cell size were used as parameters to identify developmental sequence of 5 subsets (S1, S2, S3, S4 and S5) corresponding to increasingly mature erythroblasts.

Cytospin on embryonic liver single-cell suspensions

Single-cell suspensions from E14 fetal livers were prepared as previously described. After washing step with Iscove's MEM supplemented with 2% FBS, 2.10^5 cell were used to attach on a cytospin slide (500rpm/ 5min). Cells on cytospin slides were stained with May-Grunwald-Giemsa (MGG) before observation under optical microscope.

Statistical methods

Values were expressed as mean plus or minus s.e.m. A Chi-square for non-linked genetic loci was used to assess the Mendelian allele segregation. Survival data in the warfarin treatment were plotted using the Kaplan-Meier method. A log-rank test was used to statistically compare the curves (Prism 6.0d; GraphPad). The other data were analysed by t-test, one-way and two-way ANOVA test with GraphPad Prism 6.0d. A P-value of less than 0.05 was considered statistically significant.

2.3 Results

A low plasmatic level of PS was sufficient to protect $Pros1^{lox/-}Mx1-Cre^+$ from PF

In order to reduce PS and mimic acquired PS deficiency, 8 to 10 weeks old $Pros1^{lox/lox}Mx1-Cre^+$ and $Pros1^{lox/-}Mx1-Cre^+$ mice were injected intraperitoneally 3 times with 250 µg poly I: C. After a resting period of 10 days, mice were sacrificed. Immunohistochemical analysis of sections indicated spontaneous thrombosis in lung, heart and liver sections from both $Pros1^{lox/lox}Mx1-Cre^+$ and $Pros1^{lox/lox}Mx1-Cre^+$ mice. However, no PF lesions were observed within a 2-month observation period (Fig.1, a-c). Plasmatic PS (antigenic) level was investigated by ELISA. As expected, $Pros1^{lox/lox}$ (n=16) and $Pros1^{lox/-}$ (n=8) control mice had respectively 103.1% ± 3.259% and 39.46% ± 4.576% PS antigenic level (P<0.0001) (Fig.1, d). Differently, $Pros1^{lox/lox}Mx1-Cre^+$ mice (n=17) had 48.27% ± 2.787% PS antigenic level while $Pros1^{lox/-}Mx1-Cre^+$ mice (n=11) displayed further reduced PS level: 16.63% ± 2.039% (P<0.0001) (Fig.1, e). The poly I: C-inducible $Mx1-Cre$ recombination stability was investigated over time (70 days after the last poly I: C injection) and found stable. These results suggest that very low circulating PS level (16.63% ± 2.039%) is sufficient to protect mice against PF.

Warfarin treatment reproduced PF only in a few $Pros1^{+/-}$ mice

To evaluate if a very low PS plasmatic level could be achieved, 8 to 12 old $Pros1^{+/+}$ (n=13) and $Pros1^{+/-}$ mice (n=8) received per os, 5 doses of 0.8mg warfarin per day. As a vitamin K antagonist, warfarin should prevent the gamma-carboxylation of PS requiring vitamin K, and the production of its active form, resulting in low active PS level in the circulation. We monitored mice survival and found that differently to $Pros1^{+/+}$, most of $Pros1^{+/-}$ mice succumbed to the warfarin challenge (12 vs 92%, respectively) (Fig.2, a). Only a few surviving $Pros1^{+/-}$ mice developed lesions that are compatible with PF. Interestingly, macroscopical analysis of ears skin of these mice revealed highly visible ears skin vessels at day one of the warfarin treatment. After 4 days, the hemorrhagic infarction of the skin was

more visible. 7 days later, there was a complete ear skin necrosis. Histological analysis of the developed lesions using Masson's Trichrome staining revealed that at day 1 of the treatment, a small number of thrombi were observed together with intradermal edema. 4 days later, a prominent vascular engorgement was visualised. After 7 days, there was a massive extravasation of red blood cells (RBC) in the surrounding areas of the vessels with several intra-epidermal hemorrhagic blisters (Fig.2, b). The evaluation of the formed skin lesions over time revealed thrombi occurring together with vascular wall damage. These data suggest that the endothelium may play an important role in PF development.

Fibrin deposition and vasculature disruption in whole mounted *Pros1*$^{-/-}$ embryo's dorsal skin

To investigate the role of PS in the vasculature, *Pros1*$^{+/+}$ and *Pros1*$^{-/-}$ embryos were generated by intercrossing *Pros1*$^{+/-}$ adults mice. As expected and previously described [95, 96], macroscopic observation revealed *in utero Pros1*$^{-/-}$ dead embryos between E14 and full term with large thrombi and massive hemorrhages throughout the body (Fig.3, a,b). These anomalies were never observed in *Pros1*$^{+/+}$ embryos. Histological examination of *Pros1*$^{-/-}$ embryos sections showed intracranial hemorrhages with brain necrosis. Besides, RBC were present in the extra-vascular compartments particularly in the back pointing to a severe vascular defect (Fig.3, c,d). The dorsal skin of E16 *Pros1*$^{+/+}$ and *Pros1*$^{-/-}$ embryos was than whole mounted and immunostained. Anti-fibrin and anti-PECAM1 antibodies (Ab) immunofluorescence (IF) indicated well-formed and branched vascular network in *Pros1*$^{+/+}$ embryos (Fig.3, e). In contrast, intra- and extra-vasal insoluble fibrin (Fig.3, f) was found with destruction of the vascular bad (Fig.3, g) in *Pros1*$^{-/-}$ embryos. IF with anti-VE-Cadherin and anti-Ter119 Ab showed tight vascular endothelial cell junctions with RBC within the vessels in *Pros1*$^{+/+}$ embryos (Fig.3, h). Differently, massive RBC extravasation, underdeveloped and collapsed vascular network were observed in *Pros1*$^{-/-}$ embryos (Fig.3, i). Furthermore, areas with rare and dispersed vascular structures were found in *Pros1*$^{-/-}$ (Fig.3, j). To evaluate the extend of the vasculature defect in *Pros1*$^{-/-}$, anti-PECAM1 IF was

performed in the dorsal skin of $Pros1^{+/+}$ and $Pros1^{-/-}$ embryos. Interestingly, very reduced and distributed immunostaing was found in poorly formed vascular networks with few vessels branch points in $Pros1^{-/-}$ as compare to $Pros1^{+/+}$ embryos. $Pros1^{-/-}$ and $Pros1^{+/+}$ vasculature density was quantified using an unbiased stereological approach. Although not statistically significant, the dorsal skin of $Pros1^{-/-}$ embryos displayed reduced vascular volume as compared to $Pros1^{+/+}$ embryos (18.67 ± 0.8819 vs 22.33 ± 1.856, n=3, respectively) (Fig.3,k). Vessels' branching was also examined. Approximately 2 times more branch points were found in $Pros1^{+/+}$ as compare to $Pros1^{-/-}$ embryos (11.07 ± 0.636 vs 5.7 ± 0.7572, n=3, respectively. $P<0.005$) (Fig.3, l).

One question arises from the examination of the vasculature: are the observed vascular defects secondary to thrombosis and PF or due to the absence of PS role in the vasculature? Conflicting data claiming pro- or anti-angiogenic functions of PS were previously published [96, 113, 116]. In this study, we aimed to evaluate the vasculature before PF begun.

PF starts at around E14. In practice, since the embryonic dorsal skin whole mount could not be accomplished earlier than E15.5, we then decided to perform anti-PECAM1 IF in whole mounted E11 $Pros1^{+/+}$ and $Pros1^{-/-}$ embryos to evaluate the vasculature before PF starting. Surprisingly, the size of vessels was smaller with undeveloped vasculature hierarchy in $Pros1^{-/-}$ embryos as compare to $Pros1^{+/+}$ (Fig.3, m,n). Therefore, in $Pros1^{-/-}$ embryos, the vasculature is disturbed before PF starts. These results confirmed that during PF, not only the thrombotic process is relevant. The involvement of PS in vasculature development should also be considered and PS assuredly plays a prominent role during angiogenesis.

PS complete deficiency promotes inflammation

To explore the inflammatory process in the context of PS complete deficiency, The dorsal skin of E16 $Pros1^{+/+}$ and $Pros1^{-/-}$ embryos was immunostained with anti-PECAM1 and anti-Lyve1 ab. Intriguingly, $Pros1^{-/-}$ embryos displayed massively enlarged lymphatic vessels as compared to discret ones in $Pros1^{+/+}$ (Fig.4, a,b). Unbiased stereological analysis revealed about 3 times higher lymphatic vasculature volume in $Pros1^{-/-}$ as compared to $Pros1^{+/+}$

embryos (11.43 ± 0.6984 vs 2.967 ± 0.393, n=3, respectively, P<0.0005) (Fig.4, c). Furthermore, anti-F4/80 IF showed greater macrophages infiltration in *Pros1*$^{-/-}$ than in *Pros1*$^{+/+}$ embryos (Fig.4, d,e). Thus, complete PS deficiency promotes inflammation.

PS complete deficiency causes erythropoietic and phagocytic defects.

It was previously described that *Pros1*$^{-/-}$ embryos exhibit pallor in the feet and the nose that could be due to anemia secondary to bleeding [95]. We then further explored the role of PS in erythropoiesis. Histology of major blood vessels and liver from *Pros1*$^{+/+}$ and *Pros1*$^{-/-}$ embryos revealed a high number of circulating immature RBC (Fig.5, a,b: arrows head). The percentage of circulating nucleated RBC was approximately 2 fold higher in *Pros1*$^{-/-}$ as compared to *Pros1*$^{+/+}$ embryos (7.7 ± 0.6658 vs 4.033 ± 0.1453, respectively, n=3 per group, P<0.005) (Fig.5, c) compatible with increased erythropoiesis possibly due to severe bleeding due to consumption coagulopathy and vascular damage in *Pros1*$^{-/-}$ embryos. To explore whether the anemia could be attributable to a defect in erythroid progenitor cells or exclusively secondary to bleeding, liver cell cytology from E14.5 embryos was performed. We found higher erythroid islands with a central macrophage surrounded by immature erythroblasts (Fig.5, d, e arrows) and less mature RBC (Fig.5, d, e arrows head) in *Pros1*$^{-/-}$ as compared to *Pros1*$^{+/+}$ embryos (Fig.5, d,e). Furthermore, equal numbers of liver single-cell suspension from E14.5 *Pros1*$^{+/-}$ and *Pros1*$^{-/-}$ embryos were plated *in vitro* for colonies forming assay (CFA). After 7 days, BFU-E colonies number was similar in *Pros1*$^{+/-}$ and *Pros1*$^{-/-}$ (6.833 ± 1.249, n=6 vs 7.75 ± 1.109, n=4, respectively) (Fig.5, f). Differently, fewer CFU-E colonies developed in *Pros1*$^{-/-}$ as compared to *Pros1*$^{+/-}$ (42.8 ± 4.633 vs 77.8 ± 9.566, n=5 per group, P<0.05) (Fig.5, g). To further examine the involvement of PS in the erythropoietic process, liver single-cells suspension were also analysed by flow cytometry. Cell-surface markers CD71, Ter119 and cell size were used as parameters to identify developmental sequence of 6 subsets (S0, S1, S2, S3, S4 and S5) corresponding to increasingly mature erythroblasts (Fig.5, h). *Pros1*$^{-/-}$ embryos displayed fewer mature RBC as compared to *Pros1*$^{+/-}$ (0.1 ± 0.01 vs 0.276 ± 0.04, n=3 per group, P<0.05) (Fig.5, i). These

data confirmed results obtained from cytospin and CFA experiments and suggest a prominent role of PS during erythroid cells differentiation. Since PS is a multifunctional protein that also has the capacity to stimulate macrophage phagocytosis by binding to and activating TAM RTKs [153, 179], we examined whether the lack of PS could affect phagocytosis in $Pros1^{-/-}$ embryos. Interestingly, inspection of embryonic $Pros1^{-/-}$ blood vessels showed numerous isolated nuclei that were not phagocyted by macrophages as compared to $Pros1^{+/+}$ embryos (Fig.5, b: arrows). Thus, the lack of PS also impaired phagocytosis.

Gas6-PS combined deficiency did not prevent PF and embryonic lethality observed in $Pros1^{-/-}$ **mice**

$Gas6^{-/-}$ adult mice were previously described to be protected against venous and arterial thrombosis [13]. Therefore, we hypothesized that combining Gas6 and PS deficiency could restore the hemostatic balance and rescue $Pros1^{-/-}$ embryos from PF. In this regard, $Pros1^{+/-}Gas6^{-/-}$ adult mice were intercrossed in order to obtain viable $Pros1^{-/-}Gas6^{-/-}$ mice. Among 120 litters genotyped, no viable $Pros1^{-/-}Gas6^{-/-}$ was found indicating, as for $Pros1^{-/-}$ embryos, *in utero* mortality. We then decided to set timed matings $Pros1^{+/-}Gas6^{-/-}$ to investigate the $Pros1^{-/-}Gas6^{-/-}$ embryonic phenotype. The macroscopical analysis of $Pros1^{-/-}Gas6^{-/-}$ embryos harvested at different embryonic stages revealed large blood clots and massive hemorrhages throughout the body (Fig.6, a). Interestingly, $Pros1^{-/-}Gas6^{-/-}$ embryos displayed signs of PF appearing earlier as compare to $Pros1^{-/-}$ embryos. Indeed, at E14, 80% (8/10) of $Pros1^{-/-}Gas6^{-/-}$ embryos exhibited widespread hemorrhages versus only 36% (4/11) for $Pros1^{-/-}Gas6^{+/+}$ embryos whereas at E16, 100% embryos (7/7 for $Pros1^{-/-}Gas6^{-/-}$ and 14/14 for $Pros1^{-/-}Gas6^{+/+}$) displayed widespread hemorrhages (Fig.6, c). In addition, embryos mortality rates where higher when issued from $Pros1^{+/-}Gas6^{-/-}$ matings. Indeed, at E14, 8% (3/35) dead embryos were found from $Pros1^{+/-}Gas6^{-/-}$ matings versus only 2% (1/46) from $Pros1^{+/-}Gas6^{+/+}$ matings. Similarly at E16, 25% (8/32) dead embryos were found in $Pros1^{+/-}Gas6^{-/-}$ matings versus only 4% (3/62) in $Pros1^{+/-}Gas6^{+/+}$ matings (Fig.6, d).

Furthermore, *Pros1^{-/-}Gas6^{-/-}*embryos were under represented. With 25% expected *Gas6^{-/-}* *Pros1^{-/-}* embryos (Mendelian frequency), at E14, E16 and E17.5, only 17%, 18% and 16% were respectively observed. Exclusively when issued from *Pros1^{+/-}Gas6^{-/-}* matings, from E16 onwards, nearly 10% (7/72) of embryos were found underdeveloped, macerated and necrotic indicating their earlier death as compare to *Pros1^{-/-}* embryos (Fig.6, b). Thus, combined deficiency in Gas6 and PS did not rescue *Pros1^{-/-}* embryos from fatal PF, the *Pros1^{-/-}Gas6^{-/-}* phenotype appearing more dramatic with earlier and more frequent embryonic death.

*Pros1^{-/-}Gas6^{-/-}*embryos display vascular defects and inflammation.

As for *Pros1^{-/-}* embryos, *Pros1^{-/-}Gas6^{-/-}* embryonic dorsal skin was used for immunostaining. Anti-fibrin and anti-PECAM1 Ab IF allowed the detection of intra- and extra-vasal insoluble fibrin and damaged vasculature in *Pros1^{-/-}Gas6^{-/-}* but not in *Pros1^{+/+}Gas6^{-/-}* emrbyos. IF with anti-VE-Cadherin and anti-Ter119 Ab showed tight endothelial vascular cell junctions and RBC within the vessels in *Pros1^{+/+}Gas6^{-/-}* emrbyos. In contrary, massive RBC extravasation, blood overfilled vessels and underdeveloped vascular network were observed in *Pros1^{-/-}Gas6^{-/-}* embryos (Fig.6, e). Anti-PECAM1 and anti-Lyve1 ab IF showed hyperplasic lymphatic vessels in *Pros1^{-/-}Gas6^{-/-}* as compared to *Pros1^{+/+}Gas6^{-/-}* embryos indicating ongoing inflammatory process (Fig.6, f, g).

Combined deficiency in Gas6 and PS is responsible of more severe erythropoitic defects

Previous reports indicated that Gas6 plays a critical role in the generation of erythroid progenitors and erythroblasts [81]. Here we assessed the consequence of combined PS and Gas6 deficiency in this process. Histology of major embryonic blood vessels indicated the presence of a higher number of immature erythrocytes in *Pros1^{-/-}Gas6^{-/-}* as compare to *Pros1^{+/+}Gas6^{-/-}* embryos (data not shown). Results of cytospin from fetal liver single-cells suspension showed a higher number of erythroid islands (Fig.7, a, b arrows) and less mature RBC (Fig.7, a, b arrows head) in *Pros1^{-/-}Gas6^{-/-}* compared to *Pros1^{+/+}Gas6^{-/-}* embryos. Equal number of liver cells isolated from *Pros1^{+/-}Gas6^{-/-}* and *Pros1^{-/-}Gas6^{-/-}* embryos were plated for

CFA. Differently to *Pros1$^{+/-}$Gas6$^{-/-}$*, *Pros1$^{-/-}$Gas6$^{-/-}$* contained less BFU-Es (5 ± 1, n=3 vs 8.5 ± 0.866, n=4, respectively, P<0.05) (Fig.7, c) and less CFU-Es (51.25 ± 3.75, n=4 vs 32.67 ± 6.207, n=3, respectively, P<0.05) (Fig.7, d). Moreover, very high level of hypochromic erythrocytes was exclusively found in *Pros1$^{-/-}$Gas6$^{-/-}$* suggesting troubled iron metabolism linked to inflammation and iron recycling (Fig.7, e, f arrows). Additionally, specific iron staining (Prussian blue) revealed higher iron deposition in *Pros1$^{-/-}$Gas6$^{-/-}$* embryonic tissue further confirming disturbed iron metabolism (Fig.7, g, h). Thus, the absence of PS and Gas6 leads to a more dramatic deficit in embryonic erythroid precursor cells and altered iron recycling compared to single PS deficiency.

Like for PS, several reports highlighted the role of Gas6 in phagocytosis [81, 179]. Histological investigation of major blood vessel revealed altered clearance of isolated nuclei by macrophages in *Pros1$^{-/-}$ Gas6$^{-/-}$* and not in *Pros1$^{+/+}$Gas6$^{-/-}$* (Fig.7, e, f arrows head) indicating altered phagocytosis.

2.4 Discussion

PS complete deficiency leads to fatal PF [117] [118]. The pathophysiological mechanism of PF remains enigmatic. The results of this study provide new insights into PF lesions development. As for human, we confirmed that *Pros1$^{-/-}$* mice died *in utero* from massive hemorrhages and DIC. Our first approach to understand PF etiology was to knock down *Pros1* gene in adult *Pros1$^{lox/-}$* mice by using the Mx1-Cre system to achieve null or very low PS level in order to subsequently induce PF. With 16% PS in their plasma, polyI:C treated *Pros1$^{lox/-}$Mx1cre^{+}* mice did not develop PF demonstrating that a low level of PS could still protect mice against PF. Patients with parcial PS deficiency display higher VTE risk [92]. *Pros1$^{+/-}$* mice displayed accelerated clotting in plasma [96] and increased number of thrombi in the lungs after tissue factor-induced thromboembolism challenge [95]. Similarly, the investigation of organs (liver, lung and heart) from *Pros1$^{lox/lox}$Mx1-Cre^{+}* and *Pros1$^{lox/-}$Mx1-Cre^{+}* mice treated with polyI:C (48% and 16% plasmatic PS respectively) confirms that PS

partial lack induces thrombosis. Like factor II, VII, IX, protein C, and Z, PS needs vitamin K as cofactor for post-translational γ-glutamylcarboxylation to achieve full biological activity [180]. By interfering with the vitamin K–driven γ-carboxylation process, warfarin is widely used as a long-term anticoagulation therapy in humans. In rare cases (0.01%-0.1%), large doses of warfarin treatment provoke skin necrosis as an adverse drug reaction [181]. Our second strategy was then to administer warfarin to $Pros1^{+/-}$ mice to further drop PS and induce PF. Despite the high mortality rates under this medication, only a few mice developed lesions compatible with PF. The analysis of these lesions over time revealed that during PF development, the vasculature is disrupted with more permeable and leaky vessels. Previous *in vitro* studies claimed a role of PS in vasculature development and maintenance [113] [114]. *In vivo*, the lack of PS impairs the vascular development [96]. Up to date, the mechanism of PF development in the context of PS complete deficiency is controversial [119, 182]. One hypothesis is that the lack of PS causes imbalance of the hemostatic balance and provokes thrombosis that subsequently damages the vessels. However, this hypothesis did not take into consideration that besides its role as an anticoagulant, PS exerts important roles in the endothelium, phagocytosis and immunity. Consequently, an answer to the question whether PS deficiency induced PF is exclusively secondary to thrombosis or rather due to the lack of PS signaling in endothelium or both is still awaited. In order to respond to this question, we decide to characterize the vasculature of $Pros1^{-/-}$ embryos. As expected, the lack of PS leads to thrombosis with insoluble fibrin deposition within the vessels. Nevertheless, poor vasculature hierarchy, leaky vessels and areas without any vascular structures were exclusively observed in E16 $Pros1^{-/-}$ embryos presenting PF. Since PF starts at about E14, we supposed that these vascular defects might be secondary to PF. We studied E11 $Pros1^{-/-}$ embryos and surprisingly, vascular defects were also evident before PF begins. Our findings suggest that contradictory to what is currently admitted, PS deficiency induced PF is not strictly secondary to the imbalance of pro- and anticoagulant factors, but also to the lack of PS signaling in the endothelium. Since PS plays also a role in phagocytosis [153] and inflammation [167], we investigated whether this two biological processes were altered in

Pros1⁻/⁻ embryos. Remarkably, numerous isolated nuclei were not efficiently phagocyted by macrophages in *Pros1⁻/⁻* embryos. In addition, hyperplastic lymphatic vessels and macrophage infiltration highlighted prominent signs of inflammation. Thus, the lack of PS causes inadequate phagocytosis and promotes inflammation. The role of PS in erythropoiesis was not previously addressed. We know from previous reports that *Pros1⁻/⁻* embryos exhibit pallor that could be due to anemia secondary to bleeding [95] and that Axl and Mer might influence erythropoiesis [83]. Since PS is a well known ligand for Mer, we investigated if the lack of PS could impair erythropoiesis. We found high number of circulating immature RBC and less CFU-E in E14 *Pros1⁻/⁻* embryos. These erythropoietic defects might be secondary to bleeding and consumptive coagulopathy occurring during PF but this does not rule out that PS might play a direct role in erythropoiesis. Further experiments examining the erythropoietic process before PF beginning in *Pros1⁻/⁻* will elucidate the implication of PS.

Our strategy to combine PS and Gas6 deficiencies was motivated by the hypothesis that PF derives strictly from the hemostatic imbalance due to lack of PS anticoagulant activity. Since *Gas6⁻/⁻* mice are protected against thrombosis, we expected to rebalance the hemostatic balance and rescue *Pros1⁻/⁻* from fatal PF. Intriguingly, no viable *Pros1⁻/⁻Gas6⁻/⁻* mice were observed. The investigation of *Pros1⁻/⁻Gas6⁻/⁻* embryos revealed a more severe phenotype and a higher mortality as compared to *Pros1⁻/⁻* embryos. Similar to *Pros1⁻/⁻*, vascular defects, ongoing inflammation and altered phagocytosis were observed in *Pros1⁻/⁻Gas6⁻/⁻* embryos.

Gas6 plays a prominent role in erythropoiesis and its lack decreases embryonic erythroid precursor cells [81]. The examination of the erythropoietic process in *Pros1⁻/⁻Gas6⁻/⁻* indicates more extensive erythropoiesis impairment with iron recycling defects. This could be explained by an accumulative alteration of the erythropoiesis due to the absence of both PS and Gas6.

In conclusion, our findings provide evidence that the thrombotic process occurring in the context of PF induced by PS deficiency might be less central than currently admitted. PS possibly plays an important role in vasculature development. The lack of its signalling in the endothelium might lead to vascular defects and promotes PF. Further investigations are

required to better characterise the mechanism by which PS is involved in vascular development and maintenance.

2.5 Figures:
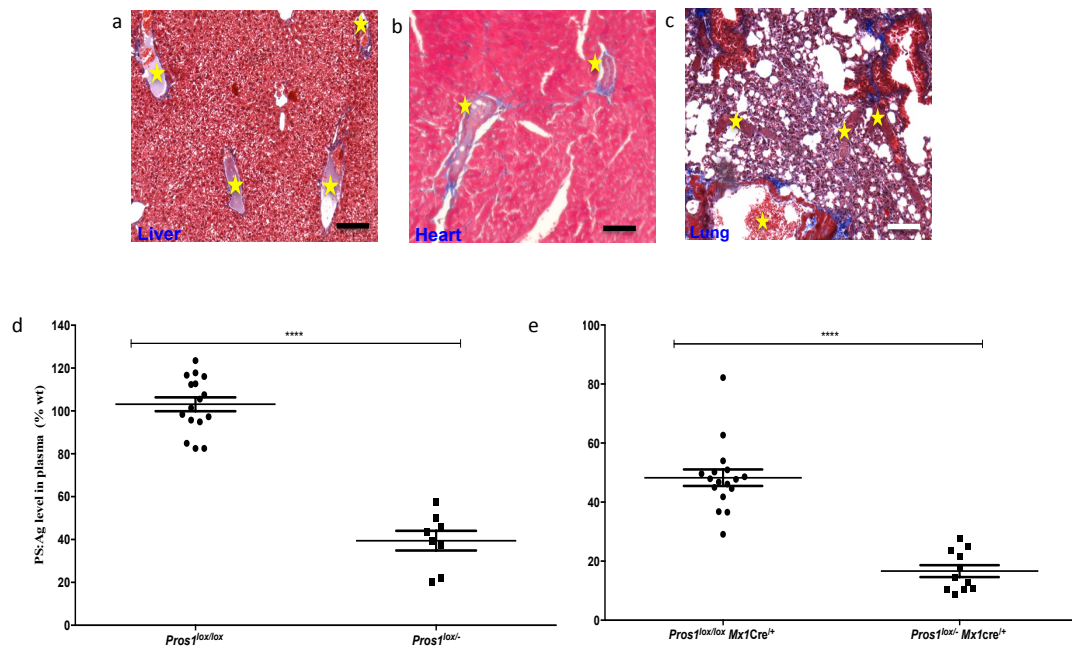
Figure 1: Partial *Pros1* gene silencing using *Mx1Cre* system

Pros1$^{lox/lox}$Mx1-Cre$^+$ and *Pros1$^{lox/-}$Mx1-Cre$^+$* mice were injected 3 times i.p. with 250 μg poly I: C every other day. Ten days after, mice were sacrificed and the organs were collected. **a, b, c**, microscopic evaluation of liver, heart and lungs stained with Masson's Trichrome, bar size 100 μm. **d,** plasmatic PS (antigenic) level measured by ELISA in *Pros1$^{lox/lox}$* (n=16), *Pros1$^{lox/-}$* (n=8), **e**, *Pros1$^{lox/lox}$Mx1-Cre$^+$* (n=17) and *Pros1$^{lox/-}$Mx1-Cre$^+$* (n=11) mice. Measurements are presented as mean±s.e.m. ****, P<0.0001.
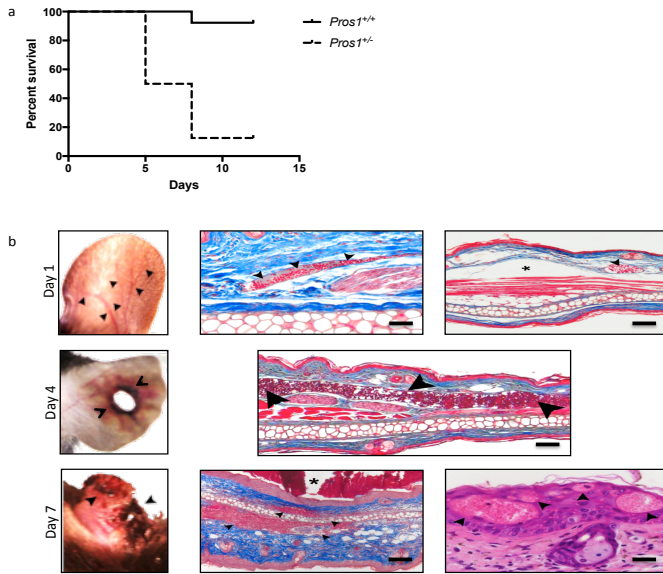
Figure 2: Warfarin treatment to reduce the level of plasmatic protein S and induce purpura fulminans

a, Kaplan Meier plots of *Pros1*^{+/+} (n=13) and *Pros1*^{+/-} (n=8) mice survival after warfarin per os treatment (5 doses of 0.8mg/ day). **b**, macroscopic images of ears from *Pros1*^{+/-} mice 1, 4 and 7 days h after warfarin treatment and corresponding microscopic evaluation (Masson's Trichrome) data were pooled from multiple independents experiments. Bar size 100μm.
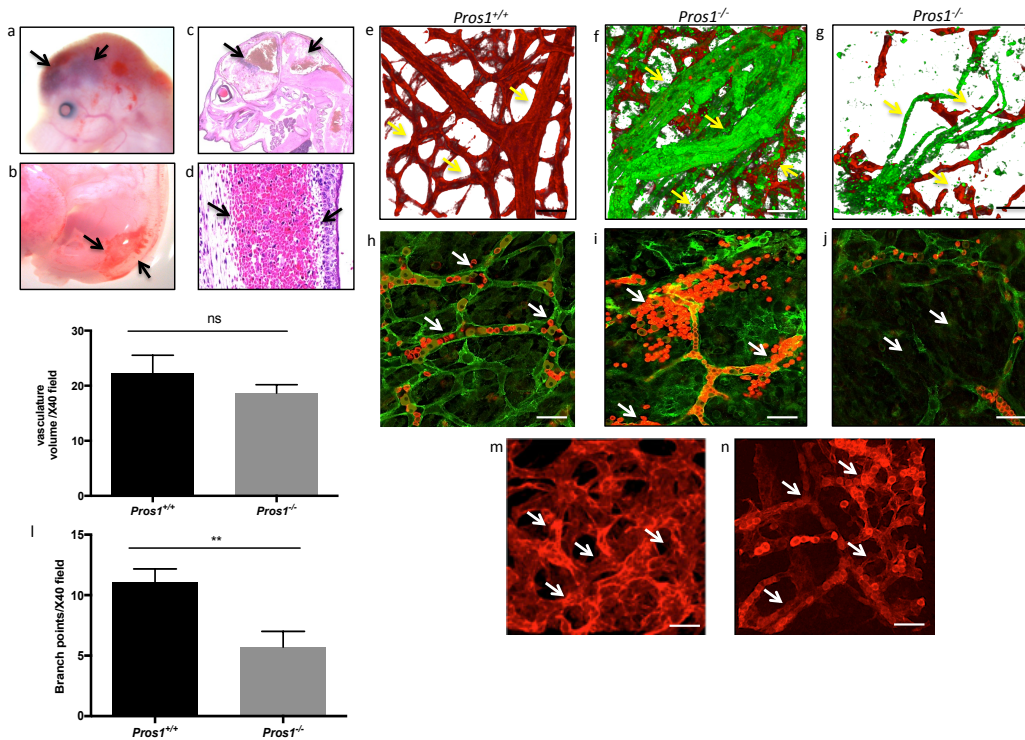
Figure 3: Complete deficiency in protein S alters vasculature

a, b, macroscopical observations of E16 *Pros1*^{-/-} embryo with purpura fulminans and corresponding microscopic evaluation of H&E stained sections **c, d. e-j**: *Pros1*^{+/+} and *Pros1*^{-/-} embryonic whole mounted dorsal skin (E16) immunofluorescence (IF) using anti-fibrin antibody (Ab) in green and anti-PECAM1 Ab in red (**e-g**), anti-VE Cadherin Ab in green and anti-Ter119 in red (**h-j**). Anti- PECAM1 IF of E11 *Pros1*^{+/+} and *Pros1*^{-/-} whole mounted embryos (**m, n**). Bar size 30μm. **k**, evaluation of vascular density and (**I**) vessels branching in *Pros1*^{+/+} (n=3) and *Pros1*^{-/-} (n=3) embryonic dorsal skin using stereology and STEPanizer software. All data are expressed as mean±s.e.m. ns, not significant **, P<0.005.
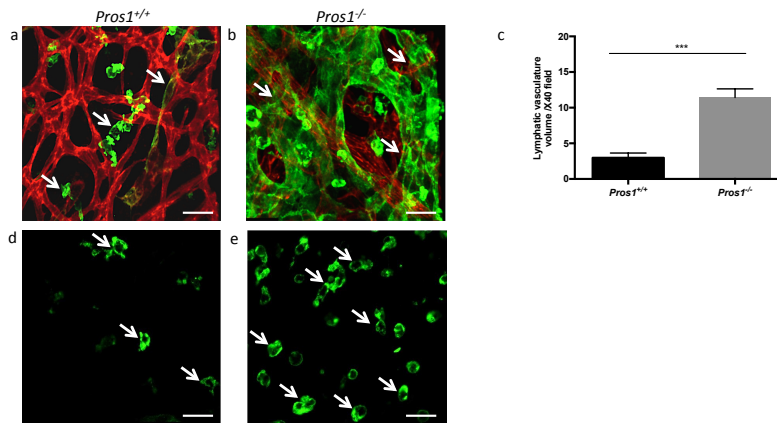
Figure 4: Protein S complete deficiency increases inflammation.

a, b, *Pros1*^{+/+} and *Pros1*^{-/-} embryonic whole mounted dorsal skin (E16) immunofluorescence using anti-Lyve1 antibody (Ab) in green and anti-PECAM1 Ab in red (**d,e**), anti-F4/80 Ab in green. Bar size 30μm. **c**, evaluation of lymphatic vasculature density in *Pros1*^{+/+} (n=3) and *Pros1*^{-/-} (n=3) embryonic dorsal skin using stereology and STEPanizer software. All data are expressed as mean±s.e.m. **, P<0.005.
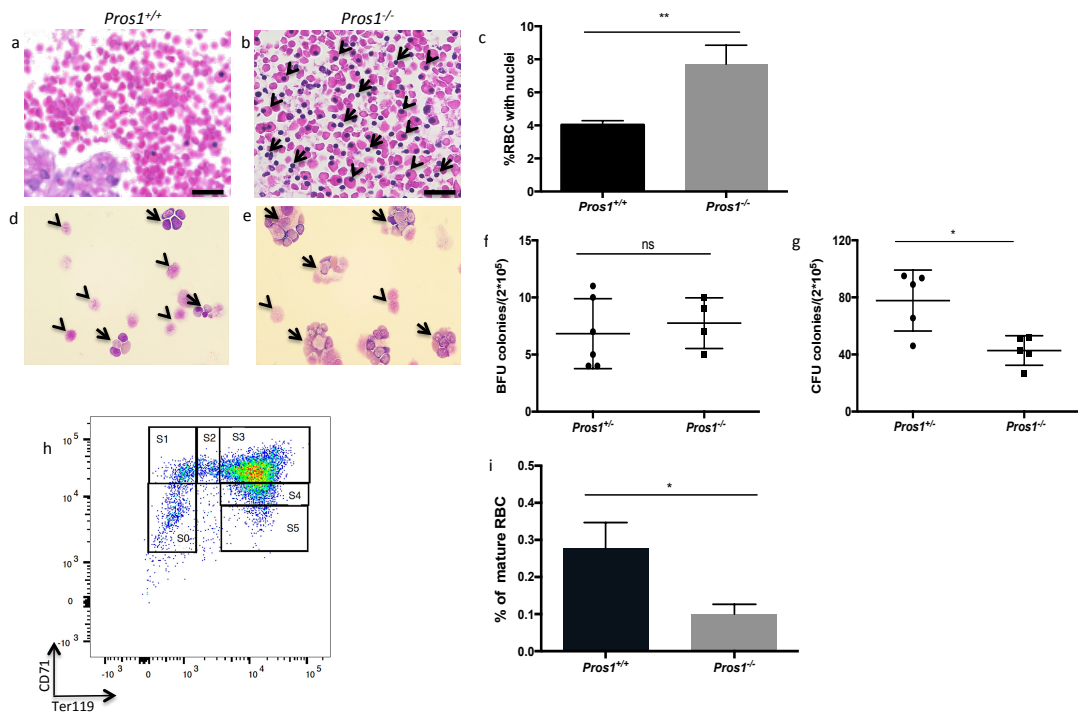
Figure 5: Protein S complete deficiency provokes erythropoietic defects.

a, b, microscopic evaluation (H&E) of embryonic (E16) major blood vessels from *Pros1*$^{+/+}$ and *Pros1*$^{-/-}$. **c,** quantification of circulating RBC that still contain their nuclei in *Pros1*$^{+/+}$ (n=3) and *Pros1*$^{-/-}$ (n=3). **d, e**, 2.10^5 liver (E14.5) single-cells suspension cytospin from *Pros1*$^{+/+}$ and *Pros1*$^{-/-}$. **f, g,** 2.10^5 liver single-cells suspension (E14) *Pros1*$^{+/-}$ (n=5) and *Pros1*$^{-/-}$ (n=4) were plated *in vitro* for colonies forming assay (CFA). BFU-E colonies were scored after 7 days and CFU-E colonies after 12 days. **h,** liver single-cells suspension (E14) were used for FACS analysis. Cell-surface markers CD71, Ter119 and cell size were used as parameters to identify developmental sequence of four 6 subsets (S0, S1, S2, S3, S4 and S5) corresponding to increasingly mature erythroblasts. **i,** evaluation of cell-surface markers CD71, Ter119 and cell size to identify mature RBC percentage (S5) in *Pros1*$^{+/-}$ and *Pros1*$^{-/-}$ (n=3 per group). All data are expressed as mean±s.e.m. ns, not significant, *, P<0.05.**, P<0.005.
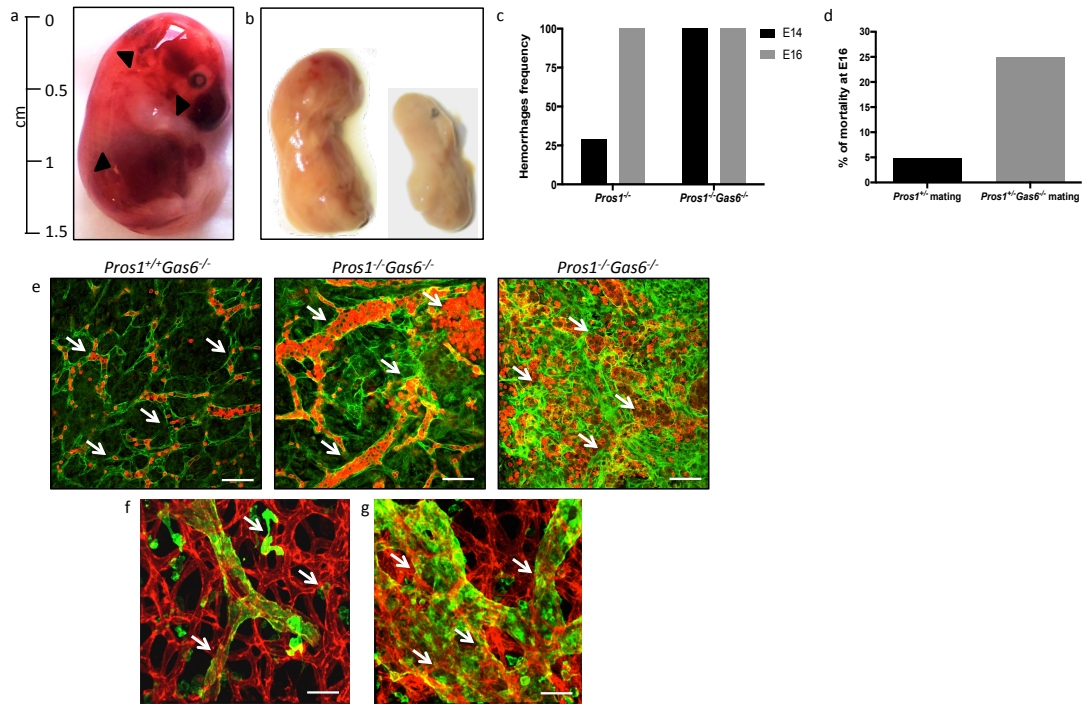
Figure 6: **Gas6/PS combined deficiency did not prevent PF**

a, macroscopical observations of E16 *Pros1⁻/⁻Gas6⁻/⁻* embryo with purpura fulminans and macerated embryos (**b**). **c**, evaluation of hemorrhages frequency in *Pros1⁻/⁻Gas6⁺/⁺* (n=11 for E14 and n=14 for E16) and *Pros1⁻/⁻Gas6⁻/⁻* (n=10 for E14 and n=7 for E16). **d**, evaluation of embryos mortality at E16 in *Pros1⁺/⁻Gas6⁺/⁺* and *Pros1⁺/⁻Gas6⁻/⁻* matings. **e**, embryonic whole mounted dorsal skin (E16) immunofluorescence using anti-VE Cadherin Ab in green and anti-Ter119 in red, (**f**,**g**) anti-Lyve1 antibody (Ab) in green and anti-PECAM1 Ab in red. Bar size 30μm.
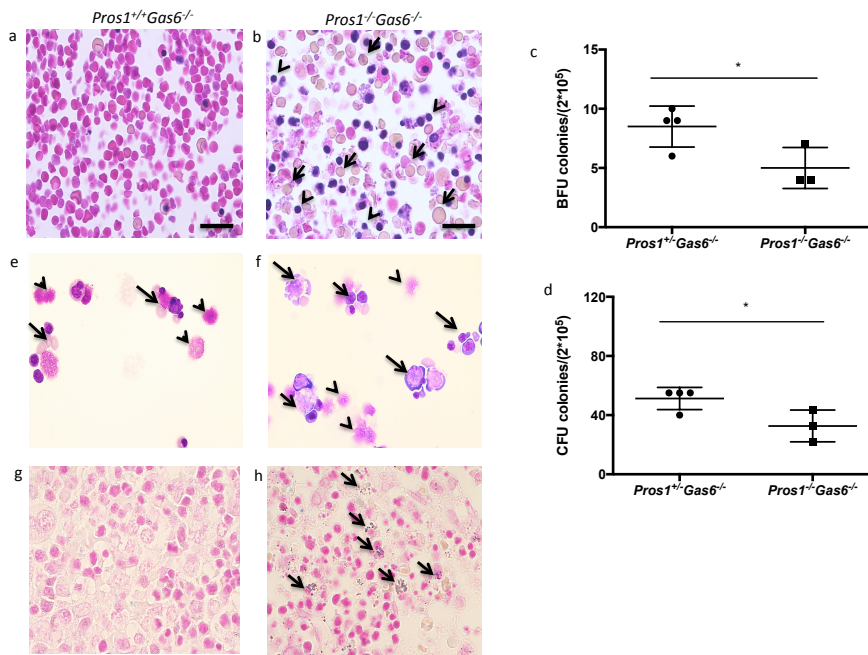
Figure 7: **Protein S and Gas6 combined deficiency leads to erythropoietic defects.**

a, b, microscopic evaluation (H&E) of embryonic (E16) major blood vessels from $Pros1^{+/+}Gas6^{-/-}$ and $Pros1^{-/-}Gas6^{-/-}$. **c**,**d**, 2.10^5 liver (E14.5) single-cells suspension cytospin from $Pros1^{+/+}Gas6^{-/-}$ and $Pros1^{-/-}Gas6^{-/-}$. **e, f,** 2.10^5 liver single-cells suspension (E14.5) $Pros1^{+/-}$ (n=5) and $Pros1^{-/-}$ (n=4) were plated *in vitro* for colonies forming assay (CFA). BFU-E colonies were scored after 7 days and CFU-E colonies after 12 days. **g,h,** microscopic evaluation (Prussian blue) of iron deposition in embryonic (E16) blood vessels from $Pros1^{+/+}Gas6^{-/-}$ and $Pros1^{-/-}Gas6^{-/-}$ liver (E14.5) All data are expressed as mean±s.e.m. *, $P<0.05$.

Chapter III. Targeting anticoagulant protein S to achieve hemostasis in hemophilia

(Manuscript Submitted)

Chapter III. Targeting anticoagulant protein S to achieve hemostasis in hemophilia

Raja Prince[1,2*], Luca Bologna[1,2*], Mirko Manetti[3], Daniela Melchiorre[4], Irene Rosa[3], Natacha Dewarrat[1,2], Poorya Amini[5], José A. Fernández[6], Laurent Burnier[6], Claudia Quarroz[1,2], Yasuhiro Matsumura[7], Johanna A. Kremer Hovinga[1,2], John H. Griffin[6], Hans-Uwe Simon[5], Lidia Ibba-Manneschi[3], François Saller[8], Sara Calzavarini[1,2**], Anne Angelillo-Scherrer[1,2**]

1) Department of Hematology and Central Hematology Laboratory, Inselspital, Bern University Hospital, University of Bern, CH-3010 Bern, Switzerland
2) Department of Clinical Research, University of Bern, Murtenstrasse 31, CH-3010 Bern, Switzerland
3) Department of Experimental and Clinical Medicine, Section of Anatomy and Histology, University of Florence, Florence, Italy
4) Department of Experimental and Clinical Medicine, Section of Internal Medicine, University of Florence, Rheumatology Unit, Careggi University Hospital, Florence, Italy
5) Institute of Pharmacology, University of Bern, Inselspital, INO-F, CH-3010 Bern, Switzerland
6) Department of Molecular and Experimental Medicine, The Scripps Research Institute, La Jolla, California 92037, USA
7) Division of Developmental Therapeutics, Research Centre for Innovative Oncology, National Cancer Centre Hospital East, Chiba, Japan
8) INSERM & UMR-S 1176, Université Paris-Sud, Université Paris-Saclay, 94270 Le Kremlin-Bicêtre, France

* Equal contribution first authorship; ** Equal contribution last authorship

Correspondence to: Prof. Anne Angelillo-Scherrer
                       Department of Hematology and Central Hematology Laboratory
                       Inselspital
                       Bern University Hospital
                       University of Bern
                       CH-3010 Bern
                       Switzerland
                       Phone: +41 31 632 33 02
                       e-mail: anne.angelillo-scherrer@insel.ch

Abstract

Improved treatments are needed for hemophilia A (HA) and B (HB), bleeding disorders affecting 400,000 people worldwide. Here we report that targeting protein S (PS), an anticoagulant acting as cofactor for activated protein C (APC) and tissue factor pathway inhibitor (TFPI), rebalances coagulation in hemophilia. PS gene targeting in hemophilic mice protected them against bleeding, especially when intra-articular. Mechanistically, these mice displayed increased thrombin generation, APC and TFPI resistance, and improved fibrin network. Blocking PS in plasma of hemophilia patients normalized *in vitro* thrombin generation. Both PS and TFPIα were detected in hemophilic mice joints. PS and TFPI expression was stronger in joints of HA than HB patients when receiving on demand therapy, e.g., during a bleeding episode. In contrast, PS and TFPI were decreased in HA patients receiving prophylaxis with coagulation factor concentrates. These results establish PS inhibition as both controller of coagulation and potential therapic target in hemophilia.

HA and HB are hereditary X-linked disorders [183-185]. They are caused by mutations in factor VIII (FVIII) gene (*F8*) or factor IX (FIX) gene (*F9*), respectively, leading to the deficiency of the encoded protein that is an essential component of the intrinsic pathway of blood coagulation (Fig. 1a). One of the major coagulation complexes is the intrinsic tenase (X-ase) complex [186] (Fig. 1a). X-ase comprises activated FIX (FIXa) as the protease, activated FVIII (FVIIIa) as the cofactor, and factor X (FX) as the substrate. Although the generation or exposure of tissue factor (TF) at the site of injury is the primary event in initiating coagulation via the extrinsic pathway, the intrinsic pathway X-ase is important because of the limited amount of available active TF *in vivo* and the presence of TFPI which, when complexed with activated FX (FXa), inhibits the TF/activated factor VII (FVIIa) complex[187] (Fig. 1a). Thus, sustained thrombin generation depends upon the activation of both FIX and FVIII[188] (Fig. 1a). This process is amplified because FVIII is activated by both FXa and thrombin, and FIX, by both FVIIa and activated factor XI (FXIa), the latter factor being previously activated by thrombin. Consequently, a progressive increase in FVIII and FIX activation occurs as FXa and thrombin are formed.

Patients with severe hemophilia often suffer from spontaneous bleeding within the musculoskeletal system, such as hemarthrosis, defined as bleeding into joint spaces. This can result in disability at a young age if left untreated[189].

Current treatment of HA and HB respectively involves FVIII and FIX replacement therapy. This therapy improves quality of life (QoL) but some drawbacks remain. Besides the short half-life of the replacement factors, the most currently challenging complication of hemophilia therapy is the development of inhibitory alloantibodies against FVIII or FIX. Inhibitors render replacement therapy ineffective, limit patient access to a safe and effective standard of care and predispose them to an increased morbidity and mortality risk.

New therapies focus on the development of products capable of decreasing the frequency of prophylactic infusions, thus potentially improving both compliance to therapy and QoL.

Besides long-lasting FVIII and FIX, novel approaches comprise the replacement of the gene necessary for production of endogenous coagulation factor, the bispecific antibody technology to mimic the coagulation function of the missing factor, and the targeting of coagulation inhibitors such as TFPI or antithrombin as a strategy to rebalance coagulation in patients with hemophilia[190]. Recently, it was shown that an APC-specific serpin rescues thrombin generation *in vitro* and restores hemostasis in hemophilia mouse models[191].

Here, we investigated whether targeting PS[192] could promote hemostasis in hemophilia by re-balancing coagulation (Fig. 1b). PS, encoded by the *PROS1* gene, acts as cofactor for APC in the inactivation of factor Va (FVa) and FVIIIa[98], and for TFPI in the inhibition of FXa[103, 193]. This dual role makes PS a key regulator of thrombin generation. The importance of PS as an anticoagulant is illustrated by the dramatic clinical manifestations observed in homozygous and compound heterozygous patients with severe PS deficiency[117]. Homozygous PS deficiency leads to purpura fulminans and disseminated intravascular coagulation (DIC) that are fatal if untreated. Heterozygous PS deficiency has variable penetrance, but can be associated with an increased risk of thromboembolic events[84, 194].

Previous studies showed that *Pros1*$^{-/-}$ mice are not viable and die *in utero* in late gestation with a phenotype quite similar to the one observed in human[95, 96]. We therefore consider *Pros1*$^{-/-}$ mice as a good model of the human disease.

Results

Loss of X-ase activity rescues *Pros1*$^{-/-}$ mice

In order to generate *F8*$^{-/-}$*Pros1*$^{-/-}$ mice, we first crossed *Pros1*$^{+/-}$ females with *F8*$^{-/-}$ males, producing 25% *F8*$^{+/-}$*Pros1*$^{+/-}$ progeny. *F8*$^{+/-}$*Pros1*$^{+/-}$ females were then bred with *F8*$^{-/-}$ males resulting in 25% *F8*$^{-/-}$*Pros1*$^{+/-}$ progeny (Extended Data Fig. 1a-c). Similar observations were made with *F9*$^{-/-}$*Pros1*$^{+/-}$ mice (Extended Data Fig. 1d-f). Of 295 pups from *F8*$^{-/-}$*Pros1*$^{+/-}$ breeding pairs, 72 (24%) were *F8*$^{-/-}$*Pros1*$^{+/+}$, 164 (56%) were *F8*$^{-/-}$*Pros1*$^{+/-}$ and 59 (20%) were *F8*$^{-/-}$*Pros1*$^{-/-}$ (χ^2=4.8, *P*=0.09). Thus, *F8*$^{-/-}$*Pros1*$^{-/-}$ mice were present at the expected Mendelian ratio. In contrast, of 219 pups from *F9*$^{-/-}$*Pros1*$^{+/-}$ breeding pairs, 56 (26%) were *F9*$^{-/-}$*Pros1*$^{+/+}$, 132 (60%) were *F9*$^{-/-}$*Pros1*$^{+/-}$ and 31 (14%) were *F9*$^{-/-}$*Pros1*$^{-/-}$ (χ^2=14.95, *P*=0.001). This is compatible with a transmission ratio distortion for *F9*$^{-/-}$*Pros1*$^{-/-}$ mice consistent with the decreased litter sizes compared to those of matings from the same genetic background (5.2±0.7 *versus* 9.8±1.8, *n*=4 matings/over 3^t generations, *P*=0.046). To confirm the genotyping results of *F8*$^{-/-}$*Pros1*$^{-/-}$ and *F9*$^{-/-}$*Pros1*$^{-/-}$ mice, FVIII and FIX, respectively, and PS levels were measured at 6-8 weeks of age (Fig. 1c-d). As expected, *F8*$^{-/-}$*Pros1*$^{-/-}$ and *F9*$^{-/-}$*Pros1*$^{-/-}$ mice did not have detectable FVIII and FIX plasma activity, respectively and PS was not detected in *F8*$^{-/-}$*Pros1*$^{-/-}$ and *F9*$^{-/-}$*Pros1*$^{-/-}$ mice plasma (Fig. 1c-d). PS plasma levels in *F8*$^{-/-}$*Pros1*$^{+/-}$ and *F9*$^{-/-}$*Pros1*$^{+/-}$ were about 50-60% less than in *F8*$^{-/-}$*Pros1*$^{+/+}$ and *F9*$^{-/-}$*Pros1*$^{+/+}$ mice (Fig. 1c-d), as previously reported[95, 96].

F8$^{-/-}$*Pros1*$^{-/-}$ and *F9*$^{-/-}$*Pros1*$^{-/-}$ mice appeared normal and showed no difference in size, weight and behavior. *F8*$^{-/-}$*Pros1*$^{-/-}$ and *F9*$^{-/-}$*Pros1*$^{-/-}$ mice viability was monitored up to 20 (*n*=4) and 16 months (*n*=2), respectively, without showing any difference compared to *F8*$^{-/-}$*Pros1*$^{+/+}$ and *F9*$^{-/-}$*Pros1*$^{+/+}$ mice, respectively.

As a complete *Pros1* deficiency in mice leads to consumptive coagulopathy[95], we assessed whether *F8*$^{-/-}$*Pros1*$^{-/-}$ and *F9*$^{-/-}$*Pros1*$^{-/-}$ mice developed signs of DIC. Platelet count, fibrinogen concentration, prothrombin time and thrombin-antithrombin complexes (TAT) were

comparable in $F8^{-/-}Pros1^{+/+}$, $F8^{-/-}Pros1^{+/-}$ and $F8^{-/-}Pros1^{-/-}$ mice (Fig. 1c), and in $F9^{-/-}Pros1^{+/+}$, $F9^{-/-}Pros1^{+/-}$ and $F9^{-/-}Pros1^{-/-}$ mice (Fig. 1d). Activated partial thromboplastin time (aPTT) was equally prolonged in $F8^{-/-}Pros1^{+/+}$ (69±2 sec), $F8^{-/-}Pros1^{+/-}$ (68±3 sec) and $F8^{-/-}Pros1^{-/-}$ (63±3 sec) mice (mean±s.e.m., n=6 per group, P=0.3) because of the absence of FVIII. Comparable data for aPTT were obtained with $F9^{-/-}Pros1^{+/+}$, $F9^{-/-}Pros1^{+/-}$ and $F9^{-/-}Pros1^{-/-}$ mice ($F9^{-/-}Pros1^{+/+}$: 68±4, $F9^{-/-}Pros1^{+/-}$: 73±4, $F9^{-/-}Pros1^{-/-}$: 67±2 sec, mean±s.e.m., n=7 per group, P=0.5). Thus, $F8^{-/-}Pros1^{-/-}$ and $F9^{-/-}Pros1^{-/-}$ mice do not present overt DIC. Moreover, histology of brain, lungs, liver and kidney of $F8^{-/-}Pros1^{-/-}$ mice did not reveal thrombosis. This was confirmed by the absence of insoluble fibrin by immunohistochemistry (Extended Data Fig. 2). Similar data were obtained with $F9^{-/-}Pros1^{+/+}$ and $F9^{-/-}Pros1^{-/-}$ mice (Extended Data Fig. 2).

Therefore, the loss of FVIII or FIX activity rescues the embryonic lethality of complete $Pros1$ deficiency. However, the rescue was only partial with the loss of FIX activity. A possible explanation is the fact that severe HB appears to be a less serious condition compared to severe HA[195-199]. Consequently, $F9$ disruption in $Pros1^{-/-}$ mice was less efficient in rebalancing coagulation than $F8$ disruption.

To explore whether restoring intrinsic X-ase activity by FVIII infusion induces DIC, thrombosis and purpura fulminans in $F8^{-/-}Pros1^{-/-}$ mice, we administered intravenously either single or multiple normal doses or overdoses of recombinant FVIII (rFVIII). During the 1 h-period following rFVIII injection at any time-point and with both normal doses and overdoses, mice were found to be lethargic with hunched posture and ruffled hair coat. However, none of them died within 72 h after rFVIII injection. Macroscopic anatomical examination of $F8^{-/-}Pros1^{-/-}$ mice 24 h after a single injection of an overdose of rFVIII revealed a combination of thrombi in numerous blood vessels and bleeding particularly in the lungs (Fig. 1e). Immunohistochemical analysis of corresponding lung sections allowed the detection of fibrin clots compatible with multiple thrombi in the lung vasculature (Fig. 1f). Nevertheless, these mice did not develop purpura fulminans.

Twenty-four h after repeated administration of a normal dose of rFVIII in $F8^{-/-}Pros1^{-/-}$ mice, blood coagulation analyses showed incoagulable prothrombin time (PT) (not shown), low fibrinogen and high TAT levels, compatible with an overt DIC (Fig. 1g). In contrast, after a single injection of a normal dose of rFVIII in $F8^{-/-}Pros1^{-/-}$ mice, fibrinogen and TAT levels were comparable to those of untreated $F8^{-/-}Pros1^{-/-}$ mice (Fig. 1g). However, numerous thrombi were visible in lung and liver (Fig. 1h-i), but not kidney sections (data not shown), 24 h after one single infusion of rFVIII or multiple rFVIII administration at normal dosage in $F8^{-/-}Pros1^{-/-}$ mice (Fig. 1j-k). None of these mice developed purpura fulminans.

Thus, rFVIII administration in $F8^{-/-}Pros1^{-/-}$ mice restored the imbalance of the coagulation promoting DIC and thrombosis but not purpura fulminans or death even after an overdose of rFVIII.

Loss of X-ase activity does not prevent lethality caused by TF-induced thromboembolism in $Pros1^{-/-}$ mice

We previously applied a TF-induced thromboembolism model[200] to $Pros1^{+/-}$ and $Pros1^{+/+}$ mice and demonstrated that although 88% of $Pros1^{+/+}$ mice survived to the challenge, only 25% of $Pros1^{+/-}$ mice were still alive 20 min after a low TF dose injection (~1.1 nM TF)[95]. When using a higher TF dosage (~4.3 nM TF), both $Pros1^{+/+}$ and $Pros1^{+/-}$ mice died within 20 min. However, $Pros1^{+/-}$ died earlier than $Pros1^{+/+}$. HA and WT mice, both with normal PS plasma levels were equally sensitive to this high TF-dose with more than 85% of them succumbing within 15 min (Fig. 2a). In contrast, >75% WT mice under thromboprophylaxis with a low molecular weight heparin (LMWH) survived (Fig. 2a). These data indicate that, in contrast with LMWH, HA does not protect mice against TF-induced thromboembolism. We then investigated $F8^{-/-}Pros1^{+/+}$, $F8^{-/-}Pros1^{+/-}$ and $F8^{-/-}Pros1^{-/-}$ mice in the same model. After the infusion of TF (~2.1 nM TF), 40-60% of the mice died ($P>0.05$), independently of their $Pros1$ genotype (Fig. 2b). However, there was a trend for $F8^{-/-}Pros1^{-/-}$ and $F8^{-/-}Pros1^{+/-}$

succumbing earlier to the thromboembolic challenge than $F8^{-/-}Pros1^{+/+}$ mice, and for $F8^{-/-}Pros1^{+/-}$ dying earlier than $F8^{-/-}Pros1^{+/+}$ mice (mean time to death: 12±4 min for $F8^{-/-}Pros1^{+/+}$, 7±2 min for $F8^{-/-}Pros1^{+/-}$, 8±3 min for $F8^{-/-}Pros1^{-/-}$ mice, n=4-6/group, P=0.43). Similar data were obtained with $F9^{-/-}Pros1^{+/+}$, $F9^{-/-}Pros1^{+/-}$ and $F9^{-/-}Pros1^{-/-}$ mice (data not shown).

Immunohistochemical analysis of lung sections allowed the detection of fibrin clots in lung arteries of $F8^{-/-}Pros1^{+/+}$ and $F8^{-/-}Pros1^{-/-}$ mice that died during the TF-induced thromboembolic challenge (Fig. 2c). Importantly, there were more thrombi in lungs from $F8^{-/-}Pros1^{-/-}$ than from $F8^{-/-}Pros1^{+/+}$ mice (n=48 *versus* 26, respectively). In addition, most arteries in $F8^{-/-}Pros1^{-/-}$ lungs were completely occluded while they were only partially occluded in $F8^{-/-}Pros1^{+/+}$ lungs.

None of the $F8^{-/-}Pros1^{-/-}$ mice that succumbed during the TF-induced thromboembolic-challenge developed purpura fulminans. Similar data were obtained with $F9^{-/-}Pros1^{+/+}$, $F9^{-/-}Pros1^{+/-}$ and $F9^{-/-}Pros1^{-/-}$ mice (not shown).

Thus, loss of intrinsic X-ase activity does not prevent lethality caused by TF-induced thromboembolism in $Pros1^{-/-}$ mice.

Loss of FVIII partially protects $Pros1^{-/-}$ mice against thrombosis in mesenteric arterioles

We then recorded thrombus formation in mesenteric arterioles by intravital microscopy, a model sensitive to defects in the intrinsic pathway of coagulation[201]. In $F8^{+/+}Pros1^{+/+}$ mice, thrombi grew to occlusive size in 20 min, and all injured arterioles were occluded (Extended Data Fig. 3). As expected, none of the arterioles of $F8^{-/-}Pros1^{+/+}$ displayed thrombosis at the end of the experiment, whereas $F8^{-/-}Pros1^{-/-}$ mice showed partial thrombi (Extended Data Fig. 3).

Emboli were generated during thrombus formation in $F8^{+/+}Pros1^{+/+}$ mice, but not in $F8^{-/-}Pros1^{+/+}$ mice. In $F8^{-/-}Pros1^{-/-}$ mice, multiple micro-emboli detached during partial thrombus growth, preventing the formation of occlusive thrombi.

$Pros1$ targeting limits but does not abrogate tail bleeding in mice with HA

The bleeding phenotype was assessed by tail transection at two different distal portions to mimic either mild (venous bleeding only) or severe (venous and arterial bleeding) bleeding.

In both mild and severe models, blood loss was reduced in $F8^{-/-}Pros1^{-/-}$ compared to $F8^{-/-}Pros1^{+/+}$ mice (Fig. 2d-e). When $F8^{-/-}Pros1^{+/-}$ mice were challenged by the mild tail transection model, they bled less than $F8^{-/-}Pros1^{+/+}$ mice (Fig. 2d). In contrast, when exposed to the severe tail transection model, both $F8^{-/-}Pros1^{-/-}$ and $F8^{-/-}Pros1^{+/-}$ mice displayed comparable blood loss (Fig. 2e). However, $F8^{-/-}Pros1^{-/-}$ mice bled significantly more than $F8^{+/-}Pros1^{+/+}$ and $F8^{+/+}Pros1^{+/+}$ mice in both models (Fig. 2d-e), indicating that the loss of $Pros1$ in $F8^{-/-}$ mice did only partially correct the bleeding phenotype of $F8^{-/-}$ mice.

Then, intravenous infusion of an anti-human PS antibody known to effectively block murine PS activity[95] was used to investigate how inhibition of PS activity altered tail bleeding (severe model) in $F8^{-/-}Pros1^{+/-}$ mice. The PS-neutralizing antibody limited blood loss in $F8^{-/-}Pros1^{+/-}$ mice to the same degree (PS-neutralizing antibody: 196±10 *versus* IgG isotype: 308±30 µL, $n=5$, $P=0.005$) as complete genetic loss of $Pros1$ (173.3±14.8 *versus* 274.3±36.9 µL, $n=6$, $P=0.02$) (Fig. 2e).

Taken together, these data demonstrate that genetic loss of $Pros1$ or inhibition of PS activity partially and indistinguishably mitigates bleeding in HA.

Pros1 targeting or PS inhibition fully protects HA or HB mice from acute hemarthrosis (AH)

Although bleeding may appear anywhere in patients with hemophilia, most of hemorrhages occur in the joints, spontaneously or in response to mechanical stress or trauma[202, 203]. To determine whether _Pros1_ loss prevents hemarthrosis in hemophilic mice, we applied an AH model to $F8^{-/-}Pros1^{+/+}$, $F8^{-/-}Pros1^{+/-}$, $F8^{-/-}Pros1^{-/-}$ and $F8^{+/+}Pros1^{+/+}$ mice. Knee swelling after injury was reduced in both $F8^{-/-}Pros1^{-/-}$ and $F8^{+/+}Pros1^{+/+}$ mice compared to $F8^{-/-}Pros1^{+/+}$ and $F8^{-/-}Pros1^{+/-}$ mice (Fig. 2f). There was also no significant difference in knee swelling between $F8^{-/-}Pros1^{-/-}$ and $F8^{+/+}Pros1^{+/+}$ mice (Fig. 2f). AH was also assessed by histology (Fig. 2g). Bleeding was observed in the joint space and synovium of $F8^{-/-}Pros1^{+/+}$ (intra-articular bleeding score, IBS=2, n=5) but not of $F8^{-/-}Pros1^{-/-}$ (IBS=0, n=5) and $F8^{+/+}Pros1^{+/+}$ mice (IBS=0, n=5) (Fig. 2g). There was much more insoluble fibrin consistent with clots in joint space and synovium from $F8^{-/-}Pros1^{+/+}$ than from $F8^{-/-}Pros1^{-/-}$ and $F8^{+/+}Pros1^{+/+}$ mice (Fig. 2g). Similar data were obtained with $F9^{-/-}Pros1^{+/+}$ and $F9^{-/-}Pros1^{-/-}$ mice (IBS=0, n=3 and IBS=2, n=3, respectively) (Extended Data Fig. 4a-b). Thus, loss of _Pros1_ in hemophilia confers full protection against AH.

These results were confirmed by the continuous subcutaneous infusion during 4 days of a PS-neutralizing antibody or an IgG isotype control antibody in $F8^{-/-}Pros1^{+/-}$ mice (starting 1 day before the induction of hemarthrosis) (knee swelling in PS-neutralizing antibody group was 0.43±0.07 _versus_ 0.69±0.09 mm in IgG isotype group, (n=9, P=0.04). The plasma PS level in PS-neutralizing antibody group was 26±6% _versus_ 45±3% in the controls (n=5, P=0.017). In addition, PS inhibition was alternatively achieved by intravenous injection of a murine PS (mPS) siRNA 2.5 days prior to the AH challenge in $F8^{-/-}Pros1^{+/-}$ and $F8^{-/-}Pros1^{+/+}$ mice (Fig. 2h-i). The assessment of the IBS confirmed the lack of intra-articular bleeding in $F8^{-/-}Pros1^{+/+}$ mice treated with mPS siRNA (IBS=0.5, n=3) when compared to those treated with control siRNA (IBS=2, n=3), (Fig. 2h). Importantly, PS expression was reduced by mPS

siRNA both in plasma (26±3%) 84±11% in controls, n=3, P=0.006) and in the synovium (Fig. 3a).

Both PS and TFPI are expressed in the synovium of mice

To understand the prominent intra-articular hemostatic effect of the genetic loss of *Pros1* and PS inhibition in hemophilic mice, knee sections were immunostained for PS and TFPI. PS staining was mainly present at the lining layer of the synovial tissue of *F8$^{-/-}$Pros1$^{+/+}$* mice with AH treated with control siRNA, whereas synovial staining for PS was remarkably reduced in *F8$^{-/-}$Pros1$^{+/+}$* mice with AH that received mPS siRNA infusion (Fig. 3a). In contrast, TFPI staining was more prominent in synovial tissue from hemophilic mice that have received the mPS siRNA than in those that were treated by the control siRNA (Fig. 3a). However, TFPI expression was comparable in synovial lining layer of both *F8$^{-/-}$Pros1$^{+/+}$* and *F8$^{-/-}$Pros1$^{-/-}$* mice (Fig. 3b).

To demonstrate further that PS is expressed by fibroblast-like synoviocytes (FLS), we performed western blots on conditioned media collected from *F8$^{+/+}$Pros1$^{+/+}$*, *F8$^{-/-}$Pros1$^{+/+}$* and *F8$^{-/-}$Pros1$^{-/-}$* murine primary FLS. As shown in Fig. 3c, media of *F8$^{+/+}$Pros1$^{+/+}$* and *F8$^{-/-}$Pros1$^{+/+}$* FLS displayed a band at a molecular weight ~75 kDa comparable to recombinant murine PS and similar to the one observed in mouse plasma and platelets. As expected, no staining was detected in media obtained from *F8$^{+/+}$Pros1$^{-/-}$* FLS (Fig. 3c).

We also studied TFPI expression in *F8$^{-/-}$Pros1$^{+/+}$* and *F8$^{-/-}$Pros1$^{-/-}$* FLS conditioned media by western blotting (Fig. 3d). All media displayed a band at a molecular weight of ~50 kDa similar to the one observed with murine placenta lysates. TFPI isoform expression was investigated using western blot analysis following protein deglycosylation because fully glycosylated TFPIα and TFPIβ migrate at the same molecular weight[204]. Deglycosylated TFPI from FLS media migrated as a single band at the molecular weight of TFPIα similar to murine placenta TFPI (positive control for TFPIα) (Fig. 3d). Thus, our data indicate that FLS express TFPIα but not TFPIβ.

Moreover, PS expression increased in $F8^{-/-}Pros1^{+/+}$ FLS 24h after stimulation with thrombin (Fig. 3f). TFPI expression was also prominent in $F8^{-/-}Pros1^{+/+}$ FLS 24h after stimulation with thrombin (Fig. 3e).

These data suggest that, within the intra-articular space, the synovium is an environment in which two key anticoagulants, PS and TFPI, are expressed and that their expression is increased by thrombin.

Both PS and TFPI are expressed in the synovium of patients with HA or HB

Human HA, HB and osteoarthritis knee synovial tissues were then analyzed for both PS and TFPI (Fig. 4a). A strong signal was found for TFPI and PS in the synovial lining and sublining layers of HA patients on demand (n=7). By contrast, immunostaining for both PS and TFPI was remarkably decreased in HA patients under prophylaxis (n=5). HB patients on demand displayed less signal for both PS and TFPI in the synovial lining and sublining layers (n=4) than HA patients on demand. Joint sections from osteoarthritis patients (n=7) did not show an intense staining for TFPI and PS similarly to hemophilic patients under prophylaxis. To evaluate which isoform of TFPI is expressed by human FLS, western blotting on conditioned media of human primary FLS isolated from healthy subjects and patients with osteoarthritis was performed. Similarly to murine FLS, human FLS express TFPI. After deglycosylation, the presence of a single band with a slightly reduced molecular weight as the one displayed by human platelet lysate indicates that FLS express TFPIα but not TFPIβ (Fig. 4b).

Monocytes in HA mice with or without PS deficiency

Induction of hemarthrosis results in a transient shift of blood monocytes towards a M1 or "inflammatory" type and an increase in M1 synovial macrophages. In the joint lavage, a temporary increase in M1 monocytes and a more sustained increase in M2 "patrolling" monocytes is observed[205]. M1 cells produce high levels of proinflammatory cytokines such

a IL-1β and TNF-α, and have limited iron internalization and release capacities, restricting thereby the elimination of catalytic iron from the joint[206, 207].

In resting condition, $F8^{-/-}Pros1^{-/-}$ mice had almost 3 times more M1 and 3 times less M2 monocytes in peripheral blood than $F8^{-/-}Pros1^{+/+}$ mice (Fig. 5a-b). However, 72 h after the induction of AH, $F8^{-/-}Pros1^{-/-}$ and $F8^{-/-}Pros1^{+/+}$ mice had comparable circulating monocytes (Fig. 5a-b). In addition, in the joint lavage, the number of M1 and M2 monocytes was comparable in $F8^{-/-}Pros1^{-/-}$ and $F8^{-/-}Pros1^{+/+}$ mice both in resting condition and 72 h after the induction of AH (Fig. 5c-d). Thus, in the context of AH, monocyte populations were comparable in $F8^{-/-}Pros1^{-/-}$ and $F8^{-/-}Pros1^{+/+}$ mice, indicating that, in this condition, monocytes polarization was preserved both in peripheral blood and in the joint. However, $F8^{-/-}Pros1^{-/-}$ mice, contrary to $F8^{-/-}Pros1^{+/+}$ mice, were fully protected against AH and thereby were expected to display less M1 and more M2 cells in knee lavage than $F8^{-/-}Pros1^{+/+}$ which presented AH.

The amount of monocyte chemotactic protein 1 (MCP-1) and IL-6, cytokines secreted by the inflamed synovium[208], was less abundant in joint lavage of $F8^{-/-}Pros1^{-/-}$ compared to $F8^{-/-}Pros1^{+/+}$ mice 72 h after the induction of AH. Similarly, we observed a trend for less IL-1β and keratinocytes-derived chemokine (KC), proinflammatory cytokines produced by synovial tissue and joint macrophages, in joint lavage from $F8^{-/-}Pros1^{-/-}$ mice than from $F8^{-/-}Pros1^{+/+}$ mice (Fig. 5e). This is consistent with the fact that $F8^{-/-}Pros1^{-/-}$ mice, contrary to $F8^{-/-}Pros1^{+/+}$ mice, did not develop AH.

Loss of *Pros1* is responsible for the lack of TFPI-dependent PS activity and resistance to APC in HA mice

The full protection against AH in HA or HB mice lacking *Pros1* in which PS was inhibited could be explained at least partly by the lack of PS cofactor activity for APC and TFPI in the joint. However, the reason for a partial hemostatic effect of the lack of *Pros1* or PS inhibition in HA mice challenged in the tail bleeding models needs to be further investigated.

Ex vivo TF-initiated thrombin generation testing has shown a correlation between the capacity of plasma to generate thrombin and the clinical severity of hemophilia[209-211]. Therefore, we investigated the impact of *Pros1* loss on thrombin generation in plasma of HA mice. TFPI-dependent PS activity was not assessed in platelet-free plasma (PFP) but in platelet-rich plasma (PRP) because previous work revealed that TFPI-cofactor activity of PS cannot be demonstrated in mouse plasma using thrombin generation tests[95]. This is explained by the lack of TFPIα in mouse plasma and its presence in mouse platelets[212].

Both thrombin peak and endogenous thrombin potential (ETP, the area under the thrombin generation curve), were significantly higher in $F8^{-/-}Pros1^{-/-}$ than in $F8^{-/-}Pros1^{+/+}$ PRP in response to 1 pM TF (1072±160 *vs* 590±10 nmol/L.min, *n*=3/group, *P*=0.04), suggesting the lack of PS TFPI-cofactor activity in $F8^{-/-}Pros1^{-/-}$ PRP (Fig. 6a). Consistent with previous work[95], both thrombin peak and ETP were comparable in PFP of $F8^{-/-}Pros1^{+/+}$ and $F8^{-/-}Pros1^{-/-}$ mice in presence of 1, 2.5 or 5 pM TF (data not shown).

To assess whether $F8^{-/-}Pros1^{-/-}$ mice exhibited defective functional APC-dependent PS activity, we used thrombin generation testing in Ca^{2+} ionophore-activated PRP in the absence of APC, in the presence of wild-type (WT) recombinant APC, or in the presence of a mutated (L38D) recombinant mouse APC (L38D APC, a variant with ablated PS cofactor activity)[213]. In this assay, APC titration showed that the addition of 8 nM WT APC was able to reduce ETP by 90% in activated PRP of WT mice whereas the same concentration of L38D APC diminished ETP by only 30% (data not shown). Based on these data, thrombin generation curves were recorded for activated PRP (3 mice/assay). The calculated APC ratio ($ETP_{+APC\ WT}$/ $ETP_{+APC\ L38D}$) indicated an APC resistance in $F8^{-/-}Pros1^{-/-}$ plasma but not in $F8^{-/-}Pros1^{+/+}$ plasma (0.87±0.13 *versus* 0.23±0.08, respectively, *P*=0.01) (Fig. 6b).

APC-dependent PS activity was also tested in PFP from $F8^{-/-}Pros1^{+/+}$ and $F8^{-/-}Pros1^{-/-}$ mice (2 mice/assay) in the presence of 2 nM WT APC and L38D APC. Calculated APC ratio showed an APC resistance in $F8^{-/-}Pros1^{-/-}$ but not in $F8^{-/-}Pros1^{+/+}$ mice (1.08±0.04 *versus* 0.25±0.09,

respectively, P=0.0003) (Fig. 6b).

Clots from HA mice lacking *Pros1* display an improved but not completely restored fibrin network

Tail bleeding models have been used to provide a measure of hemostasis *in vivo*, and tail bleeding models in mice are not only sensitive to platelet dysfunction but also to alterations in both coagulation[214] and fibrinolysis[215]. In order to better understand the differences between studied genotypes regarding tail bleeding, we used scanning electron microscopic imaging to investigate fibrin structure (Fig. 6c). Clots from $F8^{+/+}Pros1^{+/+}$ and $F8^{-/-}Pros1^{-/-}$ plasma showed a denser network of highly branched fibrin fibers compared to $F8^{-/-}Pros1^{+/+}$ plasma clots (Extended Data Fig. 6a-b). In contrast, clots from $F9^{+/+}Pros1^{+/+}$ and $F9^{-/-}Pros1^{-/-}$ plasma did not display a denser network than $F9^{-/-}Pros1^{+/+}$ plasma clots, but a trend for an augmented fibers branching (Extended Data Fig. 6c-d).

Fibrin fibers from $F8^{-/-}Pros1^{-/-}$ and $F8^{-/-}Pros1^{+/+}$ mice, and from $F9^{-/-}Pros1^{-/-}$ and $F9^{-/-}Pros1^{+/+}$ mice, displayed a larger diameter compared to fibers from $F8^{+/+}Pros1^{+/+}$ mice or $F8^{+/+}Pros1^{+/+}$ mice, respectively. Nevertheless, the fiber surface of $F8^{-/-}Pros1^{-/-}$ and $F9^{+/+}Pros1^{+/+}$ mice showed less porosity as compared to $F8^{-/-}Pros1^{+/+}$ or $F9^{-/-}Pros1^{+/+}$ mice, respectively, suggesting that $F8^{-/-}Pros1^{-/-}$ and $F9^{-/-}Pros1^{-/-}$-derived fibers might be less permeable and thereby more resistant to fibrinolysis than $F8^{-/-}Pros1^{+/+}$ or $F9^{-/-}Pros1^{+/+}$-derived fibers[216]. These data, in complement to both TFPI and APC cofactor activity results (Fig. 6a-b), help to explain why tail bleeding in $F8^{-/-}Pros1^{-/-}$ was improved when compared to $F8^{-/-}Pros1^{+/+}$ mice but not completely corrected as in $F8^{+/+}Pros1^{+/+}$ mice.

PS inhibition in human plasma completely restores thrombin generation in patients with HA

We then examined the effect of PS inhibition on thrombin generation in human HA plasma. Addition of an anti-PS antibody resulted in 2-4-fold increase of the ETP in PFP. Similar

results were obtained using an anti-human TFPI antibody directed against the C-terminal domain for efficient FXa inhibition, even in the presence of FVIII inhibitor (Fig. 6d-e). PS inhibition had a remarkable effect in PRP samples where it increased ETP more than 10 times (1912±37 and 1872±64 nM*min) (Fig. 6f and g, respectively). These data are compatible with a complete restoration of ETP in hemophilic plasma by PS inhibition (for comparison, ETP in normal plasma: 1495±2nM*min). Similar results were obtained using the anti-TFPI antibody (Fig. 6d-g). Taken together, these data confirm in humans the improvement of thrombin generation in HA PFP and PRP driven by PS inhibition that we observed in mice.

Pros1 **targeting does not increase mortality induced by endotoxemia or bacterial infection in HA mice**

Because PS is involved in the modulation of innate immunity (reviewed in[217]), we investigated the response to endotoxemia and bacterial infection of $F8^{-/-}Pros1^{+/+}$, $F8^{-/-}Pros1^{+/-}$ and $F8^{-/-}Pros1^{-/-}$ mice.

We applied the endotoxemia (LPS) model to mice, and 25 mg/kg caused about 50% - LD_{50} - mortality in $F8^{-/-}Pros1^{+/+}$ mice. In rodents, LPS promotes hypotension accompanied by the release of pro-inflammatory cytokines and nitric oxide (NO), and by the induction of nitric oxide synthase expression. These events finally result in the onset of acute pulmonary edema, myocardial dysfunction and death[218, 219]. We measured plasma PS at different time points (0, 4, 8, 12 and 16 h) and found that PS levels decreased slightly in $F8^{+/+}Pros1^{+/+}$ mice after a short period and remained below baseline for at least 12 h (1 h versus 4 h, P=0.016, Extended Data Fig. 7a). However, survival did not differ between $F8^{-/-}Pros1^{+/+}$, $F8^{-/-}Pros1^{+/-}$ and $F8^{-/-}Pros1^{-/-}$ mice (Extended Data Fig. 7b).

We then examined the response of $F8^{-/-}Pros1^{+/+}$, $F8^{-/-}Pros1^{+/-}$, $F8^{-/-}Pros1^{-/-}$ and $F8^{+/+}Pros1^{+/+}$ mice to microbial sepsis using a model that closely mimics human peritoneal sepsis (cecal ligation and puncture, CLP)[220, 221]. We found that $F8^{-/-}Pros1^{+/+}$, $F8^{-/-}Pros1^{+/-}$, $F8^{-/-}Pros1^{-/-}$

and $F8^{+/+}Pros1^{+/+}$ mice were equally sensitive to CLP (Extended Data Fig. 7c). Because hemophilia condition has been previously reported as a possible cause of impaired phagocytosis[222], we investigated bone marrow-derived macrophages (BMDM) for bacterial phagocytosis both under resting conditions and after stimulation with IFNγ and LPS. $F8^{+/+}Pros1^{+/+}$ BMDM phagocytosed more bacteria after stimulation than under resting conditions (Extended Data Fig. 7d-e). In contrast, there was no difference between resting and stimulated $F8^{-/-}$ BMDM with or without loss of *Pros1*, but $F8^{-/-}Pros1^{-/-}$ BMDM phagocytosed about 30% less bacteria than $F8^{-/-}Pros1^{+/+}$ BMDM (Extended Data Fig. 7d-e). This diminution of phagocytosis had nevertheless no relevant *in vivo* consequences as demonstrated by the results obtained with the CLP model of bacterial infection (Extended Data Fig. 7c).

Thus, HA with or without loss of *Pros1* in mice did not alter the susceptibility to endotoxemia or microbial sepsis, indicating that PS targeting for hemophilia is not expected to carry major side effects in the context of life-threatening inflammation and infection.

Conclusions

Extensive studies using genetically modified mice provide proof of concept data supporting a central role for PS and another anticoagulant, TFPI, as contributing to bleeding and serious damage in joints of hemophilic mice. Targeting *Pros1* or inhibiting PS has the ability to ameliorate hemophilia in mice as judged by the *in vivo* improvement of the bleeding phenotype in the tail bleeding assays and the full protection against hemarthrosis. Because joints display a very weak expression of TF[223] and synovial cells produce a high amount of TFPIα and PS, the activity of the extrinsic pathway is greatly reduced intra-articularly, predisposing hemophilic joints to bleed. Moreover, both TM and EPCR are expressed by FLS[224, 225], suggesting that the TM-thrombin complex activates EPCR bound-PC to generate the very potent anticoagulant, APC, in the context of AH. Importantly, the expression of TFPIα is upregulated by thrombin (Extended Data Fig. 7). Thus, AH that usually results in marked local inflammation and joint symptoms that can last for days to weeks also promotes the local generation and secretion of multiple anticoagulants, namely APC, TFPIα, and their mutual cofactor PS, that could help explain the pathophysiology of joint damage in hemophilia.

Observations using clinical samples from hemophilic human subjects are consistent with the lessons learned from murine studies. In humans, blocking PS in plasma from patients with HA with or without anti-FVIII inhibitors normalizes the ETP. Patients with HB display less intra-articular expression of TFPI and PS than patients with HA, consistent with current knowledge that patients with HB bleed less than those with HA[195-199, 226, 227]. Moreover, patients with HA receiving prophylaxis display less TFPI and PS expression in their synovia than patients receiving FVIII concentrates only in the context of bleeding, i.e., so called "on demand therapy". Finally, human FLS secrete both TFPIα and PS as observed in mice, thus strengthening the extrapolation of murine hemophilia data to humans.

The extensive findings in this report lead us to propose that targeting PS may potentially be translated to therapies useful for hemophilia. Targeting coagulation inhibitors such as TFPI or antithrombin as a strategy to rebalance coagulation in patients with hemophilia are currently

being investigated in clinical trials[190], and an APC-specific serpin rescues thrombin generation *in vitro* and restores hemostasis in hemophilia mouse models[191]. PS in human and murine joints is a novel pathophysiological contributor to hemarthrosis and constitutes an attractive potential therapeutic target especially because of its dual cofactor activity for both APC and TFPIα within the joints. In the presence of PS, hemarthrosis provokes the release of proinflammatory cytokines and increases TFPIα expression in the synovia. Targeting PS in mice protects them from hemarthrosis and the release of intra-articular cytokines (Extended Data Fig. 7). Thus, we propose that TFPIα and its cofactor PS, both produced by FLS, together with the TM-EPCR-PC pathway, comprise a potent intra-articular anticoagulant system that has an important pathologic impact on hemarthrosis. Future studies are needed to assess the merits of this new concept for targeting simultaneously the multiple anticoagulant cofactor activities of PS which involve both APC and TFPI.

Methods

Mice

$F8^{-/-}$ mice *(B6;129S4-F8^{tm1Kaz}/J) and $F9^{-/-}$ mice (B6.129P2-F9^{tm1Dws}/J)* with C57BL/6J background were obtained from The Jackson Laboratory. *Pros1$^{+/-}$* mice were progeny of the original colony, with a genetic background of 50% 129/Sv x 50% C57BL/6J, as described previously[95]. The Swiss Federal Veterinary Office approved the experiments. Mice were genotyped by a multiplex PCR that amplifies the WT (+) and the null (-) alleles of *Pros1* gene at the same time, using primers previously described[95]. Genotyping of *F8* and *F9* genes were performed accordingly to the literature[228, 229].

Preparation of murine plasma

Mice were anesthetized with pentobarbital (40 mg/kg), and whole blood was drawn from the inferior vena cava into 3.13% citrate (1 vol anticoagulant/9 vol blood). Blood was centrifuged at 1031 *g* for 10 min with the centrifuge pre-warmed to 26°C to obtain platelet rich plasma (PRP). Alternatively blood was centrifuged at 2400 *g* for 10 min at room temperature (RT), to obtain platelet-poor plasma (PPP). To obtain platelet-free plasma (PFP), an additional centrifugation at 10000 *g* for 10 min was performed.

Platelet count and measurement of coagulation parameters

Platelet counts were carried out with an automated cell counter (Procyte Dx Hematology Analyzer, IDEXX). Fibrinogen, FVIII and FIX activity were measured on an automated Sysmex CA-7000 coagulation analyzer (Sysmex Digitana). Prothrombin time (PT) and activated partial thromboplastin time (APTT) were measured on a coagulometer (*MC4plus*, Merlin Medical).

Measurement of murine PS antigen and TAT complexes by ELISA

Wells from 96-well plates (Maxisorb, Thermo) were coated with 50 µL per well of 10 µg/mL of rabbit polyclonal anti-human PS (DAKO Cytomation) and incubated overnight at 4°C. After 3 washes with TBS buffer (0.05 M tris(hydroxymethyl)aminomethane, 0.15 M NaCl, pH 7.5, 0.05% Tween 20), the plate was blocked with TBS-BSA 2%. Diluted plasma samples (dilution range: 1:300-1:600) were added to the wells and incubated at RT for 2 h. After 3 washed, 50 µL of 1µg/mL biotinylated chicken polyclonal anti-murine protein S were added and incubated for 2 h at RT. Signal was amplified by streptavidin-HRP conjugated horseradish peroxidase (Thermo) was added and plates incubated for 1 h. The plates were washed 3 times and 100 µLTMB substrate (KPL) was added. Reactions were stopped by adding 100 µL HCl (1M). Absorbance was measure at 450 nm. Standard curves were set up by using serial dilution of pooled normal plasma obtained from 14 healthy mice (8 males and 6 females, 7–12 weeks old). Results were expressed in percentage relative to the pooled normal plasma.

TAT level was measured in duplicate for each plasma sample using a commercially available ELISA (Enzygnost TAT micro, Siemens), according to the manufacturer's instructions.

Mouse tissue processing and sectioning, immunohistochemistry and microscopy

Tissue sections (4 µm) with no pre-treatment were stained with hematoxylin/eosin or Masson Trichrome or immunostained for insoluble fibrin, PS or TFPI. The following antibodies were used: fibrin (mAb clone 102-10)[175] final concentration 15.6 µg/mL, incubation for 30 min at RT, secondary antibody rabbit anti-human, (ab7155 Abcam, Cambridge, UK) 1:200 dilution, incubation for 30 min at RT; PS (MAB 4976, R&D, dilution 1:50) incubation for 30 min at RT, secondary antibody rabbit anti-rat, (ab7155 Abcam)-1:200 dilution, incubation for 30 min at RT; TFPI (PAHTFPI-S, Hematological Technologies) final concentration 18.6 µg/mL, incubation for 30 min at RT, secondary antibody rabbit anti-sheep IgG (ab7106, Abcam) 1:200 dilution, incubation for 30 min at RT. All the stainings were performed with the immunostainer BOND RX (Leica Biosystems, Muttenz, Switzerland) following

manufacturer's instructions. Whole slides were scanned using 3D HISTECH Panoramic 250 Flash II, with 20x (NA 0.8), 40x (NA 0.95) air objectives. Images processing was done using Panoramic Viewer software.

In vivo administration of FVIII to mice with complete genetic loss of *F8*

Mice, aged 6-9 week, were anesthetized with ketamine (80 mg/kg body weight) and xylazine (16 mg/kg body weight). We administered intravenously either 0.3 U/kg of recombinant FVIII (Advate®, Baxalta) to reach a FVIII level of 100% at 1 h (adequate dose) or an overdose of recombinant FVIII (2 U/kg) to reach >200% at 1 h. Either the adequate dose or the overdose was injected 1 h before and 1 h after the introduction of a jugular vein catheter (Mouse JVC 2Fr PU 10 cm, Instech) and then 4 h, 8 h and 16 h after the placement of the central line. Mice were sacrificed 24 h after the first injection. Blood was drawn and organs were harvested. FVIII, fibrinogen and TAT were measured as described above. Lungs were isolated, fixed in 4% paraformaldehyde (PFA) and embedded in paraffin.

TF-induced pulmonary embolism

A model of venous thromboembolism was adapted from Weiss et al [200] with minor modifications [95]. Mice, aged 6-9 weeks, were anesthetized with ketamine and xylazine as described above and human recombinant TF (hrTF, Dade Innovin, Siemens) was injected intravenously (2 µL/g body weight) at 4.25 nM (1:2 dilution in 0.9% NaCl) and 2.1 nM (1:4 dilution in 0.9% NaCl) were used. TF concentration in the Innovin is 400 ng·mL−1 (8.5 nM) according to T. M. Hackeng (Cardiovascular Research Institute, Maastricht, The Netherlands, personal communication). The time to the onset of respiratory arrest that lasted at least 2 min was recorded and chosen as the time to death. Experiments were terminated at 20 min. Two minutes after the onset of respiratory arrest or at the completion of the 20-min observation period, lungs were harvested and fixed in 4% PFA for 2 h at RT. Lung sections (5 µm) were stained with hematoxylin and eosin (H&E) as well as for insoluble fibrin and examined. The extent of fibrin clots in the lungs was assessed as number of intravascular thrombi in 10

randomly chosen nonoverlapping fields (×10 magnification) of lung tissue.

FeCl₃ injury thrombosis model in mesenteric arteries

A model of thrombosis in mesenteric arteries using intravital microscopy was performed according to ref[230] with minor modifications. Mice were anesthetized by intraperitoneal injection of a mixture of ketamine (80 mg/kg) and xylazine (16 mg/kg). Platelets were directly labeled in vivo by the injection of 100μL rhodamine 6G (1.0 mM). After selection of the studied field, vessel wall injury was generated by a filter paper (1 mm diameter patch of 1M Whatmann paper) saturated with 10% FeCl₃ applied topically for 1 minute. Thrombus formation was monitored in real time under a fluorescent microscope (IV-500, Micron instruments, San Diego, CA) with an FITC filter set, equiped with an affinity corrected water-immesion optics (Zeiss, Germany). The bright fluorescent labelled platelets and leucoytes allowed the observation of 1355μm X 965μm field of view through video triggered stroboscopic epi-illumination (Chadwick Helmuth, El Monte, CA). A 10X objective Zeiss Plan-Neofluar with NA0.3. was used. All scenes were recorded on video-tape using a customized low-lag silicon-intensified target camera (Dage MTI, Michigan city, IN), a time base generator and a Hi-8 VCR (EV, C-100, Sony, Japan). Time to vessel wall occlusion was measured, as determined by cessation of the blood cell flow.

Tail clipping model in HA mice

Two different tail clipping models to evaluate bleeding phenotype were assessed using an adapted protocol previously described by Ivanciu, *et al*[6]. Briefly, the distal tail of 8-10 week old mice was transected with a sharp razor at 2 mm (mild injury) and the bleeding was venous or at 4 mm (severe injury) and the bleeding was both arterial and venous[231]. Bleeding was quantified as blood lost after 30 or 10 min, respectively. In the severe injury model some *F8⁻ᐟ⁻ Pros1⁺ᐟ⁻* mice received a rabbit anti-human PS-IgG (Dako) or isotype rabbit IgG (R&D Systems) intravenously at a dose of 2.1 mg/kg 2 min before tail transection.

Acute hemarthrosis model

9-12 week old mice were anesthetized with ketamine (80 mg/kg) and xylazine (16 mg/kg). Induction of joint bleeding, knee diameter measurements and analgesic coverage were performed according to Øvlisen et al[232]. Joint diameter measurements were performed at 0 and 72 h with a digital caliper (Mitutoyo 547-301, Kanagawa). At 72 h, mice were sacrificed, both knees were isolated, fixed in 4% PFA, decalcified and embedded in paraffin. The intra-articular bleeding score (IBS) was assessed according to Hakobyan N et al[233] scoring system. Briefly, a 3-point scoring system based on examination of histological sections using light microscopy was used: score 0 represented a knee joint with the absence of bleeding and an IBS of 1 or 2 indicated a joint filled with blood with increased severity.

In vivo **PS inhibition**

10 week old mice received a continuous dose of rabbit anti-human PS-IgG (Dako Basel, Switzerland) or isotype rabbit IgG (R&D Systems) at 1 mg/kg/day through subcutaneous osmotic minipumps (model2001, Alzet).

Alternatively, a second group of 10 week old mice was treated with a single dose of mouse specific siRNA (s72206, Life Technologies) or control siRNA (4459405, In vivo Negative Control #1 Ambion, Life Technologies) at 1 mg/kg using a transfection agent (Invivofectamine 3.0, Invitrogen, Life Technologies) following the manufacturer's instructions. 2.5 days after PS inhibition, acute hemarthrosis model was performed as previously described.

Fibroblast-like synoviocytes (FLS) isolation, culture and flow cytometry

Murine FLS from 8-10 weeks old mice were isolated and cultured according to[234] . After three passages, phase contrast images of cells were taken, and cells were incubated with FITC-conjugated rat anti-mouse CD11b antibody (M1/70, Pharmingen, BD Biosciences), PE-conjugated rat anti-mouse CD90.2 antibody (30-H12, Pharmingen, BD Biosciences), FITC-

conjugated rat anti-mouse CD106 antibody (429 MVCAM.A, Pharmingen, BD Biosciences),

PE-conjugated hamster anti-mouse CD54 antibody (3E2, Pharmingen, BD Biosciences), and

fluorochrome-conjugated isotype control antibodies for 30 minutes at 4 °C in the dark. After a

final washing and centrifugation step, all incubated cells were analyzed on an LSR II flow

cytometer (BD Biosciences) and FACS Diva 7.0 software (BD Biosciences). Human FLS

from healthy individual and OA patient were purchased from Asterand, Bioscience and

cultured according to manufacture instructions.

Western blotting

 PS and TFPI were detected in human and mouse samples by sodium dodecyl sulfate-

polyacrylamide gel electrophoresis (12% gradient SDS-PAGE, Bio-Rad) under reducing

conditions. The proteins were transferred to nitrocellulose membranes (Bio-Rad), and then

visualized using: 2ug/mL monoclonal MAB-4976 (R&D system) for murine PS, 1ug/mL

polyclonal AF2975 for murine TFPI (R&D system). Recombinant murine PS[235] (30 ng),

recombinant human TFPI full length (provided by T. Hamuro, Kaketsuken, Japan), lysate of

washed platelets, PFP from $F8^{-/-}Pros1^{+/+}$ mice and placenta lysates from $F8^{+/+}Pros1^{+/+}$ mice

were used as PS, TFPIα controls. Samples from confluent murine and human FLS

conditioned media were collected after 24 h-incubation in a serum-free media (OptiMem) and

concentrated 40 times using Amicon filter devices (Millipore, 10 kDa cut-off). For TFPI

western blotting, samples were treated with a mixture of five protein deglycosidases (PNGase

F, O-Glycosidase, Neuraminidase, β1-4 Galactosidase, β-N-Acetylglucosaminidase,

Deglycosylation kit, V4931, Promega) for 12 h at 37°C before being loaded on the gel. Final

detection was completed by using a horseradish peroxidase–conjugated secondary antibody

(Dako) and the Supersignal West Dura Extended Duration Chemiluminescence Substrate

(Pierce), monitored with a Fuji LAS 3000IR CCD camera.

Immunohistochemistry on human knee synovium

Paraffin-embedded specimens of synovial tissue from twelve HA patients and four HB patients who underwent arthroplasty for severe knee arthropathy were collected at the archives of the Section of Anatomy and Histology, Department of Experimental and Clinical Medicine, University of Florence, as described elsewhere[196, 226]. Seven HA patients were treated on demand and five with secondary prophylaxis. All four HB patients were treated on demand. Synovial samples from seven osteoarthritis (OA) patients were used as controls[196, 226]. For immunohistochemistry analysis, synovial tissue sections (5 μm thick) were deparaffinized, rehydrated, boiled for 10 minutes in sodium citrate buffer (10 mM, pH 6.0) for antigen retrieval and subsequently treated with 3% H_2O_2 in methanol for 15 minutes at room temperature to block endogenous peroxidase activity. Sections were then washed in PBS and incubated with Ultra V block (UltraVision Large Volume Detection System Anti-Polyvalent, HRP, catalog number TP-125-HL, LabVision) for 10 min at RT according to the manufacturer's protocol. After blocking non-specific site binding, slides were incubated overnight at 4°C with rabbit polyclonal anti-human Protein S/PROS1 antibody (1:50 dilution, catalog number NBP1-87218, Novus Biologicals) or sheep polyclonal anti-human Tissue Factor Pathway Inhibitor (TFPI) antibody (1:500 dilution, catalog number PAHTFPI-S, Haematologic Technologies) diluted in PBS. For Protein S immunostaining, tissue sections were then incubated with biotinylated secondary antibodies followed by streptavidin peroxidase (UltraVision Large Volume Detection System Anti-Polyvalent, HRP; LabVision) according to the manufacturer's protocol. For TFPI immunostaining, tissue sections were instead incubated with HRP-conjugated donkey anti-sheep IgG (1:1000 dilution; catalog number ab97125; Abcam) for 30 min. Immunoreactivity was developed using 3-amino-9-ethylcarbazole (AEC kit, catalog number TA-125-SA; LabVision) as chromogen. Synovial sections were finally counterstained with Mayer's hematoxylin (Bio-Optica), washed, mounted in an aqueous mounting medium and observed under a Leica DM4000 B microscope (Leica Microsystems). Sections not exposed to primary antibodies or incubated with isotype-matched and concentration-matched non-immune IgG (Sigma-Aldrich) were

included as negative controls for antibody specificity. Light microscopy images were captured with a Leica DFC310 FX 1.4-megapixel digital colour camera equipped with the Leica software application suite LAS V3.8 (Leica Microsystems).

Flow cytometry on mouse blood monocytes

Blood circulating monocytes were obtained from mice before or after performing hemarthrosis as described previously[205]. Red blood cells (RBC) were lysed and discharged after centrifugation. The remaining cell pellet was resuspended and incubated for 5 minutes at 4 °C in FACS buffer containing 1% FC block (anti-CD16/CD32, eBioscience). After an additional centrifugation, cells were incubated with: PE-conjugated anti-mouse Ly-6C (HK1.4, Ebiosciences), PE-Cyanine7 conjugated anti-mouse CD3e (145-2C11, Ebiosciences), e-fluor 450 conjugated anti-mouse, CD11b (M1/70, Ebiosciences), FITC- conjugated anti-mouse CD19 (eBio1D3 Ebiosciences), and APC conjugated anti-mouse CD115 (AFS98, Ebiosciences). Cells were then washed in FACS buffer, centrifuged at 1500 g for 5 minutes at 4°C and fixed in 2% PFA. Cells were analyzed using an LSR II flow cytometer (BD Biosciences) and FACS Diva 7.0 software (BD Biosciences). Inflammatory monocytes (M1) and patrolling monocytes (M2) were identified according to the literature[205].

Flow cytometry on mouse knee lavages

Shortly after mouse sacrifice, the knee joints were punctured with a 30 G syringe (Hamilton) and joint lavage was performed 10 times with 10 µL FACS buffer. The lavage was mixed with 250 µL FACS buffer and centrifuged at 1500 g for 5 min at 4 °C. Next, supernatants were discharged and the remaining cell pellet was resuspended and incubated for 5 min at 4 °C in FACS buffer containing 1% FC block (anti-CD16/CD32, eBioscience). After an additional centrifugation, cells were incubated with: PE-conjugated anti-mouse Ly-6C (HK1.4, Ebiosciences), e-fluor 450 conjugated anti-mouse, CD11b (M1/70, Ebiosciences), PE-conjugated rat anti-mouse Ly-6C,6C (HK1.4, Ebiosciences) and APC-conjugated anti-mouse CD115 (AFS98, Ebiosciences). Cells were then washed in FACS buffer, centrifuged at

126

1500 *g* for 5 minutes at 4°C, fixed in 2% PFA and analyzed using the FACSCanto (BD Bioscences) and FACS Diva 7.0 software (BD Biosciences). Inflammatory monocytes (M1) and patrolling monocytes (M2) were identified according to the literature[205].

Plasma and knee lavages cytokines analysis

Plasma and knee lavages were analyzed using a multiplex cytokines assay (Bio-Plex Pro Mouse Cytokine 1, Bio-Rad) following the manufacturer's instruction. Briefly, $F8^{-/-}Pros1^{+/+}$ and $F8^{-/-}Pros1^{-/-}$ knee lavages (n=3-5 mice) were collected as previously described after AH. Data were analyzed using Bio-Plex manager software.

Calibrated automated thrombography assays in murine samples

Thrombin generation in PFP and PRP was determined using the calibrated automated thrombogram (CAT) method.

TFPI dependent PS activity was assessed in PRP (150 G/L), as follows. Briefly, 10 µL mouse PRP (150 G/L) was mixed with 10 µL PRP reagent (Diagnostica Stago), and 30 µL of buffer A (25 mm Hepes, 175 mm NaCl, pH 7.4, 5 mg/mL BSA). Thrombin generation was initiated at 37°C with 10 µL of a fluorogenic substrate/$CaCl_2$ mixture. Final concentrations were as follows: 16.6% mouse plasma, 1 pM hrTF, 4 µM phospholipids, 16 mM $CaCl_2$, and 0.42 mM fluorogenic substrate.

APC dependent PS activity was assessed in a CAT-based APC resistance test in mouse PFP and PRP in accordance to Dargaud Y et al[236]. PRP (150 G/L) was previously activated using 40 µM Ca^{2+} ionophore (A23187) for 5 min at 37C. Final concentrations were as follows: 16.6% mouse plasma, 22 µM A23187, 1 pM hrTF, 4 µM phospholipids, 2nM (for PFP) or 8 nM (for PRP) wild type recombinant mouse APC (wt-rmAPC)[5] or mutated recombinant mouse APC (rmAPC L38D),16 mM $CaCl_2$, and 0.42 mM fluorogenic substrate. The generation and characterization of rmAPC L38D was performed according to ref [237][213] and the purification according to ref[238][239].

For TF titration on PFP, the following reagents were used: PPP reagent and MP reagent (Diagnostica Stago).

Fluorescence was measured using a Fluoroscan Ascent® fluorometer, equipped with a dispenser. Fluorescence intensity was detected at wavelengths of 390 nm (excitation filter) and 460 nm (emission filter). A dedicated software program, Thrombinoscope® version 3.0.0.29 (Thrombinoscope bv) enabled the calculation of thrombin activity against the calibrator (Thrombinoscope bv) and displayed thrombin activity with the time. All experiences were carried out in duplicate at 37 °C and the measurements usually lasted 60 min.

Fibrin clot ultrastructure investigation

Fibrin clots were prepared at 37°C from PFP by the addition of ~5 nM TF (Dade Innovin, Siemens). They were then fixed in 2% glutaraldehyde, dehydrated, dried and sputter-coated with gold palladium for visualization using scanning electron microscopy, accordingly to Zubairova et al[240]. Semi quantitative evaluation of network density and fibers branching were performed using STEPanizer software (www.stepanizer.com).

CAT assay in human samples

Written informed consent was obtained from patients. Venous blood was drawn by venipuncture in 3.2% sodium citrate (vol/vol) and centrifuged at 2000g for 5 min. Platelet-poor plasma (PPP) was then centrifuged at 10000g for 10 minutes to obtain PFP. PFP was aliquoted, snap-frozen, and stored at −80°C until use. For PRP, blood was centrifuged at 180 g x 10 min. All subjects gave informed consent to participation. Thrombin generation was assessed in human PFP and PRP, according to ref[241] with minor changes. Briefly, 68 μL PFP or PRP (150 G/L) was incubated for 15 min at 37 °C with 12 μL of either a polyclonal rabbit anti-human PS-IgG antibody (0.42 mg/mL, Dako) or monoclonal antibodies against TFPI (0.66 μm, MW1848, Sanquin) or buffer A. Coagulation was initiated with 20 μL of a 7 : 1 mixture of the PPP low and PPP 5 pm reagents (Diagnostica Stago) for PFP samples or

with PRP reagent (Diagnostica stago) for PRP samples. After addition of 20 μL of $CaCl_2$ and fluorogenic substrate (I-1140; Bachem), the thrombin generation was followed in a Fluoroskan Ascent reader (Thermo Labsystems).

Endotoxemia model in HA mice

$F8^{-/-}Pros1^{+/+}$, $F8^{-/-}Pros1^{+/-}$, $F8^{-/-}Pros1^{-/-}$ mice were injected intraperitoneally (i.p.) with LPS from *Escherichia coli* O55:B5 (Sigma-Aldrich) at 25 mg/kg and continuously monitored for LPS-induced lethality for 72 h after LPS injection.

Cecal ligation puncture model in HA mice

A cecal ligation puncture (CLP) model was applied to 8-10 week old $F8^{-/-}Pros1^{+/+}$, $F8^{-/-}Pros1^{+/-}$, $F8^{-/-}Pros1^{-/-}$, $F8^{+/+}Pros1^{+/+}$ mice according to the protocol described by Toscano et al[13]. Briefly, mice were anesthetized by halothane. A midline laparotomy was performed to allow exposure of the cecum. The cecum was ligated as near to the ileocecal junction as possible and perforated twice with a 19-gauge needle. It was then gently squeezed to extrude a small amount of feces from the perforation sites and returned to the peritoneal cavity. The incision was closed with wound clips. Sham operated mice were also incised, cecum taken outside abdominal cavity, and returned in position without ligation or puncture. After surgery, and every 12 h, mice received 0.05 mg/kg of buprenorphine (Temgesic, Essex Chemie AG) subcutaneously up to 36 h post-surgery.

Bone marrow-derived macrophage isolation

Macrophages were derived from bone marrow (femur and tibia) from $F8^{+/+}Pros1^{+/+}$, $F8^{-/-}Pros1^{+/+}$ and $F8^{-/-}Pros1^{-/-}$ mice, and cultured according to the literature[242].

Bacterial phagocytosis assay

Mouse macrophages (0.5×10^6) were resuspended in 200 μl of DMEM medium, primed with IFNγ (Pepro Tech EC) for 2 h and consequently stimulated with 0.3 μg/mL

Lipopolysaccharide (LPS, 055:B5; Sigma-Aldrich). GFP-labeled *E. coli* GFP (M91655; GFP-*E. coli*) were opsonized with 2% mouse serum in 1 x Hank's Balanced Salt Solution (HBSS; LuBioScience GmbH) for 15 min (rotating end-over-end, 37°C). 200 µl of opsonized bacteria was then added to the cells. The cells were incubated with the bacteria for 15 min (rotating end-over-end, 37°C). Phagocytosis was stopped by adding 400 µl of ice-cold PBS with 0.02% EDTA to the cells. After one washing step with 400 µl of ice-cold PBS, the cells were analyzed by flow cytometry (FACSCalibur; BD Biosciences). In parallel mouse macrophage (0.3 x 10^6) were seeded on glass chamber, primed with IFNγ for 2h and consequently stimulated with 0.3 µg/mL LPS. GFP-*E. coli* (6 x 10^6) was added and analyzed by live cell imaging (LSM 700; Carl Zeiss Micro Imaging) using 63x /1.40 Oil DIC objective and images were processed with IMARIS software.

Statistical methods

Values were expressed as mean plus or minus s.e.m.. A Chi-square for non-linked genetic loci was used to assess the Mendelian allele segregation. Survival data in the model of TF-induced venous thromboembolism, the CLP model, and the endotoxemia model were plotted using the of Kaplan-Meier method. A log-rank test was used to statistically compare the curves (Prism 6.0d; GraphPad). The other data were analyzed by t-test, one-way and two-way ANOVA test with GraphPad Prism 6.0d. A *P*-value of less than 0.05 was considered statistically significant.

Acknowledgements

Author contributions

R.P., Lu.B., M.M., D.M., I.R., N.D., P.A., C.Q., S.Y, H.U.S., L.I.M., S.C., A.A.S. designed and performed experiments. Lu.B., R.P., M.M., D.M., I.R., N.D., P.A., J.A.F. La.B., C.Q., Y.M., J.K.H., JH.G., H.U.S., L.I.M., F.S., S.C., A.A.S. interpreted data. R.P., Lu.B., J.H.G., S.C., A.A.S. wrote the manuscript. J.A.F., La.B., Y.M., J.K.H., J.H.G., F.S. prepared reagents.

Author information

Reprints and permissions information is available at www.nature.com/reprints. The authors declare no competing financial interests. Readers are welcome to comment on the online

version of the paper. Correspondence and requests for materials should be addressed to

A.A.S. (anne.angelillo-scherrer@insel.ch).

Main figures
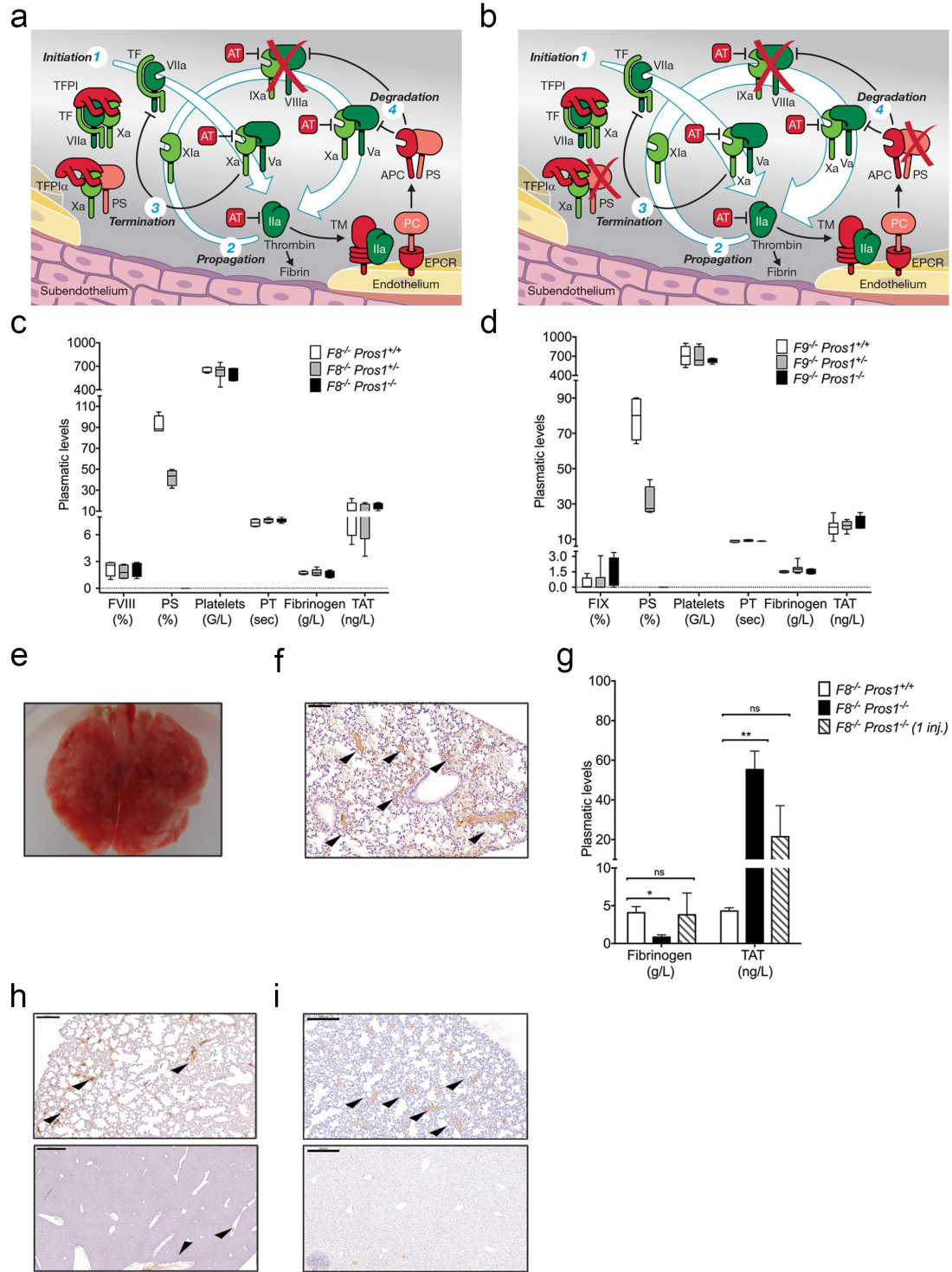
Figure 1. Loss of X-ase activity rescues *Pros1$^{-/-}$* mice. a-b, Schematic model of thrombin generation in hemophilic condition (**a**) and the experimental approach to enhance thrombin generation in severe hemophilia A and B by targeting *Pros1* (**b**). **c-d,** Murine model validation and evaluation of DIC hematologic parameters in hemophilic adult mice with and without *Pros1* deficiency: PS (antigenic), FVIII (coagulant activity) or FIX (coagulant activity) plasma levels in *F8$^{-/-}$Pros1$^{+/+}$*, *F8$^{-/-}$Pros1$^{+/-}$* and *F8$^{-/-}$Pros1$^{-/-}$* (**c**), and *F9$^{-/-}$Pros1$^{+/+}$*, *F9$^{-/-}$Pros1$^{+/-}$* and *F9$^{-/-}$Pros1$^{-/-}$* adult mice (**d**) (*n*=5/group); platelets (*n*=7/group), fibrinogen (*n*=8/group), PT (*n*=6/group) and TAT (*n*=6/group) in hemophilia A group (**c**); and platelets (*n*=5/group), fibrinogen (*n*=4/group), PT (*n*=4/group) and TAT (*n*=4/group) in hemophilia B group (**d**). **e-f,** Macroscopic image of lungs from *F8$^{-/-}$Pros1$^{-/-}$* mice 24 h after a single i.v. injection of 2 U/g recombinant FVIII (Advate®) infusion (**e**) and corresponding microscopic evaluation of fibrin clots in lung section (**f**). **g,** Recombinant FVIII (Advate®) administration in *F8$^{-/-}$Pros1$^{+/+}$* and *F8$^{-/-}$Pros1$^{-/-}$*: plasma levels of fibrinogen and TAT at 24 h following 5 injection of 0.3 U/g Advate® i.v. (injection time-points: 1 h before catheter insertion and 1 h, 4 h, 8 h and 16 h after catheter insertion) (*n*=3) (**g,** white and black columns) and 24 h after a single i.v. injection in *F8$^{-/-}$Pros1$^{-/-}$* (*n*=3) (**g,** dashed column), and representative immunohistochemistry allowing the detection of fibrin clots in lungs and liver sections in *F8$^{-/-}$Pros1$^{-/-}$* 24 h after 0.3 U/g repeated i.v. injections of Advate® (**h**) and after a single i.v. injection of 0.3 U/g Advate® i.v. (**i**). All data are expressed as mean±s.e.m.; ns, not significant; *, *P*<0.05 **; *P*<0.005.
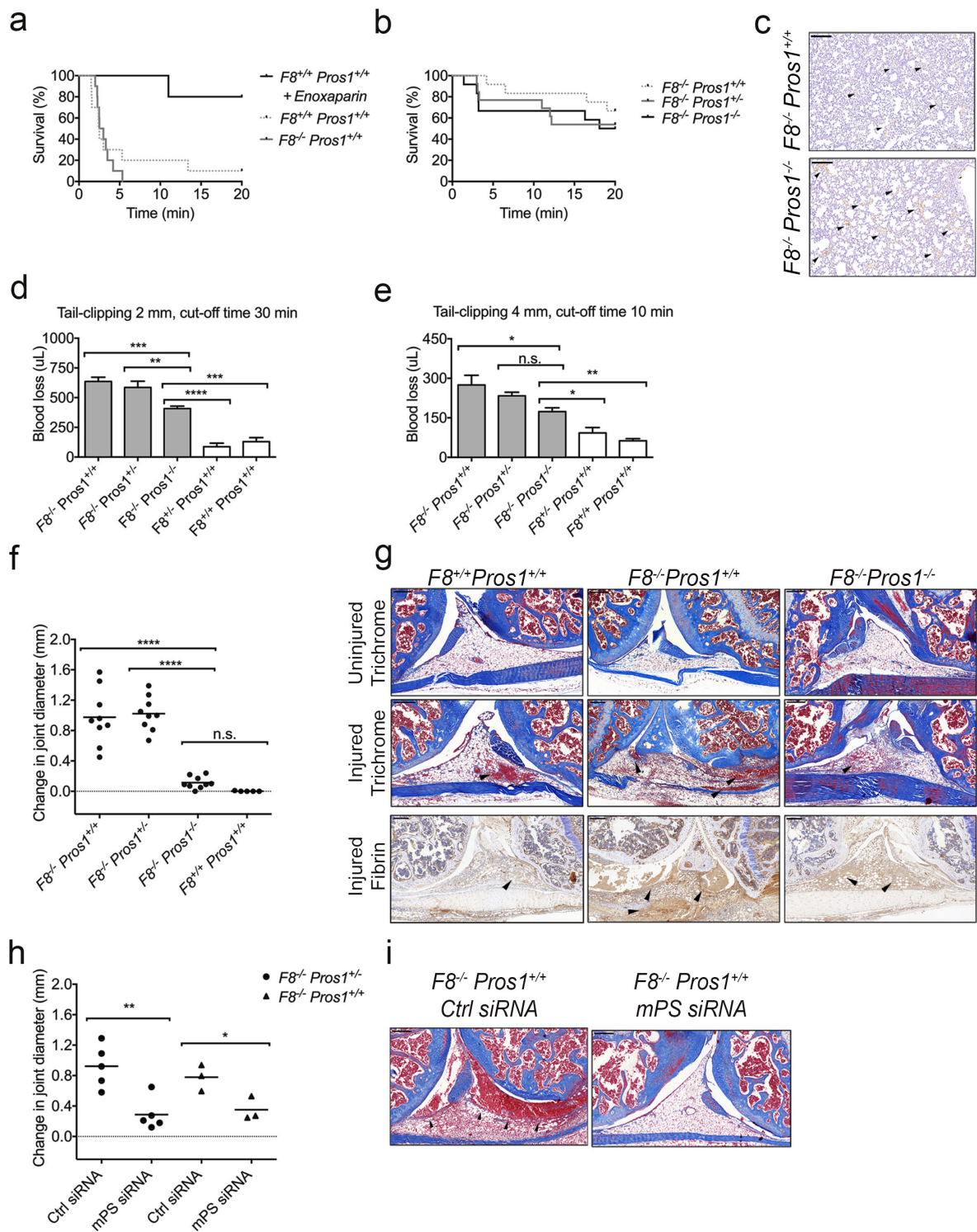
Figure 2. Murine models of thrombosis and bleeding. a-c, TF-induced venous thromboembolism in $F8^{+/+}$ $Pros1^{+/+}$, $F8^{-/-}$ $Pros1^{+/+}$, $F8^{-/-}$ $Pros1^{+/-}$ and $F8^{-/-}$ $Pros1^{-/-}$ mice (n=10/genotype). Anesthetized mice were injected intravenously via the inferior vena cava with different doses of recombinant TF (Innovin): ½ dilution (~4.3 nM TF) in **a** and ¼ dilution (~2.1 nM TF) in **b-c**. In (**a**), one group of $F8^{+/+}Pros1^{+/+}$ mice received enoxaparin 60

μg/g s.c. The time to the onset of respiratory arrest that lasted at least 2 min was recorded. Experiments were terminated at 20 min. Kaplan-Meier survival curves (**a-b**). **c,** 2 min after onset of respiratory arrest or at the completion of the 20-min observation period, lungs were excised and investigated for fibrin clots (immunostaining for insoluble fibrin, mAb clone 102-10). **d-e,** Tail bleeding model. Blood was collected after 2 mm (**d**) and 4 mm (**e**) tail transection for 30 min (**d**) and 10 min (**e**) in a fresh tube of saline; total blood loss (μl) was then measured. $F8^{+/-}Pros1^{+/+}$ and $F8^{+/+}Pros1^{+/+}$ mice (white columns) served as controls ($n = 5$ for all groups in **d**, $n=6$ for all groups in **e**). **f-i,** Acute hemarthrosis model. **f,** Difference between the knee diameter 72 h after the injury and before the injury in $F8^{-/-}Pros1^{+/+}$, $F8^{-/-}Pros1^{+/-}$, $F8^{-/-}Pros1^{-/-}$ and $F8^{+/+}Pros1^{+/+}$ mice. **g,** Microscopic evaluation (Masson's trichrome stain and immunostaining for insoluble fibrin) of the knee intra-articular space of a representative not injured and injured legs after 72 h in $F8^{+/+}Pros1^{+/+}$, $F8^{-/-}Pros1^{+/+}$ and $F8^{-/-}Pros1^{-/-}$ mice. **h,** *In vivo* mPS silencing using specific siRNA: evaluation of the joint diameter 72 h after injury in $F8^{-/-}Pros1^{+/-}$ and $F8^{-/-}Pros1^{+/+}$ mice treated with a single i.p. infusion of mPS siRNA or control siRNA. **i,** Microscopic evaluation (Masson's trichrome stain) of the knee intra-articular space of a representative injured leg after 72 h in $F8^{-/-}Pros1^{+/+}$ mice previously treated with mPS siRNA or Ctrl siRNA. Measurements are presented as mean±s.e.m. *, $P<0.05$; **, $P<0.005$; ***, $P<0.0005$; ****, $P<0.0001$.
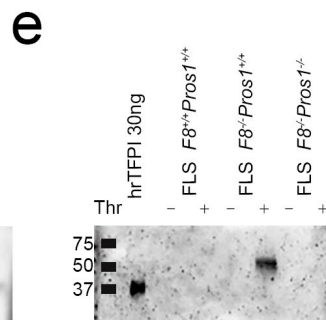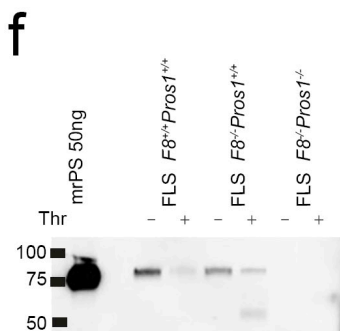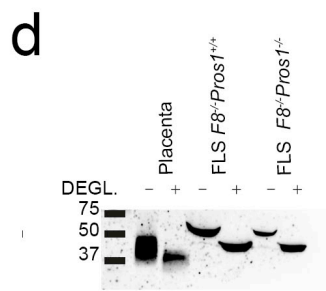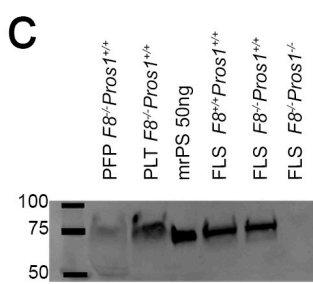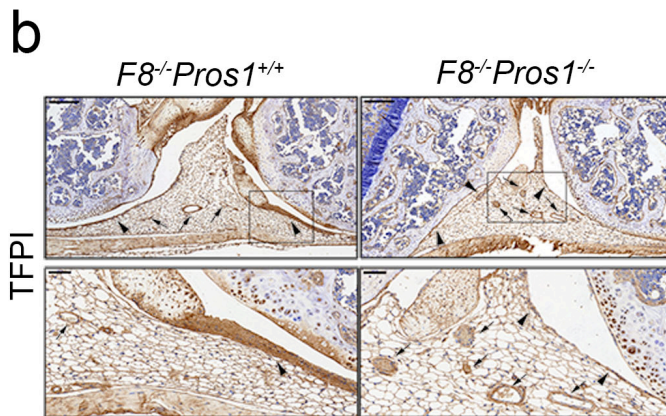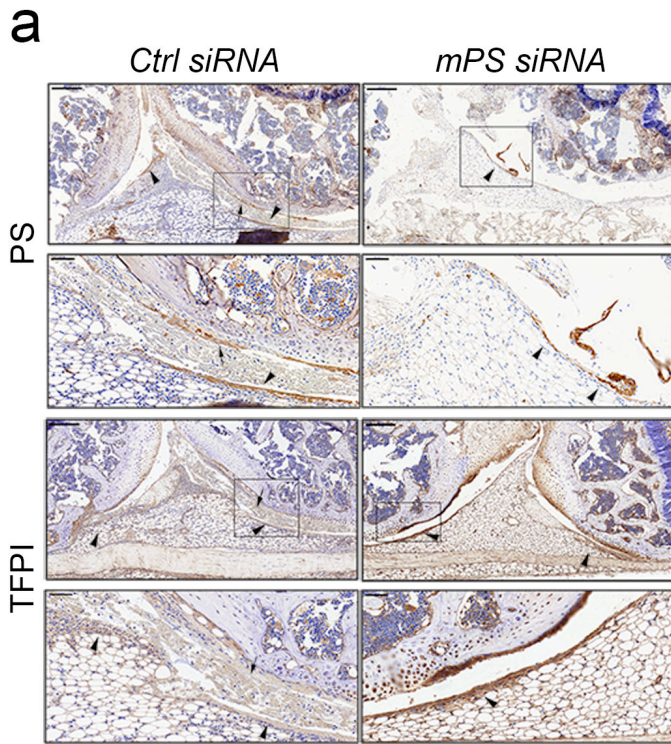
Figure 3. Both PS and TFPI are expressed in murine synovium. a, Immunostaining for PS and TFPI in the knee intra-articular space of injured knees from $F8^{-/-}Pros1^{+/+}$ mice previously treated with Ctrl-siRNA or mPS-siRNA. Arrow heads point to synovial tissue and arrows, to vascular structures, all positive for both PS and TFPI. Boxes in the upper figures (Scale bars: 200 μm) show the area enlarged in the panel below (Scale bars: 50 μm). **b,** Immunostaining for TFPI in the knee intra-articular space of not injured knees from $F8^{-/-}Pros1^{+/+}$ and $F8^{-/-}Pros1^{-/-}$ mice. **c-e,** Western blot analysis of conditioned media from primary murine fibroblast-like synoviocytes (FLS) cultures using anti-PS (c) and anti-TFPI (d) antibodies. Platelet-free plasma (PFP), protein lysates from platelets (PLT), murine PS (mPS) were used as positive controls (c). TFPI isoform expression determined by comparing molecular weights of deglycosylated TFPI and of fully glycosylated TFPI. Murine placenta was used as positive control for TFPIα. **f-e,** Western blot analysis of total protein lysates isolated from FLS after 24h of culture in presence of thrombin (Thr, +) or of a vehicle (-) using anti-PS (f) and anti-TFPI (e) antibodies. Human recombinant TFPI full length was used as positive control for TFPIα (hrTFPI). Blots are representative of three independent experiments.
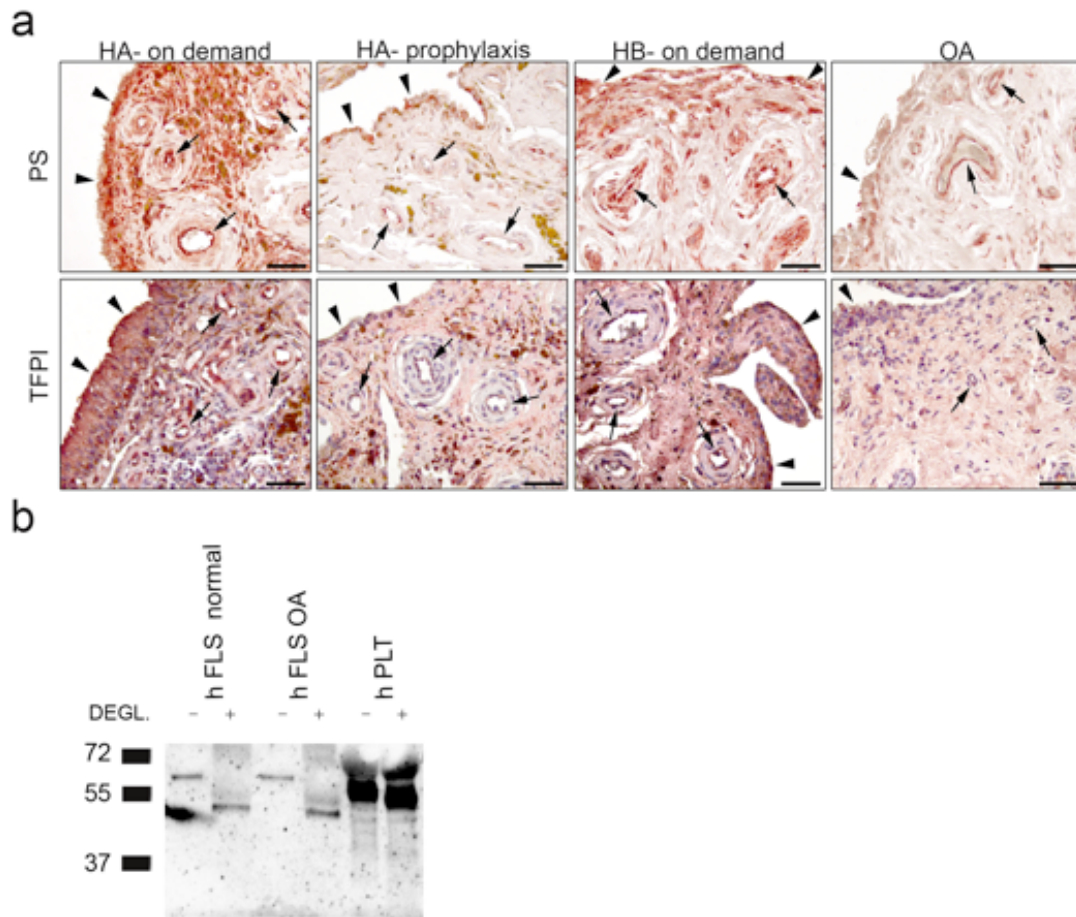
Figure 4. PS and TFPI in human synovium. a, PS and TFPI are expressed in synovial tissue of patients with HA (on demand and on prophylaxis), HB on demand or osteoarthritis (OA). Arrowheads point to synovial lining layer and arrows, to vascular structures in the sublining layer, all positive for both PS and TFPI. Scale bars: 50 μm. **b,** Western blot analysis of conditioned media of primary human FLS (hFLS) cultures from an healthy individual and an OA patient before and after deglycosylation using anti-TFPI antibody. Human platelet lysate (hPLT) was used as positive control for TFPIα. Blots are representative of three independent experiments.
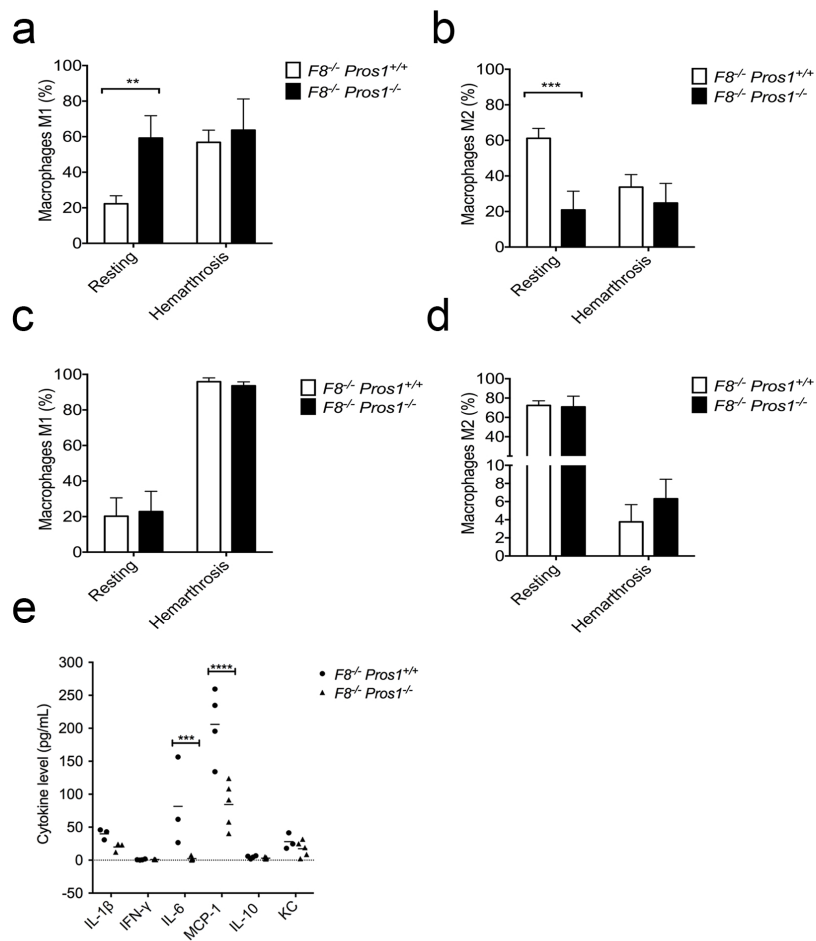
**Figure 5. Monocytes/macrophages in HA mice with or without PS deficiency. a-d,** Count of M1 and M2 monocytes in whole blood (**a-b**) and macrophages in knee lavage (**c-d**) as assessed by flow cytometry in resting condition and after hemarthrosis. **e,** Cytokines levels in knee-lavage after hemarthrosis in *F8⁻/⁻ Pros1⁺/⁺* and *F8⁻/⁻ Pros1⁻/⁻* mice. *, P<0.05; **, P<0.005; ***, P<0.0005; ****, P<0.0001.
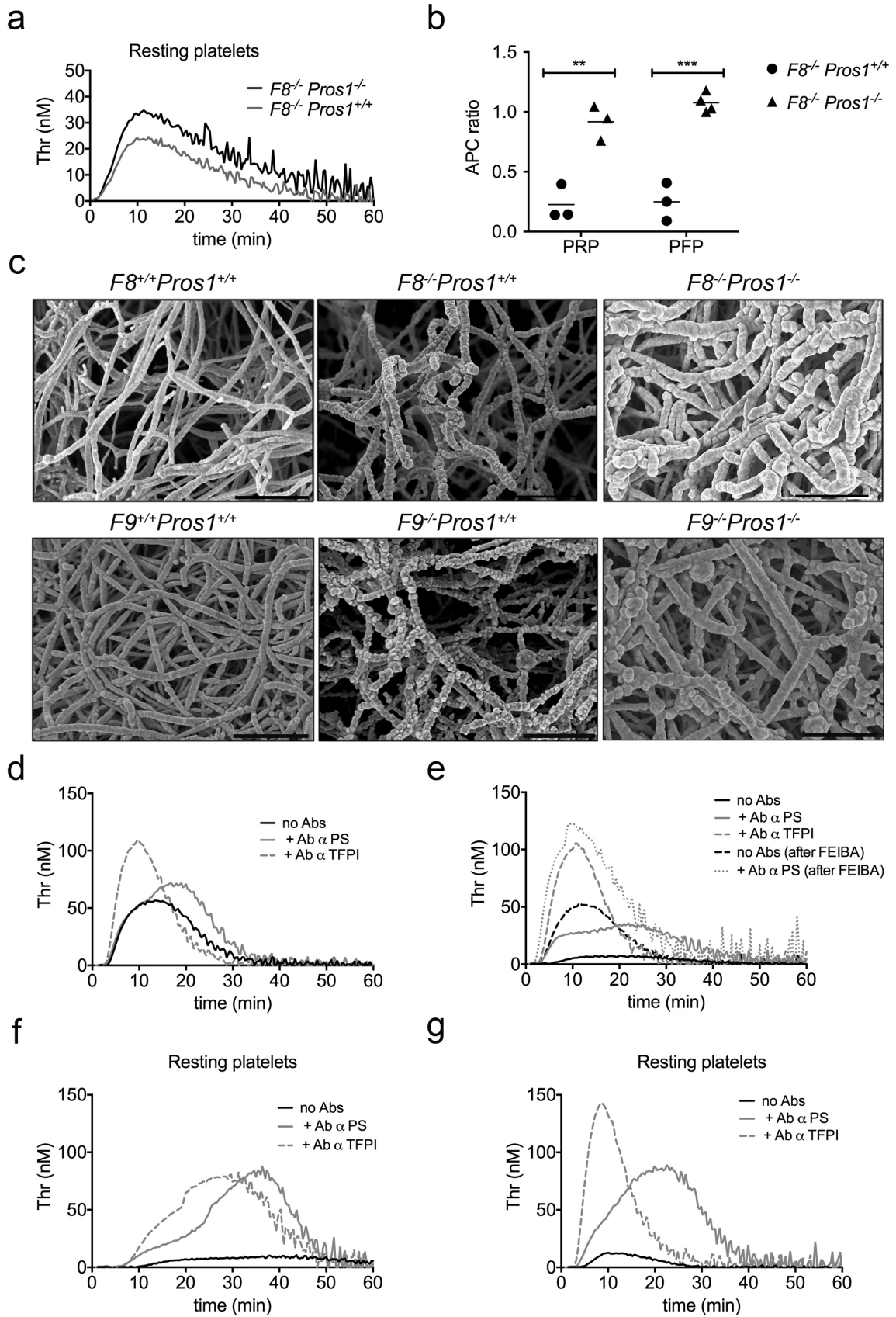
Figure 6. Thrombin generation and fibrin network in hemophilia

a, TF- (1 pM) induced thrombin generation in PRP from $F8^{-/-} Pros1^{+/+}$ and $F8^{-/-} Pros1^{-/-}$ mice depicting TFPI-dependent PS activity. **b,** APC-dependent PS activity in PRP and PFP from $F8^{-/-} Pros1^{+/+}$ and $F8^{-/-} Pros1^{-/-}$ mice. **c,** Representative scanning electron microscopy images from $F8^{+/+} Pros1^{+/+}$, $F8^{-/-} Pros1^{+/+}$ and $F8^{-/-} Pros1^{-/-}$, and from $F9^{+/+} Pros1^{+/+}$, $F9^{-/-} Pros1^{+/+}$ and $F9^{-/-} Pros1^{-/-}$ fibrin structure. **d-g,** Thrombin generation triggered by low TF concentration (1 pM) in PFP (**d-e**) and PRP (**f-g**) from severe HA patients (FVIII <1%) without (**d, f**) and with a high titer of inhibitor (**e,g**). Measurements are presented as mean±s.e.m. ******, $P<0.005$; *******, $P<0.0005$.
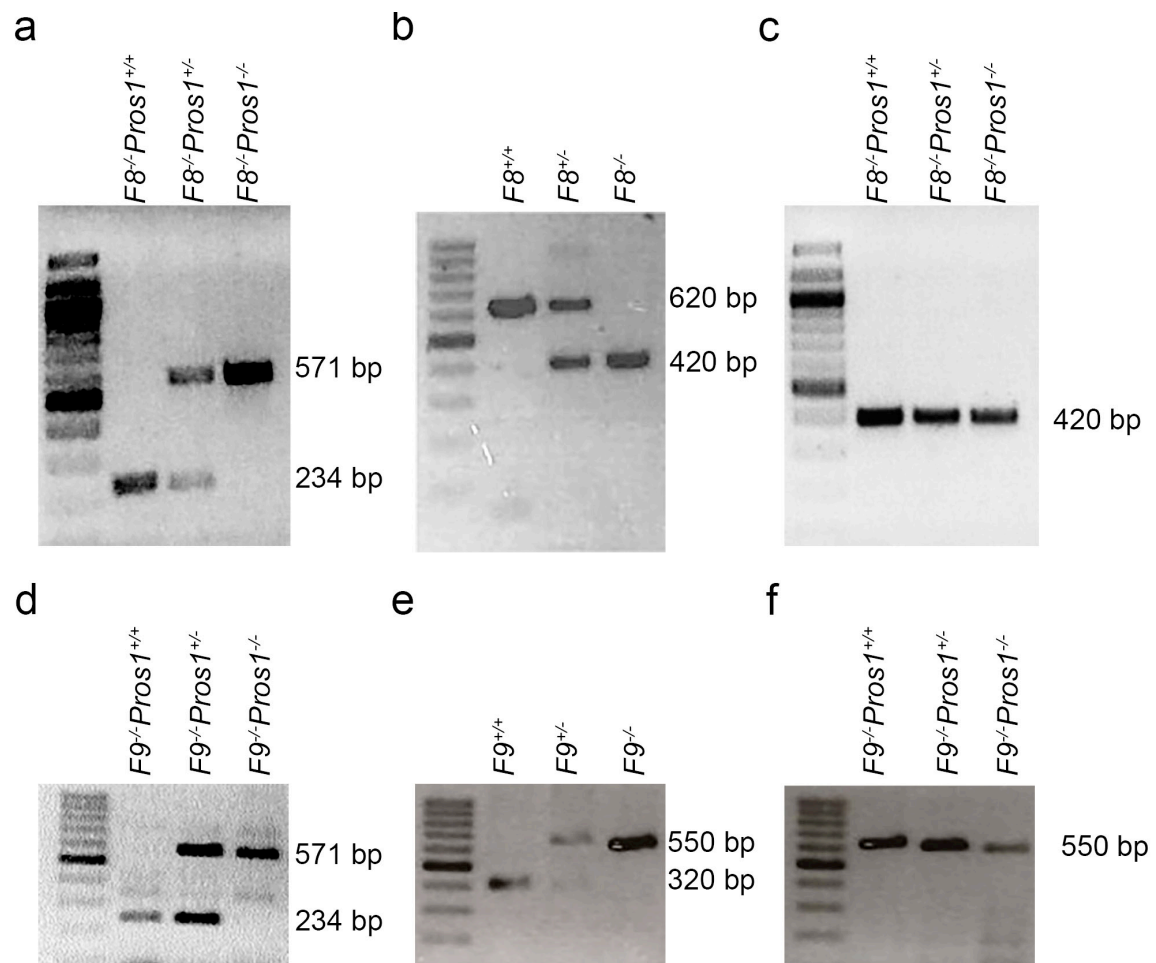
Extended Data Figure 1. Genotyping approaches. Genotypes obtained by crossing *F8^-/-^ Pros1^+/-^* (**a-c**) and *F9^-/-^Pros1^+/-^* (**d-f**) mice. a, *Pros1* alleles were amplified by a multiplex PCR. PCR products were then subjected to electrophoresis; the *wt* band has a lower molecular weight (234 bp) compared to the *null* band (571 bp), in accordance to Saller, 2009. **b,** Set-up of multiplex PCR to amplify the *wt* band (620 bp) and the *null* band (420 bp) of *F8* alleles from genomic DNA. **c,** PCR products of *F8* alleles amplification (*null* band: 420 bp) on the same samples than in (**a**). **d,** *Pros1* alleles were amplified by a multiplex PCR. PCR products were then subjected to electrophoresis; the *wt* band has a lower molecular weight (234 bp) compared to the *null* band (571 bp), in accordance to Saller, 2009. **e**, Set-up of multiplex PCR to amplify the *wt* band (320 bp) and the *null* band (550 bp) of *F9* alleles from genomic DNA. **f**, PCR products of *F9* alleles amplification (*null* band: 550 bp) on the same samples than in (**d**).
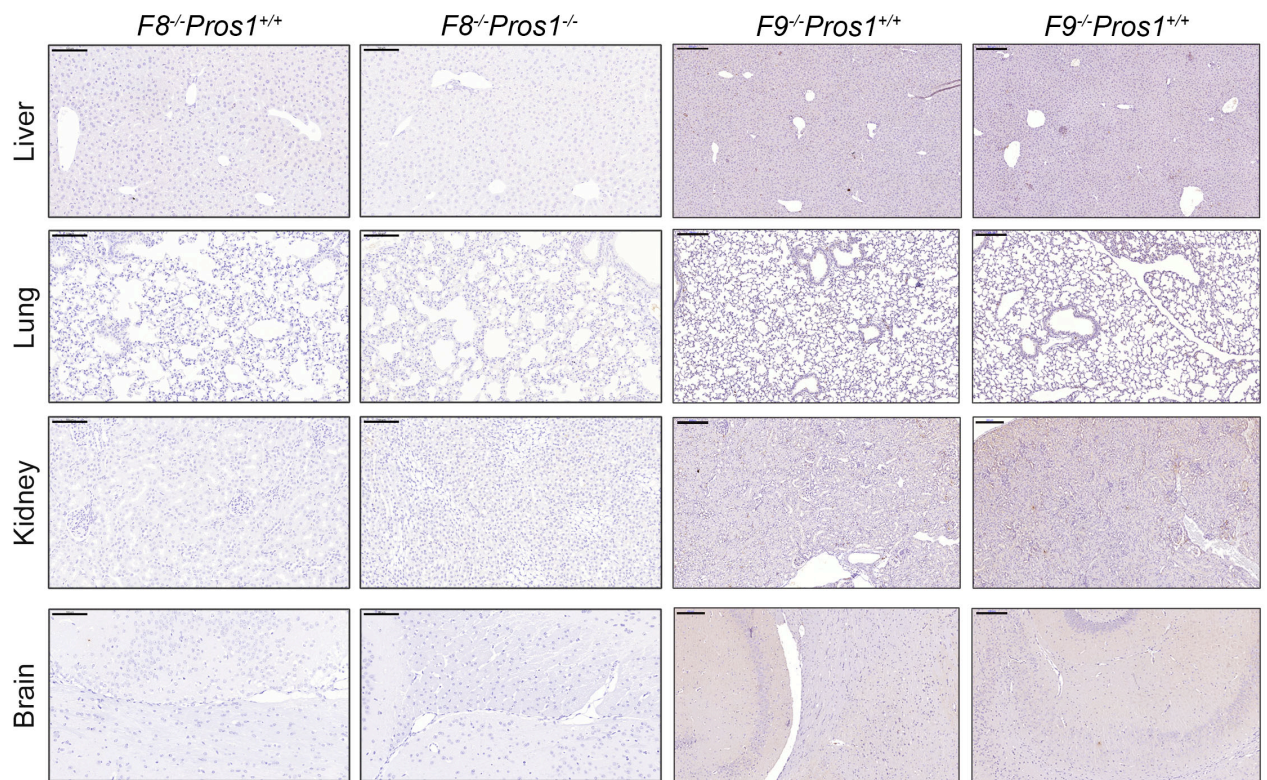
Extended Data Figure 2: Histology in physiologic condition. Immunostaining for insoluble fibrin on liver, lung, kidney, brain sections in $F8^{-/-}Pros1^{-/-}$ and in $F8^{-/-}Pros1^{+/+}$ mice as well as in $F9^{-/-}Pros1^{+/+}$ and $F9^{-/-}Pros1^{-/-}$. Scale bar: 100 μm.
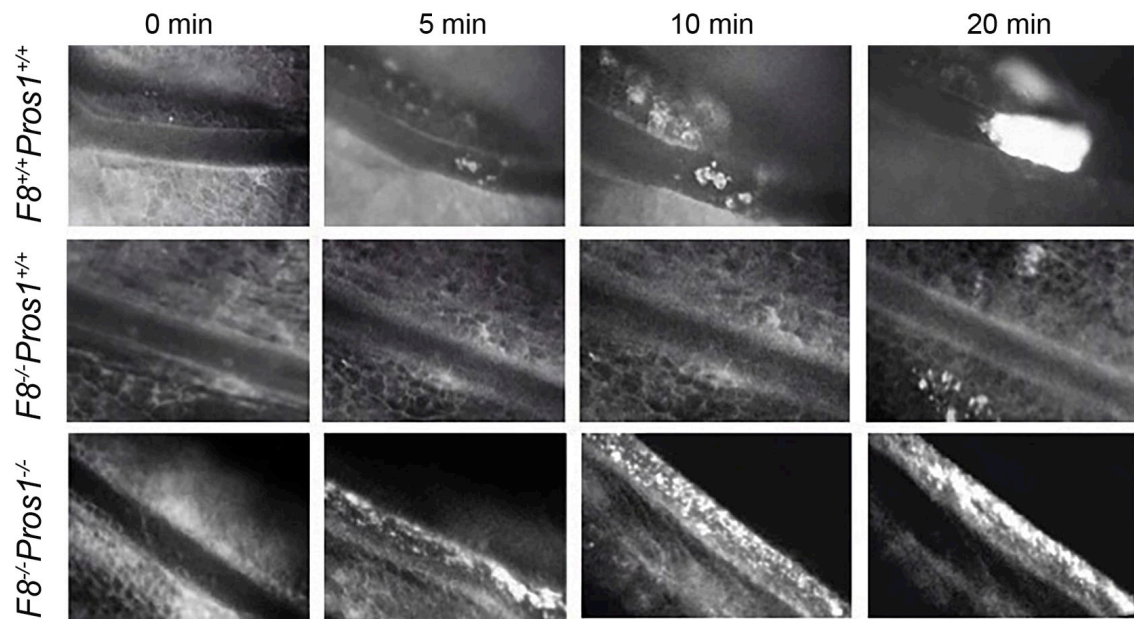
Extended Data Figure 3: Loss of FVIII partially protects *Pros1^{-/-}* mice against thrombosis in mesenteric arterioles. Thrombus formation in FeCl3-injured mesenteric arteries recorded by intravital microscopy in $F8^{+/+} Pros1^{+/+}$, $F8^{-/-} Pros1^{+/+}$ and $F8^{-/-} Pros1^{-/-}$ mice, representative experiment (n=3/genotype).
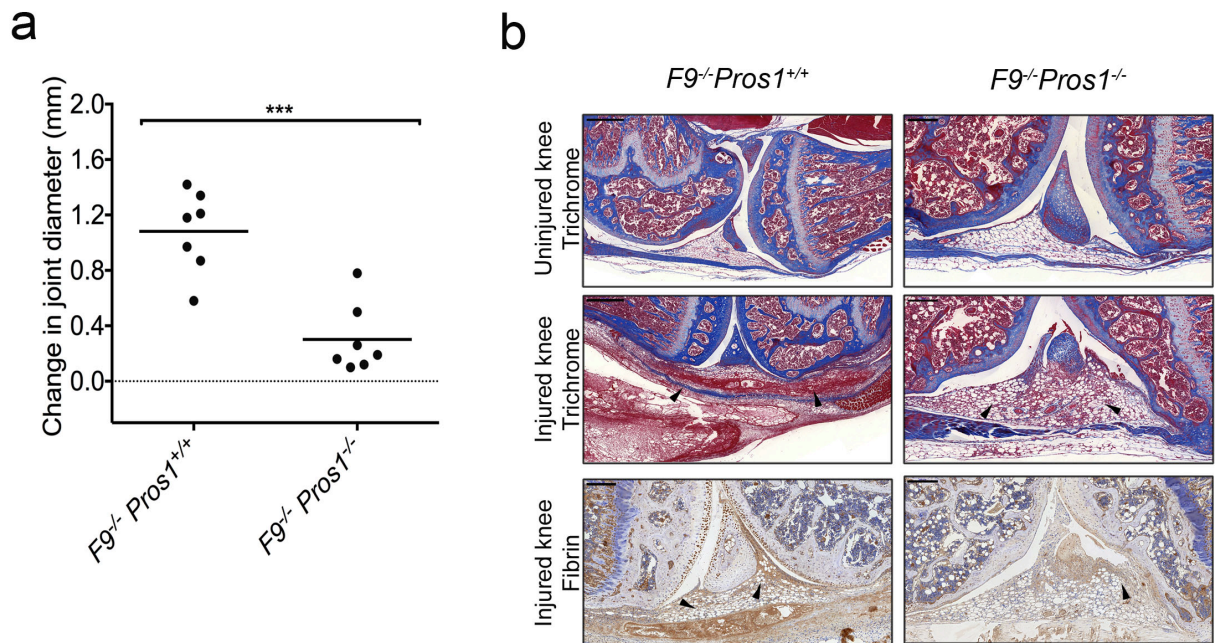
Extended Data Figure 4: Genetic loss of *Pros1* prevents hemarthrosis in mice with hemophilia B. a, Difference between the knee diameter 72 h after the injury and before the injury in $F9^{-/-}Pros1^{+/+}$, $F9^{-/-}Pros1^{+/-}$, $F9^{-/-}Pros1^{-/-}$ and $F9^{+/+}Pros1^{+/+}$ mice. **b,** Microscopic evaluation (Masson's trichrome stain and staining for insoluble fibrin, mAb clone 102-10) of the knee intra-articular space of a representative not injured and injured legs after 72 h in $F9^{+/+}Pros1^{+/+}$, $F9^{-/-}Pros1^{+/+}$ and $F9^{-/-}Pros1^{-/-}$ mice. Scale bar: 500 μm. Measurements are presented as mean±s.e.m. ***, $P<0.0005$.
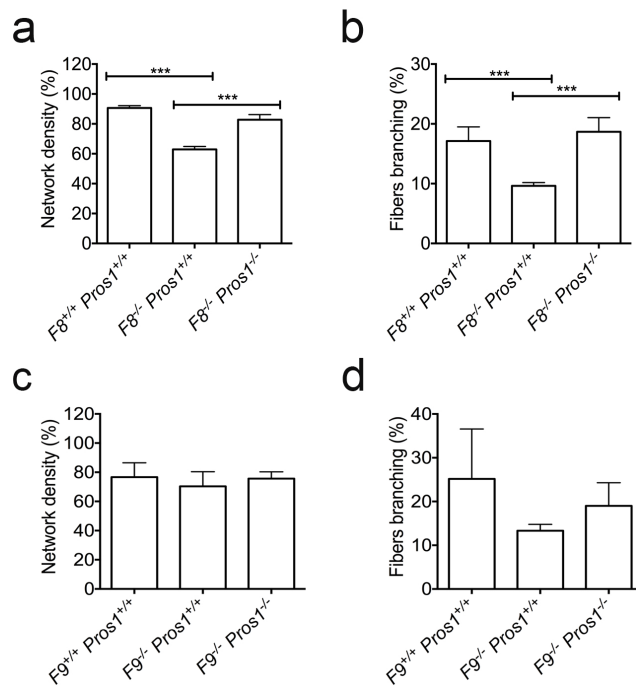
Extended Data Figure 5: Quantification of fibrin network density and fibers branching.

a-b, Fibrin network from $F8^{+/+} Pros1^{+/+}$, $F8^{-/-} Pros1^{+/+}$ and $F8^{-/-} Pros1^{-/-}$ mice. **c-d,** Fibrin network from $F9^{+/+} Pros1^{+/+}$, $F9^{-/-} Pros1^{+/+}$ and $F9^{-/-} Pros1^{-/-}$. Quantification of fibrin network density (a and c). Quantification of fibers branching (b and d). Measurements are presented as mean±s.e.m. ***, $P<0.0005$
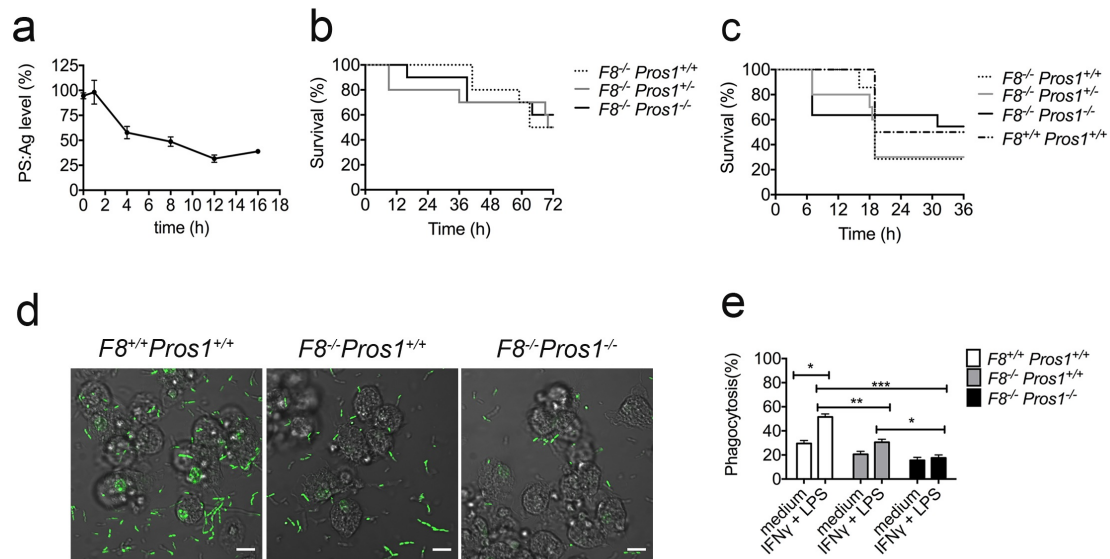
Extended Data Figure 6. Response of HA mice with or without genetic loss of *Pros1* to inflammation and infection. a, PS plasma concentration in mice challenged by LPS (25 mg/kg i.p.). **b-c,** Kaplan-Meier plots of survival after LPS treatment (25 mg/kg i.p.) (**b**) and after cecal-ligation and punction (**c**). Data were pooled from multiple independent experiments. **d,** Live confocal analysis of bacterial phagocytosis 15 min after the addition of bacteria to mouse macrophages. Bars, 10 mm. **e,** Flow cytometry analysis of bacterial phagocytosis 15 min after the addition of bacteria to mouse macrophages. Measurements are presented as mean±s.e.m. *, *P<0.05*; **, *P<0.005*; ***, *P<0.0005*.
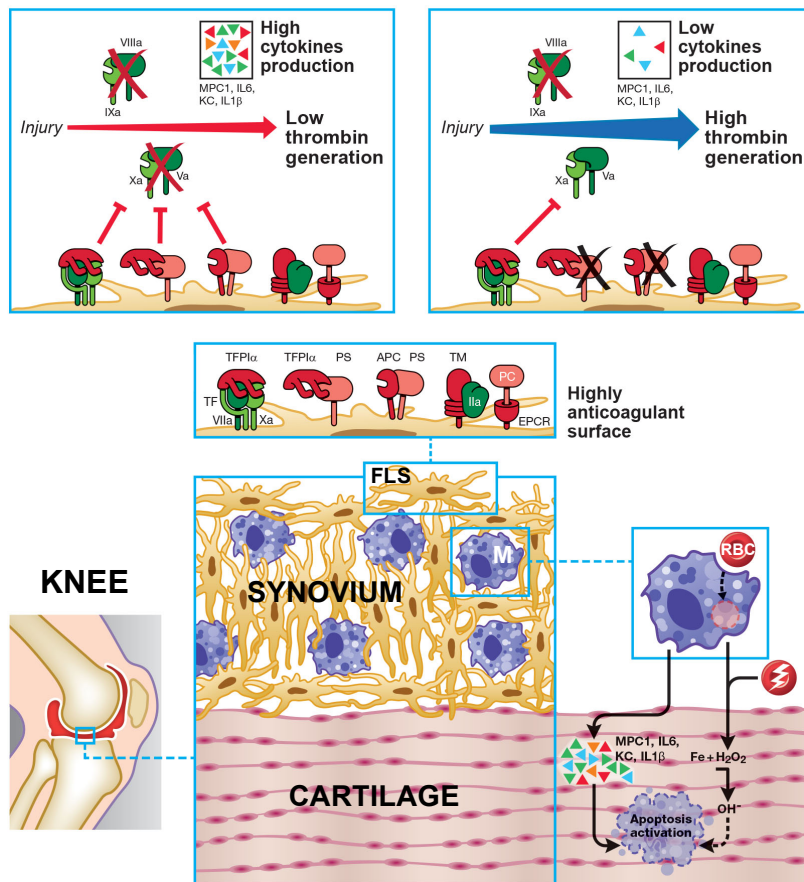
Extended Data Figure 7: Model of hemarthrosis without X-ase activity in presence (upper left) or in absence (upper right) of PS. In hemophilia, hemarthrosis account for 70-80% of all bleeds[202, 203]. The synovium is a connective tissue lining the inner surface of capsules of synovial joints, such as the knee as depicted on this figure. It makes direct contact with the synovial fluid, located at the tissue surface and composed from many rounded macrophage-like synovial cells (M) and FLS. M insure the maintenance of the synovial fluid by removing debris and FLS produce extracellular components of the synovial fluid. Because joints display a very weak expression of TF[223] and synovial cells produce a high amount of TFPIα, the activity of the extrinsic pathway is massively reduced intra-articularly, predisposing hemophilic joints to bleed. In addition, both TM and EPCR are expressed by FLS[224, 225], suggesting that the thrombomodulin-thrombin complex activates blood protein C to APC in the context of AH, a process strongly accelerated by EPCR that might

contribute to the aggravation of the local sustained bleeding process. Importantly, the expression of TFPIα is modulated by thrombin. We found that PS is also expressed by FLS and constitutes a potential therapeutic target, because of its dual cofactor activity of APC and TFPIα, that are both present within the joints. In the presence of PS, hemarthrosis provokes the release of proinflammatory cytokines (MCP-1, IL-6, KC, IL-1β) and increases TFPIα expression in the synovium. Thus, we propose that TFPIα and its cofactor PS, both produced by FLS, together with the TM-PC pathway constitute a potent intra-articular anticoagulant system that has an important impact on hemarthrosis.

After AH, the blood is cleared from the joint cavity by synovial lining cells, M and other inflammatory cells in about one week (reviewed in[243]). Iron derived from red blood cells (RBC) accumulates within the joint as hemosiderin which causes synovial inflammation ([243]). In addition, iron and H_2O_2 are responsible for the apoptosis of the chondrocytes ([243]).

Thus, AH that usually results in marked local inflammation and joint symptoms that can last for days to weeks also promotes the local secretion of anticoagulants such as TFPIα and its cofactor PS that are responsible for self-perpetuating a vicious circle.

Chapter V. Pregnancy and protein S deficiency

(Manuscript in preparation)

Chapter V. Pregnancy and protein S deficiency

Raja Prince[1,2], Sara Calzavarini[1,2], Justine Brodard[1,2], Natacha Dewarat[1,2], Desiré Reina Caro[1,2], Claudia Quarroz[1,2], José A. Fernández[3], Yasuhiro Matsumura[4], François Saller[5], John H. Griffin[3], Anne Angelillo-Scherrer[1,2]

1) Department of Hematology and Central Hematology Laboratory, Inselspital, Bern University Hospital, University of Bern, CH-3010 Bern, Switzerland

2) Department of Clinical Research, University of Bern, Murtenstrasse 31, CH-3010 Bern, Switzerland

3) Department of Molecular and Experimental Medicine, The Scripps Research Institute, La Jolla, California 92037, USA

4) Division of Developmental Therapeutics, Research Centre for Innovative Oncology, National Cancer Centre Hospital East, Chiba, Japan

5) INSERM & UMR-S 1176, Université Paris-Sud, Université Paris-Saclay, 94270 Le Kremlin-Bicêtre, France

Correspondence to: Prof. Anne Angelillo-Scherrer
                          Department of Hematology and Central Hematology Laboratory
                          Inselspital
                          Bern University Hospital
                          University of Bern
                          CH-3010 Bern
                          Switzerland
                          Phone: +41 31 632 33 02
                          e-mail: anne.angelillo-scherrer@insel.ch

4.1 Introduction:

Pregnancy is associated with various physiological changes, which may affect most of the body system. Some of these changes start immediately after conception and continue through delivery to the postpartum period in order to accommodate both the maternal and fetal needs [244]. Pregnancy is also associated with a shift of the coagulation balance with increased concentration of clotting factors, decreased concentration of some of the natural anticoagulants and diminished fibrinolytic activity. These changes occur in order to simplify healthy pregnancy and maintain placental function in order to meet the delivery's hemostatic challenge. However, it provoke a state of hypercoagulability that in one hand, protects pregnant women from fatal hemorrhage during delivery and in the other hand predispose them to thromboembolism [131].

Thrombophilia is a disorder that predisposes to develop venous thrombosis and increases the risk for venous thromboembolism (VTE). Two thrombophilia distinct categories are known: acquired thrombophilia like antiphospholipid antibody syndrome (aPL), that is strongly associated with recurrent pregnancy loss [133, 135], and inherited thrombophilias due to anticoagulant proteins deficiencies or their gene mutations. The most frequent abnormalities are factor V Leiden (FV Leiden) mutation and the prothrombin gene mutation. It was previously reported that in pregnancy, predictive rates of VTE in women with inherited thrombophilias were: 1:500 for patients carrying heterozygous mutation for FV Leiden, 1:200 for those with heterozygous mutation for prothrombin G20210A. The accumulation of more than a single mutation seems to higher the VTE incidence [137].

Antithrombin (AT), Protein C (PC) and Protein S (PS) deficiencies are also inherited thrombophilia factors that provoke VTE during pregnancy [138].

PS, a vitamin K-dependent protein (VKDP) functions as natural anticoagulant in the blood. It acts as a cofactor of activated protein C (APC) and tissue factor pathway inhibitor (TFPI) and also displays a direct anticoagulant activity. PS circulates in human plasma at a concentration of 350 nanomolar (nM) corresponding to 25 µg/mL of which 60% forms a complex with C4b-

binding protein (C4BP). The remaining 40% circulates in free form [20, 21]. The importance of PS is illustrated by life threatening skin necrosis and disseminated intravascular coagulation (DIC) named purpura fulminans (PF) that if untreated, leads to death.

In clinic, patients with hereditary partial PS deficiency mostly suffer from recurrent thrombosis with 9 fold increased VTE risk as compared to non-deficient patients [92].

Pregnant women with partial PS inherited deficiency have an elevated risk of late fetal loss [86]. Conflicting data were previously published regarding the beneficial role of thromboprophylaxis in ameliorating pregnancy outcome in patients with inherited thrombophilia. While several reports approved the benefit of using low molecular weight heparin (LMWH) and/or low dose aspirin to improve pregnancy outcome [139] [140] [141] [142], a randomized clinical trial using three treatments: aspirin and heparin, aspirin alone or placebo revealed that neither aspirin combined with heparin nor aspirin alone improved pregnancies outcome [143]. An answer to the question whether the use or heparin alone or combined with aspirin could be beneficial is still awaited.

Recently, an individual patient data meta-analysis of LMWH for prevention of placenta-mediated pregnancy complications (AFFIRM) study will integrate individual patient data from recent randomized controlled trials of LMWH for the prevention of recurrent placenta-mediated pregnancy complications. The overall objective of this meta-analysis will be to inform clinical practice and develop clinical practice guidelines [144].

A randomized clinical trial, named anticoagulants for living foetus (ALIFE) assembling about 15 years of various clinical trials piloted around the world, revealed that LMWH does not increase the chance of live birth in women with unexplained recurrent miscarriage. However, the subgroup of women with inherited thrombophilia showed a trend toward a benefit of LMWH and aspirin. According to these encouraging results, the ALIFE2 trial was initiated, and is recruiting patients since 2013 in the Netherlands, United Kingdom, and Belgium, and hopefully soon in the United States and Slovenia [145].

In this study, we used for the first time full *Pros1* knockout mice (*Pros1^{-/-}*) newly described by our group (Prince et al. manuscript in review) that are fully rescued from lethality by targeting Factor VIII (FVIII) (*F8^{-/-}Pros1^{-/-}*) and did not display any signs of PF or DIC. We did not observed pregnancy loss in *Pros1* heterozygous *(Pros1^{+/-})* females. We then investigated the effect of complete lack of PS on pregnancy outcome in mice.

4.2 Material and methods:

Mice and breeding

F8^{-/-} mice (B6;129S4-F8^{tm1Kaz}/J) with C57BL/6J background were obtained from The Jackson Laboratory. *Pros1^{+/-}* mice were progeny of the original colony, with a genetic background of 50% 129/Sv x 50% C57BL/6J, as described previously [95]. The Swiss Federal Veterinary Office approved the experiments. Mice were genotyped by a multiplex PCR that amplifies the WT (+) and the null (-) alleles of *Pros1* gene at the same time, using primers previously described [95]. Genotyping of *F8* gene was performed accordingly to the literature[228].

In order to generate *F8^{-/-}Pros1^{-/-}* mice, we first crossed *Pros1^{+/-}* females with *F8^{-/-}* males, producing 25% *F8^{+/-}Pros1^{+/-}* progeny. *F8^{+/-}Pros1^{+/-}* females were then bred with *F8^{-/-}* males resulting in 25% *F8^{-/-}Pros1^{+/-}* progeny. *F8^{-/-}Pros1^{-/-}* matings were set to evaluated pregnancy outcome when PS complete deficiency.

Timed matings and embryos harvesting

F8^{-/-}Pros1^{+/+}, F8^{-/-}Pros1^{-/-} and *F8^{+/+}Pros1^{+/+}* females were used to set timed matings in order to generate embryos at different gestational stages: E9.5, E10.5, E11.5, E12.5 E13.5, E14.5, E15.5, E16.5 and E17.5. Mating was confirmed by detection of a vaginal plug and defined as day 0.5 p.c. Embryos were harvested by dissecting the female uterus. Viability was assessed under stereomicroscope (M80, Leica) coupled to a camera (MC170 HD, Leica) and photographed. DNA was extracted from embryos tail, alternatively yolk sac, for genotyping. Embryos were then fixed in 4% paraformaldehyde (PFA) and embedded in paraffin.

Preparation of murine plasma

Pregnant $F8^{-/-}Pros1^{+/+}$, $F8^{-/-}Pros1^{-/-}$ and $F8^{+/+}Pros1^{+/+}$ females at different gestational stages were anesthetized with pentobarbital (40 mg/kg), and whole blood was drawn from the inferior vena cava into 3.13% citrate (1 vol anticoagulant/9 vol blood). Blood was centrifuged at 2400 g for 10 min at room temperature (RT), to obtain platelet-poor plasma (PPP). To obtain platelet-free plasma (PFP), an additional centrifugation at 10000 g for 10 min was performed.

Platelet count and measurement of coagulation parameters

Platelet counts were carried out with an automated cell counter (Procyte Dx Hematology Analyzer, IDEXX). Fibrinogen, prothrombin time (PT) and FVIII activity were measured on an automated Sysmex CA-7000 coagulation analyzer (Sysmex Digitana). TAT level was measured in duplicate for each plasma sample using a commercially available ELISA (Enzygnost TAT micro, Siemens), according to the manufacturer's instructions.

Tissue processing and sectioning, immunohistochemistry and microscopy

Sections (4 μm) of pregnant females tissues (liver, lung, kidney and spleen) and embryos (whole embryos and placenta) with no pre-treatment were stained with hematoxylin/eosin, Masson Trichrome or immunostained for insoluble fibrin: anti-human fibrin (mAb clone 102-10) [175] final concentration 15.6 μg/mL, incubation for 30 min at RT, secondary antibody rabbit anti-human, (ab7155 Abcam, Cambridge, UK) 1:200 dilution, incubation for 30 min at RT. The staining was performed with the immunostainer BOND RX (Leica Biosystems, Muttenz, Switzerland) following manufacturer's instructions. Whole slides were scanned using 3D HISTECH Panoramic 250 Flash II, with 20x (NA 0.8), 40x (NA 0.95) air objectives. Images processing was done using Panoramic Viewer software.

Aspirin or LMWH treatment in $F8^{-/-}Pros1^{-/-}$ pregnant females

From 7 p.c (E7) until the pregnancy end (≈E20), $F8^{-/-}Pros1^{-/-}$ pregnant females received daily

freshly prepared aspirin in drinking water (Aspegic, 30µg/mL Lysine acetylsalicylate, Sanofi) According to literature [245], this low quantity was administered to obtain an amount similar to that prescribed in clinical practice, that is around 200 mg/day. Alternatively, $F8^{-/-}Pros1^{-/-}$ pregnant females were anesthetized with ketamine (80 mg/kg body weight) and xylazine (16 mg/kg body weight) and an osmotic minipump (model #1003D, Alzet, CA) delivering at a rate of 0.25 µL/hour was inserted subcutaneously in the subscapular region. The osmotic pumps contained LMWH (Clexane, 100µg/mL, Sanofi). Females were monitored during for the rest of the pregnancy. Pups were weaned after 21 days and ears tag used for genotyping

Statistical methods

Values were expressed as mean plus or minus s.e.m. A Chi-square for non-linked genetic loci was used to assess the Mendelian allele segregation. Survival data on embryos were plotted using the Kaplan-Meier method. A log-rank test was used to statistically compare the curves (Prism 6.0d; GraphPad). The other data were analysed by t-test, one-way and two-way ANOVA test with GraphPad Prism 6.0d. A P-value of less than 0.05 was considered statistically significant.

4.3 Results

PS deficiency and pregnancy

From $F8^{-/-}Pros1^{+/-}$ breeding pairs, 295 pups were obtained. 72 (24%) were $F8^{-/-}Pros1^{+/+}$, 164 (56%) were $F8^{-/-}Pros1^{+/-}$ and 59 (20%) were $F8^{-/-}Pros1^{-/-}$ (χ^2=4.8, P=0.09). $F8^{-/-}Pros1^{-/-}$ mice were present at the expected Mendelian ratio. Thus the partial lack of PS in $F8^{-/-}Pros1^{+/-}$ females did not causes pregnancy loss. We next studied the effect of complete PS deficiency on pregnancy outcome using $F8^{-/-}Pros1^{-/-}$ breedings. Intriguingly, we did not observe any litters from 4 $F8^{-/-}Pros1^{-/-}$ matings monitored during 4 months. $F8^{-/-}Pros1^{-/-}$ males fertility was checked in more than 15 different matings with $F8^{-/-}Pros1^{+/-}$ females and litters size was found normal. We then hypothesized that $F8^{-/-}Pros1^{-/-}$ females might be sterile or experience

pregnancy loss.

$F8^{-/-}Pros1^{-/-}$ females are not sterile and exhibit high abortion rates

To rule out if the complete lack of PS causes infertility or rather pregnancy loss, we set time plugged $F8^{-/-}Pros1^{-/-}$ females. $F8^{-/-}Pros1^{+/+}$, $F8^{+/+}Pros1^{+/+}$ were used as control females. Vaginal plugs were observed in all females. They were than sacrificed at different gestational stages and embryos collected. Uterus from $F8^{-/-}Pros1^{+/+}$ control females at E16 contained several embryos showing normal devlopment (Fig.1,a). Contrarily, $F8^{-/-}Pros1^{-/-}$ females uterus, at the same pregnany stage, showed several macerated embryos with few ones with normal size or exclusively macerated and necrotic embryos (Fig.1,b). Macroscopical examination of the embryos revealed that in contrast to embryos coming from $F8^{-/-}Pros1^{+/+}$ females (Fig.1,c), some embryos coming from $F8^{-/-}Pros1^{-/-}$ females exhibit hemorrhages (Fig.1,d). Staining for fibrin clots did not reveal any evidence of increased thrombosis in placentas of $F8^{-/-}Pros1^{-/-}$ pregnancies as compared to $F8^{-/-}Pros1^{+/+}$ and $F8^{+/+}Pros1^{+/+}$ pregnancies. Almost no dead embryos was found in $F8^{-/-}Pros1^{+/+}$ and $F8^{+/+}Pros1^{+/+}$ control females. Differently, very high embryonic mortality was found in $F8^{-/-}Pros1^{-/-}$ females: 57% (41/71) at E11-E12, 66% (36/54) at E14-E15 and 59% (16/27) at E16-E17. No viable embryos were present after E18 (Fig.1,e). Besides, litter size decreases along with the pregnancy progression (Fig.1,f). Among embryos collected between E9.5 and E10.5, only 33% carryed the $F8^{-/-}Pros1^{-/-}$ genotype versus 50% expected, and no $F8^{-/-}Pros1^{-/-}$ live embryos were collected after E12.5 (Fig.1,g). Differently, all embryos collected from $F8^{-/-}Pros1^{+/+}$ and $F8^{+/+}Pros1^{+/+}$ females were alive and present at the expected Mendelian frequency. Recurrent pregnancy loss never affected $F8^{-/-}Pros1^{-/-}$ females survival. Thus, PS complete deficiency is a severe inherited thrombophilia incompatible with pregnancy positive outcome.

Hemostatic imbalance with no overt DIC in pregnant $F8^{-/-}Pros1^{-/-}$ females

We recently described that combined deficiency of PS and F8 rescued $Pros1^{-/-}$ lethal phenotype. The hemostatic balance is perfectly restored in $F8^{-/-}Pros1^{-/-}$ mice. Taking into

159

account that pregnancy provokes a shif in the hemostatic equilibrium and leads to a state of hypercoagulability [131], we decided to examine hemostasis in $F8^{-/-}Pros1^{-/-}$ pregnant females. Hematological blood parameters, fibrinogen concentration, prothrombin time (PT) and TAT were investigated. Interestingly, as compared to control females ($F8^{-/-}Pros1^{+/+}$ and $F8^{+/+}Pros1^{+/+}$), at E12-E16, we observed an overall trend of low fibrinogen levels in $F8^{-/-}Pros1^{-/-}$ with 1.1±0.1 g/L, 2.0±0.2 g/L for $F8^{-/-}Pros1^{+/+}$ and 2.1±0.2 for $F8^{+/+}Pros1^{+/+}$, (P<0.005) (Fig.2, a). TAT complexes were found increased in $F8^{-/-}Pros1^{-/-}$ with 24.3±2.6 ng/L, 16.3±1.2 ng/L for $F8^{-/-}Pros1^{+/+}$ and 13.1±1.8 for $F8^{+/+}Pros1^{+/+}$ (P<0.05), (Fig.2, b), whereas PT was normal in all genotypes. Platelet count was reduced in $F8^{-/-}Pros1^{-/-}$ as compared to $F8^{-/-}Pros1^{+/+}$ pregnant females. Indeed, we found 881±78G/L in $F8^{-/-}Pros1^{+/+}$ (n=3) vs 434±129G/L in $F8^{-/-}Pros1^{-/-}$ (n=2) at E12, 635±114G/L in $F8^{-/-}Pros1^{+/+}$ vs 429±142G/L in $F8^{-/-}Pros1^{-/-}$ (n=2 per group) at E14, 930±78G/L, (n=2) vs 636±66G/L, (n=3) at E15. Differently, platelets count was comparable beween both genotypes at E16 (842±142G/L vs 936±183G/L, (n=3 per group) (Fig.2, c). Especially, during the whole pregnancy period, $F8^{-/-}Pros1^{-/-}$ showed more activated platelet as compared to $F8^{-/-}Pros1^{+/+}$ and $F8^{+/+}Pros1^{+/+}$ (Fig.2,d). Thus, during pregnancy, the achieved hemostatic balance in $F8^{-/-}Pros1^{-/-}$ is disturbed.

Thromboprophylaxis protects $F8^{-/-}Pros1^{-/-}$ females from poor pregnancy outcome

Since the antithrombotic prophylaxis is extremely debated in ameliorating pregnancy outcome in inherited thrombophilia, we treated $F8^{-/-}Pros1^{-/-}$ with LMWH or low dose aspirin. Attractively, LMWH almost prevented pregnancy loss. Pregnancy outcome was also positive with low dose aspirin. From both treatements, newborns appeared morphologically normal (Fig.3, a). However, the litter size was slightly reduced in the LMWH group (6±1) as compared to $F8^{-/-}Pros1^{+/-}$ females (8±1). The litters of the aspirin treated group were more reduced (3±1). (P<0.05) (Fig.3, b). Thus, aspirin or better LMWH treatment prevented pregnancy loss, indicating that thromboprophylaxis might apply to pregnancy in very severe inherited thrombophilias.

4.4 Discussion

The beneficial role of thromboprophylaxis in pregnant women with inherited thrombophilia is intensely debated. Conflicting data were previously published. While several reports approved the profit of using LMWH and/or low dose aspirin to improve pregnancy outcome [139] [140] [141] [142], other studies revealed the opposite [143]. Here, we reported that LMWH greatly reduces abortion rates in severe inherited thrombophilia setting but did not completely rescue abortion. Less efficiently, low dose aspirin leads to positive pregnancy outcome too.

The murine experimental model system shares similarities with humans regarding the chorioallantoic placentation that occurs approximately at the end of first trimester in humans and corresponds to E9 in mice. Both species form a hemochorial placenta where maternal cells are eroded and zygote-derived trophoblast cells become directly exposed to maternal blood [246]. Pregnant women with partial PS exhibit high risk of late fetal loss [86]. The pathophysiology of this poor pregnancy outcome is not well understood. We used $F8^{-/-}$ $Pros1^{+/-}$ mice to examine the effect of partial PS deficiency in pregnancy. Intriguingly, $F8^{-/-}$ $Pros1^{+/-}$ females displayed no fetal loss and normal litter size. This might be explained by fact that 50% circulating PS in $F8^{-/-}Pros1^{+/-}$ pregnant mice is sufficient to prevent abortion. Differently, the complete lack of PS in $F8^{-/-}Pros1^{-/-}$ females provokes pregnancy loss. In this severe inherited thrombophilia condition, high embryos mortality rates were observed with no $F8^{-/-}Pros1^{-/-}$ live embryos collected after E12. The early death of $F8^{-/-}Pros1^{-/-}$ embryos starting from E11 might be caused by the lack of PS in both mother and foetus since $F8^{-/-}Pros1^{+/-}$ embryos survive as long as PS expression is maintained in the uteroplacental unit. In multifetal human pregnancies, retention of a dead foetus is coupled with amplified platelet activation, thrombin generation, and a higher risk of DIC in the mother and in morbidity of the surviving foetus [247]. Similarly to humans, dead and macerated embryos present within mice uterus produce toxic factors that damage surviving foetus [248]. The assessment of DIC parameters in $F8^{-/-}Pros1^{-/-}$ pregnant mice revealed low fibrinogen concentration, decreased platelet count and increased TAT levels. The complete lack of PS leads to a severe

prothrombotic phenotype that is equilibrated in $F8^{-/-}Pros1^{-/-}$. We presume that the pregnancy associated hypercoagulable state imbalances hemostasis in $F8^{-/-}Pros1^{-/-}$ and promotes DIC. However, histological investigations of liver, kidney and lung sections from pregnant $F8^{-/-}Pros1^{-/-}$ mice at different gestational stages revealed no evidence of augmented fibrin deposition. In addition, increased platelets activation is typical in female suffering from abortion. Therefore, it is not clear whether the observed DIC is due to the hemostatic imbalance in $F8^{-/-}Pros1^{-/-}$ during pregnancy or to the effect of intrauterine retained dead foetus. In humans, LMWH is being tested to prevent placental dysfunction and the related sequelae in a subset of women with heritable thrombophilia. The risk-to-benefit balance of such prophylaxis is questioned [145]. In this study, we treated $F8^{-/-}Pros1^{-/-}$ pregnant mice with enoxaparin. This was efficient in reducing fetal death. However, litter size were slightly reduced as compared to control females ($F8^{-/-}Pros1^{+/-}$).

Our findings allow us to propose two scenarios: the first one is that abortion in $F8^{-/-}Pros1^{-/-}$ mice is strictly due to hemostatic imbalance which might provoke thrombosis, disturb the uteroplacental circulation, and causes placental failure. This scenario seems improbable because of 2 reasons: i) there was no increased fibrin deposition in $F8^{-/-}Pros1^{-/-}$ pregnant females and embryos placentas, ii) the rescue with enoxaparin treatment was not total with reduced litter size and even worse with aspirin. The second scenario is that observed abortion in $F8^{-/-}Pros1^{-/-}$ mice is due to lack of PS anticoagulation effect, that is reverted partially by enoxaparin, but is also due to the lack of PS role in uteroplacental vasculature to support the establishment of the trophoblast invasion of the spiral arteries of the uterus. The latter scenario arises from the know role of PS in vasculature development and maintainace [113] [114].

The treatment of $F8^{-/-}Pros1^{-/-}$ pregnant mice with low dose aspirin showed less efficient protection from abortion as compared to enoxaparin. These findings are in line with previous clinical observation [141]. It is known that aspirin mainly prevents the initiation of thrombus formation and that new nonanticoagulant roles of LMWH have emerged, some of which are

directly related to trophoblast function [249]. Thus, any beneficial effects of LMWH prophylaxis might not necessarily reflect a causal thrombotic link between thrombophilia mutations and pregnancy loss. Last but not least, platelets play a role into gestational requirements. Any roles for platelets are likely to result from their activation in the circulation. Nevertheless, the molecular mechanisms of platelet activation in pregnancy remain largely unknown. Characterisation of platelets activation and role in the placental beds in complete PS deficient will provide great insights into the physiopathology of inherited thrombophilia associated fetal loss.

In humans, the setting of ongoing clinical trials evaluating the role of LMWH in preventing placental dysfunction in PS deficiency may need to be adjusted. The role of PS in placental vasculature should also be assessed.

4.5 Figures
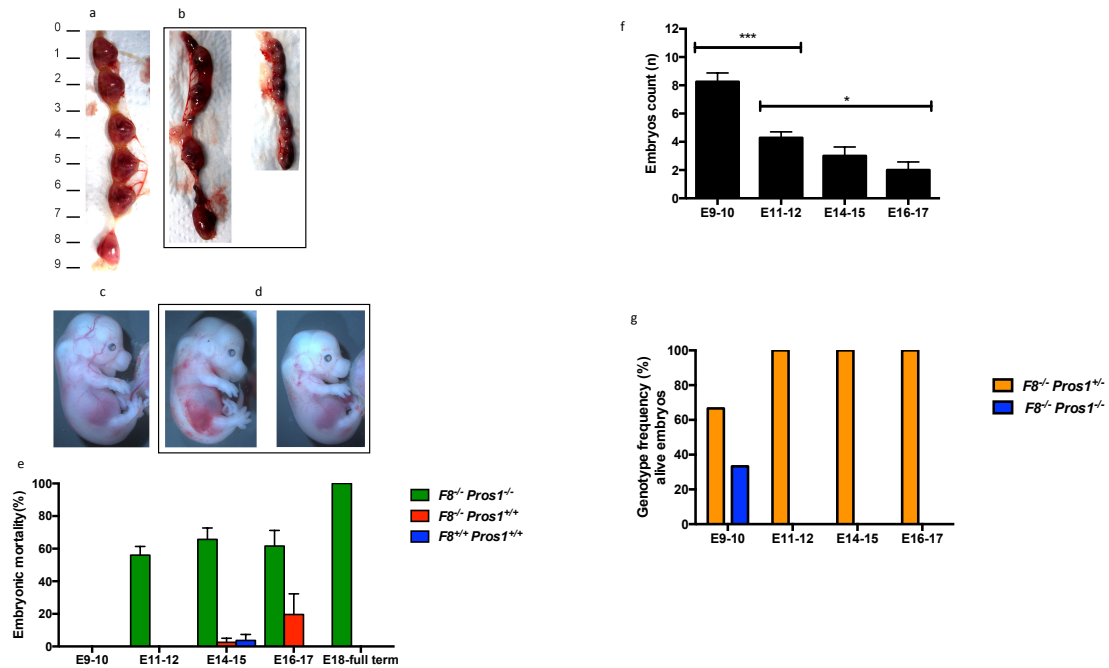
Figure 1: Pregnancy outcome in *F8*$^{-/-}$*Pros1*$^{-/-}$ females.

a, macroscopy of uterus from *F8*$^{-/-}$*Pros1*$^{+/+}$ control females at E16 with several embryos showing normal develepement. **b**, *F8*$^{-/-}$*Pros1*$^{-/-}$ females macroscopy of uterus at E16 with several macerated embryos and few ones with normal size or exclusively macerated and necrotic embryos. **c**, macroscopical examination of embryos from *F8*$^{-/-}$*Pros1*$^{+/+}$ female. **d**, macroscopical examination of embryos with hemorrhages coming from *F8*$^{-/-}$*Pros1*$^{-/-}$ female. **e**, evaluation of embryos mortality in *F8*$^{-/-}$*Pros1*$^{-/-}$ females at: E9-E10 (n=4), E11-E12 (n=4), E14-E15 (n=5), E16-E17 (n=4). *F8*$^{-/-}$*Pros1*$^{+/+}$ females at: E11-E12 (n=2), E14-E15 (n=5), E16-E17 (n=4). *F8*$^{+/+}$*Pros1*$^{+/+}$ females at: E11-E12 (n=2), E14-E15 (n=3), E16-E17 (n=4). **f**, **g**, evaluation of litter size and genotype frequency in alive embryos from *F8*$^{-/-}$*Pros1*$^{-/-}$ females at: E9-E10 (n=4), E11-E12 (n=4), E14-E15 (n=5), E16-E17 (n=4). All data are expressed as mean±s.e.m. ns, not significant, ***P<0.0005 *P<0.05.
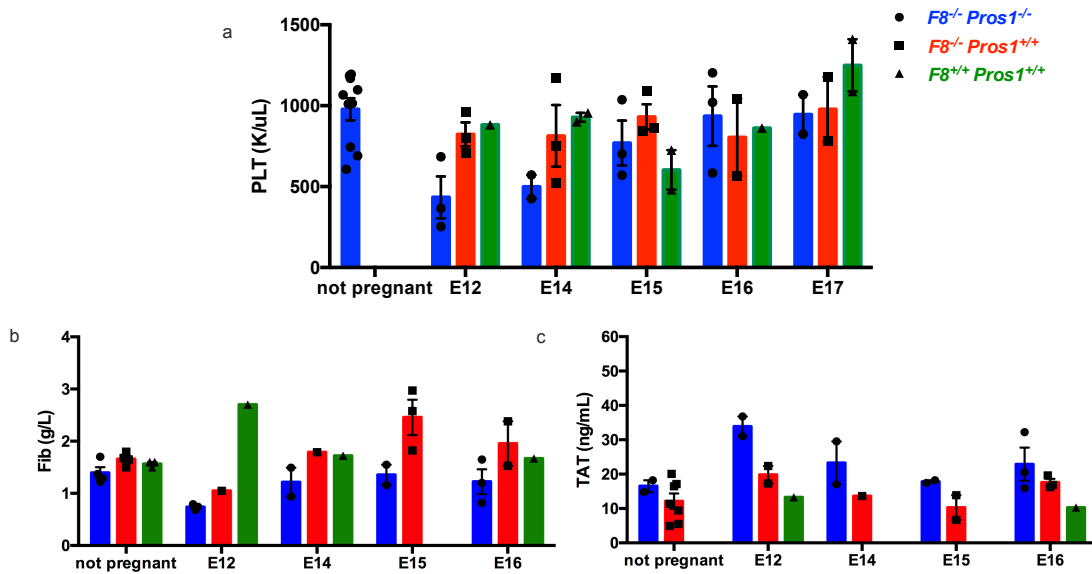
Figure 2: Evaluation of DIC parameters and platelets during pregnancy

a, Evaluation of platelet count in $F8^{-/-}Pros1^{-/-}$, $F8^{-/-}Pros1^{+/+}$, $F8^{+/+}Pros1^{+/+}$ pregnant mice from E12 until E17, **b-c**, fibrinogen concentration and thrombin anti-thrombin complexes in $F8^{-/-}Pros1^{-/-}$, $F8^{-/-}Pros1^{+/+}$, $F8^{+/+}Pros1^{+/+}$ pregnant mice from E12 until E16. All data are expressed as mean±s.e.m.
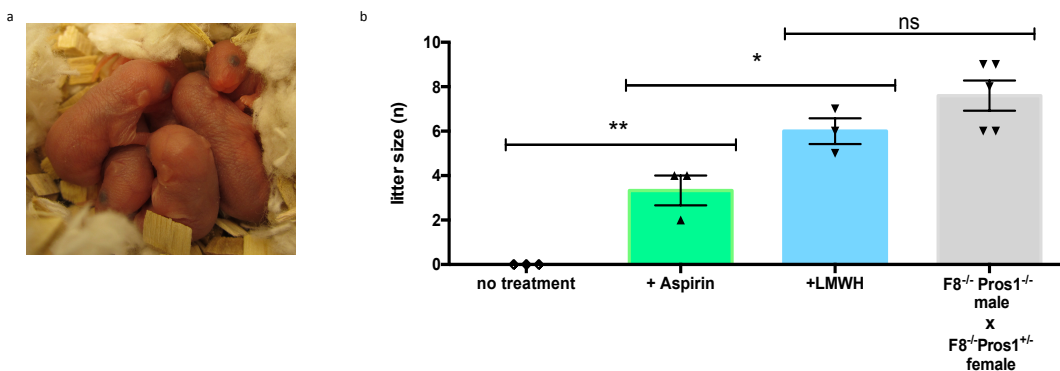
Figure 3: Pregnancy rescue in $F8^{-/-}Pros1^{-/-}$

a, Macroscopical image of pups produced by $F8^{-/-}Pros1^{-/-}$ female treated with enoxaparin (100μg/mL) from E7 until birth. **b**, evaluation of pups litter size of $F8^{-/-}Pros1^{-/-}$ female without thromboprophylaxis, with aspirin (30μg/mL) or LMWH (100μg/mL) and $F8^{-/-}Pros1^{+/-}$ crossed with $F8^{-/-}Pros1^{-/-}$. All data are expressed as mean±s.e.m. ns, not significant, **P<0.005 *P<0.05.

Chapter V. Discussion and perspectives

Hemostasis maintains blood in a fluid state and prevents its loss after vessel damage. Upon injury, the coagulation system activation leads to the formation of a thrombus. The equilibrium between pro- and anticoagulant forces is tightly balanced and the deficiency of any of the coagulation factors or of the anticoagulants could conduct to a disequilibrium provoking bleeding or thrombosis.

PS is a natural anticoagulant. Its role in hemostatsis and thrombosis has been extensively studied. In clinic, patients with hereditary PS deficiency mostly suffer from VTE.

[92]. In case of complete PS deficiency, newborns present a combination of an extensive skin necrosis and DIC named PF and died within hours if untreated [117, 118]. It has been considered for a long time that PF essentially results from the imbalance between pro- and anticoagulant factors due to the absence of PS anticoagulant effect. Recent reports [95, 96] demonstrated that PS deficiency in mice recapitulates the aspects of PS deficiency in human. It was proposed that PF might not be exclusively a consequence of the lack on PS anticoagulant effect but could also result from the absence of PS signaling in endothelium and subsequent vascular disturbance [95, 96].

Murine model with PS deficiency: a valuable tool to better understand PF

Our results showed in Chapter II confirmed that as for human, $Pros1^{-/-}$ mice died *in utero* from the consequences of purpura fulminans and DIC. We hypothesized that silencing $Pros1$ gene in adult mice to achieve null or very low PS level could reproduce PF. To this end, we knocked out $Pros1$ in adult $Pros1^{lox/-}$ mice by using the Mx1-Cre system. $Pros1^{lox/-}Mx1\text{-}Cre^{+}$ mice displayed 16% circulating PS and thrombosis in the liver, heart and lung. However, they did not develop PF demonstrating that very low level of PS could still protect against PF. PS needs vitamin K as cofactor for post-translational γ-glutamylcarboxylation to achieve full biological activity. By interfering with the vitamin K–driven γ-carboxylation process, warfarin is widely used as a long-term anticoagulation therapy in humans. Our second

hypothesis was to administer warfarin to $Pros1^{+/-}$ mice to further decrease PS and induce PF. Despite high mortality rates, only a few $Pros1^{+/-}$ mice developed under warfarin lesions compatible with PF. Analysing these lesions over time revealed that thrombosis occurred together with vasculature disruption. Previous studies [113] [114] [96] claimed the involvement of PS in the vasculature development and maintenance. However, the hypothesis that vascular damages occurring during PF are exclusively due to thrombosis resulting from the imbalance between pro- and anticoagulant factors did not take into consideration that besides its role as an anticoagulant, PS exerts important roles in endothelium, phagocytosis [34] [157] and inflammation [167]. Clarification whether PS deficiency induced PF is exclusively secondary to thrombosis or is also due to the lack of PS signaling in endothelium or both is awaited. In order to elucidate this issue, we decided to characterize $Pros1^{-/-}$ embryonic vasculature. As expected, the lack of PS leads to vascular thrombosis. Nevertheless, poor vasculature hierarchy, leaky vessels and areas without any vascular structures were exclusively observed in $Pros1^{-/-}$ embryos. Higher inflammation, altered phagocytosis and erythropoiesis were concomitant with PF. Furthermore, vascular defects were also present before PF begins. Our findings suggest that contradictory to what is currently admitted, PS deficiency induced PF is not strictly secondary to the imbalance of pro- and anticoagulant factors, but also to lack of PS signaling in endothelium.

Targeting Gas6 gene to rebalance hemostasis in $Pros1^{-/-}$

Strongly motivated by our conclusion that in PS complete deficiency, PF is not uniquely caused by the imbalance of pro- and anticoagulant factors, we attempted to rebalance hemostasis in $Pros1^{-/-}$ by intercrossing $Pros1^{+/-}Gas6^{-/-}$ mice. $Gas6^{-/-}$ mice exhibit a well-known antithrombotic phenotype [13]. We hypothesized that combining PS and Gas6 deficiencies might restore the hemostatic balance and rescue $Pros1^{-/-}$ from fatal PF. Intriguingly, no viable $Pros1^{-/-}Gas6^{-/-}$ mice were observed. Embryonic investigation revealed a more dramatic phenotype with earlier and higher mortality. Similar to $Pros1^{-/-}$, vascular defects, ongoing inflammation, altered phagocytosis and erythropoiesis were observed in

Pros1^{-/-}Gas6^{-/-}. This finding further support that PF might not strictly result from the hemostatic imbalance due to the lack of PS anticoagulant activity.

In conclusion, the results presented in Chapter II provide evidence that the thrombotic process occurring during PS deficiency induced PF should be less central than currently admitted. PS possibly plays an important role in vasculature development and maintenance. The lack of its anticoagulant effect provokes thrombosis. Besides, the absence of PS signalling in the endothelium might lead to vascular defects and further worsen PF. Further investigations are required to better characterize the mechanism by which PS is involved in vascular development and maintenance.

FVIII or _FIX_ gene silencing rescues *Pros1*^{-/-} mice from lethality and restores hemostasis in hemophilia

FVIII deficiency (hemophilia A : HA) and *FIX* deficiency (hemophilia B : HB) are bleeding diseases sustained by the loss of FVIII or FIX activity that remarkably impairs the generation of thrombin and imbalances hemostasis [250]. Patients with severe hemophilia frequently suffer from spontaneous recurrent muscle and joint bleeding, such as hemarthrosis, which leads to severe and progressive musculoskeletal damage [251]. This can result in disability at a young age if left untreated [189]. The main treatment is replacement therapy: the administration of the deficient clotting factor to achieve adequate hemostasis. The main complication of such therapy is the development of neutralising antibodies. New therapies focus on the development of products capable of decreasing the frequency of prophylactic infusions. Besides long-lasting FVIII and FIX, novel approaches comprise the replacement of the gene necessary for the production of endogenous coagulation factor, the bispecific antibody technology to mimic the coagulation function of the missing factor, and the targeting of coagulation inhibitors such as TFPI or antithrombin as strategy to rebalance coagulation in patients with hemophilia [252].

The disequilibrium of the hemostatic balance caused by PS complete lack allows us to hypothesize that FVIII or FIX /PS combined deficiency might be a suitable strategy to achieve hemostasis in HA and HB and rescue $Pros1^{-/-}$ mice from lethal PF. Attractively, HA and HB mice completely lacking PS ($Pros1^{-/-}F8^{-/-}$ and $Pros1^{-/-}F9^{-/-}$) were viable, displayed normal hemostatic parameters and did not presented PF. One of the most pertinent findings of this study is the complete prevention from acute and chronic hemarthrosis in $Pros1^{-/-}F8^{-/-}$ and $Pros1^{-/-}F9^{-/-}$ mice. Recombinant FVIII administration in $Pros1^{-/-}F8^{-/-}$ mice restored the imbalance of the coagulation and promoted DIC and thrombosis but not PF or death even after an overdose of recombinant FVIII. An important interrogation remains: why FVIII full reconstitution in $Pros1^{-/-}F8^{-/-}$ mice did not provoke PF? Further investigations are required to better clarify the mechanism of PF development in the context of PS complete deficiency. The extensive findings in this chapter of the work lead us to propose that targeting PS may potentially be translated to therapies useful for hemophilia.

Pregnancy and PS deficiency: Pros or cons thromboprophylaxis

Pregnancy is associated with a shift of the coagulation balance leading to a hypercoagulable state that protects pregnant women from fatal hemorrhage during delivery but predispose them to thromboembolism. Interestingly, pregnant women with PS inherited thrombophilia have an elevated risk of late fetal loss [86]. Some clinical studies reported that heparin and/or low dose aspirin treatment could ameliorate pregnancy outcomes [139] while others showed no benefit from thromboprophylaxis [143]. To develop clinical practice guidelines for this controversial situation, the AFFIRM study is assembling individual patient data from recent randomized controlled trials where heparin was administered for the prevention of recurrent placenta-mediated pregnancy complications [144]. To better understand how the lack of PS could affect pregnancy outcome, we assessed pregnancy in $F8^{-/-}Pros1^{+/-}$ mice. Intriguingly, we did not observe fetal loss and litter size was normal in these mice. We supposed that 50% circulating PS in $F8^{-/-}Pros1^{+/-}$ pregnant mice was sufficient to prevent abortion. We then took advantage from females with complete PS deficiency ($F8^{-/-}Pros1^{-/-}$) available in our

laboratory to investigate pregnancy in this severe thrombophilia condition. We did not observed any litter from plugged $F8^{-/-}Pros1^{-/-}$ females demonstrating that complete deficiency in PS during gestation is incompatible with a positive pregnancy outcome. Embryos examination at different gestational stages revealed dead and macerated embryos from E11.5 onwards. Some of them showed hemorrhages and thrombosis but no PF. With 50% expected $F8^{-/-}Pros1^{-/-}$ embryos, only 33% were found with no live $F8^{-/-}Pros1^{-/-}$ embryos collected after E12.5. We suppose that the early death of $F8^{-/-}Pros1^{-/-}$ embryos could result from the lack of PS in both the mother and the fetus, since $F8^{-/-}Pros1^{+/-}$ embryos survive as long as PS expression is maintained in the uteroplacental unit. In multifetal human pregnancies, retention of a dead fetus is coupled with amplified platelet activation, thrombin generation, and a higher risk of DIC in the mother and in morbidity of the surviving foetus [247]. Similarly to humans, dead and macerated embryos present within mice uterus produce toxic factors that damage surviving littermates [248]. The evaluation of DIC parameters in $F8^{-/-}Pros1^{-/-}$ pregnant mice revealed decreased fibrinogen concentration and platelet count with higher thrombin-antithrombin levels. Indeed, the complete lack of PS leads to a severe prothrombotic phenotype that is rebalanced in $F8^{-/-}Pros1^{-/-}$. We postulate that the pregnancy associated hypercoagulable state imbalances the achieved hemostasis in $F8^{-/-}Pros1^{-/-}$ and promotes DIC. However, histological investigations of liver, kidney and lung sections from $F8^{-/-}Pros1^{-/-}$ pregnant mice and placentas at different gestational stages revealed no signs of fibrin deposition. In addition, increased platelets activation is typical in female suffering from abortion. Therefore, it is not clear whether the observed DIC signs are due to the hemostatic reimbalance in $F8^{-/-}Pros1^{-/-}$ during pregnancy or to the effect of intrauterine retained dead fetus. In humans, LMWH is being tested to prevent placental dysfunction and the related sequelae in a subset of women with heritable thrombophilia. The risk-to-benefit balance of such prophylaxis is questioned [145]. In this study, we treated $F8^{-/-}Pros1^{-/-}$ pregnant mice with LMWH (enoxaparin) or low dose aspirin. These treatments were efficient in reducing fetal death. However, litter size was reduced as compared to control females.

In conclusion, the results presented in Chapter III suggest that abortion in $F8^{-/-}Pros1^{-/-}$ mice is

due to the hemostatic imbalance that provoke thrombosis and might disturb the uteroplacental circulation causing placental failure. This scenario seems questionable since there was no increased fibrin deposition in $F8^{-/-}Pros1^{-/-}$ pregnant mice and placentas. Furthermore, litter size was reduced with enoxaparin and even inferior with aspirin. It is tempting to suppose that observed abortion in $F8^{-/-}Pros1^{-/-}$ mice is due to lack of PS anticoagulation effect (that is reverted by enoxaparin treatment) but also due to the lack of PS role in uteroplacental vasculature to support the establishment of the trophoblast invasion of the spiral arteries of the uterus.

Previous clinical observations indicated that low dose aspirin had less efficient protection from abortion as compare to LMWH [141]. It is known that aspirin mainly prevents the initiation of thrombus formation and that new nonanticoagulant roles of LMWH have emerged, some of which are directly related to trophoblast function [249]. Thus, any beneficial effects of LMWH prophylaxis might not necessarily reflect a causal thrombotic link between thrombophilia mutations and pregnancy loss. Also, platelets play a role into gestational requirements. Any roles for platelets are likely to result from their activation in the circulation. However, the molecular mechanisms of platelet activation in pregnancy remain largely unknown. Characterization of platelet activation and of the role in the placental beds in complete PS deficieny will provide great insights into the physiopathology of inherited thrombophilia associated fetal loss.

General conclusion and perspectives

The equilibrium between pro- and anticoagulant forces is meticulously maintained in physiological situations. This thesis confirmed that complete PS deficiency causes DIC and PF. The etiological factor of PF is debated, although mainly considered to result from the lack of PS anticoagulant effect. Previous reports revealed vascular defects in $Pros1^{-/-}$ mice embryos. Our findings support these data. Indeed, warfarin treatment reproduces PF and indicates vascular wall damage. Examination of our $Pros1^{-/-}$ embryos revealed leaky and underdeveloped vasculature. The obtained results from PS and Gas6 combined deficiency

further suggest that during PF, PS might play other roles than anticoagulation.

Our findings suppose that PS plays a prominent role in vasculature. The next step of this work will be to examine the role of PS in vascular development and maintenance. An immunostaining of the vascular wall and the endothelial cell junctions will be performed in order to determine the mechanism of vascular leakage in absence of PS. Furthermore, we will take advantage of the unique viable murine model with complete lack of PS ($F9^{-/-}Pros1^{-/-}$). $F9^{-/-}Pros1^{-/-}$ mice will be used to perform *in vivo* angiogenesis assays : Matrigel plugs, investigation and quantification of vasculature in postnatal mouse brain by immunostaining and stereology. Taking into account the well know role of VEGF and its receptor VEGFR2 in vascular development and maintainance, our future aim is to investigate a possible pathway involving VEGF/VEGFR2 and PS, perhaps via the TAM receptors, in PF development.

The hemostatic balance was perfectly restored in mice with combined PS and F8/F9 deficiency and prevented PF in $Pros1^{-/-}$ mice, paradoxically suggesting that PF in $Pros1^{-/-}$ mice principally results from the hemostatic imbalance. The hypercoagulable state related to pregnancy restored the hemostatic imbalance in $F8^{-/-}Pros1^{-/-}$ females. Thromboprophylaxis was beneficial but did not fully prevent pregnancy loss further advocating an additional role for PS in pregnancy. This work will be persued by examining the role of PS in vasculature during pregnancy. We will investigate the uteroplacental vasculature by whole mounting immunostained placentas. Angiogenic factors (VEGF, sflt) will also be measured in plasma. Since platelets play a prominent role in pregnancy, their activation will be evaluated.
Furthermore, the setting of ongoing clinical trials evaluating the role of LMWH in preventing placental dysfunction in PS deficiency may need to be adjusted and take into account the role of PS in placental vasculature.
The achieved hemostasis in $F8^{-/-}Pros1^{-/-}$ and $F9^{-/-}Pros1^{-/-}$ provides the first evidence that inhibiting PS completely prevents hemarthrosis and ameliorates bleeding. The next step of this project is to develop a suitable compound to inhibit PS such as SIRNA or antisense

oligonucleotides. Next, we will conduct *in vivo* experiments in primates and clinical trials in hemophilia patients. I will also follow the master of translation and entrepreneurship in medicine (sitem-Insel School, University of Bern). This master will allow us to possess the necessary combination of scientific and medical knowledge and entrepreneurship skills to successfully coordinate the commercialization of biomedical products.

Chapter VI: Appendices

I- Endogenous GAS6 contributes to immune homeostasis in response to endotoxemia and infection

II- The Gas6-Axl Protein Interaction Mediates Endothelial Uptake of Platelet Microparticles

Endogenous GAS6 contributes to immune homeostasis in response to endotoxemia and infection

(Manuscript submitted)

Endogenous GAS6 contributes to immune homeostasis in response to endotoxemia and infection

Laurent Burnier[1,2], Raja Prince[1,3,4], Didier Le Roy[5], Sara Calzavarini[1,3,4], Thierry Roger[5], François Saller[6], Sylvain Clauser[6], Anne C. Brisset[1], Linda Kadi[1], Marc Chanson[7], Stéphanie Rignault[8], Michael Racine[1], Peter Carmeliet[9,10], Greg Lemke[11], Glenn K. Matsushima[12], François Feihl[8], Delphine Borgel[6], Lucas Liaudet[13], Thierry Calandra[5] & Anne Angelillo-Scherrer[1,3,4]

1) Service and Central Laboratory of Hematology, Centre Hospitalier Universitaire Vaudois and University of Lausanne, rue du Bugnon 46, CH-1011 Lausanne, Switzerland, phone: +41.21.314.42.22, e-mail: anne.angelillo-scherrer@chuv.ch
2) Department of Biomedical Sciences, University of Copenhagen, Ole Maaløes Vej 5, 2200 Copenhagen, Denmark, phone +45.35.32.58.33, email: laurent.burnier@bric.ku.dk
3) University Clinic of Hematology and Central Hematology Laboratory, Bern University Hospital and the University of Bern, Inselspital, CH-3010 Bern, Switzerland, phone: +41.31.632.33.02, e-mail: anne.angelillo-scherrer@insel.ch
4) Department of Clinical Research, University of Bern, Murtenstrasse 31, CH-3010 Bern, Switzerland, phone: +41.31.632.09.55, e-mail: anne.angelillo-scherrer@insel.ch
5) Infectious Diseases Service, Centre Hospitalier Universitaire Vaudois and University of Lausanne, rue du Bugnon 46, CH-1011 Lausanne, Switzerland, phone: +41.21.314.10.10, e-mail: thierry.calandra@chuv.ch
6) Université Paris-Sud, Laboratoire d'hématologie, EA 4531, 92296 Châtenay-Malabry Cedex, France ; AP-HP, Hôpital Necker, Service d'Hématologie Biologique, 75015 Paris, France, phone : +33.1.46.83.59.54, e-mail : delphine.borgel@u-psud.fr
7) Laboratory of Clinical Investigation III, Department of Pediatrics, Faculty of Medicine and University Hospitals of Geneva Micheli-du-Crest 24, CH-1211 Geneva 14, Switzerland, phone: +41.22.372.46.11, e-mail: Marc.Chanson@hcuge.ch
8) Division of Clinical Physiopathology and Medical Teaching, Centre Hospitalier Universitaire Vaudois and University of Lausanne, rue du Bugnon 46, CH-1011 Lausanne, Switzerland, phone: 021.314.14.23, e-mail: Francois.Feihl@chuv.ch
9) Laboratory of Angiogenesis and Neurovascular link, Vesalius Research Center, Department of Oncology, University of Leuven, Leuven, B-3000, Belgium, phone: +32.16.34.57.72, e-mail: Peter.Carmeliet@med.kuleuven.ac.be
10) Laboratory of Angiogenesis and Neurovascular link, Vesalius Research Center, VIB, Leuven, B-3000, Belgium, phone: +32.16.34.57.72, e-mail: Peter.Carmeliet@med.kuleuven.ac.be
11) Salk Institute for Biological Studies, La Jolla, CA 92037, USA, phone: +1.858.453.4100, e-mail: lemke@salk.edu
12) UNC Neuroscience Center, University of North Carolina at Chapel Hill, Chapel Hill, NC 27599, USA, phone: +1-919-966-0408, e-mail: gkmats@med.unc.edu
13) Service of Adult Intensive Care Medicine, Centre Hospitalier Universitaire Vaudois and University of Lausanne, rue du Bugnon 46, CH-1011 Lausanne, Switzerland, phone: +41.21.314.05.14, e-mail: Lucas.Liaudet@chuv.ch

Editorial correspondence to: Anne Angelillo-Scherrer
University Clinic of Hematology and Central Hematology Laboratory & Bern University Hospital and the University of Bern, Inselspital
CH-3010 Bern, Switzerland
phone: +41.31.632.33.02
e-mail: anne.angelillo-scherrer@insel.ch

Key words: GAS6, TYRO3, AXL, MERTK, cytokines, LPS, sepsis, innate immunity

Figures: 6

ABSTRACT

Sepsis is a severe life-threatening infection with organ dysfunction triggering interplay of host pro- and anti-inflammatory processes. There are currently no proven pharmacological therapies for sepsis. The product of growth arrest-specific gene 6 (*Gas6*) plays at the interface of coagulation and inflammation, and therefore at the interface between blood and pathogens. It contributes to the protection from cellular stress, such as inflammation and apoptosis. Here we explored whether endogenous GAS6 is protective in the context of endotoxemia and bacterial infection. In mice, *Gas6* deficiency enhanced lethality in endotoxemia and bacterial sepsis, caused by an overproduction of numerous cytokines provoking a systemic inflammatory response and drop in blood pressure. In response to endotoxin, macrophages secreted GAS6 that dampened cytokine release in an autocrine manner. Thus, in the absence of GAS6 and in the presence of pathogens, macrophages overproduce pro-inflammatory cytokines. Indeed, treatment of *Gas6*$^{-/-}$ macrophages with exogenous GAS6 decreased cytokine release, thereby restoring the wild-type phenotype. In humans, GAS6 rose in plasma during endotoxemia. These observations in humans corroborate data in mice and point to endogenous GAS6 as a major modulator of innate immunity, a potent immuno-modulator and protective factor for sepsis.

INTRODUCTION

Sepsis and related complications are the leading causes of death in the intensive care unit. In the USA, about 750,000 patients are diagnosed with sepsis annually, resulting in greater than 200,000 deaths per year [253]. In Europe, the hospital mortality of sepsis ranges from 20% to 47% [254]. Clinical manifestations result from the interplay between infectious organisms and host responses. In the early phases of sepsis, pathogens and microbial products, such as endotoxin (lipopolysaccharide, LPS) stimulate the host immune response. Both pro- and anti-inflammatory responses occur rapidly after sepsis onset with an initial prominent hyperinflammatory phase accompanied by fever, hypermetabolism and shock [255]. The host's response is complex, prolonged and responsible for both infection clearance and organ injury [256]. Its dysregulation could favor secondary infections contributing to mortality [257]. To date, no proven pharmacological therapies for sepsis are available [258], and there is an urgent need for novel therapeutic targets.

Based on previous studies that report increased GAS6 plasma levels in severe sepsis [172, 259], we decided to investigate GAS6, as a likely candidate for sepsis treatment. GAS6 is a secreted vitamin K-dependent protein, structurally similar to protein S [7], which interacts with activated phospholipid membranes and TAM receptor tyrosine kinases (TYRO3, AXL and MERTK) [43, 152, 260, 261]. TAM activation leads to intracellular signaling involving PI3K/Akt and interferon (IFN) receptor/signal transducers and activators of transcription (STAT)/suppressor of cytokine signaling (SOCS) pathways. In non immune cells, the PI3K pathway is a major signaling pathway downstream GAS6 [44, 45, 262], whereas in dendritic cells the main pathway operates via IFN/STAT/SOCS [167].

Previous work indicates that the loss of TAM receptors on macrophages causes a chronically high expression of MHC class II levels that is further increase after LPS stimulation. This in turn induces an excessive production of pro-inflammatory cytokines, such as. IL-12 and TNF-α [263]. In line with this results, MERTK activation has been shown to inhibit TNF-α expression by monocytes/macrophages thus protecting mice from lethal endotoxic shock

[166]. More recently, pharmacological intervention with exogenous GAS6 attenuates neutrophil migration and lung injury in sepsis [264].

The results of the present study support the idea that endogenous GAS6 influences the host response to endotoxemia and infection by modulating innate immunity. A rise of plasma GAS6 in healthy volunteers during endotoxin challenge corroborates experimental data in mice and suggests that endogenous GAS6 is a protective factor for severe sepsis, by dampening the inflammation state of macrophages after their initial activation by endotoxin.

MATERIAL AND METHODS

Healthy volunteers

Eight healthy young men [265] were enrolled after approval by the institutional ethics committee (Commission Cantonale (VD) d'Ethique de la Recherche sur l'Etre Humain) and written consent. Inclusion criteria were good health and no medication. A complete history, physical examination and 12-lead electrocardiography were performed. Blood was collected for each participant before and after 2 ng/kg LPS i.v. injection.

Mice

$Gas6^{+/+}$, $Gas6^{+/-}$ and $Gas6^{-/-}$ mice were progeny of the original colony, with a genetic background of 50% 129/Sv x 50% Swiss [13]. BALB/cAnNCrl $Gas6^{-/-}$ mice were backcrossed for >10 generations on a BALB/cAnNCrl background. $Tyro3^{-/-}$, $Axl^{-/-}$ and $Mertk^{-/-}$ mice were progeny of the original colony on a 50% 129/Sv x 50%C57BL/6 background [33]; control WT mice had the same genetic background. Animal experiments were approved by the Swiss Federal Veterinary Office and performed according to our institution's guidelines for animal experiments.

Murine endotoxemia model

Swiss/129/Sv or 129/Sv/C57BL/6 mice were injected intraperitoneally (i.p.) with LPS from *Escherichia coli* O55:B5 (Sigma-Aldrich) at 2 doses (25 or 50 mg/kg) and continuously monitored for LPS-induced lethality for 72 hours after LPS injection.

Arterial blood pressure measurements

Male $Gas6^{+/+}$ and $Gas6^{-/-}$ mice were i.p. injected with 40 mg/kg *E. coli* LPS or an equivalent volume of isotonic saline. After 6 hours, arterial blood pressure was measured inserting a 1.4 F micro-tip pressure catheter (Millar Instruments) into the right carotid artery of anesthetized mice (ketamine 80 mg/kg and xylazine 10 mg/kg). Signals were recorded with a Powerlab/4SP A/D converter (ADInstruments).

Recombinant human Gas6

Recombinant GAS6 (rGAS6) was expressed and purified from HEK293 cells transfected with an epitope-tagged cDNA, as described [266].

Gas6 and protein S ELISA

Plates were coated overnight at 4°C with goat polyclonal antibody against human and mouse GAS6 (AB885 at 10 µg/mL and AF986 at 1 µg/mL, respectively; R&D Systems) in 0.1 M $NaHCO_3$ pH 8.2. The plates were blocked with PBS containing 1% BSA, 5% sucrose and 0.05% NaN_3. rGAS6, mouse GAS6 (986-GS, R&D Systems) and samples diluted in PBS and 1% BSA were incubated overnight at 4°C. After washing, plates were incubated with biotinylated goat antibodies directed against human or mouse GAS6 (BAF885 at 2 µg/mL and BAF986 at 0.5 µg/mL, respectively; R&D Systems). Signals were revealed using avidin-HRP (BD Pharmingen) and the OPD substrate (Sigma-Aldrich). The detection limit of the ELISA was 0.6 and 0.1 ng/mL for human and mouse GAS6, respectively. Human GAS6 levels were expressed in percentage relative to the level of Gas6 in a pool of normal plasma in order to minimize technical variations and to facilitate the comparison of GAS6 levels between clinical samples.

To measure protein S in murine plasma, plates were coated overnight at 4°C with 10 µg/ml of rabbit polyclonal anti human-protein S (DAKO Cytomation). After rinsing with TBS buffer (0.05 M tris(hydroxymethyl)aminomethane, 0.15 M NaCl, pH 7.5, 0.05% Tween 20), the

plate was blocked with TBS-BSA 2%. Plasma samples were added to the wells and incubated at room temperature for 2 hours. Standard curves were established by using dilution of pooled plasma obtained from 14 healthy mice (8 males and 6 females, 7–12 weeks old). Plates were washed and 1 µg/ml biotinylated chicken polyclonal anti-murine protein S was applied for 2 hours at room temperature. Signals were revealed using a streptavidin-HRP conjugated horseradish peroxidase (Thermo) the TMB substrate (KPL).

Mouse protein cytokine array

Plasma samples or macrophage supernatants were applied to a mouse protein cytokine array (62 cytokines; RayBiotech). The array membranes were processed according to the manufacturer's instructions. Briefly, membranes were blocked with a blocking buffer, and then 1 mL of a plasma pool (corresponding to 8 mice) or supernatant was individually added and incubated at room temperature for 2 hours. Finally, the results with immuno-reactivity were assessed and quantified by using a VerSaDoc Imaging System (Bio-Rad) and graphed.

Measurement of sAXL, sMERTK, sTYRO3 cytokines and NO levels

Antigenic evaluation of TAM soluble receptors (sAXL, sMERTK, sTYRO3), IFN-γ, TNF-α and IL-6 in mouse plasma was performed using commercial antibodies (R&D Systems) and ELISA kits (R&D Systems). Nitrate and nitrite were measured by a colorimetric assay according to manufacturer's instructions (Cayman Chemical).

Western blotting for signal transduction and quantification of phosphorylated IκBα

For Western blotting, MBDMs were washed with cold PBS and lysed directly on plates at 4°C with Cell Lysis Buffer (Cell Signaling Technology) supplemented with Complete Mini protease inhibitors cocktail (Roche Diagnostics) and 1 mM NaF. Lysates were centrifuged 10 minutes at 17'000 x g, 4°C and then supernatants were kept at -80°C until use. Proteins were quantified using BCA Protein Assay Kit (Pierce Biotechnology) separated by SDS-PAGE and transferred onto nitrocellulose (Amersham). Phosphorylation of Akt (at Ser473), ERK1/2

(Thr202/Tyr204), p38 (Thr180, Tyr182) and JNK (Thr183/185) was determined using 1:1000 dilutions of rabbit antibodies (Cell Signaling Technologies) incubated overnight at 4°C. For total protein control, membranes were stripped in 62.5 mM Tris-HCl pH=6.8, 2% SDS, 100 µM β-mercaptoethanol for 30 minutes at 50°C, and reprobed with antibodies (Cell Signaling Technologies) directed against the total form of the protein (dilution 1:1000). All primary antibodies were detected by HRP-conjugated swine anti-rabbit antibodies (dilution 1:3000, DakoCytomation). Membranes were incubated with ECL (Amersham) and exposed to Hyperfilm (Amersham). Phosphorylated and total IκBα were quantified in macrophages by an ELISA kit (PathScan ELISA kits, Cell Signaling Technology) according to manufacturer's instructions.

SOCS1 and SOCS3 quantification by qPCR

Gene expression of SOCS1 and SOCS3 was quantified by real-time qPCR, relative to the expression of GAPDH, using an ABI PRISM 7000 (Applied Biosystems) real-time cycler and the following primers: GAPDH forward, 5′-CAACGGGAAGCCCATCAC-3′; reverse, 5′-CGGCCTCACCCCATTTG-3′; SOCS1 forward, 5′-CCGTGGGTCGCGAGAAC-3′; reverse, 5′-AACTCAGGTAGTCACGGAGTACCG-3′; SOCS3 forward, 5′-TCCCATGCCGCTCACAG-3′; reverse, 5′-ACAGGACCAGTTCCAGGTAATTG-3′. Each reaction contained 4 µl SYBR Green PCR Master Mix (Applied Biosystems), 50 nM primer pair, 5 µl diluted cDNA (obtained with SuperScript II Reverse Transcriptase (Invitrogen) according to manufacturer instructions) and water to a final volume of 20 µl. PCR parameters were as follows: initial denaturation at 95°C for 10 min followed by 40 cycles of 15 s at 60°C. The relative gene expression levels in each sample were determined using the comparative deltadeltaCt method, and the GAPDH gene as the endogenous control.

Bacterial sepsis models

In a first model, *E. coli* O18 strain, a gift of A.S. Cross [267], was cultured in BHI medium (Brain Heat Infusion, Becton Dickinson) for 3-4 hours at 37° until $OD_{620nm} = 0.4$ (about $3*10^8$

CFU/ml). BALB/cAnNCrl $Gas6^{+/+}$ and $Gas6^{-/-}$ mice were injected i.p. with $1.5*10^4$ to $2.5*10^5$ CFU. The inoculum was plated immediately after inoculation on blood agar plates to determine viable counts.

In a second model, cecal ligation and puncture, mice were anesthetized by halothane. A midline laparotomy was performed to allow exposure of the cecum. The cecum was ligated as near to the ileocecal junction as possible and perforated twice with a 19-gauge needle. It was then gently squeezed to extrude a small amount of feces from the perforation sites and returned to the peritoneal cavity. The incision was closed with wound clips. Sham operated mice were also incised, cecum taken outside abdominal cavity, and returned in position without ligation or puncture. After surgery, and every 12 hours, mice received 0.05 mg/kg of buprenorphine (Temgesic, Essex Chemie) subcutaneously.

Murine bone marrow-derived macrophages

Bone marrow-derived macrophages (BMDMs) were obtained by culturing bone marrow cells for 7 days in IMDM containing Glutamax (Invitrogen) supplemented with 10% FBS (Invitrogen), 100 IU/mL penicillin, 100 μg/mL streptomycin (Amimed, BioConcept), 50 μM β-mercaptoethanol and 30% L929 conditioned medium as a source of M-CSF.

Statistical analyses

Values were expressed as mean ± SEM. All the data were plotted and analyzed by ANOVA (one-way or two-way, and Bonferroni post-test) or Student's *t*-test using GraphPad Prism (Prism 5.0f). Survival data were plotted using the Kaplan-Meier method and compared using Log-rank test .$P < .05$ was considered statistically significant.

RESULTS

Plasma GAS6 levels rose following LPS challenge in healthy volunteers and mice

Previous studies have shown that plasma GAS6 levels rise in patients with severe sepsis [172, 259]. To corroborate this observation, a small group of healthy volunteers were subjected to intravenous (i.v.) LPS injection in order to mimic acute generalized inflammatory response, a key component in sepsis. GAS6 levels were monitored in plasma participants before and every 30 minutes after LPS injection [265]. GAS6 increased sharply after LPS reaching its maximal concentration after 90 minutes (about two-fold from baseline levels, P<0.001, Figure 1A). Sustained high GAS6 levels were maintained over the whole observation period (360 minutes). These results suggest that LPS directly promoted a rapid and stable GAS6 release in plasma.

We applied the LPS model to mice, at 25 or 50 mg/kg, causing about 25% - LD_{25} - or 75% - LD_{75} - mortality in $Gas6^{+/+}$ mice, respectively. In steady state, circulating GAS6 in $Gas6^{+/+}$ mice was 24 ± 2 ng/mL (Figure 1B), and peaked to 55 ± 10 and 66 ± 6 ng/mL 1 hour after a LPS challenge of 25 and 50 mg/kg, respectively ($P < .001$ between 0 and 1 hour for both LPS doses). GAS6 was still elevated up to 4 hours ($P < .001$ versus baseline) following LPS injection but with a downward trend to baseline levels. Moreover, GAS6 was higher after LPS 50 than 25 mg/kg ($P < .01$, Figure 1B). Since protein S shares sequence/structure homology with GAS6 and has preferential binding to TAM receptors, we also measured plasma protein S in parallel of GAS6. Whereas GAS6 level increased immediately after the injection of LPS, protein S decreased slightly after a short period and remained below baseline for at least 12 hours (1 hour vs. 4 hours, $P = 0.016$, Figure 1C). Thus, in plasma, bacterial product triggers an immediate rise of GAS6, but not of protein S.

Genetic loss of TAM or *Gas6* receptors enhanced vulnerability to endotoxemia

To investigate the role of GAS6 in the host response to endotoxemia, we challenged mice deficient in any of the TAM receptors with LPS (Figure 2A). We established that $Axl^{-/-} Tyro3^{-/-}$, or $Mertk^{-/-}$ mice were more vulnerable to LPS than WT ($n = 7-11$, $Axl^{-/-}$ versus WT: $P =$

.0002; *Tyro3*$^{-/-}$ versus WT: P = .0002; *Mertk*$^{-/-}$ versus WT: P = .0002). *Axl*$^{-/-}$, *Tyro3*$^{-/-}$, or *Mertk*$^{-/-}$ mice were comparably sensitive to LPS challenge (P > .05). Our data on *Mertk*$^{-/-}$ are in line with those reported by Camenisch *et al*. [166].

Since only GAS6, and not protein S, was increased in sepsis, we examined whether endogenous GAS6 is an active player in the endotoxic response in *Gas6*$^{+/+}$, *Gas6*$^{+/-}$ and *Gas6*$^{-/-}$ mice. After LPS injection, *Gas6*$^{-/-}$ mice showed an increased vulnerability compared to *Gas6*$^{+/+}$ and *Gas6*$^{+/-}$ mice (Figure 2B-C). In particular, whereas most of the *Gas6*$^{-/-}$ mice succumbed in the first 48 hours after 25 mg/kg LPS treatment, 73% of the *Gas6*$^{+/+}$ mice survived (Figure 2B). Using higher LPS dosage (50 mg/kg), all *Gas6*$^{-/-}$ mice died within 48 hours (Figure 2C) whereas 25% of *Gas6*$^{+/+}$ mice were still alive; the median survival was 34 hours for *Gas6*$^{+/+}$ versus 14.5 hours for *Gas6*$^{-/-}$ mice. Survival after LPS challenge in *Gas6*$^{+/-}$ mice, whose circulating GAS6 was about 50% of the WT level (Supporting Figure S1A) did not differ from *Gas6*$^{+/+}$. Thus, the loss of *Gas6* or any TAM receptors enhanced vulnerability of mice to endotoxemia.

In rodents, LPS promotes hypotension accompanied by the release of pro-inflammatory cytokines and nitric oxide (NO), and by the induction of nitric oxide synthase expression. These events finally result in the onset of acute pulmonary edema, myocardial dysfunction and death [218, 219]. To investigate whether *Gas6*$^{-/-}$ mice were more susceptible to hypotension during endotoxemia, arterial blood pressure was measured. *Gas6*$^{-/-}$ and *Gas6*$^{+/+}$ mice did not differ at steady state; however, 6 hours after LPS injection, mean blood pressure was significantly reduced in *Gas6*$^{-/-}$ mice (Figures 2D-E).

Soluble receptor AXL (sAXL) rose in murine plasma in response to LPS

During inflammation, TAM receptors can be cleaved and released in the bloodstream. *Gas6*$^{-/-}$ mice presented at baseline soluble sAXL levels higher than *Gas6*$^{+/+}$ mice (21.3 ± 1.3 vs 6.7 ± 0.3 ng/mL, Figure 3A). Although 25 mg/kg LPS treatment increased sAXL in both genotypes during the first 7 hours, *Gas6*$^{-/-}$ mice showed a 2-fold increased sAXL compared to *Gas6*$^{+/+}$ mice, as further confirmed by cytokines antibody array (cytokine # 1, Figure 3B). We were

unable to detect the soluble forms of TYRO3 and MERTK in murine plasma by ELISA both in $Gas6^{-/-}$ and $Gas6^{+/+}$ mice.

Circulating cytokines were elevated in $Gas6^{-/-}$ mice during endotoxemia

Sixty-two pro-inflammatory and immunomodulatory cytokines were quantified in plasma in a relative scale manner at different time points after LPS injection (50 mg/kg i.p.) using an antibody array. Cytokines levels were generally higher in $Gas6^{-/-}$ mice 1 hour after LPS challenge (Figure 3B), several cytokines being at least 50% higher in $Gas6^{-/-}$ than $Gas6^{+/+}$ plasma after LPS injection (after 1 hour: 46/62 cytokines, 4 hours: 6/62, 7 hours: 29/62, Supporting Table S1) but also at steady-state (52/62) [242]. Indeed, 1 hour after LPS injection, IFN-γ, IL-10, IL-12p40/p70, IL-12 p70, IL-1β, IL-6, KC were at least 50% higher in $Gas6^{-/-}$ than $Gas6^{+/+}$ plasma. After 4 hours, IL-1β and TNF-α, and after 7 hours, IL-10, MCP1 and TARC were at least 50% higher. Antigenic assays for TNF-α and IFN-γ further confirmed the increased concentration of both cytokines in $Gas6^{-/-}$ 1 hour after LPS injection (Figure 3C-D). In addition, we measured TNF-α levels also in $Axl^{-/-}$, $Tyro3^{-/-}$, and $Mertk^{-/-}$ mice plasma after LPS challenge (25 mg/kg). Both $Axl^{-/-}$ mice (14 ± 1 ng/mL) and $Mertk^{-/-}$ mice (50 ± 13 ng/mL) mice showed 3-10 fold increase of TNF-α levels compared to WT (5 ± 1 ng/mL) ($P = .0002$ and $P = .009$ respectively, $n = 7$-9), whereas for $Tyro3^{-/-}$, TNF-α levels were comparable to WT (8 ± 2 ng/mL, $P = .14$, $n = 7$).

Although NO enhances bacterial destruction, it is also well known to promote the vasodilation. We therefore evaluated the total amount of NO by measuring nitrate and nitrite concentrations in plasma. In WT mice, NO increased drastically after LPS injection (1 and 7 hours, depending of the murine background, Supporting Figure S1B-C). In comparison, NO level increased only slightly in $Gas6^{-/-}$ mice and did not differ significantly from baseline in $Axl^{-/-}$ and $Tyro3^{-/-}$ mice (Supporting Figure S1B-C).

Since steroids inhibit inflammatory cytokines, we assessed whether dexamethasone (DXM) affects GAS6 concentration in murine plasma (Figure 3E) or whether the lack of GAS6 would

impair the immunomodulatory effect of the glucocorticoid (Figure 3F). Intraperitoneal DXM injection in the presence or absence of LPS did not modify plasma GAS6 in comparison to vehicle controls. Moreover, in the absence of GAS6, DXM was still a potent inflammatory cytokines inhibitor (Figure 3F).

Thus, during endotoxemia, numerous circulating pro- and anti-inflammatory cytokines were higher in *Gas6*^{-/-} than *Gas6*^{+/+} mice. In addition, TNF-α was higher in the absence of *Axl* or *Mertk*, although the absence of *Tyro3* appeared to have less significance on TNF-α levels. However, NO levels were higher in *Gas6*^{+/+} than *Gas6*^{-/-} mice. DXM treatment, however, did not modify the release of GAS6 in plasma upon LPS challenge.

Macrophages lacking Gas6 overproduced cytokines

GAS6 and TAM receptors are expressed by macrophages, platelets and endothelial cells but not by circulating lymphocytes and neutrophils [15, 171]. Therefore, we focused on macrophages as they may constitute the main source of circulating GAS6 and cytokines during sepsis [259, 268].

We observed that BMDMs released GAS6 when stimulated by LPS (Figure 4A). Next, we assessed the role of *Gas6* by measuring the release of TNF-α in *Gas6*^{+/+} and *Gas6*^{-/-} BMDMs stimulated with LPS. *Gas6*^{-/-} BMDMs released significantly more TNF-α than *Gas6*^{+/+} BMDMs in a dose-dependent manner (Figure 4B). Moreover rGAS6 (400 ng/mL) reduced TNF-α release from *Gas6*^{-/-} BMDMs, thereby restoring a *Gas6*^{+/+} phenotype (Figure 4B). We observed a comparable restoration of the WT phenotype in a time-course experiment (Supporting Figure S1D). Similarly, IL-6 secretion was enhanced in *Gas6*^{-/-} BMDMs (Figure 4C) compared to *Gas6*^{+/+} BMDMs and its level rose progressively with LPS dose. Increased IL-6 levels in *Gas6*^{-/-} BMDMs were dampened by adding rGAS6 (400 ng/mL) to the cell culture medium (Figure 4C).

These results indicate that after LPS stimulation macrophages released GAS6 that in turn prevented exaggerated cytokine release. However, co-treatment of $Gas6^{-/-}$ BMDMs with rGAS6 partially restored the $Gas6^{+/+}$ phenotype for all the examined cytokines.

GAS6 immunomodulatory function acted through SOCS1/3 pathway in BMDMs

Signal transduction mediated by GAS6 in other cell types than dendritic cells is known to involve the activation of PI3K and its downstream target, Akt [260]. In addition, MERTK regulates PI3K and NF-κB activation in dendritic cells [269]. Since it has been shown that the PI3K/Akt signaling pathway negatively regulates LPS-induced acute inflammation [270], we assessed whether the absence of $Gas6$ affects Akt activation in BMDMs. Moreover, downstream targets of the PI3K/Akt pathway and the TLR4 pathway include the MAPK pathways (p38, ERK1/2, JNK) [263]. Thus, we stimulated BMDMs with LPS (40 ng/mL) and assessed the phosphorylation of Akt, p38, ERK1/2 and JNK, as well as the total form of each protein. Western blotting and densitometry quantification (data not shown) of three independent experiments did not highlight a difference of target protein phosphorylation between $Gas6^{+/+}$ and $Gas6^{-/-}$ BMDMs (Supporting Figure S1E). Consequently, we did not notice a modification of the phosphorylation state of IκB-α between $Gas6^{+/+}$ and $Gas6^{-/-}$ BMDMs (Figure 5A).

GAS6 induces the cytokine and TLR suppressors SOCS1 and SOCS3 in dendritic cells, as shown by an increased mRNA expression of SOCS1/3 in cell lysates [167] and in the synovia of mice in a collagen-Induced arthritis model [271]. Quantitative RT-PCR of BMDMs stimulated with LPS at different time points was performed. In absence of GAS6, mRNA expression of SOCS1 was reduced (Figure 5B). A similar pattern was also observed for SOCS3 although only as a trend (Supporting Figure S1F). The same pattern has been described in [271]. Thus, the lack of GAS6 weakened the regulation of the TLR signaling pathway in BMDMs by dampening at least SOCS1 activation.

***Gas6* deficiency conferred susceptibility to microbial sepsis with exaggerated inflammation**

We examined the response of *Gas6*^{+/+} and *Gas6*^{-/-} mice to microbial sepsis using two models of peritonitis. In the first model, *Gas6*^{+/+} mice were inoculated i.p. with the *E. coli* strain O18 [24]. Plasma GAS6 levels increased by 50% after 4 hours (39 ± 2 at baseline and 59 ± 4 ng/mL after 4 hours, $P < .05$, $n = 9\text{-}10$) and remained elevated for at least 24 hours. Higher dose of *E. coli* ($2.5*10^6$ CFU) induced much higher levels of IL-6 in *Gas6*^{-/-} than *Gas6*^{+/+} mice (143 ± 20 versus 53 ± 14 ng/mL, $P = .004$, $n = 5\text{-}6$).

In the second model of peritonitis, which closely mimics human peritoneal sepsis (cecal ligation and puncture, CLP) [220, 221], plasma GAS6 levels were higher after 8 and 24 hours in mice with peritonitis compared to sham-operated mice (Figure 6A). *Gas6*^{-/-} mice were more sensitive to CLP than *Gas6*^{+/+} mice: 83% of *Gas6*^{-/-} versus 55% of *Gas6*^{+/+} mice died 48 hours after peritonitis-inducing surgery (Figure 6B). All shams survived to 48 hours. Thus, *Gas6* deficiency in mice conferred susceptibility to microbial sepsis.

DISCUSSION

Here we show that the *Gas6* influences host responses to endotoxemia and bacterial infection by modulating innate immunity. Endogenous GAS6 exhibits strong anti-inflammatory activities both *in vivo* and *in vitro*, by attenuating endotoxin-induced activation of macrophages and blunting systemic inflammatory response. A first insight came from a report showing that MERTK activation inhibits TNF-α production by monocytes/macrophages and alleviates endotoxic shock in mice [166]. A second insight was provided by data demonstrating that macrophages lacking the three cognate GAS6 receptors (TYRO3/AXL/MERTK or TAM) are chronically hyperactivated as indicated by their high expression of MHC class II and CD86 in steady-state with further aberrantly increase after endotoxin stimulation and excessive production of pro-inflammatory cytokines [33]. Finally,

a third study demonstrated that activation of TAM signaling provides a negative feedback of TLR- and cytokine-driven immune response in dendritic cells [167]. Based on these reports, we hypothesized that endogenous GAS6 might be involved in protection against systemic inflammatory response to infection and/or in the development of immune dysfunction observed in severe sepsis.

To test our hypothesis, we performed experimental studies using $Gas6^{+/+}$, $Gas6^{+/-}$ and $Gas6^{-/-}$ mice. First, we observed in $Gas6^{-/-}$ mice the same vulnerability to endotoxin challenge as in $Mertk^{-/-}$ mice [166], characterized by a reduced survival associated with an overproduction of TNF-α. Moreover, survival curves after endotoxin challenge in $Axl^{-/-}$ and $Tyro3^{-/-}$ were comparable to those of $Mertk^{-/-}$ and $Gas6^{-/-}$ mice. Second, $Gas6^{-/-}$ mice mortality was also increased in the CLP model. We demonstrated that plasma GAS6 relatively increased both in endotoxemia and microbial peritonitis models. We showed that macrophages secrete cytokines and GAS6 after endotoxic treatment in order to prevent an over-stimulation, by the activation of the IFNR/STAT1/SOCS pathway through TAM signaling as it was postulated previously [33, 42]. We describe here that in BMDMs, SOCS1 and although to a less extent SOCS3 are decreased in absence of GAS6. Consequently, endogenous GAS6 dampens mortality induced by endotoxemia and sepsis, acting through TAM receptors as a negative feedback in the inflammation process.

Besides GAS6, soluble TAM receptors are generated by proteolytic cleavage of their ectodomains upon LPS stimulation [39]. These soluble forms might possibly sequester GAS6 and antagonize the cell-associated TAM receptors [272]. Soluble AXL was higher in steady-state and after endotoxin challenge in $Gas6^{-/-}$ than $Gas6^{+/+}$ mice, but we were unable to detect circulating sTYRO3 or sMERTK in mice. GAS6 has a higher affinity for AXL than TYRO3 or MERTK so it is plausible that compensatory regulation is occurring for AXL in the absence of GAS6 in $Gas6^{-/-}$ mice.

The data obtained in mice were corroborated by observations in humans. In healthy volunteers, GAS6 rose in plasma in response to endotoxin, reaching its maximal concentration at 90 minutes and was then sustained for the next 4.5 hours. In comparison,

under the same conditions, TNF-α has been reported to peak in plasma at 120 minutes and to progressively return to baseline [265], suggesting that the time course of plasma GAS6 after LPS injection in humans differs from that of TNF-α.

In patients with severe sepsis, high plasma GAS6 levels correlated with the degree of organ dysfunction [259]. In our murine endotoxemia model, mild GAS6 deficiency in *Gas6*^{+/-} mice did not affect mortality whereas total absence of GAS6 increased mortality in both endotoxemia and microbial sepsis models. Thus, our data argue for a homeostatic role of endogenous GAS6, acting on macrophages, and suggest that GAS6 might appear as a potential early and reliable marker of infection and sepsis, as has been proposed. Indeed, currently, no single clinical or biological marker of sepsis has gained general acceptance [273, 274]. In addition to previous observations [172, 259], this work suggests that GAS6 and its soluble receptor should be investigated further as early biomarkers of sepsis. This is of relevance regarding that GAS6 plays a beneficial role in sepsis. Endogenous GAS6 attenuates the systemic inflammatory response in the early phase of sepsis, leading to death if the immune reaction is not dampened, but might also participate to hypo-inflammatory response in a later phase of sepsis, favoring fatalities due to primary infection or the development of secondary infections. Recently, a pharmacological intervention with recombinant GAS6 showed a rescue of the mortality induced by CLP, reduced both cytokine levels in plasma and cellular infiltration in the lungs [264].

Both GAS6 and protein S are ligands for TAM receptors but previous publications showed that plasma protein S, in contrast to GAS6, may be reduced in the context of sepsis in human, most probably because of consumptive coagulopathy. The effect on protein S was, however, less prominent than on antithrombin or protein C [275]. In addition, initial and sequential differences in plasma protein S between survivors and non survivors were not significant and initial protein S levels had no prognostic value for prediction of subsequent death [276]. We observed that protein S significantly decreased in mice after LPS, most probably secondary to the consumptive coagulopathy occurring in this context. The role of protein S in LPS and

sepsis murine models is beyond the scope of the current manuscript and will be further investigated.

In conclusion, our data presented here point to GAS6 as a major modulator of innate immunity and thereby provide novel insights into the mechanism of the systemic inflammatory response. GAS6 may constitute a protective factor for sepsis and, consequently, a potential target for the treatment of sepsis.

FIGURES
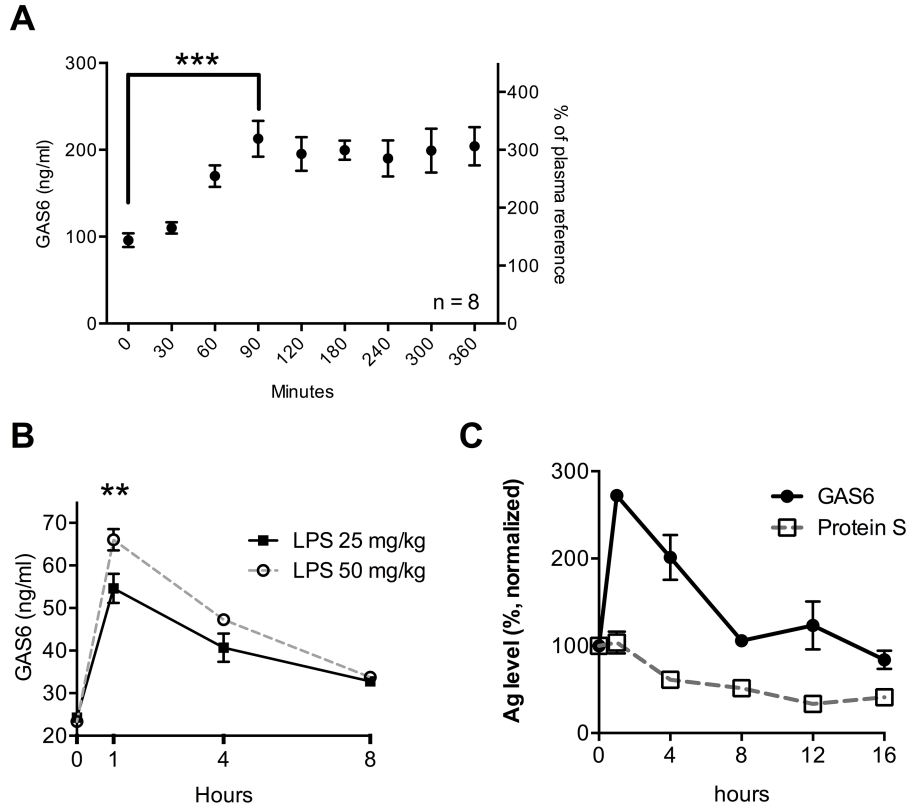
FIGURE 1: LPS PROMOTES GAS6 RELEASE IN HUMAN AND MOUSE PLASMA

(A) GAS6 levels in plasma of healthy volunteers (n=8) at steady-state (t0) and after 2 ng/kg

LPS i.v. injection (***P < .001 t0 *vs* any time points ≥ 60 min, repeated measures ANOVA

and Bonferroni's multiple comparison test). (B) GAS6 levels in plasma of *Gas6$^{+/+}$* mice at

steady-state and at different time points after LPS injection (** P < .01, 25 vs. 50 mg/kg).

Data from two independent experiments. (C) GAS6 and protein S levels in plasma of *Gas6$^{+/+}$*

mice at different time points after LPS (25 mg/kg) injection.
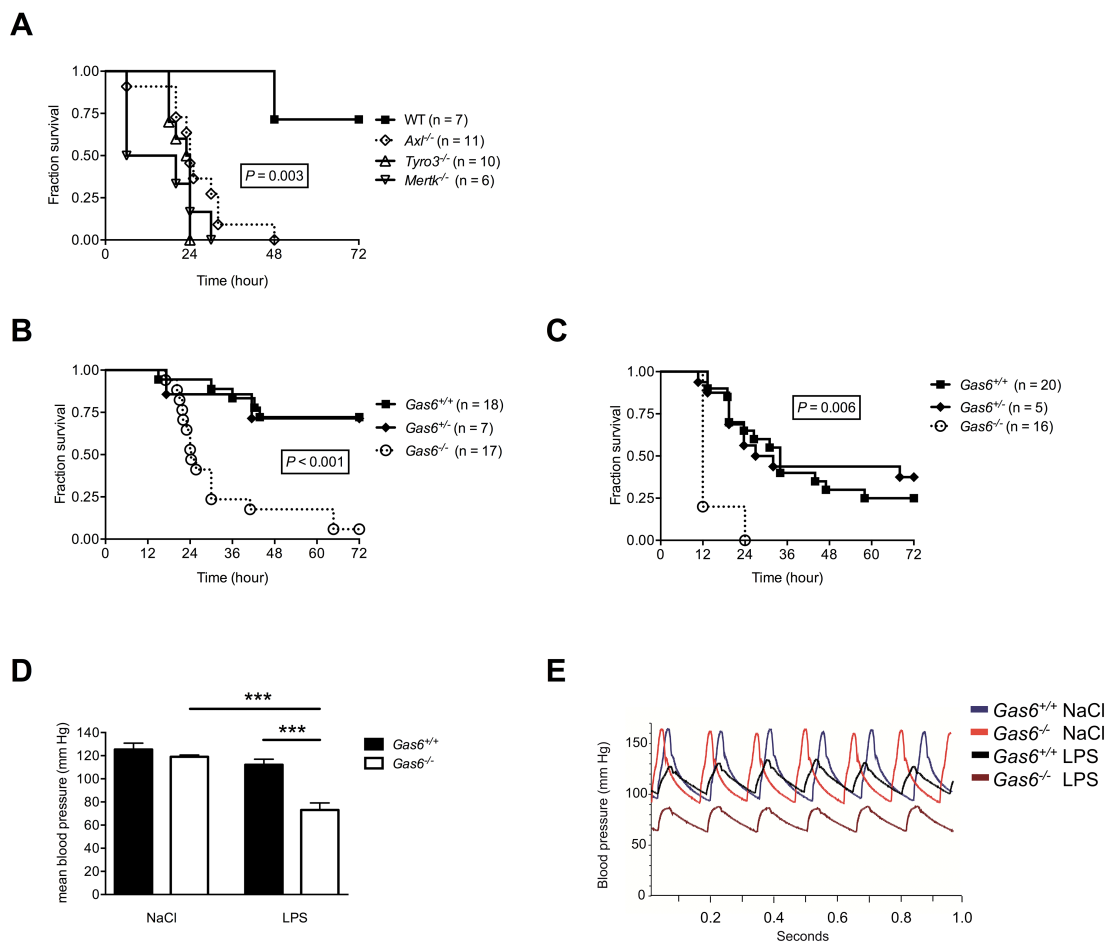
Figure 2: Lack of *GAS6* or of its receptors in mice enhances vulnerability to endotoxemia

(A-B) Kaplan-Meier plots of the survival of $Gas6^{+/+}$, $Gas6^{+/-}$ and $Gas6^{-/-}$ mice treated with LPS 25 mg/kg (A) and 50 mg/kg (B) intraperitoneally (i.p.). Data are pooled from multiple independent experiments. (C) Mean blood pressure measured in the carotid artery did not differ between $Gas6^{+/+}$ ($n = 3$) and $Gas6^{-/-}$ mice ($n = 3$) in steady state (mean ± SEM, $P > .05$) but was lower in $Gas6^{-/-}$ mice ($n = 7$) compared to $Gas6^{+/+}$ mice ($n = 6$) 6 hours after LPS injection (40 mg/kg) (*** $P < .001$). Data from two independent experiments. (D) Representative traces of arterial blood pressure measured in mice 6 hours after i.p. injection of NaCl 0.9% or 40 mg/kg LPS. Data from two independent experiments. (E) Kaplan-Meier

plots of the survival of WT and mice lacking any one of the cognate GAS6 receptors treated

with 25 mg/kg LPS. Data from two independent experiments
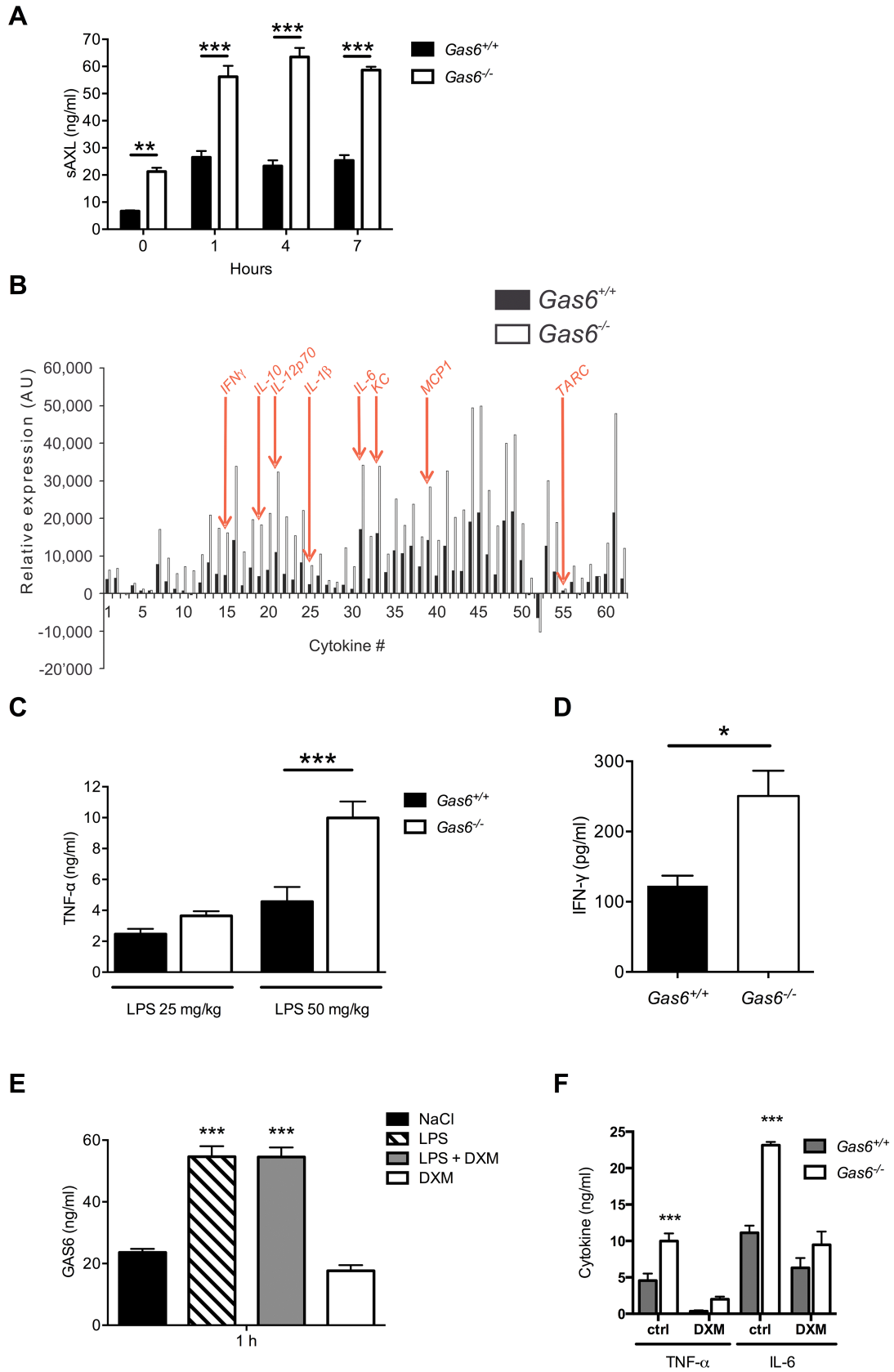
FIGURE 3: GAS6 RAISES IN PLASMA DURING ENDOTOXEMIA AND DOWN-REGULATES ITS SOLUBLE RECEPTOR AXL AND NUMEROUS CIRCULATING CYTOKINES

(A) Comparison between plasma levels of sAXL in $Gas6^{-/-}$ than in $Gas6^{+/+}$ mice before and after LPS injection (25 mg/kg); ** $P < .01$, *** $P < .001$. (B) Cytokines antibody array was performed using pool of $Gas6^{-/-}$ and $Gas6^{+/+}$ plasma (n=8 mice each group) 1 hour after LPS injection (50 mg/kg). Cytokines are numbered from 1 to 62 on the *x*-axis and their relative expression is indicated on the *y*-axis in arbitrary units (AU). Cytokines that are commonly significantly increased during endotoxemia are indicated in red. Cytokine listed in Supporting Table S2. (C-D) Plasmatic TNF-α (C) and IFN-γ (D) levels in $Gas6^{-/-}$ and $Gas6^{+/+}$ mice 1 hour after LPS injection (*** $P < .001$, $P < .05$). Data from two independent experiments. (E) dexamethasone (DXM) doesn't control plasmatic GAS6. (F) The absence of GAS6 doesn't impair the immunomodulatory effect of DXM.
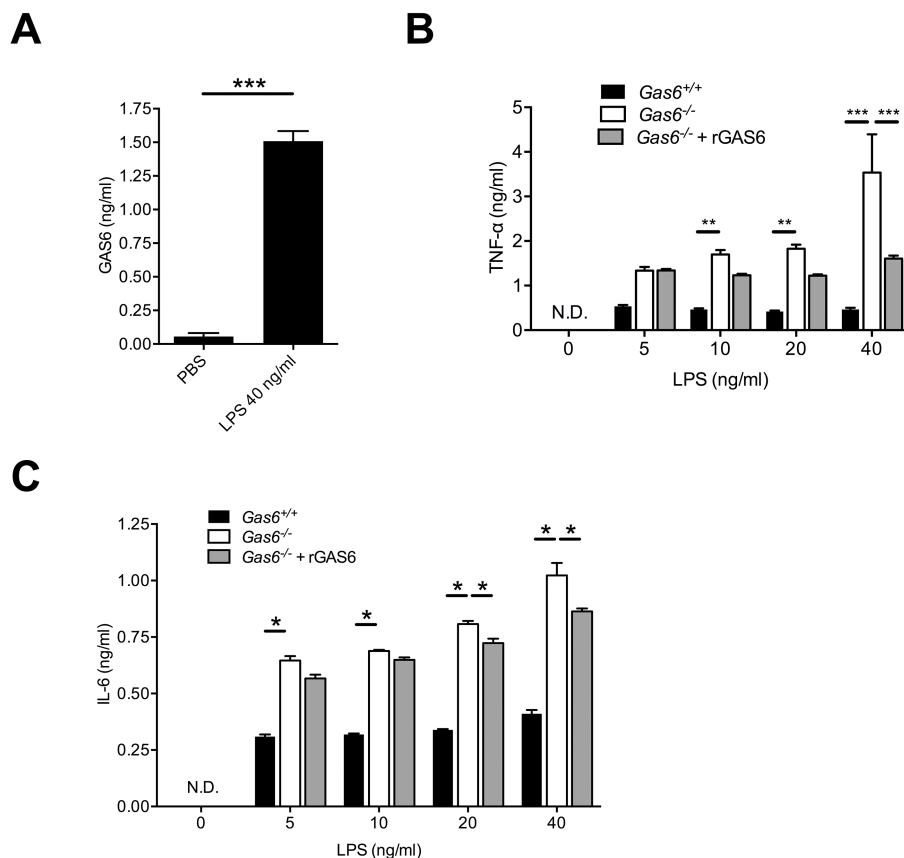
FIGURE 4: MACROPHAGES LACKING GAS6 OVERPRODUCE CYTOKINES IN RESPONSE TO ENDOTOXIN

(A) Secreted GAS6 by bone marrow-derived macrophages (BMDMs) after 24 hours stimulation with 40 ng/ml LPS (*** P < .001). (B) TNF-α released by *Gas6*^{-/-} BMDMs and *Gas6*^{+/+} BMDMs after 5-40 ng/ml LPS stimulation. Addition of rGAS6 (400 ng/ml) *Gas6*^{-/-} BMDMs conditioned media was able to reduce TNF-α release from *Gas6*^{-/-} BMDMs (** P < .01, *** P < .001). (C) IL-6 secretion by *Gas6*^{-/-} BMDMs and *Gas6*^{+/+} BMDMs after LPS treatment (* P < .05); addition of rGAS6 (400 ng/ml) to the cell culture media reduced IL6 released by *Gas6*^{-/-} BMDMs.

A
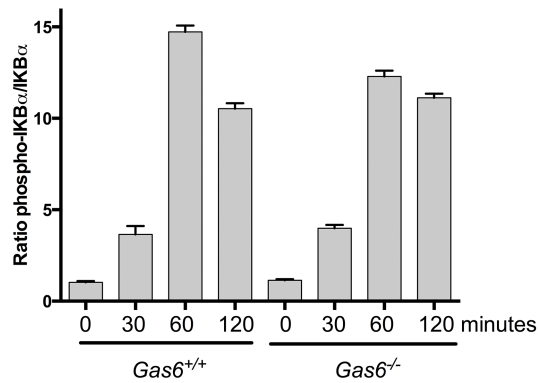
B
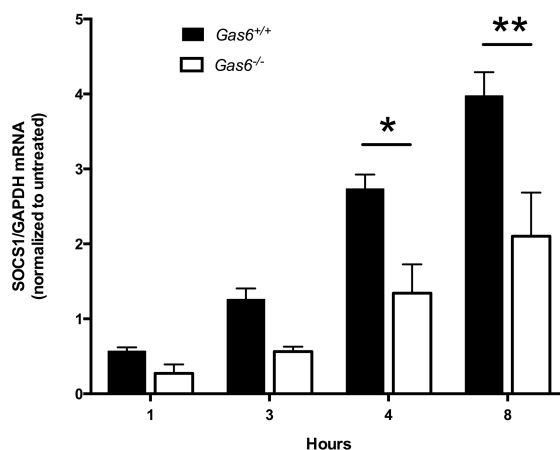
FIGURE 5: SOCS1 PATHWAY IS DAMPEND IN *GAS6*^{-/-} MACROPHAGES

(A) Kinetics of IκB phosphorylation after LPS (40 ng/ml) stimulation in BMDMs (3 independent experiments). (B) Relative mRNA expression of suppressor of cytokine signaling (SOCS)1 quantified by qPCR using GAPDH as housekeeping gene and normalized to nonstimulated cells (0 hour). BMDMs were incubated for 1 to 8 hours with 40 ng/ml of lipopolysaccharide (LPS). (* P < .05, ** P < .01).
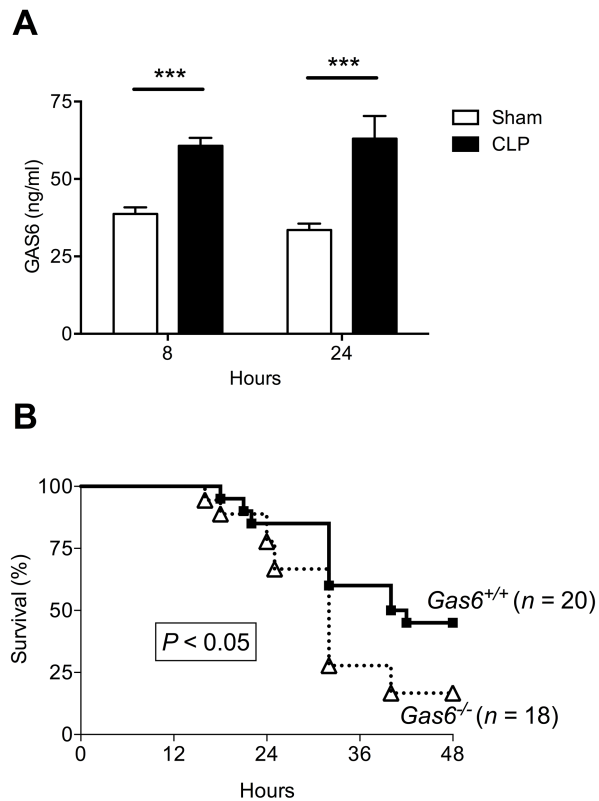
FIGURE 6: *GAS6^{-/-}* MICE ARE MORE SUSCEPTIBLE TO MICROBIAL SEPSIS.

(A) GAS6 plasma levels after 8 and 24 h from CLP compared to sham-operated mice (*** P < .001). (B) CLP survival in *Gas6^{-/-}* and *Gas6^{+/+}* mice. Data from three independent experiments (P < .05).

Disclosures: none.

The Gas6-Axl Protein Interaction Mediates Endothelial Uptake of Platelet Microparticles

Chapter VII. Bibliography

1. Furie, B. and B.C. Furie, *Mechanisms of thrombus formation.* N Engl J Med, 2008. **359**(9): p. 938-49.
2. Day, I.S.C.f.W.T., *Thrombosis: a major contributor to the global disease burden.* J Thromb Haemost, 2014. **12**(10): p. 1580-90.
3. Gaertner, F. and S. Massberg, *Blood coagulation in immunothrombosis-At the frontline of intravascular immunity.* Semin Immunol, 2016.
4. Foley, J.H. and E.M. Conway, *Cross Talk Pathways Between Coagulation and Inflammation.* Circ Res, 2016. **118**(9): p. 1392-408.
5. Lentz, S.R., *Thrombosis in the setting of obesity or inflammatory bowel disease.* Blood, 2016. **128**(20): p. 2388-2394.
6. Schneider, C., . King RM., Philipson, L.,, *Genes Specifically Expressed at Growth Arrest of Mammalian Cells.* cell, 1988. **54**: p. 787-793.
7. Manfioletti, G., et al., *The protein encoded by a growth arrest-specific gene (gas6) is a new member of the vitamin K-dependent proteins related to protein S, a negative coregulator in the blood coagulation cascade.* Mol Cell Biol, 1993. **13**(8): p. 4976-85.
8. Funakoshi, H., et al., *Identification of Gas6, a putative ligand for Sky and Axl receptor tyrosine kinases, as a novel neurotrophic factor for hippocampal neurons.* J Neurosci Res, 2002. **68**(2): p. 150-60.
9. Llacuna, L., et al., *Growth arrest-specific protein 6 is hepatoprotective against murine ischemia/reperfusion injury.* Hepatology, 2010. **52**(4): p. 1371-9.
10. Yanagita, M., *The role of the vitamin K-dependent growth factor Gas6 in glomerular pathophysiology.* Curr Opin Nephrol Hypertens, 2004. **13**(4): p. 465-70.
11. Nakano, T., et al., *Vascular smooth muscle cell-derived, Gla-containing growth-potentiating factor for Ca(2+)-mobilizing growth factors.* J Biol Chem, 1995. **270**(11): p. 5702-5.
12. Avanzi, G.C., et al., *GAS6, the ligand of Axl and Rse receptors, is expressed in hematopoietic tissue but lacks mitogenic activity.* Exp Hematol, 1997. **25**(12): p. 1219-26.
13. Angelillo-Scherrer, A., et al., *Deficiency or inhibition of Gas6 causes platelet dysfunction and protects mice against thrombosis.* Nat Med, 2001. **7**(2): p. 215-21.
14. Balogh, I., et al., *Analysis of Gas6 in human platelets and plasma.* Arterioscler Thromb Vasc Biol, 2005. **25**(6): p. 1280-6.
15. Laurance, S., C.A. Lemarie, and M.D. Blostein, *Growth arrest-specific gene 6 (gas6) and vascular hemostasis.* Adv Nutr, 2012. **3**(2): p. 196-203.
16. Di Scipio, R.G., et al., *A comparison of human prothrombin, factor IX (Christmas factor), factor X (Stuart factor), and protein S.* Biochemistry, 1977. **16**(4): p. 698-706.
17. Fair, D.S. and R.A. Marlar, *Biosynthesis and secretion of factor VII, protein C, protein S, and the Protein C inhibitor from a human hepatoma cell line.* Blood, 1986. **67**(1): p. 64-70.
18. Fair, D.S., R.A. Marlar, and E.G. Levin, *Human endothelial cells synthesize protein S.* Blood, 1986. **67**(4): p. 1168-71.

19. Lemke, G. and C.V. Rothlin, *Immunobiology of the TAM receptors.* Nat Rev Immunol, 2008. **8**(5): p. 327-36.

20. Dahlback, B., *The tale of protein S and C4b-binding protein, a story of affection.* Thromb Haemost, 2007. **98**(1): p. 90-6.

21. Suleiman, L., C. Negrier, and H. Boukerche, *Protein S: A multifunctional anticoagulant vitamin K-dependent protein at the crossroads of coagulation, inflammation, angiogenesis, and cancer.* Crit Rev Oncol Hematol, 2013. **88**(3): p. 637-54.

22. Stenflo, J., *Contributions of Gla and EGF-like domains to the function of vitamin K-dependent coagulation factors.* Crit Rev Eukaryot Gene Expr, 1999. **9**(1): p. 59-88.

23. Long, G.L., et al., *Human protein S cleavage and inactivation by coagulation factor Xa.* J Biol Chem, 1998. **273**(19): p. 11521-6.

24. Lu, D., et al., *The effect of N-linked glycosylation on molecular weight, thrombin cleavage, and functional activity of human protein S.* Thromb Haemost, 1997. **77**(6): p. 1156-63.

25. Lai, C. and G. Lemke, *An extended family of protein-tyrosine kinase genes differentially expressed in the vertebrate nervous system.* Neuron, 1991. **6**(5): p. 691-704.

26. Crosier, P.S., et al., *Isolation of a receptor tyrosine kinase (DTK) from embryonic stem cells: structure, genetic mapping and analysis of expression.* Growth Factors, 1994. **11**(2): p. 125-36.

27. Fujimoto, J. and T. Yamamoto, *brt, a mouse gene encoding a novel receptor-type protein-tyrosine kinase, is preferentially expressed in the brain.* Oncogene, 1994. **9**(3): p. 693-8.

28. Ohashi, K., et al., *Cloning of the cDNA for a novel receptor tyrosine kinase, Sky, predominantly expressed in brain.* Oncogene, 1994. **9**(3): p. 699-705.

29. Mark, M.R., et al., *rse, a novel receptor-type tyrosine kinase with homology to Axl/Ufo, is expressed at high levels in the brain.* J Biol Chem, 1994. **269**(14): p. 10720-8.

30. Dai, W., et al., *Molecular cloning of a novel receptor tyrosine kinase, tif, highly expressed in human ovary and testis.* Oncogene, 1994. **9**(3): p. 975-9.

31. Lai, C., M. Gore, and G. Lemke, *Structure, expression, and activity of Tyro 3, a neural adhesion-related receptor tyrosine kinase.* Oncogene, 1994. **9**(9): p. 2567-78.

32. Linger, R.M., et al., *TAM receptor tyrosine kinases: biologic functions, signaling, and potential therapeutic targeting in human cancer.* Adv Cancer Res, 2008. **100**: p. 35-83.

33. Lu, Q. and G. Lemke, *Homeostatic regulation of the immune system by receptor tyrosine kinases of the Tyro 3 family.* Science, 2001. **293**(5528): p. 306-11.

34. Prasad, D., et al., *TAM receptor function in the retinal pigment epithelium.* Mol Cell Neurosci, 2006. **33**(1): p. 96-108.

35. O'Bryan, J.P., et al., *axl, a transforming gene isolated from primary human myeloid leukemia cells, encodes a novel receptor tyrosine kinase.* Mol Cell Biol, 1991. **11**(10): p. 5016-31.

36. Janssen, J.W., et al., *A novel putative tyrosine kinase receptor with oncogenic potential.* Oncogene, 1991. **6**(11): p. 2113-20.

37.   Rescigno, J., A. Mansukhani, and C. Basilico, *A putative receptor tyrosine kinase with unique structural topology.* Oncogene, 1991. **6**(10): p. 1909-13.

38.   Wang, X.M., et al., *[Single calcium channel analysis and electron spin resonance (ESR) spectral study on the myocardial effects of ginsenoside Rb2].* Zhongguo Zhong Yao Za Zhi, 1994. **19**(10): p. 621-4, 640.

39.   Sather, S., et al., *A soluble form of the Mer receptor tyrosine kinase inhibits macrophage clearance of apoptotic cells and platelet aggregation.* Blood, 2007. **109**(3): p. 1026-33.

40.   Graham, D.K., et al., *Cloning and mRNA expression analysis of a novel human protooncogene, c-mer.* Cell Growth Differ, 1994. **5**(6): p. 647-57.

41.   Stitt, T.N., et al., *The anticoagulation factor protein S and its relative, Gas6, are ligands for the Tyro 3/Axl family of receptor tyrosine kinases.* Cell, 1995. **80**(4): p. 661-70.

42.   Lemke, G., *Biology of the TAM receptors.* Cold Spring Harb Perspect Biol, 2013. **5**(11): p. a009076.

43.   Nagata, K., et al., *Identification of the product of growth arrest-specific gene 6 as a common ligand for Axl, Sky, and Mer receptor tyrosine kinases.* J Biol Chem, 1996. **271**(47): p. 30022-7.

44.   Goruppi, S., et al., *Gas6-mediated survival in NIH3T3 cells activates stress signalling cascade and is independent of Ras.* Oncogene, 1999. **18**(29): p. 4224-36.

45.   Goruppi, S., E. Ruaro, and C. Schneider, *Gas6, the ligand of Axl tyrosine kinase receptor, has mitogenic and survival activities for serum starved NIH3T3 fibroblasts.* Oncogene, 1996. **12**(3): p. 471-80.

46.   Angelillo-Scherrer, A., et al., *Role of Gas6 receptors in platelet signaling during thrombus stabilization and implications for antithrombotic therapy.* Journal of Clinical Investigation, 2005. **115**(2): p. 237-246.

47.   Ma, Y.Q., J. Qin, and E.F. Plow, *Platelet integrin alpha(IIb)beta(3): activation mechanisms.* J Thromb Haemost, 2007. **5**(7): p. 1345-52.

48.   Cosemans, J.M., et al., *Potentiating role of Gas6 and Tyro3, Axl and Mer (TAM) receptors in human and murine platelet activation and thrombus stabilization.* J Thromb Haemost, 2010. **8**(8): p. 1797-808.

49.   Tjwa, M., *Gas6 promotes inflammation by enhancing interactions between endothelial cells, platelets, and leukocytes.* Blood, 2008. **111**(8).

50.   Robins, R.S., et al., *Vascular Gas6 contributes to thrombogenesis and promotes tissue factor up-regulation after vessel injury in mice.* Blood, 2013. **121**(4): p. 692-9.

51.   Laurance, S., et al., *Gas6-induced tissue factor expression in endothelial cells is mediated through caveolin-1-enriched microdomains.* J Thromb Haemost, 2014. **12**(3): p. 395-408.

52.   Sinauridze, E.I., et al., *Platelet microparticle membranes have 50- to 100-fold higher specific procoagulant activity than activated platelets.* Thromb Haemost, 2007. **97**(3): p. 425-34.

53.   Happonen, K.E. and B. Dahlback, *Gas6 fueling tumor-mediated thrombosis.* Blood, 2016. **127**(6): p. 672-3.

54.   Blostein, M.D., et al., *Elevated plasma gas6 levels are associated with venous thromboembolic disease.* J Thromb Thrombolysis, 2011. **32**(3): p. 272-8.

55. Munoz, X., et al., *Human vitamin K-dependent GAS6: gene structure, allelic variation, and association with stroke.* Hum Mutat, 2004. **23**(5): p. 506-12.

56. Melaragno, M.G., et al., *Increased expression of Axl tyrosine kinase after vascular injury and regulation by G protein-coupled receptor agonists in rats.* Circ Res, 1998. **83**(7): p. 697-704.

57. Melaragno, M.G., et al., *Gas6 inhibits apoptosis in vascular smooth muscle: role of Axl kinase and Akt.* J Mol Cell Cardiol, 2004. **37**(4): p. 881-7.

58. Son, B.K., et al., *Statins protect human aortic smooth muscle cells from inorganic phosphate-induced calcification by restoring Gas6-Axl survival pathway.* Circ Res, 2006. **98**(8): p. 1024-31.

59. Korshunov, V.A., et al., *Axl, a receptor tyrosine kinase, mediates flow-induced vascular remodeling.* Circ Res, 2006. **98**(11): p. 1446-52.

60. Healy, A.M., et al., *Gas 6 promotes Axl-mediated survival in pulmonary endothelial cells.* Am J Physiol Lung Cell Mol Physiol, 2001. **280**(6): p. L1273-81.

61. D'Arcangelo, D., C. Gaetano, and M.C. Capogrossi, *Acidification prevents endothelial cell apoptosis by Axl activation.* Circ Res, 2002. **91**(7): p. e4-12.

62. Li, D.W., et al., *Contribution of endothelial progenitor cells to neovascularization (Review).* Int J Mol Med, 2012. **30**(5): p. 1000-6.

63. Zuo, P.Y., et al., *Growth arrest-specific gene 6 protein promotes the proliferation and migration of endothelial progenitor cells through the PI3K/AKT signaling pathway.* Int J Mol Med, 2014. **34**(1): p. 299-306.

64. Kim, Y.S., et al., *Gas6 stimulates angiogenesis of human retinal endothelial cells and of zebrafish embryos via ERK1/2 signaling.* PLoS One, 2014. **9**(1): p. e83901.

65. Doherty, M.J., et al., *Vascular pericytes express osteogenic potential in vitro and in vivo.* J Bone Miner Res, 1998. **13**(5): p. 828-38.

66. Collett, G., et al., *Receptor tyrosine kinase Axl modulates the osteogenic differentiation of pericytes.* Circ Res, 2003. **92**(10): p. 1123-9.

67. Konishi, A., et al., *Hydrogen peroxide activates the Gas6-Axl pathway in vascular smooth muscle cells.* J Biol Chem, 2004. **279**(27): p. 28766-70.

68. Cavet, M.E., et al., *Gas6-Axl pathway: the role of redox-dependent association of Axl with nonmuscle myosin IIB.* Hypertension, 2010. **56**(1): p. 105-11.

69. Lo, C.M., et al., *Nonmuscle myosin IIb is involved in the guidance of fibroblast migration.* Mol Biol Cell, 2004. **15**(3): p. 982-9.

70. Gallagher, P.J., et al., *Alterations in expression of myosin and myosin light chain kinases in response to vascular injury.* Am J Physiol Cell Physiol, 2000. **279**(4): p. C1078-87.

71. Jin, C.W., et al., *Gas6 delays senescence in vascular smooth muscle cells through the PI3K/ Akt/FoxO signaling pathway.* Cell Physiol Biochem, 2015. **35**(3): p. 1151-66.

72. Koury, M.J., *Erythropoietin: the story of hypoxia and a finely regulated hematopoietic hormone.* Exp Hematol, 2005. **33**(11): p. 1263-70.

73. Baron, M.H., *Concise Review: early embryonic erythropoiesis: not so primitive after all.* Stem Cells, 2013. **31**(5): p. 849-56.

74. Fandrey, J., *Oxygen-dependent and tissue-specific regulation of erythropoietin gene expression.* Am J Physiol Regul Integr Comp Physiol, 2004. **286**(6): p. R977-88.

75. Santini, V., *Clinical use of erythropoietic stimulating agents in myelodysplastic syndromes.* Oncologist, 2011. **16 Suppl 3**: p. 35-42.

76. Cao, Y., *Erythropoietin in cancer: a dilemma in risk therapy.* Trends Endocrinol Metab, 2013. **24**(4): p. 190-9.

77. Pinevich, A.J. and J. Petersen, *Erythropoietin therapy in patients with chronic renal failure.* West J Med, 1992. **157**(2): p. 154-7.

78. Hayat, A., D. Haria, and M.O. Salifu, *Erythropoietin stimulating agents in the management of anemia of chronic kidney disease.* Patient Prefer Adherence, 2008. **2**: p. 195-200.

79. F. Stickel, B.H., M. Heim, A. Geier, C. Hirschi,B. Terziroli, K. Wehr and F.N.a.T.G. A. De Gottardi, *Critical review of the use of erythropoietin in the treatment*
of anaemia during therapy for chronic hepatitis C. Journal of Viral Hepatitis, 2011(19): p. 77–87.

80. Marti-Carvajal, A.J., et al., *Erythropoiesis-stimulating agents for anemia in rheumatoid arthritis.* Cochrane Database Syst Rev, 2013(2): p. CD000332.

81. Angelillo-Scherrer, A., *Role of Gas6 in erythropoiesis and anemia in mice.* The Journal of Clinical Investigation, 2008. **118**.

82. Chasis, J.A., *Erythroblastic islands: specialized microenvironmental niches for erythropoiesis.* Curr Opin Hematol, 2006. **13**(3): p. 137-41.

83. Tang, H., et al., *TAM receptors and the regulation of erythropoiesis in mice.* Haematologica, 2009. **94**(3): p. 326-34.

84. Schwarz, H.P., et al., *Plasma protein S deficiency in familial thrombotic disease.* Blood, 1984. **64**(6): p. 1297-300.

85. Beauchamp, N.J., et al., *The prevalence of, and molecular defects underlying, inherited protein S deficiency in the general population.* Br J Haematol, 2004. **125**(5): p. 647-54.

86. Seligsohn, U. and A. Lubetsky, *Genetic susceptibility to venous thrombosis.* N Engl J Med, 2001. **344**(16): p. 1222-31.

87. Kinoshita, S., et al., *Protein S and protein C gene mutations in Japanese deep vein thrombosis patients.* Clin Biochem, 2005. **38**(10): p. 908-15.

88. Ikejiri, M., et al., *The association of protein S Tokushima-K196E with a risk of deep vein thrombosis.* Int J Hematol, 2010. **92**(2): p. 302-5.

89. Pintao, M.C., et al., *Protein S levels and the risk of venous thrombosis: results from the MEGA case-control study.* Blood, 2013. **122**(18): p. 3210-9.

90. ten Kate, M.K. and J. van der Meer, *Protein S deficiency: a clinical perspective.* Haemophilia, 2008. **14**(6): p. 1222-8.

91. Thomson, J.J., A. Retter, and B.J. Hunt, *Novel management of post varicella purpura fulminans owing to severe acquired protein S deficiency.* Blood Coagul Fibrinolysis, 2010. **21**(6): p. 598-600.

92. Brouwer, J.L., et al., *Difference in absolute risk of venous and arterial thrombosis between familial protein S deficiency type I and type III. Results from a family cohort study to assess the clinical impact of a laboratory test-based classification.* Br J Haematol, 2005. **128**(5): p. 703-10.

93. Lijfering, W.M., et al., *Clinical relevance of decreased free protein S levels: results from a retrospective family cohort study involving 1143 relatives.* Blood, 2009. **113**(6): p. 1225-30.

94. Brouwer, J.L., et al., *The pathogenesis of venous thromboembolism: evidence for multiple interrelated causes.* Ann Intern Med, 2006. **145**(11): p. 807-15.

95. Saller, F., et al., *Generation and phenotypic analysis of protein S-deficient mice.* Blood, 2009. **114**(11): p. 2307-14.

96. Burstyn-Cohen, T., M.J. Heeb, and G. Lemke, *Lack of protein S in mice causes embryonic lethal coagulopathy and vascular dysgenesis.* J Clin Invest, 2009. **119**(10): p. 2942-53.

97. Rosing, J., et al., *Effects of protein S and factor Xa on peptide bond cleavages during inactivation of factor Va and factor VaR506Q by activated protein C.* J Biol Chem, 1995. **270**(46): p. 27852-8.

98. Walker, F.J., *Regulation of activated protein C by a new protein. A possible function for bovine protein S.* J Biol Chem, 1980. **255**(12): p. 5521-4.

99. Maurissen, L.F., et al., *Re-evaluation of the role of the protein S-C4b binding protein complex in activated protein C-catalyzed factor Va-inactivation.* Blood, 2008. **111**(6): p. 3034-41.

100. Shen, L. and B. Dahlback, *Factor V and protein S as synergistic cofactors to activated protein C in degradation of factor VIIIa.* J Biol Chem, 1994. **269**(29): p. 18735-8.

101. Ahnstrom, J., et al., *Activated protein C cofactor function of protein S: a novel role for a gamma-carboxyglutamic acid residue.* Blood, 2011. **117**(24): p. 6685-93.

102. Hackeng, T.M. and J. Rosing, *Protein S as cofactor for TFPI.* Arterioscler Thromb Vasc Biol, 2009. **29**(12): p. 2015-20.

103. Hackeng, T.M., et al., *Protein S stimulates inhibition of the tissue factor pathway by tissue factor pathway inhibitor.* Proc Natl Acad Sci U S A, 2006. **103**(9): p. 3106-11.

104. Ndonwi, M., E.A. Tuley, and G.J. Broze, Jr., *The Kunitz-3 domain of TFPI-alpha is required for protein S-dependent enhancement of factor Xa inhibition.* Blood, 2010. **116**(8): p. 1344-51.

105. Castoldi, E., et al., *Hereditary and acquired protein S deficiencies are associated with low TFPI levels in plasma.* J Thromb Haemost, 2010. **8**(2): p. 294-300.

106. Mitchell, C.A., S.M. Kelemen, and H.H. Salem, *The anticoagulant properties of a modified form of protein S.* Thromb Haemost, 1988. **60**(2): p. 298-304.

107. Heeb, M.J., et al., *Protein S binds to and inhibits factor Xa.* Proc Natl Acad Sci U S A, 1994. **91**(7): p. 2728-32.

108. Hackeng, T.M., et al., *Human protein S inhibits prothrombinase complex activity on endothelial cells and platelets via direct interactions with factors Va and Xa.* J Biol Chem, 1994. **269**(33): p. 21051-8.

109. Heeb, M.J., et al., *Plasma contains protein S monomers and multimers with similar direct anticoagulant activity.* J Thromb Haemost, 2006. **4**(10): p. 2215-22.

110. Heeb, M.J., et al., *Plasma protein S contains zinc essential for efficient activated protein C-independent anticoagulant activity and binding to factor Xa, but not for efficient binding to tissue factor pathway inhibitor.* FASEB J, 2009. **23**(7): p. 2244-53.

111. Stavenuiter, F., et al., *Platelet protein S directly inhibits procoagulant activity on platelets and microparticles.* Thromb Haemost, 2013. **109**(2): p. 229-37.

112. Gasic, G.P., et al., *Coagulation factors X, Xa, and protein S as potent mitogens of cultured aortic smooth muscle cells.* Proc Natl Acad Sci U S A, 1992. **89**(6): p. 2317-20.

113. Benzakour, O., et al., *Evidence for a protein S receptor(s) on human vascular smooth muscle cells. Analysis of the binding characteristics and mitogenic properties of protein S on human vascular smooth muscle cells.* Biochem J, 1995. **308 (Pt 2)**: p. 481-5.

114. Liu, D., et al., *Protein S confers neuronal protection during ischemic/hypoxic injury in mice.* Circulation, 2003. **107**(13): p. 1791-6.

115. Zhu, D., et al., *Protein S controls hypoxic/ischemic blood-brain barrier disruption through the TAM receptor Tyro3 and sphingosine 1-phosphate receptor.* Blood, 2010. **115**(23): p. 4963-72.

116. Fraineau, S., et al., *The vitamin K-dependent anticoagulant factor, protein S, inhibits multiple VEGF-A-induced angiogenesis events in a Mer- and SHP2-dependent manner.* Blood, 2012. **120**(25): p. 5073-83.

117. Mahasandana, C., et al., *Neonatal purpura fulminans associated with homozygous protein S deficiency.* Lancet, 1990. **335**(8680): p. 61-2.

118. Mahasandana, C., et al., *Homozygous protein S deficiency: 7-year follow-up.* Thromb Haemost, 1996. **76**(6): p. 1122.

119. Chalmers, E., et al., *Purpura fulminans: recognition, diagnosis and management.* Arch Dis Child, 2011. **96**(11): p. 1066-71.

120. Lund, C.J. and J.C. Donovan, *Blood volume during pregnancy. Significance of plasma and red cell volumes.* Am J Obstet Gynecol, 1967. **98**(3): p. 394-403.

121. Bernstein, I.M., W. Ziegler, and G.J. Badger, *Plasma volume expansion in early pregnancy.* Obstet Gynecol, 2001. **97**(5 Pt 1): p. 669-72.

122. Lurie, S. and Y. Mamet, *Red blood cell survival and kinetics during pregnancy.* Eur J Obstet Gynecol Reprod Biol, 2000. **93**(2): p. 185-92.

123. Milman, N., et al., *Serum erythropoietin during normal pregnancy: relationship to hemoglobin and iron status markers and impact of iron supplementation in a longitudinal, placebo-controlled study on 118 women.* Int J Hematol, 1997. **66**(2): p. 159-68.

124. Whittaker, P.G., S. Macphail, and T. Lind, *Serial hematologic changes and pregnancy outcome.* Obstet Gynecol, 1996. **88**(1): p. 33-9.

125. Stephansson, O., et al., *Maternal hemoglobin concentration during pregnancy and risk of stillbirth.* JAMA, 2000. **284**(20): p. 2611-7.

126. Kuvin, S.F. and G. Brecher, *Differential neutrophil counts in pregnancy.* N Engl J Med, 1962. **266**: p. 877-8.

127. Kuhnert, M., et al., *Changes in lymphocyte subsets during normal pregnancy.* Eur J Obstet Gynecol Reprod Biol, 1998. **76**(2): p. 147-51.

128. Matthews, J.H., et al., *Pregnancy-associated thrombocytopenia: definition, incidence and natural history.* Acta Haematol, 1990. **84**(1): p. 24-9.

129. Burrows, R.F. and J.G. Kelton, *Fetal thrombocytopenia and its relation to maternal thrombocytopenia.* N Engl J Med, 1993. **329**(20): p. 1463-6.

130. Saha, P., D. Stott, and R. Atalla, *Haemostatic changes in the puerperium '6 weeks postpartum' (HIP Study) - implication for maternal thromboembolism.* BJOG, 2009. **116**(12): p. 1602-12.
131. Stirling, Y., et al., *Haemostasis in normal pregnancy.* Thromb Haemost, 1984. **52**(2): p. 176-82.
132. Francalanci, I., et al., *D-dimer plasma levels during normal pregnancy measured by specific ELISA.* Int J Clin Lab Res, 1997. **27**(1): p. 65-7.
133. Miyakis, S., et al., *International consensus statement on an update of the classification criteria for definite antiphospholipid syndrome (APS).* J Thromb Haemost, 2006. **4**(2): p. 295-306.
134. Levine, J.S., D.W. Branch, and J. Rauch, *The antiphospholipid syndrome.* N Engl J Med, 2002. **346**(10): p. 752-63.
135. Opatrny, L., et al., *Association between antiphospholipid antibodies and recurrent fetal loss in women without autoimmune disease: a metaanalysis.* J Rheumatol, 2006. **33**(11): p. 2214-21.
136. Gerhardt, A., et al., *Prothrombin and factor V mutations in women with a history of thrombosis during pregnancy and the puerperium.* N Engl J Med, 2000. **342**(6): p. 374-80.
137. Benedetto, C., et al., *Coagulation disorders in pregnancy: acquired and inherited thrombophilias.* Ann N Y Acad Sci, 2010. **1205**: p. 106-17.
138. Battinelli, E.M., A. Marshall, and J.M. Connors, *The role of thrombophilia in pregnancy.* Thrombosis, 2013. **2013**: p. 516420.
139. Brenner, B., et al., *Gestational outcome in thrombophilic women with recurrent pregnancy loss treated by enoxaparin.* Thromb Haemost, 2000. **83**(5): p. 693-7.
140. Kupferminc, M.J., et al., *Low-molecular-weight heparin for the prevention of obstetric complications in women with thrombophilias.* Hypertens Pregnancy, 2001. **20**(1): p. 35-44.
141. Gris, J.C., et al., *Low-molecular-weight heparin versus low-dose aspirin in women with one fetal loss and a constitutional thrombophilic disorder.* Blood, 2004. **103**(10): p. 3695-9.
142. Folkeringa, N., et al., *Reduction of high fetal loss rate by anticoagulant treatment during pregnancy in antithrombin, protein C or protein S deficient women.* Br J Haematol, 2007. **136**(4): p. 656-61.
143. Kaandorp, S.P., et al., *Aspirin plus heparin or aspirin alone in women with recurrent miscarriage.* N Engl J Med, 2010. **362**(17): p. 1586-96.
144. Rodger, M.A., et al., *Low-molecular-weight heparin for prevention of placenta-mediated pregnancy complications: protocol for a systematic review and individual patient data meta-analysis (AFFIRM).* Syst Rev, 2014. **3**: p. 69.
145. Middeldorp, S., *Inherited thrombophilia: a double-edged sword.* Hematology Am Soc Hematol Educ Program, 2016. **2016**(1): p. 1-9.
146. Serhan, C.N., N. Chiang, and T.E. Van Dyke, *Resolving inflammation: dual anti-inflammatory and pro-resolution lipid mediators.* Nat Rev Immunol, 2008. **8**(5): p. 349-61.
147. Bosurgi, L., et al., *Paradoxical role of the proto-oncogene Axl and Mer receptor tyrosine kinases in colon cancer.* Proc Natl Acad Sci U S A, 2013. **110**(32): p. 13091-6.

148. Scott, R.S., et al., *Phagocytosis and clearance of apoptotic cells is mediated by MER.* Nature, 2001. **411**(6834): p. 207-11.
149. Cohen, P.L., et al., *Delayed apoptotic cell clearance and lupus-like autoimmunity in mice lacking the c-mer membrane tyrosine kinase.* J Exp Med, 2002. **196**(1): p. 135-40.
150. Tibrewal, N., et al., *Autophosphorylation docking site Tyr-867 in Mer receptor tyrosine kinase allows for dissociation of multiple signaling pathways for phagocytosis of apoptotic cells and down-modulation of lipopolysaccharide-inducible NF-kappaB transcriptional activation.* J Biol Chem, 2008. **283**(6): p. 3618-27.
151. Seitz, H.M., et al., *Macrophages and dendritic cells use different Axl/Mertk/Tyro3 receptors in clearance of apoptotic cells.* J Immunol, 2007. **178**(9): p. 5635-42.
152. Nakano, T., et al., *Cell adhesion to phosphatidylserine mediated by a product of growth arrest-specific gene 6.* J Biol Chem, 1997. **272**(47): p. 29411-4.
153. Anderson, H.A., et al., *Serum-derived protein S binds to phosphatidylserine and stimulates the phagocytosis of apoptotic cells.* Nat Immunol, 2003. **4**(1): p. 87-91.
154. D'Cruz, P.M., et al., *Mutation of the receptor tyrosine kinase gene Mertk in the retinal dystrophic RCS rat.* Hum Mol Genet, 2000. **9**(4): p. 645-51.
155. Gal, A., et al., *Mutations in MERTK, the human orthologue of the RCS rat retinal dystrophy gene, cause retinitis pigmentosa.* Nat Genet, 2000. **26**(3): p. 270-1.
156. Xiong, W., et al., *Gas6 and the Tyro 3 receptor tyrosine kinase subfamily regulate the phagocytic function of Sertoli cells.* Reproduction, 2008. **135**(1): p. 77-87.
157. Chung, W.S., et al., *Astrocytes mediate synapse elimination through MEGF10 and MERTK pathways.* Nature, 2013. **504**(7480): p. 394-400.
158. Happonen, K.E., et al., *The Gas6-Axl Protein Interaction Mediates Endothelial Uptake of Platelet Microparticles.* J Biol Chem, 2016. **291**(20): p. 10586-601.
159. Buckley, C.D., et al., *The resolution of inflammation.* Nat Rev Immunol, 2013. **13**(1): p. 59-66.
160. Coombes, J.L. and F. Powrie, *Dendritic cells in intestinal immune regulation.* Nat Rev Immunol, 2008. **8**(6): p. 435-46.
161. Lambrecht, B.N. and H. Hammad, *The role of dendritic and epithelial cells as master regulators of allergic airway inflammation.* Lancet, 2010. **376**(9743): p. 835-43.
162. Beutler, B., et al., *Genetic analysis of host resistance: Toll-like receptor signaling and immunity at large.* Annu Rev Immunol, 2006. **24**: p. 353-89.
163. Iwasaki, A. and R. Medzhitov, *Toll-like receptor control of the adaptive immune responses.* Nat Immunol, 2004. **5**(10): p. 987-95.
164. Banchereau, J. and V. Pascual, *Type I interferon in systemic lupus erythematosus and other autoimmune diseases.* Immunity, 2006. **25**(3): p. 383-92.
165. Liew, F.Y., et al., *Negative regulation of toll-like receptor-mediated immune responses.* Nat Rev Immunol, 2005. **5**(6): p. 446-58.

166. Camenisch, T.D., et al., *A novel receptor tyrosine kinase, Mer, inhibits TNF-alpha production and lipopolysaccharide-induced endotoxic shock.* J Immunol, 1999. **162**(6): p. 3498-503.

167. Rothlin, C.V., et al., *TAM receptors are pleiotropic inhibitors of the innate immune response.* Cell, 2007. **131**(6): p. 1124-36.

168. Paquette, R.L., et al., *Interferon-alpha and granulocyte-macrophage colony-stimulating factor differentiate peripheral blood monocytes into potent antigen-presenting cells.* J Leukoc Biol, 1998. **64**(3): p. 358-67.

169. Sharif, M.N., et al., *Twist mediates suppression of inflammation by type I IFNs and Axl.* J Exp Med, 2006. **203**(8): p. 1891-901.

170. Scutera, S., et al., *Survival and migration of human dendritic cells are regulated by an IFN-alpha-inducible Axl/Gas6 pathway.* J Immunol, 2009. **183**(5): p. 3004-13.

171. Carrera Silva, E.A., et al., *T cell-derived protein S engages TAM receptor signaling in dendritic cells to control the magnitude of the immune response.* Immunity, 2013. **39**(1): p. 160-70.

172. Gibot, S., et al., *Growth arrest-specific protein 6 plasma concentrations during septic shock.* Crit Care, 2007. **11**(1): p. R8.

173. Ekman, C., et al., *Plasma concentrations of Gas6 (growth arrest specific protein 6) and its soluble tyrosine kinase receptor sAxl in sepsis and systemic inflammatory response syndromes.* Crit Care, 2010. **14**(4): p. R158.

174. Stalder, G., et al., *Study of Early Elevated Gas6 Plasma Level as a Predictor of Mortality in a Prospective Cohort of Patients with Sepsis.* PLoS One, 2016. **11**(10): p. e0163542.

175. Hisada, Y., et al., *Discovery of an uncovered region in fibrin clots and its clinical significance.* Sci Rep, 2013. **3**: p. 2604.

176. Tschanz, S., J.P. Schneider, and L. Knudsen, *Design-based stereology: Planning, volumetry and sampling are crucial steps for a successful study.* Ann Anat, 2014. **196**(1): p. 3-11.

177. Tschanz, S.A., P.H. Burri, and E.R. Weibel, *A simple tool for stereological assessment of digital images: the STEPanizer.* J Microsc, 2011. **243**(1): p. 47-59.

178. Koulnis, M., et al., *Identification and analysis of mouse erythroid progenitors using the CD71/TER119 flow-cytometric assay.* J Vis Exp, 2011(54).

179. van der Meer, J.H., T. van der Poll, and C. van 't Veer, *TAM receptors, Gas6, and protein S: roles in inflammation and hemostasis.* Blood, 2014. **123**(16): p. 2460-9.

180. Chatrou, M.L., et al., *Vascular calcification: the price to pay for anticoagulation therapy with vitamin K-antagonists.* Blood Rev, 2012. **26**(4): p. 155-66.

181. Pourdeyhimi, N. and Z. Bullard, *Warfarin-induced skin necrosis.* Hosp Pharm, 2014. **49**(11): p. 1044-8.

182. Price, V.E., et al., *Diagnosis and management of neonatal purpura fulminans.* Semin Fetal Neonatal Med, 2011. **16**(6): p. 318-22.

183. Bolton-Maggs, P.H. and K.J. Pasi, *Haemophilias A and B.* Lancet, 2003. **361**(9371): p. 1801-9.

184. Hoyer, L.W., *Hemophilia A.* N Engl J Med, 1994. **330**(1): p. 38-47.

185. Mannucci, P.M. and E.G. Tuddenham, *The hemophilias--from royal genes to gene therapy.* N Engl J Med, 2001. **344**(23): p. 1773-9.

186. Mann, K.G., R.J. Jenny, and S. Krishnaswamy, *Cofactor proteins in the assembly and expression of blood clotting enzyme complexes.* Annu Rev Biochem, 1988. **57**: p. 915-56.

187. Broze, G.J., Jr., *The role of tissue factor pathway inhibitor in a revised coagulation cascade.* Semin Hematol, 1992. **29**(3): p. 159-69.

188. Repke, D., et al., *Hemophilia as a defect of the tissue factor pathway of blood coagulation: effect of factors VIII and IX on factor X activation in a continuous-flow reactor.* Proc Natl Acad Sci U S A, 1990. **87**(19): p. 7623-7.

189. Berntorp, E. and A.D. Shapiro, *Modern haemophilia care.* Lancet, 2012. **379**(9824): p. 1447-56.

190. Hartmann, J. and S.E. Croteau, *2016 Clinical Trials Update: Innovations in Hemophilia Therapy.* Am J Hematol, 2016.

191. Polderdijk, S.G., et al., *Design and characterization of an APC-specific serpin for the treatment of hemophilia.* Blood, 2016.

192. DiScipio, R.G. and E.W. Davie, *Characterization of protein S, a gamma-carboxyglutamic acid containing protein from bovine and human plasma.* Biochemistry, 1979. **18**(5): p. 899-904.

193. Ndonwi, M. and G. Broze, Jr., *Protein S enhances the tissue factor pathway inhibitor inhibition of factor Xa but not its inhibition of factor VIIa-tissue factor.* J Thromb Haemost, 2008. **6**(6): p. 1044-6.

194. Comp, P.C. and C.T. Esmon, *Recurrent venous thromboembolism in patients with a partial deficiency of protein S.* N Engl J Med, 1984. **311**(24): p. 1525-8.

195. Biss, T.T., et al., *The use of prophylaxis in 2663 children and adults with haemophilia: results of the 2006 Canadian national haemophilia prophylaxis survey.* Haemophilia, 2008. **14**(5): p. 923-30.

196. Melchiorre, D., et al., *Clinical, instrumental, serological and histological findings suggest that hemophilia B may be less severe than hemophilia A.* Haematologica, 2016. **101**(2): p. 219-25.

197. Nagel, K., et al., *Comparing bleed frequency and factor concentrate use between haemophilia A and B patients.* Haemophilia, 2011. **17**(6): p. 872-4.

198. Schulman, S., et al., *Validation of a composite score for clinical severity of hemophilia.* J Thromb Haemost, 2008. **6**(7): p. 1113-21.

199. Tagariello, G., et al., *Comparison of the rates of joint arthroplasty in patients with severe factor VIII and IX deficiency: an index of different clinical severity of the 2 coagulation disorders.* Blood, 2009. **114**(4): p. 779-84.

200. Weiss, E.J., et al., *Protection against thrombosis in mice lacking PAR3.* Blood, 2002. **100**(9): p. 3240-4.

201. Gailani, D. and T. Renne, *Intrinsic pathway of coagulation and arterial thrombosis.* Arterioscler Thromb Vasc Biol, 2007. **27**(12): p. 2507-13.

202. Fischer, K., et al., *Trends in bleeding patterns during prophylaxis for severe haemophilia: observations from a series of prospective clinical trials.* Haemophilia, 2011. **17**(3): p. 433-8.

203. Stephensen, D., et al., *Changing patterns of bleeding in patients with severe haemophilia A.* Haemophilia, 2009. **15**(6): p. 1210-4.

204. Piro, O. and G.J. Broze, Jr., *Comparison of cell-surface TFPIalpha and beta.* J Thromb Haemost, 2005. **3**(12): p. 2677-83.

205. Nieuwenhuizen, L., et al., *Hemarthrosis in hemophilic mice results in alterations in M1-M2 monocyte/macrophage polarization.* Thromb Res, 2014. **133**(3): p. 390-5.

206. Ovlisen, K., et al., *IL-1 beta, IL-6, KC and MCP-1 are elevated in synovial fluid from haemophilic mice with experimentally induced haemarthrosis.* Haemophilia, 2009. **15**(3): p. 802-10.

207. Roosendaal, G., et al., *Synovium in haemophilic arthropathy.* Haemophilia, 1998. **4**(4): p. 502-5.

208. Harigai, M., et al., *Monocyte chemoattractant protein-1 (MCP-1) in inflammatory joint diseases and its involvement in the cytokine network of rheumatoid synovium.* Clin Immunol Immunopathol, 1993. **69**(1): p. 83-91.

209. Beltran-Miranda, C.P., et al., *Thrombin generation and phenotypic correlation in haemophilia A.* Haemophilia, 2005. **11**(4): p. 326-34.

210. Dargaud, Y., et al., *Evaluation of thrombin generating capacity in plasma from patients with haemophilia A and B.* Thromb Haemost, 2005. **93**(3): p. 475-80.

211. Santagostino, E., et al., *Severe hemophilia with mild bleeding phenotype: molecular characterization and global coagulation profile.* J Thromb Haemost, 2010. **8**(4): p. 737-43.

212. Maroney, S.A., et al., *Temporal expression of alternatively spliced forms of tissue factor pathway inhibitor in mice.* J Thromb Haemost, 2009. **7**(7): p. 1106-13.

213. Preston, R.J., et al., *Multifunctional specificity of the protein C/activated protein C Gla domain.* J Biol Chem, 2006. **281**(39): p. 28850-7.

214. Dejana, E., et al., *Bleeding time in laboratory animals. III - Do tail bleeding times in rats only measure a platelet defect? (the aspirin puzzle).* Thromb Res, 1979. **15**(1-2): p. 199-207.

215. Flight, S.M., et al., *Textilinin-1, an alternative anti-bleeding agent to aprotinin: Importance of plasmin inhibition in controlling blood loss.* Br J Haematol, 2009. **145**(2): p. 207-11.

216. He, S., et al., *The role of recombinant factor VIIa (FVIIa) in fibrin structure in the absence of FVIII/FIX.* J Thromb Haemost, 2003. **1**(6): p. 1215-9.

217. Rothlin, C.V., et al., *TAM receptor signaling in immune homeostasis.* Annu Rev Immunol, 2015. **33**: p. 355-91.

218. Buras, J.A., B. Holzmann, and M. Sitkovsky, *Animal models of sepsis: setting the stage.* Nat Rev Drug Discov, 2005. **4**(10): p. 854-65.

219. Rudiger, A. and M. Singer, *Mechanisms of sepsis-induced cardiac dysfunction.* Crit Care Med, 2007. **35**(6): p. 1599-608.

220. Baker, C.C., et al., *Evaluation of factors affecting mortality rate after sepsis in a murine cecal ligation and puncture model.* Surgery, 1983. **94**(2): p. 331-5.

221. Remick, D.G., et al., *Comparison of the mortality and inflammatory response of two models of sepsis: lipopolysaccharide vs. cecal ligation and puncture.* Shock, 2000. **13**(2): p. 110-6.

222.	Mannhalter, J.W., et al., *A functional defect in the early phase of the immune response observed in patients with hemophilia A.* Clin Immunol Immunopathol, 1986. **38**(3): p. 390-7.

223.	Drake, T.A., J.H. Morrissey, and T.S. Edgington, *Selective cellular expression of tissue factor in human tissues. Implications for disorders of hemostasis and thrombosis.* Am J Pathol, 1989. **134**(5): p. 1087-97.

224.	Dargaud, Y., et al., *The potential role of synovial thrombomodulin in the pathophysiology of joint bleeds in haemophilia.* Haemophilia, 2012. **18**(5): p. 818-23.

225.	Xue, M., et al., *Endothelial protein C receptor is overexpressed in rheumatoid arthritic (RA) synovium and mediates the anti-inflammatory effects of activated protein C in RA monocytes.* Ann Rheum Dis, 2007. **66**(12): p. 1574-80.

226.	Melchiorre, D., et al., *RANK-RANKL-OPG in hemophilic arthropathy: from clinical and imaging diagnosis to histopathology.* J Rheumatol, 2012. **39**(8): p. 1678-86.

227.	Quick, A.J. and C.V. Hussey, *Hemophilia B (PTC deficiency, or Christmas disease).* AMA Arch Intern Med, 1959. **103**(5): p. 762-75.

228.	Bi, L., et al., *Targeted disruption of the mouse factor VIII gene produces a model of haemophilia A.* Nat Genet, 1995. **10**(1): p. 119-21.

229.	Lin, H.F., et al., *A coagulation factor IX-deficient mouse model for human hemophilia B.* Blood, 1997. **90**(10): p. 3962-6.

230.	Angelillo-Scherrer, A., et al., *Connexin 37 limits thrombus propensity by downregulating platelet reactivity.* Circulation, 2011. **124**(8): p. 930-9.

231.	Maroney, S.A., et al., *Absence of hematopoietic tissue factor pathway inhibitor mitigates bleeding in mice with hemophilia.* Proc Natl Acad Sci U S A, 2012. **109**(10): p. 3927-31.

232.	Ovlisen, K., et al., *Hemostatic effect of recombinant factor VIIa, NN1731 and recombinant factor VIII on needle-induced joint bleeding in hemophilia A mice.* J Thromb Haemost, 2008. **6**(6): p. 969-75.

233.	Hakobyan, N., et al., *Haemarthrosis model in mice: BSS - Bleeding Severity Score assessment system.* Haemophilia, 2016. **22**(5): p. 790-8.

234.	Armaka, M., et al., *A standardized protocol for the isolation and culture of normal and arthritogenic murine synovial fibroblasts.* Protocol Exchange, 2009.

235.	Fernandez, J.A., et al., *Species-specific anticoagulant and mitogenic activities of murine protein S.* Haematologica, 2009. **94**(12): p. 1721-31.

236.	Dargaud, Y., et al., *Standardisation of thrombin generation test--which reference plasma for TGT? An international multicentre study.* Thromb Res, 2010. **125**(4): p. 353-6.

237.	Harmon, S., et al., *Dissociation of activated protein C functions by elimination of protein S cofactor enhancement.* J Biol Chem, 2008. **283**(45): p. 30531-9.

238.	Burnier, L., J.A. Fernandez, and J.H. Griffin, *Antibody SPC-54 provides acute in vivo blockage of the murine protein C system.* Blood Cells Mol Dis, 2013. **50**(4): p. 252-8.

239.	Mosnier, L.O., X.V. Yang, and J.H. Griffin, *Activated protein C mutant with minimal anticoagulant activity, normal cytoprotective activity, and*

preservation of thrombin activable fibrinolysis inhibitor-dependent cytoprotective functions. J Biol Chem, 2007. **282**(45): p. 33022-33.

240. Zubairova, L.D., et al., *Circulating Microparticles Alter Formation, Structure, and Properties of Fibrin Clots.* Sci Rep, 2015. **5**: p. 17611.

241. Maurissen, L.F., et al., *Thrombin generation-based assays to measure the activity of the TFPI-protein S pathway in plasma from normal and protein S-deficient individuals.* J Thromb Haemost, 2010. **8**(4): p. 750-8.

242. Angelillo-Scherrer, A., et al., *Role of Gas6 in erythropoiesis and anemia in mice.* J Clin Invest, 2008. **118**(2): p. 583-96.

243. Pulles, A.E., et al., *Pathophysiology of hemophilic arthropathy and potential targets for therapy.* Pharmacol Res, 2017. **115**: p. 192-199.

244. Bremme, K.A., *Haemostatic changes in pregnancy.* Best Pract Res Clin Haematol, 2003. **16**(2): p. 153-68.

245. Bakhti, A. and D. Vaiman, *Prevention of gravidic endothelial hypertension by aspirin treatment administered from the 8th week of gestation.* Hypertens Res, 2011. **34**(10): p. 1116-20.

246. Georgiades, P., A.C. Ferguson-Smith, and G.J. Burton, *Comparative developmental anatomy of the murine and human definitive placentae.* Placenta, 2002. **23**(1): p. 3-19.

247. Erez, O., et al., *Evidence of maternal platelet activation, excessive thrombin generation, and high amniotic fluid tissue factor immunoreactivity and functional activity in patients with fetal death.* J Matern Fetal Neonatal Med, 2009. **22**(8): p. 672-87.

248. An, J., et al., *Heparin rescues factor V Leiden-associated placental failure independent of anticoagulation in a murine high-risk pregnancy model.* Blood, 2013. **121**(11): p. 2127-34.

249. Kingdom, J.C. and S. Drewlo, *Is heparin a placental anticoagulant in high-risk pregnancies?* Blood, 2011. **118**(18): p. 4780-8.

250. Franchini, M. and P.M. Mannucci, *Hemophilia A in the third millennium.* Blood Rev, 2013. **27**(4): p. 179-84.

251. Peyvandi, F., I. Garagiola, and G. Young, *The past and future of haemophilia: diagnosis, treatments, and its complications.* Lancet, 2016. **388**(10040): p. 187-97.

252. Hartmann, J. and S.E. Croteau, *2017 Clinical trials update: Innovations in hemophilia therapy.* Am J Hematol, 2016. **91**(12): p. 1252-1260.

253. Angus, D.C., et al., *Epidemiology of severe sepsis in the United States: analysis of incidence, outcome, and associated costs of care.* Crit Care Med, 2001. **29**(7): p. 1303-10.

254. Vincent, J.L., et al., *Sepsis in European intensive care units: results of the SOAP study.* Crit Care Med, 2006. **34**(2): p. 344-53.

255. Hotchkiss, R.S., G. Monneret, and D. Payen, *Sepsis-induced immunosuppression: from cellular dysfunctions to immunotherapy.* Nat Rev Immunol, 2013. **13**(12): p. 862-74.

256. Angus, D.C. and T. van der Poll, *Severe sepsis and septic shock.* N Engl J Med, 2013. **369**(21): p. 2063.

257. Hotchkiss, R.S., G. Monneret, and D. Payen, *Immunosuppression in sepsis: a novel understanding of the disorder and a new therapeutic approach.* Lancet Infect Dis, 2013. **13**(3): p. 260-8.

258. Jones, A.E. and M.A. Puskarich, *The Surviving Sepsis Campaign guidelines 2012: update for emergency physicians.* Ann Emerg Med, 2014. **63**(1): p. 35-47.

259. Borgel, D., et al., *Elevated growth-arrest-specific protein 6 plasma levels in patients with severe sepsis.* Crit Care Med, 2006. **34**(1): p. 219-22.

260. Saller, F., et al., *Role of the growth arrest-specific gene 6 (gas6) product in thrombus stabilization.* Blood Cells Mol Dis, 2006. **36**(3): p. 373-8.

261. Varnum, B.C., et al., *Axl receptor tyrosine kinase stimulated by the vitamin K-dependent protein encoded by growth-arrest-specific gene 6.* Nature, 1995. **373**(6515): p. 623-6.

262. Angelillo-Scherrer, A., et al., *Role of Gas6 receptors in platelet signaling during thrombus stabilization and implications for antithrombotic therapy.* J Clin Invest, 2005. **115**(2): p. 237-46.

263. Beutler, B., *Inferences, questions and possibilities in Toll-like receptor signalling.* Nature, 2004. **430**(6996): p. 257-63.

264. Giangola, M.D., et al., *Growth arrest-specific protein 6 attenuates neutrophil migration and acute lung injury in sepsis.* Shock, 2013. **40**(6): p. 485-91.

265. Pluess, T.T., et al., *Intravenous fish oil blunts the physiological response to endotoxin in healthy subjects.* Intensive Care Med, 2007. **33**(5): p. 789-97.

266. Clauser, S., et al., *Development of a novel immunoassay for the assessment of plasma Gas6 concentrations and their variation with hormonal status.* Clin Chem, 2007. **53**(10): p. 1808-13.

267. Cross, A.S., et al., *Role of lipopolysaccharide and capsule in the serum resistance of bacteremic strains of Escherichia coli.* J Infect Dis, 1986. **154**(3): p. 497-503.

268. Belge, K.U., et al., *The proinflammatory CD14+CD16+DR++ monocytes are a major source of TNF.* J Immunol, 2002. **168**(7): p. 3536-42.

269. Sen, P., et al., *Apoptotic cells induce Mer tyrosine kinase-dependent blockade of NF-kappaB activation in dendritic cells.* Blood, 2007. **109**(2): p. 653-60.

270. Schabbauer, G., et al., *PI3K-Akt pathway suppresses coagulation and inflammation in endotoxemic mice.* Arterioscler Thromb Vasc Biol, 2004. **24**(10): p. 1963-9.

271. van den Brand, B.T., et al., *Therapeutic efficacy of Tyro3, Axl, and Mer tyrosine kinase agonists in collagen-induced arthritis.* Arthritis Rheum, 2013. **65**(3): p. 671-80.

272. Ekman, C., J. Stenhoff, and B. Dahlback, *Gas6 is complexed to the soluble tyrosine kinase receptor Axl in human blood.* J Thromb Haemost, 2010. **8**(4): p. 838-44.

273. Vincent, J.L., *Procalcitonin: THE marker of sepsis?* Crit Care Med, 2000. **28**(4): p. 1226-8.

274. Boucher, B.A. and S.D. Hanes, *Searching for simple outcome markers in sepsis: an effort in futility?* Crit Care Med, 1999. **27**(7): p. 1390-1.

275. Takahashi, H., et al., *Plasma protein S in disseminated intravascular coagulation, liver disease, collagen disease, diabetes mellitus, and under oral anticoagulant therapy.* Clin Chim Acta, 1989. **182**(2): p. 195-208.

276. Fourrier, F., et al., *Septic shock, multiple organ failure, and disseminated intravascular coagulation. Compared patterns of antithrombin III, protein C, and protein S deficiencies.* Chest, 1992. **101**(3): p. 816-23.